STRUCTURAL GEOMETRY, TECTONIC HISTORY AND DEFORMATION MECHANISMS IN THE MOINE THRUST ZONE NEAR ULLAPOOL N.W. SCOTLAND

D.A. WINTER B.Sc. M.Sc. DIC

Thesis submitted for the degree of Doctor of Philosophy at the University of Edinburgh

1984

The laboratory work for Chapter 6 was carried out at St. Andrews University by Dr. G. Oliver, the remainder of the thesis is all my own work.

Signed.

CONTENTS

LIST OF FIGURES

* SEE ALSO ENCLOSURE 4.

Fig. 2.4.
Diagrammatic section from Elliott & Johnson (1980), to show the disposition of the "Torridonian" rocks in the Foreland and Assynt basins prior to movement on the thrusts. Displacement estimates for the Loch Broom thrust by Elliott & Johnson (op. cit.) are based on the width of the eroded anticline. The original positions of the Langwell and the Achall portions of the Loch Broom thrust sheet are marked. See fig. 2.5 and section 2.3.2.

Fig. 2.5.
Sketch map of the two "Torridonian" basins prior to thrust movement, with the present day thrust front marked. The original thrust front prior to movement on the Loch Broom thrust is also marked, note that it represents a ramp that is oblique to the transport direction. This ramp terminated in the north at the large lateral ramp in the Moine thrust. See fig 2.2a and section 2.3.2

Fig. 2.6.
Stratigraphic separation diagram for the Ullapool thrust sheet: Note that the northern termination is marked by diminishing stratigraphic separation as the displacement decreases. However the southern termination was against a lateral ramp in the Loch Broom thrust. See fig. 2.7 & 2.8.

Fig. 2.7.
Geological map of the Ullapool thrust sheet: The diminishing stratigraphic separation northwards is clearly seen. The bedding dips are a result of rotation during the emplacement of the thrust sheet.

Fig. 2.8.
Hangingwall sequence diagram for the Ullapool thrust. Viewed down the thrust dip, i.e., down the line of transport.

a). The Ullapool thrust is initiated at a lateral ramp in the Loch Broom thrust as an attempt to reduce friction at the ramp.

b). With movement on the Ullapool thrust, the hangingwall,the Looch Broom and Moine thrusts are folded. Deformation within the Ullapool thrust sheet produces extensional strains which are taken up by extensional faulting. These faults are later cut and truncated by the reactivated extensional movement on the Moine thrust. See 2.4.

Fig. 2.9.
Stereogram of poles to bedding in Sheet IV at Achall. Note the spread of dips as a result of rotation on the extension faults in Sheet IV. Lower hemisphere projection. See 2.5.1.1.

Fig. 2.10.
Diagram to show relationship between tectonic veins and bedding parallel stylolites. These are illustrated with respect to the stress system active during the extensional faulting. Material desolved by pressure solution along the stylolites is deposited in the veins. With rotation of bedding by movement on the faults, earlier veins and stylolites are also rotated. Later episodes of veining during increments of slip produce cross-cutting relationships. See 2.5.1.1.

Fig. 2.11.
Sketch diagram to illustrate styles of folding in Sheet IV. See 2.5.1.2.

a). Folds formed by a shear couple acting on the bedding planes during rotation on the extensional faults. The folds may have amplified from a small perturbation.
b). Folds formed by drag on a fault plane.

Fig. 2.12.
Stereograms of poles to NE-SW extension faults and tectonic veins.

a). NE-SW extension faults; the spread of the poles is a result of the listric geometry of the faults. Lower hemisphere projection.

b). Tectonic veins which formed synchronously with the faults. The spread of the poles is a result of rotation firstly on the NE-SW extension faults, and secondly on the NW-SE extension faults. Lower hemisphere projection. See 2.5.1.3a.

Fig. 2.13.
Sketch diagram to illustrate the development of secondary synthetic and antithetic extension faults. These are a result of hangingwall deformation to accomodate rotation on the first order listric extension faults. See 2.5.1.3a.

Fig. 2.14.
a). Stereogram of poles to NW-SE extension faults in Sheet IV. Lower hemisphere projection.

b). Stereogram of poles to tectonic veins which formed concomitantly with the NW-SE extension faults. Lower hemisphere projection.
See 2.5.1.3b.

Fig 2.15
Sketch block diagram to show the development of crystal fibre growths at small steps in a fault plane. Crystal fibre growths grow in the lee of the steps, with their long axes representing the X direction of the deformation strain ellipsoid. Any small change in the movement vector of the fault will be reflected in the fibre growths by a change in their orientation. Fibre growths build up incrementally in steps,(see small diagram). Material forming the fibres is removed from the steps by pressure solution. See 2.5.1.3b.

Fig 2.16.
a). Stereogram of poles to strike slip faults in Sheet IV. Lower hemisphere projection.

b). Stereogram of the long axes of the crystal fibre growths on the strike slip fault planes. Lower hemisphere projection. See 2.5.1.3c.

Fig. 2.17.
Diagrams to illustrate the Andersonian relationship between fault geometry and the principal stesses for a). reverse faults, b).extension faults, and c). strike slip faults. $_1$ = maximum principal stess, $_3$ = minimum principal stress. See 2.5.1.3c.

Fig 2.18.
Block diagram to show the geometric relationship between an extension fault and concomitant tectonic veins. Such veins have been interpreted as pre-failure fracture arrays, Sibson (1981). See 2.5.1.4.

Fig. 2.19.
Sketch diagrams to illustrate the classification of extension faults of Wernicke & Burchfiel (1982), a). non-rotational, b). listric, and c). planar rotational, note that the angle between the fault plane and the bedding remains constant during displacement, hence the fault planes also rotate.

d). sketch diagram to illustrate the most likely relationship between classes of extension faults observed in Sheet IV at Achall, not to scale.
See 2.5.1.5.

Fig. 2.20.
Extension map from Wernicke & Burchfiel (1982) for planar rotational faults. As the majority of the faults in Sheet IV are planar rotational faults, then the map can give a minimum estimate of extension as it is not possible to produce a restored section. The map gives an approximate estimate of 30% extension in Sheet IV.

See 2.6.

* Fig.2.21.
a). Section through Sheet IV from Coward (1983) who interprets some of the faults as thrusts which are components of a surge zone.

b). Section through Sheet IV with the faults interpreted as extension faults.
Note that the reactivated extensional movement on the Moine thrust truncates the faults in both of the sections. See 2.6. and 2.2.1.

Fig.3.1. Deformation of a thrust sheet at a ramp-
(a) Back thrusts may form as a result of compressive stresses produced when a thrust sheet moves against a ramp.

(b) Synthetic splay thrusts may also form above a ramp, again as a result of compressive stresses.

Fig.3.2.
Extension faults occur in the thrust sheets at the apex of the ramp: these commonly form as a response to bending stresses within the thrust sheet as it moves from the ramp onto the flat.

Fig.3.3.
The ramp induced internal deformation of the thrust sheet can be totally accommodated by folding: in (a) a thrust is shown soon after some initial movement, with continuing motion the fold crest flattens (b).

* NOW ADDED TO ENCLOSURE 2.

Fig.3.4.
A fold may develop in the competent units prior to movement up the ramp. With movement onto the upper flat the fold limb becomes over-steepened, and in some cases may become overturned, Berger& Johnson (1980).

Fig.3.5.
Possible fault orientations in a thrust sheet at a ramp, predicted by theoretical analysis. The stippled areas are where the stresses are tensile. Note the position at the apex of the ramp, from Wiltschko (1979a).

Fig.3.6.
Extension faults above the ramp in the Loch Broom thrust at Achall occur where compressive stresses would be expected. The extension faults are the N.W-S.E extension faults of Sheet IV which have propagated up through the Loch Broom thrust

Fig.3.7.
A hanging wall sequence diagram to illustrate the accretion of a horse and the resulting deformation of the hangingwall. (a) shows a thrust prior to accreting the horse. (b) with accretion the thrust and the hangingwall are folded and extended. This extension may be taken up by extension faults (c).

Fig.3.8.
A hangingwall sequence diagram to illustrate the sequential accretion of horses onto a thrust sheet. With each successive accretion, the hangingwall becomes more extended, (a,b) which may eventually lead to the formation of a drop fault, (c).

Fig.3.9.
Accretion of horses to adjacent hangingwall sites can produce a complex hangingwall deformation. This hangingwall seqence diagram shows that successive accretions causes folding of horses and extension in the hangingwall, (a,b). Further accretion, (c), can cause folding in areas of the hangingwall which were previously in extension.

Fig.3.10.
Hangingwall sequence diagram to demonstrate the development ot the internal geometry of the Ullapool thrust sheet. The thrust sheet initiated at a large lateral ramp in the Loch Broom thrust, (a). With movement the thrust sheet was deformed into a large warp, with extension occurring at the crest.This extension was accommodated by extension faulting both in the strike and dip directions of the thrust sheet.

Fig.3.11.
Geological map of the Ullapool thrust sheet. Note the situation of the extension faults at the thickest part of the thrust sheet.

Fig.3.12.
Cross section along the line A-A' on fig.3.11, parallel to the tectonic transport direction. Note the lens shape of the thrust sheet. The Ullapool sheet is a large horse plucked from a lateral ramp in the Loch Broom thrust. The late extensional movement on the Moine thrust truncates the Loch Broom thrust.

Fig.3.13.
Diagram to show the shape of a horse; the bounding fault planes meet the main thrust plane at a branch line, these line surround the horse. Horses are often lensoid in shape, the section X-X' shows a typical cross section.

Fig.3.14.
Diagram to show the ralationship between the principal stresses and a thrust plane. An increase in the angle θ causes an increase in the normal stress σ_n and hence also τ, friction on the thrust plane will also rise.

Fig.3.15.
Diagrams to show the formation of ramps as a result of lateral changes in their glide plane.

(a) Ramps may form as links connecting planes of high pore fluid pressure.

(b) Old extension faults which have previously displaced the glide horizon may become reactivated as thrust ramps.

(c) Fossil hills may provide a similar situation to old extension faults

(d) Folding may occur prior to thrusting, thickening the layers. The short steep limbs of folds are commonly thrust out and are often sites of ramps.

Fig.3.16.
Two diagrams to show the geometry of a horse that is formed from a simple ramp.

(a) The footwall is undeformed, and the incipient fracture is shown.

(b) With accretion and movement over the ramp, the bedding rotates to become foreland dipping and right way up.

Fig.3.17
Two diagrams to show the geometry of a horse derived from a ramp which cuts through a folded footwall.

(a) Geometry before movement.

(b) After accretion and movement up the ramp, and the bedding is rotated to become hindward dipping but inverted.

* Fig.3.18.
Cross section along the line A-A' on encl.3 to show the present day disposition of the large quartzite horse. Note that the late extensional movement on the Moine thrust truncates the extension faults in Sheet IV.

Fig.3.19.
Cross section drawn along a line parallel to the transport direction of an aperity. Note that at the leading edge of an asperity the thrust cuts down section in transport direction.

Fig.3.20.
Diagrammatic cross section through the horses at Creag nam Broc to show the geometry of horse E. Horse E was either derived from an asperity whose original position wsa on the top of Sheet IV, or it was was plucked off of Sheet IV by movement on the Creag man Broc fault, which then moved the horse to its present position.

Fig.3.21.
Diagrams to illustrate the formation of horses from an anastomosing thrust zone-

(a) As a fracture deforms the rock a field of work hardening develops around it, and which strengthens the fracture. Continuing deformation will then shift the deformation to the weaker host rock, and a lens of the work hardened rock removed.

(b) A fault plane may become indurated by its own fault rock or vein. The deformation may then shift to the host rock. Small horses of fault rock may form.

(c) If a thrust is continually forming an irregular fracture, then the irregularities will be sheared off as horses.

Fig.3.22.
Sketch diagram to show the development of a horse 'stratigraphy' from an anastomosing thrust zone. As the thrust is always picking up asperities from the footwall, these horses will be stratigraphically older away from the thrust.

Fig.3.23.
A hangingwall sequence diagram viewed down the transport direction, to illustrate horse stacking at Creag nam Broc.

(a) The Loch Broom thrust has ramped into the Pipe Rock Member and accreted horses from the ramp.

(b) An asperity formed, which contains An-t-Sron Formation and Durness Formation, has become detached and accreted, and folded the older horses.

(c) The Loch Broom thrust then ramped up to the Eilean Dubh Member at the top of Sheet IV. Horse E was then accreted either as an asperity from the top of Sheet IV or, it was plucked off of Sheet IV by the Creag nam Broc fault, which then emplaced it to its present position.

(d) The accretion of horse E folded the other horses. This diagram shows the present geometry of the horses.

* NOW ADDED TO ENCLOSURE 3.

Fig.3.24.
Diagram of the classification of horses. Horses can be divided into three main groups, (i) horses derived from ramps, (ii) horses derived from asperities and (iii) horses derived from anastomosing thrust zones. Each group produces distinct geometries.

Fig.4.1.
Schematic diagram to show the geometry of Sheet IV prio to movement on the extension faults. Sheet IV comprises of Durness Formation and it is bounded by ramps. It is a large asperity.

Fig.4.2.
Figures 4.2a and 4.2b show foreland dipping duplexes, i.e. the faults dip towards the foreland, from Boyer & Elliott (1982): thes duplexes are derived from ramps and are always forward facing. However, fig.4.2c which shows Sheet IV which is also foreland dipping but hindward facing, i.e. the bedding dips towards the hinterland.

Fig.4.3.
Fig.4.3a- A Mohr circle diagram to show the stress conditions to show the effect of pore fluid pressure on the stress circle. The σ_3 point on the normal stress axis moves to the left to σ_3'.

Fig.4.3b- A Mohr circle diagram to show the stress conditions for hydraulic fracture. Hydraulic fracture occurs when $\sigma_3' = -T_o$.

Fig.4.4.
Fig.4.4a is a Mohr circle diagram to show the stress conditions for shear failure. Note that σ_3 is in the compressive field of the diagram to the right of the shear stress axis, and that $\Delta\sigma > 4T_o$. This stress condition will cause shear failure only, fig.4.4b.

Fig.4.5.
Fig.4.5a is a Mohr circle diagram to show the stress condition for hydraulic fracture, note that $\Delta\sigma < 4T_o$ and that σ_3 lies in the tension field. The largest circle is the maximum case for hydraulic fracture. Fig.4.5b shows the resulting structures.

Fig.4.6
Fig.4.6a is a Mohr circle diagram to show the stress condition for simultaneous shear failure and hydraulic fracture. Note that $\Delta\sigma > 4T_o$ but $< 5.7T_o$. Fig.4.6b shows the resulting structures, note that the veins are not displaced by the fault but form off of the fault, these are termed feather veins.

Fig.4.7.
Sketch block diagram to show the orientation of the principal effective stresses within Sheet IV.

Fig.4.8.
Graphs of λ against σ'. In fig.4.8a the overburden is 5km thick, note that λ =0.65-7 in order to cause failure, with σ_x as σ_3, but would need to rise to 0.7-0.8 to cause failure with $\sigma_y = \sigma_3$. In fig.4.8b the overburden is 10km thick, λ has to rise to 0.85 for failure with $\sigma_x = \sigma_3$ and 0.9 when $\sigma_y = \sigma_3$.

Fig.4.9.
Schematic graph to illustrate the stress history in Sheet IV during tectonic loading against time. With failure when $\sigma_x = \sigma_3$ and $\lambda =$ 0.65, σ_x will approach the value of p and σ_y will then become σ_3, if λ = 0.7-0.8 failure can occur and σ_y will also approach the value of p. After failure and with continued loading σ_x and σ_y will again start to increase. Further failure will occur when σ_x- p reaches a critical value, likewise for σ_y. The two lateral stresse will increase step wise until loading ceases.

Fig.4.10.
Block diagram (not to scale) to illustrate the structures which form with failure when λ =0.65 and $\sigma_x = \sigma_3$. The faults are the N.E.-S.W set in Sheet IV.

Fig.4.11.
Block diagram (not to scale) to show the style of structures which form with failure when $\sigma_y = \sigma_3$. The resulting N.W-S.E faults and concomittant veins crosscut the N.E.-S.W set of structures.

Fig.4.12.
Schematic block diagrams to show rotation of originally upright hydraulic fractures so that slip can occur along them.

Fig.4.13.
Diagrammatic graph to show the changes in the principal stresses with time during erosion. Note that at first the lateral stresses decrease more rapidly than p, and so when σ_x- p further slip is possible. The lateral stress will decrease more slowly than the overburden stress and hence a situation may arise when $\sigma_y > \sigma_z$. If $\sigma_y = 3\ \sigma_x$ then failure can occur producing strike slip faults. This has happened in SheetIV ,see section 2.5.1.3c, and the strike slip faults cut both sets of extension faults.

Fig.4.14.
Block diagram to show the geometry of the strike slip faults in Sheet IV in the Achall quarry.

Fig.4.15.
Diagram to show the geometry of the Creag nam Broc fault.

(a) cross section illustrating the extensional geometry of the Creag nam Broc fault, see plate.4.1.

(b&c) these diagrams show the expected geometry if the Creag nam Broc fault was a folded thrust as interpreted by Peach et al (1907) and Elliott & Johnson (1980).

Fig.5.1.-5.4.
Hangingwall sequence diagrams to ilustrate the structural evolution of the Moine thrust zone between Knockan an Loch Broom. see text for details

FIGURE CAPTIONS

Fig. 6.1 Map to show sample localities with corresponding Hbrel values. Note that there is no real trend of values, and that low values of Hbrel occur at Stoer as well as near to the thrust.

Fig. 6.2a A histogram of all Hbrel values, showing an obvious peak in the Hbrel range 140-180.

Fig. 6.2b Graph diagram to show range of Hbrel values for each sample population.

Fig. 6.3 Graph of Hbrel value against vertical distance below the thrust zone. Note the spread of values especially of the Stoer population. No marked thermal gradient is seen, however the wide spread may hide any gradient.

Fig. 6.4 A histogram of all b_o- spacing indexes. Note the widespread of values which is probably due to compositional effects, see text.

Fig. 6.5 Profiles of maximum temperatures developed by overthrusting 10 km thick thrust sheet for various parameter values. From Brewer (1981).

Fig. 6.6a Diagram to show simple thrust sheet emplacement model and configuration of thermal gradients before and immediately after thrusting.

Fig. 6.6b 'Sawtooth' thermal gradient produced immediately after thrusting.

Fig. 6.7a Graph to show change in temperature with time and depth with a thick thrust sheet. The initial rapid heat loss is clearly shown. Although illustrated for a 15 km thrust sheet, a 10 km thrust sheet will have similar profiles, from Oxburgh & Turcotte (1974).

Fig. 6.7b Graph to show temperture as a function of depth and time in the footwall of a thrust sheet 15 km thick. The initial heat flux into the footwall is obvious, from Oxburgh & Turcotte.

Fig. 6.8 Temperature as a function of time on the interface between the thrust sheet and the footwall. The temperatures on the 10 km thick thrust sheet profile are for the foreland metamorphism at the thrust, and the temperatures, for a 15 km thick thrust sheet, in the rocks beneath the Moine thrust at the Stack of Glencoul. See text for discussion.

Fig. 6.9 Sawtooth thermal profile for the 15 km thick Moine thrust sheet on top of the incipient Glencoul thrust sheet. Relaxation profiles are added with time taken for that set of re-equilibration taken from Fig. 6.10.

Fig. 6.10 Schematic diagram to show the relationship between the structural evolution of the thrust belt with the thermal events and their possible age relationships.

NOTE: The Key to the ornaments used on the text-figures is to be found on Enclosure 4 in the back-pocket of thesis.

LIST OF PLATES

PLate.2.14. View kooking N.N.W of the Creag nam Broc fault. Secimens shown in plate.2.15 were collected from immediately below the fault (A) on the plate.

Plate.2.15a-d.

(a) thin cataclasite zones cross-cut the dolomites of Sheet IV ca 10m below the Creag nam Broc fault.

(b) Note that calcite veins cross-cut cataclasite zones yet in plate 2.15a, the cataclasit zonez cross-cut the veins. This indicates that there is a cyclicity of cataclasis and tectonic veining, see section 2.9.

(c) The dolomite is cut by more cataclasite zones so that it is a microbreccia. This specimen was m below the fault.

(d) The dolomite at the fault is intensely cataclasised, note the increase in veining.

Plate.2.16. Extension faults in the Sheet IV at Knockan, note the listric form and the small horses (arrow).

Plate .4.1 Intense veining in the Durness Formation below the Glencoul thrust at Loch Glencoul.

ABSTRACT

The Moine thrust is an example of a foreland thrust belt. The thrusts propagated from the hinterland towards the foreland so that higher, older thrusts were deformed by movement on the younger, lower thrusts. The Moine thrust was later reactivated as a low angle extension fault and cut through the structures which had originally deformed it. Horses are an important structural component of the thrust zone, and were accreted to the thrust sheets by collapse of footwall ramps and asperities. The bedding geometry within the horses is classified, and allows an insight into the original geometry of the ramps and asperities.

The extension faults, tectonic veins, hydraulic fractures and stylolites in the lowest thrust sheet (Sheet IV) are considered to have formed as a result of gravitational loading by the overlying thrust sheets. Using a semi-quantitative model it is shown that high pore fluid pressures were needed to form the extensional structures. Differential stress was estimated from Sheet IV by using twin analysis in carbonates, and by a new method based on observations of modes of rock failure. The palaeostress estimates support a two stage model of thrust movement: firstly, a compressional stage, during the initiation and propagation of the thrusts, when differential stress was ca. 1300 bars; and secondly a loading event during translation of the thrust sheets, when differential stress was ca. 500 bars. It is suggested that the driving mechanism during this second stage was gravity spreading. Fault rocks show that the dominant deformation mechanism was cataclasis along the thrust planes.

Illite crystallinity studies show a widespread heating event in the foreland which is interpreted as a thermal response to thrust sheet emplacement. Temperatures reached 275°C approximately 20 Ma after the main thrusting event. Three stages of movement are proposed at 440-430 Ma, ca 425 Ma, and 425-414 Ma. This is based on the relationships between syn-thrusting intrusions and thrust planes combined with radiometric dates from the Moine sediments.

ACKNOWLEDGEMENTS

I am greatly indebted to my supervisor, Dr M.R.W. Johnson for his encouragement and assistance. I thank Professors G.Y. Craig and Sir Frederick Stewart for letting me freely use the resources of the geology department at Edinburgh. I am especially grateful to Professor Craig and Dr Johnson for their labours on my behalf during an early financial crisis, without them this thesis would have remained uncompleted.

I would like to thank the following for much useful discussion:- Mr G. Aktas (Edinburgh), Dr J.F. Boyle (Bergen), Professor M.P. Coward (Imperial College), Dr R.F. Cheeney (Edinburgh), Dr A.B. Hayward (B.P. Exploration, London), Dr K.R. Gill (Edinburgh), Dr S. Kelly (Sheffield), Mr Lin Maobing (Chengdu, China), Mr A.R. Martin (Edinburgh), Dr B.A. Martin (B.P. Exploration, Aberdeen), Dr G. Oliver (St Andrews), Mr D.R.M. Pattison (Edinburgh), Dr J. Ridley (ETH, Zurich), Dr J. Warburton (B.P. Exploration, Madrid).

I would like to thank Drs N.J. Price (Imperial College), D. Powell (Bedford College) and A.D. Gibbs (Britoil) for initiating my interest in structural geology.

I am also very grateful to Mr & Mrs Mitchell of Ardmair Bay near Ullapool for making my fieldwork that much easier and more enjoyable.

For technical services at Edinburgh I would like to thank Mr C. Chaplin, Mrs F. Tullis and Mrs D. Baty.

Last but not least, I thank Denise McGuire for undertaking the typing with much patience.

The work was carried out under the tenure of a Natural Environment Research Council Grant which is gratefully acknowledged.

CHAPTER 1. INTRODUCTION

The Moine thrust zone marks the northwest boundary of the Caledonian orogenic belt in Great Britain, fig. 1.1, and extends 190 km from Eriboll in the north to Sleat on Skye in the south. The first detailed account of the thrust zone was given by Peach et al(1907) after their geological survey of the NW Highlands in the last two decades of the nineteenth century. Although subsequent work in NW Scotland has included detailed sections of the thrust zone, Bailey (1935), Christie (1960, 1963), Johnson (1960, 1961), Soper & Wilkinson (1975), more attention was paid to the structure, metamorphism and stratigraphy of the Moine in the interior of the Caledonian orogen, Johnstone et al (1969), Johnstone (1975), Johnson (1975), Powell (1974), Ramsay (1963). It has been only recently in the light of advances in the understanding of the geometric evolution of thrust belts, pioneered by Dahlstrom (1970) and Elliott (1976a), that great attention has been given to the structural evolution of the Moine thrust zone, Coward (1980, 1982, 1983), Elliott & Johnson (1978, 1981)

The aim of this research was to study the portion of the Moine thrust zone between Knockan, which is situated at the southern edge of the Assynt culmination, in the north, and Loch Broom near Ullapool in the south, fig. 1.1. This portion of the thrust zone varies in width from 0 to 1.8 km where small culminations at Achall and Langwell are developed, fig. 1.1. Despite the deceptively simple appearance of the thrust zone in this portion, detailed study revealed a complex structural evolution. Chapter 2 first describes the geometry and emplacement history of the thrust zone, and then deals with the fault rock products of the thrust planes. In this chapter it is put forward that the Moine thrust was firstly deformed by structures which formed above lower thrusts, i.e. by piggy-back thrusting but it then truncated these structures when it acted as a low angle extension fault. Chapter 3 deals with the internal deformation of the thrusts, and then there follows a description and discussion of horses, which are a major structural component in this section of the thrust zone.

The occurrence of extensive normal faulting, veining and stylolite formation in Sheet IV is explained in Chapter 4, by proposing that this extensional deformation is a result of gravitational loading by the overlying thrust sheets. This semi-quantitative model shows that pore fluid pressures must have been high in Sheet IV and also leads to a new method of estimating differential stress. These three chapters are then summarised in Chapter 5. In Chapter 6, the thermal effects of thrusting are described and discussed.

1.1 STRATIGRAPHY

The stratigraphic units of the area are summarised in encl 4.

1.1.2 The Lewisian Gneiss Complex

The Lewisian gneiss was first described in detail by Peach et al. (1907), who recognised that the Lewisian complex could be chronologically divided into two main divisions. This was confirmed by Sutton & Watson (1951) who recognised an early Scourian episode separated in time by a period of dyke intrusion from the Laxfordian event. The Scourian gneiss consists of banded gneisses ranging from ultramafic to acid with some metasediments. These gneisses have been radiometrically dated and ages range from 2900-2600 Ma, Giletti et al. (1961), Moorbath et al. (1969). The Scourian gneisses are intruded by a basic dyke swarm termed the Scourie dykes and these dykes post date all Scourian tectonic and metamorphic features. Dates of 2400-2200 Ma have been obtained from the dykes, Evans & Tarney (1964), Moorbath et al. (1969). The Laxfordian events post-date and deform both the Scourian gneisses and the Scourie dykes, Sutton & Watson (1951), Watson (1983). The deformation and metamorphism was accompanied by the intrusion of granitic sheets and pegmatites which have been dated at 1700-1750 Ma, Lyon et al. (1973), Watson (1983).

1.1.2 The "Torridonian" Sediments.

The "Torridonian" is the name given to a thick sequence, mainly of arkosic red beds which rest with marked unconformity upon the Lewisian. The "Torridonian" sediments were first described by Peach et al. (1907). However, subsequent studies based on field mapping and radiometric dating have shown that the "Torridonian" sediments can be divided into at least two groups; the older Stoer Group separated by an angular unconformity from the Torridon Group, Stewart (1969).

The Stoer Group consists of over 2 km thickness of red arkosic sandstones with locally derived breccias and conglomerates; local mudstones and a volcanic mudflow also occur. Dating of nannofossils from the mudstones suggests a Middle Riphean age, Downie (1962), which agrees with the recalculated Rb/Sr age of 968 Ma: Smith et al. (1983). The Stoer Group was deposited in fault-controlled basins.

The Torridon Group is much more extensive and oversteps the Stoer Group onto the Lewisian. Red and purple arkosic sandstones are predominant in the group, but grey and red shales do occur. Nannofossils from shales of the Torridon Group give an Upper Riphean age which is confirmed by a recalculated Rb/Sr date of ~777 Ma. Smith et al. (1983). The Torridon Group was deposited in a large alluvial fan, shales in the sequence may record a marine influence.

Prior to the deposition of the Cambro-Ordovician sequence the "Torridonian" sediments were folded into large warps which trend N-S, and have a wavelength of approximately 50 km. A large syncline in the west of the present day outcrop defines the "foreland basin", Soper & Barber (1979), Elliott & Johnson (1980). A smaller Assynt basin lay to the east and is only exposed in the thrust zone. Peneplanation of these large structures occurred before the deposition of the Cambro-Ordovician which oversteps from the Torridon Group onto the Lewisian to produce the renowned double unconformity.

1.1.3 The Cambro-Ordovician Sediments.

The Cambrian and Lower Ordovician strata are shown in encl 4. The stratigraphy has been described in detail firstly by Peach et al. (1907) and more recently by Swett (1969). The latter divided the Cambro-Ordovician sequence into three major formations; the Eriboll Formation, the An-t-Sron Formation and the Durness Formation, fig. 1.2.

The Eriboll Formation consists of two members; the Basal Quartzite Member and the Pipe Rock Member. The former comprises of quartz-arenites, sometimes with a conglomerate at its base and exhibits tabular cross sets. These Basal Quartzites pass up conformably into the Pipe Rock Member which again comprises of mature quartz arenites which become more thinly bedded towards the top of the member. However, the Pipe Rock Member is notable for vertical bioturbation structures (pipes), which are burrows of the Skolithus and Monocraterion, Hallam & Swett (1966). Salterella has also been found which confirms that at least the Pipe Rock Member has a Lower Cambrian age. The Eriboll Formation was deposited in a shallow sub-tidal or inter-tidal environment, Swett et al. (1971).

The An-t-Sron Formation also consists of two members: the Fucoid Beds and the Salterella Grit. The Fucoid Beds are dolomitic siltstones with sandstones, shales and carbonates. The presence of the trilobite Ollenellus confirms a Lower Cambrian age, Cowie (1974). Flattened worm casts, Planolites, were originally mistaken for fucoid markings - hence the name of the member. The Salterella Grit (originally called Serpulite Grit) consists of mature, cross bedded quartzites separated by thin shales. Olenellid trilobites have been found, Cowie (1974). The Fucoid Beds represent a short marine transgression from the tidal environment at the top of the Eriboll Formation. The Salterella Grit represents a regression which did not persist as it was soon covered by carbonates.

A thick sequence of carbonates comprises the Durness Formation which has been divided into seven members. Only the first three members are found in the study area and Assynt, and they are described here. The remaining four members; the Sangamore, Balnakiel, Croisaphuill and Durine members, only occur at Durness. In the present study area the latter four members have been removed by thrusting.

The lowest member, the Ghrudaidh Member, consists of a sequence of dark grey and white, massive crystalline dolomites. Occasionally chert nodule horizons and oolitic horizons occur. Salterella and Planolites have been reported, Walton (1983). This member is followed conformably by the Eilean Dubh Member which is more flaggy and well-bedded. Oolitic horizons occur at various levels in the member, as do chert nodule horizons. The overlying Sailmhor Member consists of massive dolomites and these often have a mottled appearance, due to diagenetic changes. The member is marked by the occurrence of extensive chert layers and nodules. All three members have been extensively affected by diagenetic changes consisting of a complex sequence of dolomitisation, silification and calcitisation, Swett (1969).

1.1.4 The Moine Metasediments.

The metasediments only occur to the east of the Moine thrust zone. They rest with unconformity on Lewisian gneiss which occurs as large "inliers" now regarded as either thrust slices or isoclinal fold cores. The metasediments are divided into three divisions; the Morar, Glenfinnan and Loch Eil divisions.

The Morar Division consists of alternating psammites and pelites; these display rare sedimentary structures such as cross-beddings, slump structures, and shrinkage cracks, Johnstone et al. (1969). The Morar Division has a slide contact with the Glenfinnan Division which is made up of thinly bedded psammites, quartzites and pelites which contain sheets and lenses of garnet-amphibolite which may be of sedimentary origin. The Loch Eil Division occurs to the east of the Glenfinnan Division and is composed of psammitic schist with some pelites.

The age of the metasediments and the relationships between the divisions is still a subject of research. However dates of 1240±96 Ma for the Morar Division and 1050±46 Ma for the Glenfinnan Division have recently been obtained, Brook et al. (1976, 1977). The metasediments cannot be younger than 815±30 - 730±20 Ma which are dates obtained from pegmatites which intrude the them, van Breemen et al. (1974). These dates which indicate a Precambrian metamorphic event only occur in the SW Moines. It has been argued that the metasediments in Sutherland have not undergone any Precambrian deformation, and therefore may be younger than the SW Moines, Soper & Wilkinson (1975).

The Moine metasediments have suffered several phases of deformation, two of the earliest of which have been assigned to the Precambrian, Powell (1974). In the Precambrian they were firstly deformed by major and minor isoclinal folds, accompanied by interleaving of Lewisian with Moine metasediments either as thrust slices or cores of folds, and secondly by further folding to form major tight folds with an intense axial planar cleavage. Concurrent with the first phase of deformation the metasediments suffered regional high grade metamorphism and migmatisation. A major thrust occurs within the Moine outcrop; it has displaced Lewisian with its cover of the Glenfinnan division onto the uninverted Morar Division. This thrust has been traced for 180 km along strike and is known as the Sgurr Beag slide, Sutton & Watson (1962), Tanner et al. (1970), Rathbone & Harris (1979) and Baird (1982).The Sgurr Beag slide is considered to have been active prior to movement on the Moine thrust. Elliott & Johnson (1980), Soper & Barber (1982). Even where the Lewisian is absent the Glenfinnan Division is in tectonic contact with the Morar Division. The slide is folded by large Caledonian folds, which become more intense towards the interior of the orogen.

The structures which formed in the Moine thrust zone, overprint the polyphase Moine structures, Barber & May (1976) and are outlined in section 2.2.

1.2 THRUST TECTONICS AND CURRENT RESEARCH IN THE MOINE THRUST ZONE

Recent research in the Moine thrust zone has applied the principles and empirical rules of thrust geometry that were first established in the Canadian Rockies, Dahlstrom (1970), and have since been applied to the Rockies of the USA, Royse et al. (1975) and the Appalachians, Elliott (1976a), Hatcher (1981), Boyer & Elliott (1982). These rules are based on the simple observation that thrusts follow easy slip horizons as flats and cut across competent units as ramps, always cutting up section in the direction of transport (however a thrust may cut up or down section along strike), thus producing a staircase section. Movement of the thrust sheet over the ramps produces folds in the hangingwall, which will deform any higher thrust. These observations have been used to establish that thrusts propagate from the hinterland towards the foreland; thus the structurally higher thrusts are folded as a result of movement over ramps by lower thrust sheets, fig. 1.3. Collapse of footwall ramps leads to the development of duplex systems, fig. 1.4.,Elliott & Johnson (1980), Boyer & Elliott (1982).

Using these simple rules and constructing balanced cross sections c.f. Dahlstrom (1969), Elliott & Johnson (1980) reinterpreted the Moine thrust zone in the area around the Assynt culmination. They argued that the Moine thrust zone was a thin skinned foreland thrust belt, and that the Moine thrust formed first and became folded by the movement on the lower Glencoul and Ben More thrust sheets. They also showed that the duplex systems (the schuppen or imbricate zones of Peach et al. (1907)) were formed by ramp collapse. Boyer & Elliott (1982) show that duplexes form by progressive collapse of ramps, i.e. the individual thrusts in a duplex propagate sequentially towards the foreland, fig. 1.4. Coward (1980) demonstrated comparable structures and structural histories at Eriboll in Sutherland. Further detailed mapping showed that in several places thrusts "disobey the rules" and cut down section in the transport direction and across earlier structures. This is especially notable on the Glencoul thrust in Assynt where Coward (1982, 1983) demonstated the existence of "surge zones" which are large "landslide type" sheets, fig. 1.5 from Coward (1982). Further, the Moine thrust itself shows evidence of late

extensional movement, Coward (1983), see 2.2.1., and cuts through earlier structures which originally deformed it. Coward (1983) suggests that these later movements are a result of gravity spreading, Price (1973), Chapple (1976), Elliott (1976a), caused by a thickened and uplifted crust in the Highlands which may have been due to the intrusion of late Caledonian granitic batholiths. An opposite viewpoint is taken by Soper & Barber (1982) who argue that the Moine thrust zone is a thick-skinned thrust belt similar to the Wind River thrusts in the Rocky Mountains, U.S.A. Brewer et al. (1981). Soper & Barber (op cit) suggest that the Moine thrust steepens about 30 km behind the present day thrust front so that the detachment horizon is in the lower crust giving the thrust a sigmoidal form. They also suggest that the Moine thrust and slides in the Moine metasediments such as the Sgurr Beag slide and the Meadie and Navier slides join at a roof thrust which has since been eroded away. The steep ramp would require a horizontal compression in order to overcome gravity at the ramp, Wiltschko (1979b); this is contradictory to the thin skinned model which suggests that gravity spreading is the driving mechanism. The occurrence of differential slip within the thrust zone may indicate that the gravitational potential varies along the length of the thrust sheet, Coward (1983); this could be due to an increase in the surface slope and an increase in erosion caused by thckening and uplift at the rear of the thrust sheet, hence aiding forward motion of the thrust sheet, Elliott (1976a). The problem of the driving mechanism and the thin-skinned versus thick-skinned models are still subjects of debate. However, the reactivation of the Moine thrust as a low angle extension fault described in 2.2.1. is consistent with the gravity spreading and the thin-skinned model.

Elliott & Johnson (1980) were the first to apply the thrust rules established in the Rockies to the Moine thrust zone. These authors used balanced cross sections across the Assynt culmination to show that the thrusts had propagated from the hinterland towards the foreland, and that movement by structurally lower, younger thrusts over footwall ramps caused deformation within the thrust sheets and folded the structurally higher, older thrust planes. Further mapping by Coward and co-workers at Leeds University in Eriboll, Assynt and the southern part of the Moine thrust zone, Coward (1980, 1982, 1983), Butler (1982b), Fischer & Coward (1982) showed that although the interpretation of Elliott & Johnson (op cit) was fundamentally correct, there are areas where the thrusts contravene the 'thrust rules' and that locally, downcutting extensional geometries occur. This is especially notable in the Assynt area where Coward (1982) demonstrated large scale, landslide type bodies which were termed 'surge zones'. These workers also showed that in many places the Moine thrust itself has an extensional geometry, and was the last thrust to be active, Coward (1982, 1983).

Both Peach et al. (1907) and Elliott & Johnson (1980) have studied the area covered by this thesis. The author's own new mapping has changed little of the lithological relationships in the area, apart from detail complex faulting structures in the Achall valley. However, the present work differs markedly in interpretation of some of the structures seen in the thrust zone, from both Peach et al. (1907) and Elliott & Johnson (1980), and shows that extensional geometries are important components of the thrust zone.

The areas covered by this thesis were chosen for study in order to achieve the following:

i) To understand the structure of the Achall culmination in the light of the recent advances, in the understanding of thrust tectonics

ii) To elucidate the structure at the southern termination of the Assynt culmination at Knockan

iii) To expand and continue the pilot study by Drs G. Oliver and M. Johnson in assessing the thermal effects of thrusting, by using illite crystallinity studies.

The small size of the areas and their relatively good exposure would allow a detailed understanding of the structural geometry, and allow examination of localities where cross cutting relationships of faults appeared to disagree with thrusting rules, mentioned earlier (see 1.2.).

Access was not allowed in the Langwell-Strath Kanaird area so new mapping was restricted to the Achall culmination - Loch Broom and the Knockan areas (see page 11). Mapping of theses areas revealed the importance of extensional faulting and established the late movement on the Moine thrust, and confirmed Cowards (1983) hypothesis that the late movement was extensional. The mapping differs from that of Peach et al. only in detail, and from Elliott & Johnson (1980) in the interpretation of the Achall culmination and the Knockan areas. The interpretation of the extension faults led to the new model of tectonic loading described in Chapter 4.

Fig. 1.1

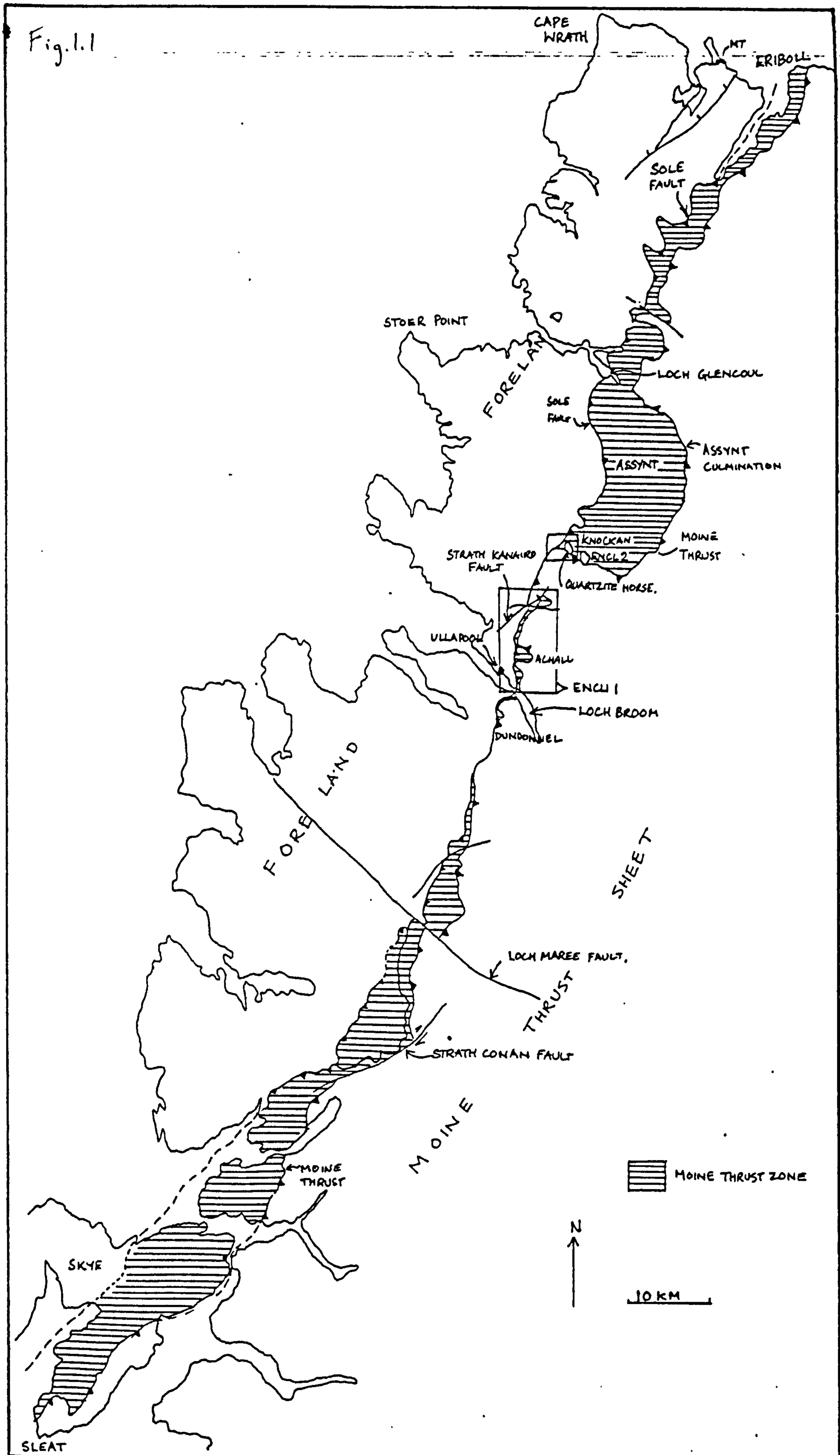
CAPE WRATH
MT ERIBOLL
SOLE FAULT
STOER POINT
FORELAND
LOCH GLENCOUL
SOLS FAULT
ASSYNT
ASSYNT CULMINATION
KNOCKAN
MOINE THRUST
STRATH KANAIRD FAULT
ENCL 2
QUARTZITE HORSE.
ULLAPOOL
ACHALL
ENCL 1
LOCH BROOM
DUNDONNEL
FORELAND
SHEET
LOCH MAREE FAULT.
THRUST
STRATH CONAN FAULT
MOINE
MOINE THRUST
SKYE
SLEAT
MOINE THRUST ZONE
N
10 KM

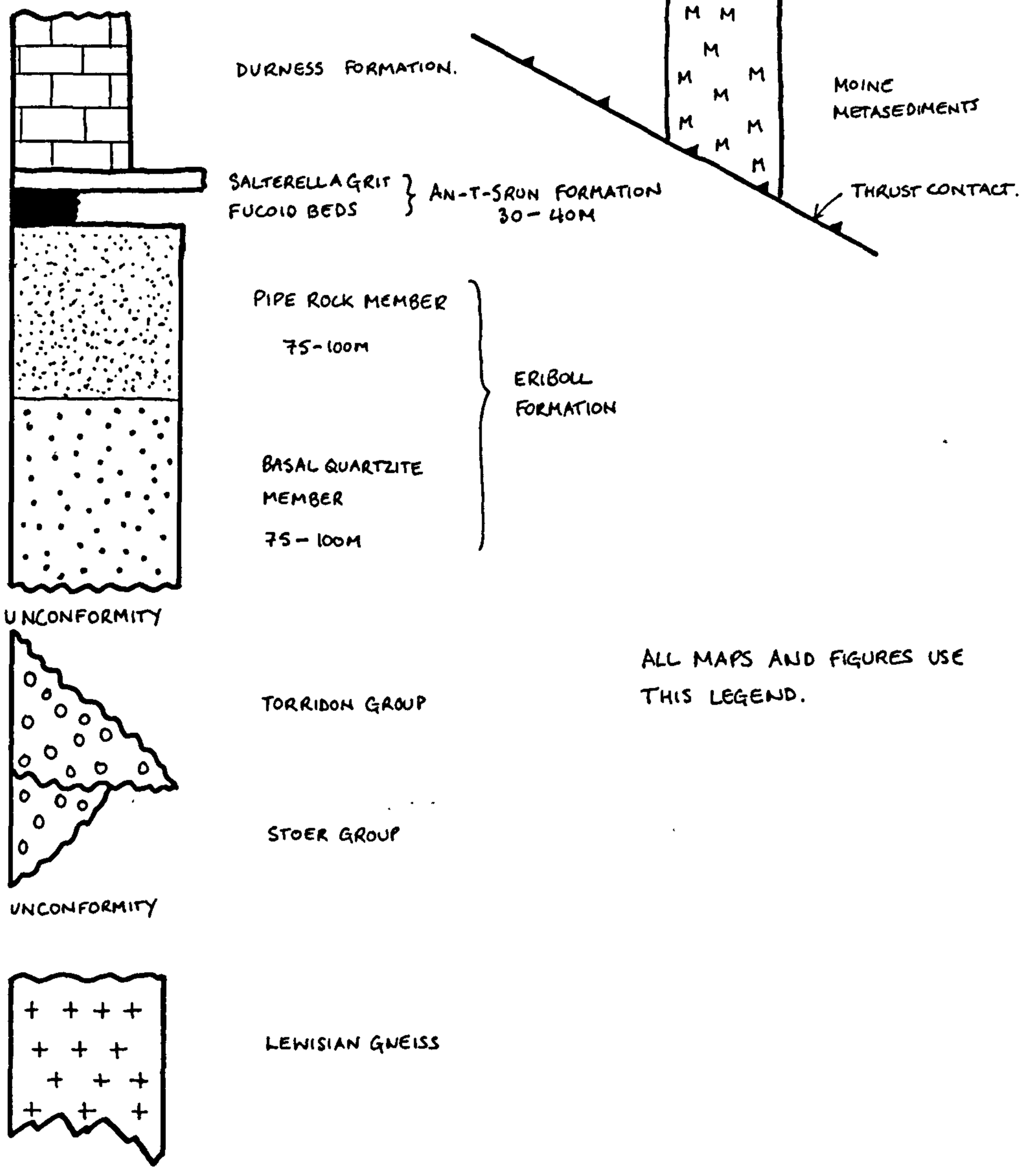

Fig.1.2.

The stratigraphic succession in the foreland and the Moine thrust zone.

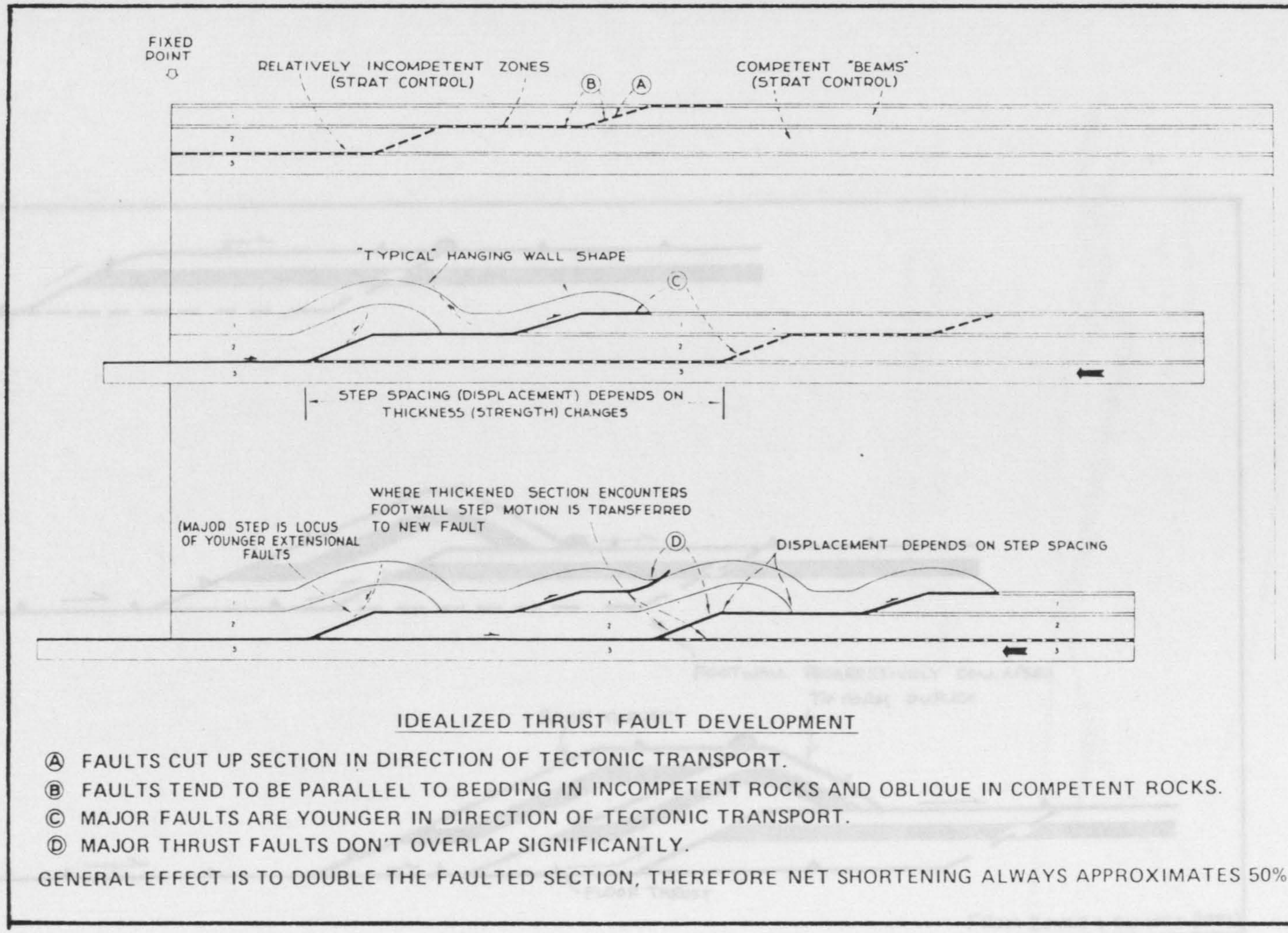

Fig.1.3.

Diagram to illustrate the concept of 'piggy-back' thrusting. From Royse et al. (1975)

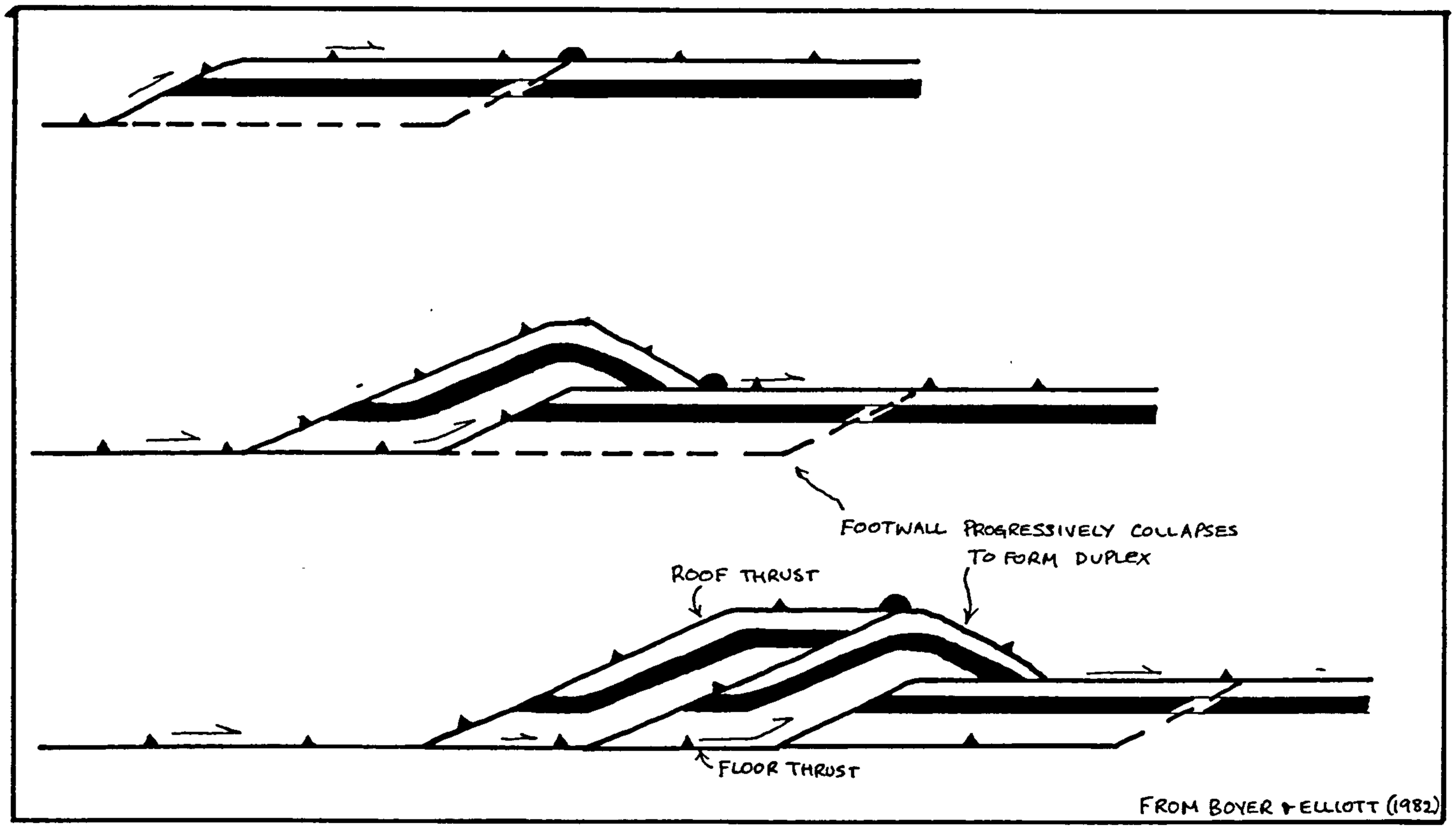

Fig.1.4.

Diagram to show the progressive collapse of a footwall ramp to produce a duplex, from Boyer & Elliott (1982).

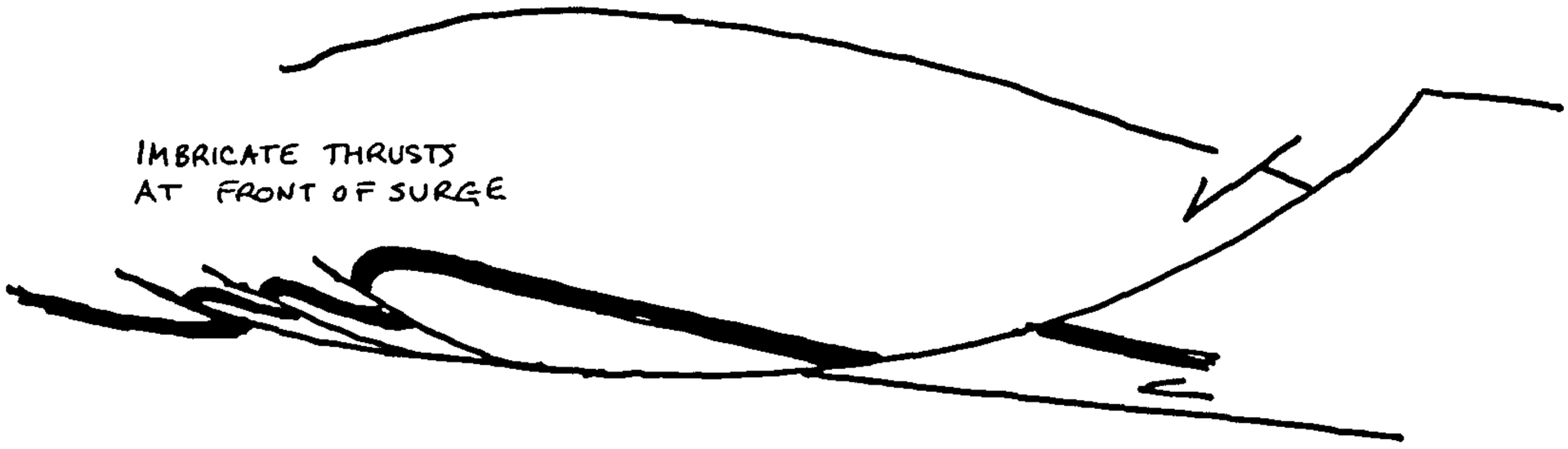

FIG 1.5 LANDSLIDE-LIKE SURGE ZONE WHICH MOVES UNDER ITS OWN BODY WEIGHT.

CHAPTER TWO

THE STRUCTURAL GEOMETRY OF THE MOINE THRUST ZONE BETWEEN LOCH BROOM AND THE ASSYNT CULMINATION.

2.1 Introduction

The section of the Moine thrust zone studied in this chapter lies between the villages of Elphin-Knockan in the north to Loch Broom in the south. Knockan is situated at the southern extremity of the Assynt culmination where the thrust zone changes from a thick wide zone involving a number of thrust sheets, to a single thrust plane, the Moine thrust. However, in southern part of the section, from Langwell [GR.174023] to Loch Broom, the thrust zone again becomes more complex, with thin thrust sheets developed beneath the main Moine thrust. These thin thrust sheets have produced a culmination between Langwell and Glen Achall 1-2 km west of Loch Achall, and at Ullapool, see encl 1. Within the culminations small tectonic slices termed horses are well developed, Elliott & Johnson (1980), Butler (1982a), Boyer & Elliott (1982). These are fully described and explained in 3.2.

The stratigraphy involved in this section of the Moine thrust zone is the same as described in 1.1

The most structurally complex areas, covering approximately half of the section studied, were mapped by the author. These areas were at the northern part of the section in the vicinity of Knockan Crag and Elphin village, see encl 2, and in the southern part of the section from Alt-an-Strathan valley south to Loch Broom at Corry Point [GR.146919]. These two areas were mapped at a scale of 1:10,000 or 6 inches to 1 mile, during the autumn of 1980 and the early summer of 1981. Sheet IV in Glen Achall was mapped on a scale of 1:5,000 during the summer of 1981, and spring 1982. Clean copies of the original survey maps were used to construct the map, enclosure 1, in areas where the author did not map due to access problems. This includes all of enclosure 1 north of Alt-an-strathan valley.

The thrust zone is cross-cut by a series of normal faults which trend N.E.-S.W., some of which are fairly large, e.g. the Strath Kanaird Fault and its splays described by Peach et al. (1907), encl. 1. These may be of possible Mesozoic age perhaps related to early openings of the Atlantic Ocean, Roberts (1974), Kent (1975). Many smaller faults cross-cut the thrust zone approximately perpendicular to its strike, i.e. N.W-S.E., and have a different orientation to the large Strath Kanaird-type faults. Open upright warps with axes plunging south east are also developed folding the thrust planes, their origin is unclear.

2.1.1. Nomenclature.

Peach et al. (1907) used names to identify individual thrust planes within the Moine thrust zone and correlated them with the thrust planes within the Assynt culmination which have the same position relative to the Moine thrust plane. For example, the thrust plane carrying a thrust sheet of Lewisian gneiss in the Ullapool area, was named the Ben More thrust, but where this thrust crossed Loch Broom and outcrops in Strath Beag at Dundonnell, it was named the Kinlochewe thrust. This is misleading as it wrongly assumes a continuity of the thrust sheets beneath the Moine thrust. To avoid confusion Elliott & Johnson (1980) used a numbering system where the highest thrust plane was numbered T_I (i.e. the Moine thrust), with its thrust sheet, Sheet I. Any thrust sheets that were present beneath T_I were numbered T_{II}, Sheet II, etc. This system works well but would need to be applied over the whole Moine thrust zone to be useful. As names are still used over the rest of the thrust zone outside the Ullapool area, I have renamed the thrusts in order to avoid confusion. T_I remains as the Moine thrust, however T_{II} of Elliott & Johnson (1980), the Ben More/Kinlochewe thrust of Peach et al. (1907) is renamed the Loch Broom thrust, as Loch Broom crosses the thrust. T_{III} of Elliott & Johnson (1980) is named the Ullapool thrust, as it outcrops entirely within the Ullapool area. The major tectonic units are shown on inset on Encl. 1.

The lowest fault plane within the thrust zone is commonly called the 'Sole thrust', Peach et al. (1907), Elliott & Johnson (1980), Coward (1980, 1982). However, in this section of the thrust zone the 'Sole thrust' has either no stratigraphic separation across it, or in a few localities, i.e. Glen Achall [GR 147953], it displaces younger stratigraphic units onto older. By definition, a thrust fault must place older rocks onto younger unless the rocks involved have been previously deformed, Dahlstrom (1971), Elliott & Johnson (1980). As the stratigraphic units above the 'Sole thrust' show no major inversions, and the deformation displayed is syn-thrusting, then the 'Sole thrust' is not technically a thrust, but a décollement plane with extensional displacement. Hereafter the 'Sole thrust' is referred to as the Sole fault. The Sole fault is discontinuous in this section, see encl. 1, and is only developed beneath culminations.

2.2 STRUCTURAL GEOMETRY: THE MOINE THRUST.

The Moine thrust is continuous along the complete length of the section between Knockan and Loch Broom. Upon it rests the Moine thrust sheet commonly called the Moine nappe, which consists of the Moine metasediments. These metasediments pass downwards into mylonites which lie immediately above the Moine thrust. In the section studied the mylonites are ~50 m thick, and they are excellently exposed at Drumrunie [GR 170057] and Knockan Crag [GR 189093]. The mylonites are deformed by at least four phases of deformation:-

D1- this deformation produced a mylonitic fabric which is occasionally peserved in small tectonic augen, which also show rare intrafolial, isoclinal F1 folds. These folds plunge to around 104°. A prominent lineation is marked on foliation surfaces and this also plunges to around 104°; it is a mineral lineation defined by phyllosilicates and quartz.

D2- is the main mylonitisation phase; small isoclines which are intrafolial to the D2 foliation fold the D1 foliaation and the L1 lineation. The folds plunge gently both to the S.E. and the N.E. and are true sheath folds which have been described from many ductile shear zones, Quinquis et al. (1980), Berthé & Brun (1980). These folds have an axial planar foliation that is the dominant mylonitic foliation.This dips consistently between 10°-15° to the S.E.

D3-is marked by tight to open asymmetric folds, which verge to the N.W. and plunge gently both to the N.E. and S.W. There is no axial planar foliation or lineation associated with the folds.

D4-is marked by two sets of kink folds:-

i) a compressional set of kinks, which plunges down the dip of thrust planes, i.e. gently to the S.E. ii) an extensional set which plunges along the thrust strike both N.E. and S.W. and verge to the NW and whose axial planes dip steeply SE.

To the south of Knockan Crag, see encl 2, the Moine thrust has a glide plane usually at the top of the Saltarella Grit Member of the An-t-Sron Formation, but occasionally the thrust ramps along strike to glide at the top of the Fucoid Bed Member or within the Durness Formation. Where the thrust ramps up into the Durness Formation small culminations are developed, examples of which can be seen near to Drumrunie Lodge [GR 163042]. These small culminations are often only between 10-20 m in thickness and of the order of 100 m strike length. The thrust plane dips at 8-12° to the S.E. along the section between Knockan Crag and Langwell. From Langwell south to Loch Broom the thrust zone becomes more complex with the development of the Loch Broom thrust sheet and the Ullapool thrust sheet. It can be demonstrated that the Loch Broom thrust has a displacement of at least 25 km, Elliott & Johnson (1980), see 2.3.2. The Loch Broom thrust carried the Moine thrust piggy back style to its present position, although later movement on the Moine hrust must have occurred as it cross-cuts the Loch Broom hrust in several places, see 2.2.1.

2.2.1. Late movement on the Moine thrust: The case for an extensional Moine 'thrust'

The Moine thrust has certainly cut through structures which deformed the original thrust. The most obvious example occurs on the north limb of the Achall culmination, see encl 3. Here the Loch Broom thrust has ramped up into the Durness Formation, folded the overlying Moine thrust and produced the Achall culmination. However at a point approx 200 m N.E. of Creag nam Broc [GR 155950] the Moine thrust clearly truncates the Loch Broom thrust to rest directly upon the Durness Formation of Sheet IV. Moreover, it also truncates the Creag nam Broc fault, which is an extension fault developed during the evolution of Sheet IV, the lowest thrust sheet, and detachment of the Sole fault. This observation leads to the obvious conclusion that the Moine thrust has moved at a later date than the Sole fault.

From studying the hangingwall stratigraphy of the Loch Broom thrust sheet and with the use of a stratigraphic separation diagram for the Loch Broom thrust, it can be shown that prior to much movement the Loch Broom thrust had an irregular section with large lateral ramps, fig 2.1, see 2.3. With movement on the Loch Broom thrust the stratigraphic units within the Loch Broom thrust sheet and the Moine thrust were folded into a broad synform, the Loch na Maoile synform, encl 1. However, the Moine thrust is not folded by the Loch na Maoile synform as would be expected from piggy back thrusting. Instead the Moine thrust appears to cut through the fold. This can be explained by invoking later movement on the Moine thrust which cut through the folds which originally deformed it. Figure 2.2 is a hangingwall sequence diagram which demonstrates the structural history of movement on the thrust planes.

In figure 2.2 it is shown that prior to any movement on the Loch Broom thrust, the Moine thrust had ramped laterally from the Lewsian Gneiss up to the Eilean Dubh Member, and the Loch Broom thrust was initiated along an irregular thrust plane. With movement on the Loch Broom thrust, the hangingwall and the Moine thrust were folded. Later movement upon the Moine thrust cut through and truncated the folds, see fig. 2.2a,b,c.

There are several lines of evidence which support this interpretation, and lead to interesting revelations about the Moine thrust itself:-

i) At Loch na Maoile approx 2 km E. of Strath Kanaird, there are two large horses of Durness Formation which have been accreted onto the Moine thrust, see encl. 1. These two horses rest on a 'thrust' which has a stratigraphic separation so that younger Durness Formation has been placed onto older Fucoid Beds and Pipe Rock. This suggests the 'thrusts' have cut down through the stratigraphy in the direction of transport, indeed it indicates that the thrusts beneath the two horses of Durness Formation are in fact low angle extension faults.

ii) The Loch Broom thrust sheet has been internally deformed to produce the Loch na Maoile synform but the structure is very open and does not affect the way up of the stratigraphic units. The presence of the Durness Formation horses indicates that the Moine thrust has cut down section, from the Durness Formation to the Pipe Rock and Fucoid Beds within the Loch Broom thrust sheet. Furthermore, study of encl. 1, in the vicinity of Langwell, shows that the Moine thrust has cut down section from the Lewisian Gneiss in the Loch Broom thrust sheet, truncated the Loch Broom thrust, onto the Durness Formation in a Sheet IV horse and then down onto the foreland at the top of the An-t-Sron Formation, see fig 2.3.

iii) At Knockan Crag, encl.2, the Moine thrust plane is the youngest structure as it cross-cuts extension faults associated with the Sole fault. See section 2.6.

iv) Perhaps the most convincing evidence is the geometry of the Moine thrust plane with respect to its footwall. The foreland Cambro-Ordovician succession has a mean dip of ~18° to the S.E. see encl 1. However, the Moine thrust plane only dips at between 8°-12°, and has a shallower dip than its footwall. In many more recent thrust belts, foreland stratigraphic units commonly dip only

2°-5° towards the hinterland, Dahlstrom (1970), Royse et al. (1975). If it is assumed that the foreland units had a similar dip during the thrusting, then it can be seen that the Moine thrust may be either horizontal,or dipping gently towards the foreland. Thrusts which climb up section must have a dip which is greater than that of the footwall. This is obviously not so with Moine thrust, which consistently cuts down section in the direction of tectonic transport.

The above evidence indicates that the Moine thrust at the present depth of erosion disobeys the basic rules for thrusting of Dahlstrom (1970) and Elliott (1976a), and consistently cuts down section in the direction of transport. The geometry indicates that the latest movements on the Moine thrust were on a low angle extension fault and suggests that either gravity sliding or gravity spreading was the driving mechanism behind movement and that the older Moine thrust was superseded by the later extensional fault plane, and is now nowhere exposed. Comparable extensional geometries have been described in the Moine thrust zone in the Kinlochewe area,Coward (1982).

The thickness of the Moine thrust sheet is unknown, but the Moine metasediments with inliers of deformed Lewisian Gneiss are continuously exposed up to 50 km east of the thrust zone, on the Ross-shire coast, Harris et al (1979). The thrust sheet has been thickened by the Sgurr Beag slide prior to movement on the Moine thrust, Elliott & Johnson (1980), and recent work has shown that more slides and thrusts such as the Navier and Meadie slides exist, Mendum (1978).

Displacement on the Moine thrust plane along this section of the thrust is uncertain: it must be greater than 25 km as Eliott & Johnson (1980) showed that Loch Broom thrust has a displacement of 25 km (see 2.3.2). Also the displacement on the later,extensional Moine thrust cannot be estimated. However movement on the extensional Moine 'thrust' may have been relatively small because although the thrust has cut through the Achall and Langwell antiforms and the Loch na Maoile synform,the metasediments of the Moine thrust sheet are folded into two corresponding antiforms with a broad synform between (encl 1). If displacement on the extensional Moine thrust has been large then it would be reasonable to expect that the geometries in the hangingwall would be different than those of the footwall.

2.3 THE LOCH BROOM THRUST SHEET

The Loch Broom thrust sheet lies upon the Loch Broom thrust, which outcrops from Strath Kanaird to Loch Broom then onto Dundonnell in Strath Beag. Only the section of the thrust sheet between Strath Kanaird and Loch Broom concerns us here. The stratigraphy involved in the Loch Broom thrust sheet is the same as that of the undisturbed foreland which is described in section.1.1. All the stratigraphic units are present from the Lewisian gneiss through the Torridon Group up to the Eilean Dubh Member of the Durness Formation.

2.3.1 The Structural Geometry of the Loch Broom thrust sheet.

Because of the late extensional movements on the Moine thrust it is impossible to estimate the original thickness of the Loch Broom thrust sheet. However, as the later movement of the Moine thrust picked up two horses of the Durness Formation (see 2.2.1), it is reasonable to assume that the original thickness of the Loch Broom thrust sheet included the Eilean Dubh Member. Study of the hanging-wall sequence diagram, fig 2.2, shows that prior to movement the Loch Broom thrust was non-planar with dominant glide horizons in the Lewisian Gneiss and the quartzites of the Eriboll Formation linked by long lateral ramps. Figure 2.8, shows that as it moved the thrust

plane achieved planarity and consequently two shallow culminations were developed, where before movement the thrust sheet was thickest. These two culminations are situated at Langwell and Achall. In between the two culminations, in the vicinity of Loch na Maoile, encl 1., there is the wide Loch na Maoile synform whose axis plunges down the dip direction of the thrust.

Where the Loch Broom thrust is the structurally lowest thrust plane it is planar and by constructing structure contours on the thrust plane it can be shown that it dips 12-15° to 127°. Using the "bow and arrow" rule of Elliott (1976b), which states that the maximum dip direction is the direction of transport of the thrust sheet, 127° is taken as the direction of transport.

Horses are a common feature along the Loch Broom thrust and they are principally made up of the quartzites of the Eriboll Formation, but the An-t-Sron Formation and the Durness Formation also occur in these horses, see encl.1 and 3. The horses vary in size from <10 m strike length, e.g. the small horses of the Durness formation on the N.W. flanks of Meall Mor [GR 139948] up to >100 m -<300 m for quartzite horses on the N.E. slopes of Creag non Broc [GR153958]. The origin and detailed geometry of the horses is discussed in Section 3.2.

2.3.2 Displacement on the Loch Broom thrust.

By using restored balanced cross-sections through the thrust belt in the Assynt district recent work has shown that prior to the thrusting the Torridon Group rocks were deposited in two basins, separated by a large anticline, defined by the opening direction of the 'double' unconformity between the Cambrian, Torridonian and Lewisian gneiss, fig 2.4, Elliott & Johnson (1980). These basins were named the "foreland basin" which at the present day outcrops to the west of the thrust belt on the foreland, and the "Assynt basin" found only within the thrust sheets. The width of the anticline separating the two basins was calculated to be 22.5 km. After the warping which produced the two basins, the Eriboll Formation was deposited unconformably, producing the double unconformity, fig 2.4 . From the

geometry of the double unconformity, it is possible to determine from which margin of the basin the thrust sheet originated. Eliott & Johnson (1980) calculated that the eastern margin of the foreland basin lies approximately 3 km behind the present day outcrop of the thrust front, and therefore the western edge of the Assynt basin must be approximately 25.5 km behind the thrust front.

The Torridon Group only outcrops within the Loch Broom thrust sheet in the vicinity of Creag nam Broc. At Creag-nam-L'uamha [GR 147968] the Torridon Group rocks are overlain by the Eriboll Formation with a shallower dip than that of the Torridon Group. This geometry indicates an eastwards opening basin, which must be the Assynt basin. As a result of folding during movement on the Loch Broom thrust the Torridon Group does not outcrop again further south until Dundonnell. This evidence suggests that displacement on the Loch Broom thrust at Achall is at least 25.5 km. At Langwell, the Eriboll Formation rests directly upon the Lewisian gneiss with no Torridon Group developed, therefore, the Loch Broom thrust sheet must have been derived from the crest of the large anticline between the two Torridonian basins. This means that displacement on the Loch Broom thrust at Langwell is less than 25 km, and suggests that prior to movement the Loch Broom thrust sheet lay obliquely across the western margin of the Assynt basin, the Loch Broom thrust sheet was derived from a ramp that was oblique to the thrusting direction with an orientation N.W.-S.E. The north-western end of the ramp was on the anticline and terminated against the large lateral ramp in the Moine thrust; the south eastern end was within the Assynt basin, fig 2.5.

2.4 THE ULLAPOOL THRUST SHEET.

The Ullapool thrust sheet rests upon the Ullapool thrust which was called T_{III} by Elliott & Johnson (1980). The Ullapool thrust runs from Meall Mor, where it joins the Loch Broom thrust, southwards to Loch Broom, under which it must rejoin the Loch Broom thrust as it does not outcrop on the south shore of Loch Broom. encl.1. The northern junction with the Loch Broom thrust is obscured by a late crosscutting extension fault, but from the stratigraphic separation diagram, fig 2.6, it is clear that stratigraphic separation rapidly diminishes near the junction.

The stratigraphy involved in the thrust sheet includes the Torridon Group through the Cambro-Ordovician sequence to the Ghrudaidh Member of the Durness Formation. Bedding planes within the thrust sheet dip moderately at 30°-50° to the S.E., fig.2.7. This dip is a result of internal deformation which is described in 3.1.2. The Ullapool thrust is planar and dips 15° to 127°, as shown by structure contours, and this direction is taken as the transport direction using the "bow and arrow" rule, Elliott (1976b). For most of its length along strike the footwall of the Ullapool thrust consists of the Salterella Grit of the An-t-Sron Formation, however, there are two small asperities of the Ghrudaidh Member (see 3.2.2.) The thrust plane is excellently exposed at the Corry Bridge road section [GR 142929].

At the top of the Corry Burn [Gr148932] there is imbrication involving the An-t-Sron Formation and Durness Formation. However, the exposure is so poor that it is impossible to determine the structural relationships between the imbrication and the overlying Loch Broom thrust.

The hangingwall sequence diagram, fig 2.8., shows that the Ullapool thrust originated beneath a long lateral ramp in the Loch Broom thrust, and must have been formed in an attempt to smooth the ramp, see 3.2.1.2.

2.4.1 Displacement on the Ullapool thrust.

Although the absence of Lewisian gneiss within the Ullapool thrust sheet suggests that it originated within one of the Torridonian basins, the geometry of the Cambrian/Torridon Group unconformity is unclear on this point. But the hangingwall sequence diagrams, fig 2.8., show that when the Ullapool thrust was initiated the Loch Broom thrust was active at the top of the An-t-Sron formation. As the Loch Broom thrust itself was derived from the Assynt basin then it is unlikely, indeed impossible, for the Ullapool thrust sheet to have been derived from the Assynt basin. The Ullapool thrust sheet must be derived from the foreland basin whose eastern margin lies 3 km behind the present thrust front, Elliott & Johnson (1980). Therefore displacement on the Ullapool thrust must be less than 3 km.

2.5 SHEET IV.

Sheet IV is a series of lensoid horses which are developed above the Sole fault, but below the Loch Broom, Ullapool and Moine thrusts The horses of Sheet IV were accreted to both the Loch Broom and Ullapool thrusts, see encl 1. The largest of them is at Achall which has an areal extent of approx 1.75 km^2. A small horse of Sheet IV outcrops at Strath Kanaird [GR 1602] and a large area of Sheet IV occurs at Knockan/Elphin which is described later, section 2.6. and encl.2. The Achall Sheet IV is shown on encl.3.

The lithologies involved in Sheet IV are the dolomites and limestones of the Durness Formation. The roof thrust of Sheet IV can be either the Loch Broom, Ullapool, or Moine thrusts, but Sheet IV is always structurally the lowest thrust sheet with the Sole fault as the floor fault, see encl.1.

2.5.1 Structural geometry of Sheet IV.

The Sole fault is everywhere planar and is only developed where Sheet IV horses occur. From structure contours constructed on the fault plane it can be seen to dip 15°-20° to 125°, which is sub-parallel to the bedding dip of the foreland stratigraphic units. The Sole fault is therefore a bedding plane fault.

A quarry at Achall allows the geometry of Sheet IV to be examined closely, supplemented by some well exposed areas at Creag nam Broc and at Knockan.

2.5.1.1 Bedding plane geometry and its structural importance in Sheet IV.

The bedding plane geometry within Sheet IV dips consistently to the S.E. at moderate to steep dips of 20°-50°, and occasionally as steep as 70°-90°, fig 2.9. This variation in dip is caused by rotation on listric extension faults within Sheet IV. The bedding planes can be divided into two groups:- i) 'active' bedding planes, which have suffered bedding plane slip and ii) 'inactive' bedding planes, which show no signs of movement.See plate 2.6

i) Active bedding planes: these bedding planes are commonly marked by a narrow layer of gouge/cataclasite which is commonly between 2 mm and 1 cm in thickness. The gouge/cataclasite consists predominantly of very fine grained dolomite with some clay minerals which are present on a crude anastomosing foliation. The foliation surfaces are marked by slickenside lines which indicate that at least some of the movement occurred after the formation of the foliation planes. It is likely that the active bedding planes were the planes of slip during rotation of the individual fault blocks on the listric normal faults. The active bedding planes are not often developed, and they therefore divide the Durness Formation into thick, mechanically isotropic units, commonly between 5-10 m thick.

ii) Inactive bedding planes: are marked by stylolites and have not been used for any movement. They are crosscut by small faults, hydraulic fractures, and tectonic veins associated with the extension faulting, see plate 2.7. The styolites and tectonic veins share a similar stress field and it can be shown that the two are coeval, e.g. some veins terminate onto the stylolites and the stylolites terminate into veins, fig 2.10a. With rotation of the fault blocks, veins formed during later movements will crosscut the stylolites and a further generation of stylolites will form with the newer veins, fig 2.10b. The stylolites are marked by a thin layer of clay minerals, and have a wavy toothed pattern. They form parallel to the minimum principal stress with the teeth parallel to the maximum principal stress, see fig 2.10a. Material is removed along the stylolite by pressure solution and deposited as carbonate vein fillings in the veins, leaving behind the insoluble clay mineral residue, Alvarez et al. (1976), Geiser & Sansome (1981).

The reason why one bedding plane was 'active' while others remained inactive is unclear. Presumably the active bedding planes developed along planes of low cohesive strength. These may have been provided by i) a zone of pore fluid pressure higher than the ambient pore pressure, or ii) a dolomitic shale bed. The establishment of low cohesion planes would enable shear stresses acting upon the beds during rotation on the listric faults to initiate sliding.

2.5.1.2 Folding in Sheet IV.

Folding is rare within Sheet IV at Achall, presumably because of the mechanical strength of the thick units between the active bedding planes. However, there are a few localities where folding does occur within the more anisotropic Eilean Dubh Member. The folds are periclinal, angular chevron style folds, with occasional box folds, plate 2:1: they plunge gently to the N.E. and S.W., with interlimb angles of 90°. An axial planar pressure solution cleavage is

developed, spaced at 2 mm-2 cm intervals. How these folds relate to the other structural elements is uncertain. There are two possibilities:-

i) The folds may be a result of a compressional tectonic event separate from extensional events. This event could have occurred during the early propagation of the Loch Broom thrust, as it ramped up through the Durness Formation. At this stage the Durness Formation would have been deformed under a compressional stress regime. Although it is advocated in 4.5.2. that the compressive strength of the dolomites was too high to deform extensively during the thrust initiation, local deformation may have occurred if a 'weak' point developed, either at a stress concentration around a perturbation, or an area of higher pore pressure which would cause a decrease in the strength of the dolomite and allow deformation to take place.

ii) The folds may be a result of shear stresses acting upon the bedding planes during rotation of the fault blocks, fig 2.11a. Rotation of the bedding planes would be accompanied by bedding plane slip on the active bedding planes. However,the folds are restricted to areas where 'active' bedding planes are closely spaced. This occurs more often in the Eilean Dubh Member where dolomitic shales are common.

Any small physical perturbation e.g. a bedding plane irregularity, may have triggered a buckle perturbation, which then developed into a buckle fold, Biot (1965). The usual mechanically isotropic nature of the Durness Formation explains why folds are rarely developed.

Drag folds are developed adjacent to faults, but only in the Eilean Dubh Member which is more thinly bedded and hence more anisotropic. They are related to movements on the faults, The folds produced are macroscopic with wavelength of 10 m. Larger, more open, roll over warps occur in the hangingwall of some of the listric extension faults, fig 2.11b.

2.5.1.3 Faults and tectonic veins.

Extension faulting and tectonic veining constitute the dominant structural style within Sheet IV Two sets of extension faults are developed:- i) a N.E.-S.W. striking set and ii) a N.W.-S.E. striking set, both with related sets of tectonic veins. The extension faults are crosscut by a system of strike slip faults with small displacement The faulting is best described from the Achall quarry where the best exposure is obtained. *See Encl.3.*

2.5.1.3a The N.E.-S.W. set of extension faults.

The N.E.-S.W. set of extension faults occur as conjugate pairs, with large synthetic, i.e. with displacement in direction of transport, faults with a listric form, and smaller antithetic faults which are planar (plate 2.2.). Displacement on the synthetic listric faults is greater than 5 m, whilst on the antithetic faults displacement varies between 0.5-4 m. Their orientation is shown in fig 2.12. The faults commonly have a layer of gouge/cataclasite along the fault plane ranging in thickness between 1-3 cm. Several of the antithetic faults have calcite/dolomite veins which are intruded along the fault plane, and can be up to 1 cm thick. These veins indicate that the faults failed by a combination of shear failure and extensional failure, Price (1966). The vein filling is massive and shows no fibrous crystal growth such as those described by recent workers on tectonic veining, Durney & Ramsay (1973), Ramsay (1980). The veins are limited to the antithetic faults where displacements are relatively small. This may suggest that any larger displacement would have destroyed the veins by cataclasis.

The exact relationship between the synthetic and antithetic faults with respect to the fault development is not entirely clear. The antithetic faults could be a product of extensional strains induced in the individual fault blocks by rotation on the synthetic listric faults, fig.2.13., and hence they have developed slightly later than the synthetic faults.

2.5.1.3b The N.W.-S.E. set of extension faults.

The N.W.-S.E. set of extension faults are the largest faults seen in the Achall quarry, plate 2.3. The faults strike between 090°-150° and dip moderately 30°-50° both to the N.E. and S.W., fig 2.14. A layer of gouge/cataclasite is developed along the fault planes which can be between 1-3 cm thick. Calcite fibre growths (sometimes referred to as slickencrysts, Gretener (1977a)), are also developed on the fault plane, on the leeward side of asperities (steps). Where two asperities on opposite fault walls meet and lock, a high stress concentration is the result. Material will be removed from areas of high stress concentration by pressure solution, and deposited in the lee of asperities where there is a void and a low stress concentration. Crystal growth will occur with crystals developing as fibres growing in the X direction of the strain ellipsoid associated with the faulting deformation. With movement the fibres build up as incremental steps and layers. Any slight change in the movement direction and hence a change in the orientation of the strain ellipsoid, causes a shift in the orientation of the crystal fibres, Durney & Ramsay (1973), Elliott (1976b), fig. 2.15.

These fibre growths are admirably displayed on the fault surfaces at the Achall quarry. Also at this locality examples of multilayers of fibre growth can be seen with slightly different fibre growth directions indicating changes in orientation of the strain ellipsoid.

The N.W.-S.E. faults cross cut and displace the N.E.-S.W. set. Displacement on the larger N.W.-S.E. faults is unknown as markers cannot be followed across the faults, but displacement on small faults is often up to 3 m. Displacement on the N.W.-S.W.faults appears to die out by branching into two or more faults, plate.2.4. Bedding adjacent to one ofthe faults has a dip of 90°, which can be explained by double rotation, once by movement on the N.E.-S.W. set

of faults, and again by the N.W.-S.E. fault. A small fault, which appears to be a splay from the a main N.W.-S.E. fault has a markedly listric geometry and is asymptotic to and terminates in a dolomitic shale bed. Price (1977) showed that very high pore fluid pressures can cause sub-horizontal fractures to form, and that the lower the pore pressure the steeper the angle of failure. The flattening of faults into dolomitic shale beds may indicate the these were zones of high pore fluid pressure.

Both sets of extension faults have sub-parallel arrays of fractures and small faults with displacements of < 10 cm. Although the small faults are distributed throughout the dolomites the fracture spacing becomes closer nearer to the faults. Fractures developed sub-parallel to the Creag nam Broc fault are more dominant than bedding up to 10 m from the fault. At < 5 m from the fault the bedding is hard to determine. The sub-parallel fractures are interpreted as pre-failure fracture arrays. With stress build up the rock would deform as a zone of fractures with small displacements. On increase in stress and strain the fracture zone would be incapable of taking-up all the deformation, causing the deformation to become concentrated into a single fracture plane. A similar process is described in many examples of experimental rock deformation, where pre-failure fracturing is commonly observed, Jaeger & Cook (1976), Price (1966).

2.5.1.3c <u>The strike slip faults</u>.

The strike slip faults are only sporadically seen. In the Achall quarry they occur as a system of spaced fracture zones commonly 3 m wide or less, mostly striking N-S and dipping at 60°-90° to both the E and W, fig 2.16a. They display fibre growth structures, which plunge gently south, fig 2.16b. There are no multilayer fibre growths, suggesting that movement on the faults was of short duration and displacements were probably small. Fault gouge/cataclasite only has a limited development occurring where the deformation has been

concentrated onto a single fault plane. Most of the faults have a dextral displacement, however, some of the strike-slip faults have orientations similar to the N.E.-S.W. set and have a sinistral movement. These faults are best explained as being original N.E.-S.W. faults which have been reactivated as strike slip faults. The most likely N.E.-S.W. faults to be reactivated are those whose orientation deviates from the usual N.E.-S.W. orientation towards a N-S orientation.

The strike slip faults certainly displace the N.E.-S.W. faults, plate 2.5, and appear to cut the N.W.-S.E. faults, although this is not so clear. They are, therefore, the latest faults to be developed in the Achall Sheet IV.

If the Andersonian relationship between the fault orientation and the position of the principal stress axis is accepted, Anderson (1951), fig 2.17, then the strike slip faults represent a significant departure from the stress field for the extension faults. Instead of a vertical maximum principal stress σ_{max}, i.e. loading, it acted horizontally sub-parallel to the strike of the main thrust planes, and the minimum principal stress acted parallel to the transport direction. In section 4.4 a model is put forward that interprets the strike slip faults as products of a change in the orientation of the stress system due to rapid unloading by erosion of the overlying thrust sheets.

2.5.1.4 Tectonic Veins.

Tectonic veins are well developed within Sheet IV. They have an intimate relationship with the extension faults and are products of the same stress system. The veins are intensely developed close to the faults, and are usually sub-parallel to the strike fo the faults. The relationship is shown in fig 2.18. Similar geometries have been described by other authors, notably Phillips (1972), Sibson (1977, 1981), and Fyfe et al. (1978).

The veins have variable forms:-

i) Upright veins: these, the most common veins are usually < 10 mm wide and have length width ratios of >10:1, plate 2.5.

ii) En echelon vein arrays, plate 2.6: these are more rarely developed.

iii) Vein networks are seen in the Ghrudaidh Member and they become more intense near to the faults.

The vein fillings are usually i) calcite or dolomite, ii) calcite/dolomite, iii) calcite/quartz, iv) quartz. The vein fillings in the calcite, dolomite and calcite/quartz veins are usually massive, with large subhedral crystals plate. 2.7, very occasionally fibrous, plate.2.8. The calcite crystals are commonly twinned. Quartz veins are rare, and they have a fibrous habit similar to the vein textures described by Durney & Ramsay (1973). Some of these show at least two increments of opening and the fibres are curved indicating that slight changes in the dilation direction occured, this is probably a result of rotation on the listric extension faults.

Recent work on vein textures has shown that fibrous textures develop during repeated crack opening, and with successive opening individual 'walls' of fibres build up in an incremental fashion, Durney & Ramsay (1973). The opening and sealing by vein material has been termed the crack-seal mechanism, Ramsay (1980). Sibson (1981) showed that reopening of the veins indicates that the tensile strength of the vein is less than the tensile strength of the host rock. The veins in Sheet IV show no sign of incremental opening, suggesting that they may have formed during only one opening increment, and then remained sealed. This can be interpreted in two ways:-

i) Following Sibson (1981) it can be suggested that the vein fillings had an equal or higher tensile strength than the host rock or

ii) It is possible that the orientation of the vein with respect to the operative stress field became unsuitable for re-opening due to rotation of the veins in the fault blocks between the listric faults.

Veins also occur adjacent to bedding planes both active and inactive, plate 2.9. Veins adjacent to inactive bedding planes are closely associated with stylolites, see section 2.5.1.1., with pressure solution along the stylolites providing the infilling material. The occurrence of veins which branch off active bedding planes suggests that the active bedding planes are planes of high pore fluid pressure, a plane of super weakness of Gretener (1981). The high pore fluid pressure may cause hydraulic fracture in the overlying unit, Fyfe et al. (1978).

The timing between vein generation and fault failure is far from clear. Sibson (1981) and Sibson et al. (1975) suggest that the veins are products pre-failure dilatancy and stress cycling. As stress builds up, pre-failure dilatancy occurs and the veins form by hydraulic fracture. The formation of the vein lowers the pore fluid pressure in the rock and induces 'wet dilatancy hardening', Sibson et al. (1975). Differential stresses will rise until a critical value is reached and failure occurs and stress drops. This cycle will be repeated many times at each movement of the fault.

2.5.1.5. CLASSIFICATION OF THE EXTENSION FAULTS.

Wernicke & Burchfiel (1982) divided extension faults into two broad groups; rotational and non-rotational. Rotational faults were further divided into two subgroups; i) where both the beds and the fault planes are rotated, and where the fault geometry is either planar (planar rotational) or listric and ii) where only the beds are rotated and the fault plane is non-rotational and has a listric geometry.

In the non-rotational class, neither the bedding nor the faults are rotated. Figure 2.19a,b,c, illustrates the geometry of the classes. Listric faults always produce a differential tilt between the hangingwall and the footwall because the hangingwall strata have moved down a curved plane. Whereas with a set of planar rotational faults the beds will all tilt by the same amount.

Some of the rotation on the NE-SW extension faults in Sheet IV is differential, indicating that some of the faults are listric and curve downwards into the Sole fault. However, many of the faults show a planar rotational geometry with no differential tilt, see plate 2.2 and fig. 2.19d. The NW-SE extension faults also show a planar rotational geometry.

The total amount of extension in Sheet IV on the NE-SW faults cannot be calculated by balancing a cross-section as there is little control on stratigraphic position within Sheet IV. But as the majority of the faults in Sheet IV are planar rotational then a minimum extension can be obtained by using the extension map of Wernicke and Burchfiel (1982), fig. 2.20. This gives an estimated extension in Sheet IV of around 30% on the NE-SW extension faults.

2.6. THE STRUCTURAL GEOMETRY OF THE KNOCKAN AREA.

At Knockan the Moine thrust climbs up a large lateral ramp from a glide plane at the top of the An-t-Sron Formation up into the Eilean Dubh Member. This ramp defines the southern boundary of the Assynt culmination. The Durness Formation in Sheet IV, which rests upon the Sole fault, covers a tract of poorly exposed ground and extends as far north as the Loch Borralan intrusions. The Durness Formation is deformed by a comparable set of structures as Sheet IV at Achall. These are truncated by the later extensional movement on the Moine thrust, but join and curve into the Sole fault. In thrust emplacement terms the Sheet IV at Knockan is chronologically comparable to Sheet IV at Achall.

Beneath the Moine thrust but above Sheet IV are two large horses which are comprised of Eriboll Formation, Torridon Group, and Lewisian gneiss. The thrust plane beneath these horses is nowhere exposed. These two horses have been previously interpreted as klippen of the Ben More thrust sheet, Peach et al. (1907), Christie (1963), Elliott & Johnson (1980). The most westerly of the two horses consists entirely of Eriboll Formation. Bedding is gently folded into a series of open folds which gently plunge N.E., encl.2. Pipes in the Pipe Rock show that the beds are right way up, this is contrary to Elliott & Johnson (1980) who advocated that the horse was inverted. The horse is extensively deformed by extension faults which are related to movement on the Sole fault.

Enclosure 2 is a geological map of the Durness Formation in Sheet IV at Knockan. The structures seen in the area are a 'family' of extension faults, stylolites which are sub-parallel to bedding, and hydraulic fractures and veins, which are comparable to those seen in Sheet IV at Achall, see 2.5. The structures are superbly displayed in a line of cliff sections which runs NE from Knockan Crag GR.189093 to GR 233103, and in an excellent road section in Knockan village at GR 213107 plate 2.16. Inland from the road sections the faults are distinguished by gullies and can be divided into two main sets i) a NNE-SSW striking set and ii) a NE-SW to E$\bar{W}$ set, NW-SE striking faults are rarer than at Achall. Differential tilt across the faults indicate that some of the faults have a listric geometry (see encl. 2). Tectonic veins are common, these strike sub-parallel to the faults and have moderate to steep dips to SE and NW. (Encl. 2). Folds are rare, where they do occur at GR 196097, the folds are kink folds occurring as conjungate boxlike folds, and plunge both to the NE and SE with axial planes which are steeply dipping to the W and E. These folds are interpreted as localised compression perhaps due to accommodation problems during extension faulting or from a pre-extension faulting compression event (see section 2.5.1.2). The Moine thrust cuts across all of the extensional structures above, and is the latest structure seen.

The 'family' of extensional structures comparable to those at Achall suggest a similar origin. The structures are interpreted as the result of tectonic loading, and the deformation in Sheet IV is dominantly extensional. This is at variance with the interpretation of Coward (1983), who advocated that the Durness Formation at Knockan was a compressional imbricate zone with local surge zones (see section from Coward (1983) on encl. 2).

2.7. FAULT ROCK PRODUCTS IN THE MOINE THRUST ZONE BETWEEN LOCH BROOM AND THE ASSYNT CULMINATION.

Due to bad exposure the actual thrust planes are rarely exposed so a systematic study of fault rocks such as those described by House & Gray (1982) in the Appalachians, and Sibson (1975, 1977) in the Outer Isles Thrust Zone, could not be undertaken. This study is an interpretation from observations based on few samples. For fault rock nomenclature I follow Sibson's (1977) classification of fault rocks. All the fault rocks studied are cataclasites and belong to the elastic-frictional regime of Sibson (1977). Although the Moine Thrust has mylonites in its hanging wall they were derived from deeper levels in the thrust zone and brought up to the present level by the brittle thrust.

Fault rock specimens from the Moine thrust plane were collected from the classic Knockan Crag locality [GR189093] described by Peach et al. (1907) and Christie (1960, 1963). The Moine thrust plane also outcrops in a stream section, NE of Creag nam Broc [GR 149958] and on the Loch Broom shore near to Corry Point [GR 143923] but the outcrops are very weathered and no good sample of fault rock could be collected. The thrust plane of the Loch Broom thrust only outcrops in a few places to the NW of Creag nam Broc [GR 149958] and at Corry Point [GR 143923]. Again both outcrops are weathered and no good sample of fault rock was obtained. For the Ullapool thrust we are more fortunate as a road cutting has been made at Corry Bridge [GR 143923] which affords an excellent section through the thrust, and several good samples were collected. Fault rocks from Sheet IV were collected from the Creag nam Broc fault [GR 149958] and from the Achall quarry [GR 149953] where excellent samples were found.

2.7.1 Fault Rock from the Moine thrust plane.

At Knockan Crag the fault rock varies in thickness from 2-7 cm and occurs between Moine mylonites in the hanging wall and dolomites of the Durness Formation in the footwall.

The thickness along strike is unclear, but similar thicknesses of fault rock occur at Achall and Corry Point. Christie (1963) included the fault rock at Knockan in his 'secondary mylonite' group, and referred to it as kakirite. However, following the fault rock classification of Sibson (1977), the fault rock can be classified as a proto-cataclasite grading to cataclasite.

The proto-cataclasite consists of between 40-60% rock fragments and 40-60% matrix. The rock fragments can be recognized as Moine mylonites, dolomites of the Durness Formation and vein calcite and dolomite. The clasts vary in shape from sub-angular to well rounded. The well rounded clasts usually being limited to the dolomite and the vein material, plate 2.10. The size of the dolomite and mylonite fragments varies from < 1 mm - 10 mm. No fragments were seen of the rest of the Cambrian succession, the Lewisian gneiss or the Torridon Group. This indicates that cataclasite only contains material from the immediately adjacent hangingwall and footwall and it has not been displaced up the fault plane. The matrix is very fine grained and generally unresolvable in thin section; it has a green colour caused by chlorite with small flecks of white mica, plate 2.10. At some points within the matrix, a crude pressure solution cleavage is developed especially close to inpinging clasts. This suggests that areas of the matrix around two clasts have suffered a higher strain than the remainder of the cataclasite which has a random fabric, plate 2.11. There is no clast shape orientation and no evidence of any straining of the clasts, therefore, no ductile strain has taken place.

The cataclasite is cut by calcite/dolomite veins, which cut across both the clasts and the matrix. These veins are commonly < 1 mm wide and are single straight veins with tapering ends, plate 2.12a,b. Vein material is also found as clasts within the cataclasite, which suggests that there is a cyclicity of cataclasis and veining. The implications of which are discussed later,see 2.8.

2.7.2 Fault Rocks from the Ullapool thrust.

The fault rocks were collected from the Corry Bridge road cutting [GR149958), see plate 2.13a,b,for actual locations of specimens. Specimens were collected from the Torridon Group and Eriboll quartzites from the hangingwall, Durness Formation dolomites of the footwall and the fault rock from the thrust plane.

The quartzites were collected from two small horses in the hangingwall of the thrust, see plate 2.13a. The rocks can be classified as cataclasites with narrow zones of ultracataclasite, plate 2.13c. These zones have a variable orientation and are only recognizable in thin section. The clasts, which make up approximately 30%-60% of the rock are remnant grains of the original quartzite; they are well rounded or occasionally sub-angular, with a grain size of 1mm. The quartz grains show a moderate undulose extinction, the significance of which is unclear; it may be due to straining before cataclasis, or to the beginnings of ductile strain during cataclasis. The matrix consists of very fine grained quartz with minor mica content. No foliation is developed and there is no shape orientation, hence the rock has a random fabric, fig 2.13c.

The fault rock derived from the Torridon Group of the hangingwall can be classified as a proto-cataclasite, grading to a crush breccia. This consists of intact "Torridonian" arkose, surrounded by cataclasite rich in mica. The fragments are large but <1cm, and there is no preferred shape orientation.

A sample of the dolomite from the footwall was taken immediately adjacent to the thrust plane. The rock can be classified as a cataclasite grading to ultracataclasite, and is totally derived from the dolomite of the Ghrudaidh Member. Remnant clasts do exist, but as the original rock was fine grained it is very hard to distinguish between original rock and cataclasite. Under plane polarised light the cataclasite shows as a darker shade than the original rock. The cataclasis is sometimes so intense that the product is an ultracataclasite which either has gradational boundaries with the cataclasite or has very sharp boundaries and occurs in narrow zones, indicating that deformation was localised on a microscopic scale. The cataclasite is veined by thin calcite/dolomite veins, which are also cut by the cataclasite and ultracataclasite zones, but as cataclasis is so strong no remnant clasts survive; this evidence of cross-cutting between cataclasite, ultracataclasites and veins again indicates a cyclicity of cataclasis and veining.

2.7.3 Fault Rocks of Sheet IV.

The fault rocks from Sheet IV were collected from the Creag nam Broc fault, see plate 2.14 , and from the Achall quarry.

At Creag nam Broc samples were collected at 1m intervals below the Creag nam Broc fault in order to investigate the change in deformation as the fault was approached. Between 10 m and 3 m below the fault the dolomites of the Ghrudaidh Member are little deformed, retaining the dominantly sedimentary fabric, but they are crossed by narrow cataclasite zones which meet in small areas of microbrecciation, see plate 2.15a. At 3 m from the fault the deformation becomes more intense with an increase in the intensity of veining. The veins cross-cut the cataclasite zones as well as being cut themselves by the cataclasites, indicating a cyclicity between cataclasis and tectonic veining, see plate 2.15b. At 1 m below the fault the dolomite was approximately 50% cataclasite in a network of cataclasite zones, see plate 2.15c. However, adjacent to the fault cataclasite was dominant, plate 2.15d. Tectonic veining is intense, showing the cross-cutting relationships described above. The zones of cataclasite occur along fractures which are conjugate pairs and are parallel to minor extension faults associated with the main Creag

nam Broc fault. With the increase in deformation as the main fault is approached the intensity of the fracturing and cataclasis increases until at the fault a microbreccia is produced. Comparable fabrics have been described from the Saltville thrust in the Appalachians, House & Gray (1982).

2.8 DEFORMATION CYCLES IN FAULT ROCKS.

The evidence from the samples described above suggests that deformation in the fault rocks occurred in cycles of cataclasis and tectonic veining. Furthermore, in specimen K1 from the Moine Thrust plane, pressure solution cleavage is crudely developed. This ordered fabric suggests that a low strain rate must have been operative for its development. The cataclasis which produced the predominant random fabric is a fast strain rate process, Sibson (1977). Veins, which both cross-cut the cataclasite fabric and are incorporated into it, cannot have been evolved during the cataclasis process otherwise they would have been destroyed. This evidence from the fault rock fabric leads to the conclusion that deformation occurred in cycles of fast-strain rate, cataclastic deformation producing a random fabric, and slower strain-rate deformation producing a crude pressure-solution cleavage and tectonic veining.

Cataclasis, which involves the mechanical movement and fracturing of grains, is a dilatant process, Sibson (1977), and therefore during cataclasis permeability and porosity must be high. However, recent experimental work has shown that during sliding experiments, permeability, and hence porosity decreases with the increase in shear stress acting upon the fault plane, Chu et al. (1981), Morrow et al. (1981), Morrow et al, (1982). These experiments were carried out using actual fault gouges from the San Andreas Fault zone both at low

confining pressures (up to 220b), Chu et al. (1981), and high confining pressures (>2 kb), Morrow et al. (1981), with strain rates of 10^{-6} sec^{-1}, which is equivalent to a natural stain rate of 10^{-14}-10^{-15} sec^{-1}, the so-called average crustal strain rate. However, it is known that during cataclasis strain rates can be as high as 10^{-10}-10^{-12} sec^{-1} during fast seismic slip, Sibson (1975, 1977). The two contrary lines of evidence can be accommodated if permeability is controlled by the strain rate. Further evidence to justify this approach exists: some faults are known to be channelways for fluid transport Sibson (1977), Sibson et al. (1975), leading to the development of tectonic vein systems in fault zones. Yet some faults act as impermeable barriers; Lachenbrach & Sass (1980) in a study of the San Andreas fault show that there are two hydro-geological provinces either side of the fault with no fluid transport across the fault. Wallace & Morris (1979) described small faults in a mine, some of which are tight and impermeable and others very permeable.

Let us consider a hypothetical fault, which is active and already initiated, that is , we are only concerned with movement on an already existant fault. Prior to further failure, shear stress acting on the fault plane is low and deformation is by slow strain rate aseismic shear. As shear stress rises, the rock around the fault deforms by pre-failure dilatancy, with formation of small fractures and the migration of pore fluids into the fractures. The fluid migration produces an abrupt drop in the ambient fluid pressure causing an increase in the strength of the rock, i.e. a strain hardening effect, Sibson (1973). This dilatancy has been noted prior to large earthquakes; Sibson et al. (1975) calculated that for earthquakes of magnitude M5-M8 on the Richter Scale, pre-failure dilatancy exists for 0.3-83 years respectively, during which time the fault zone is permeable. With the influx of the fluid into the fault zone, fluid pressure will begin to rise causing a decrease in the strength of the rock and the fault zone. When the shear stress equals or exceeds the frictional resistance on the fault plane failure will occur, and the dilatant zone will collapse with the expulsion up the fault plane of remaining fluids in the fractures. Evidence of this fluid migration is outflow of water along spring lines near faults after shallow earthquakes, Sibson et al. (1975), With the expulsion of fluids the pore fluid pressures drop and the

deformation reverts to a slow aseismic shear after release of the shear stress. This causes compaction of the cataclasite and allows the development of pressure solution foliation at high strain points i.e. grain to grain contacts. During this stage the cataclasite will be relatively impermeable and may be equivalent to the deformation simulated by the experimental work of Chu et al. (1981) and Morrow et al. (1981, 1982).

This idealised fault model can explain why some faults appear to be fluid conduits whilst others are impermeable - it depends on what stage the faulting has reached in the sequence described above. The time when faults are impermeable is longer than when they are permeable and for an average sized earthquake of M5-6, a fault zone will only be dilatant for 0.3-2 years, Sibson et al. (1975). The above model can also explain the apparently contradictory fault rock fabrics seen in the cataclasites. Sibson et al. (1975) showed that for a fault with 1 km displacement, there will be 10^3-10^4 of the above cycles. The Moine thrust has moved at least 77 km, Elliott & Johnson (1980), so the number of cycles involved is very large indeed. Moreover, because cataclasis is a destructive process, evidence of only 2 or maybe 3 cycles may be present in a fault rock.

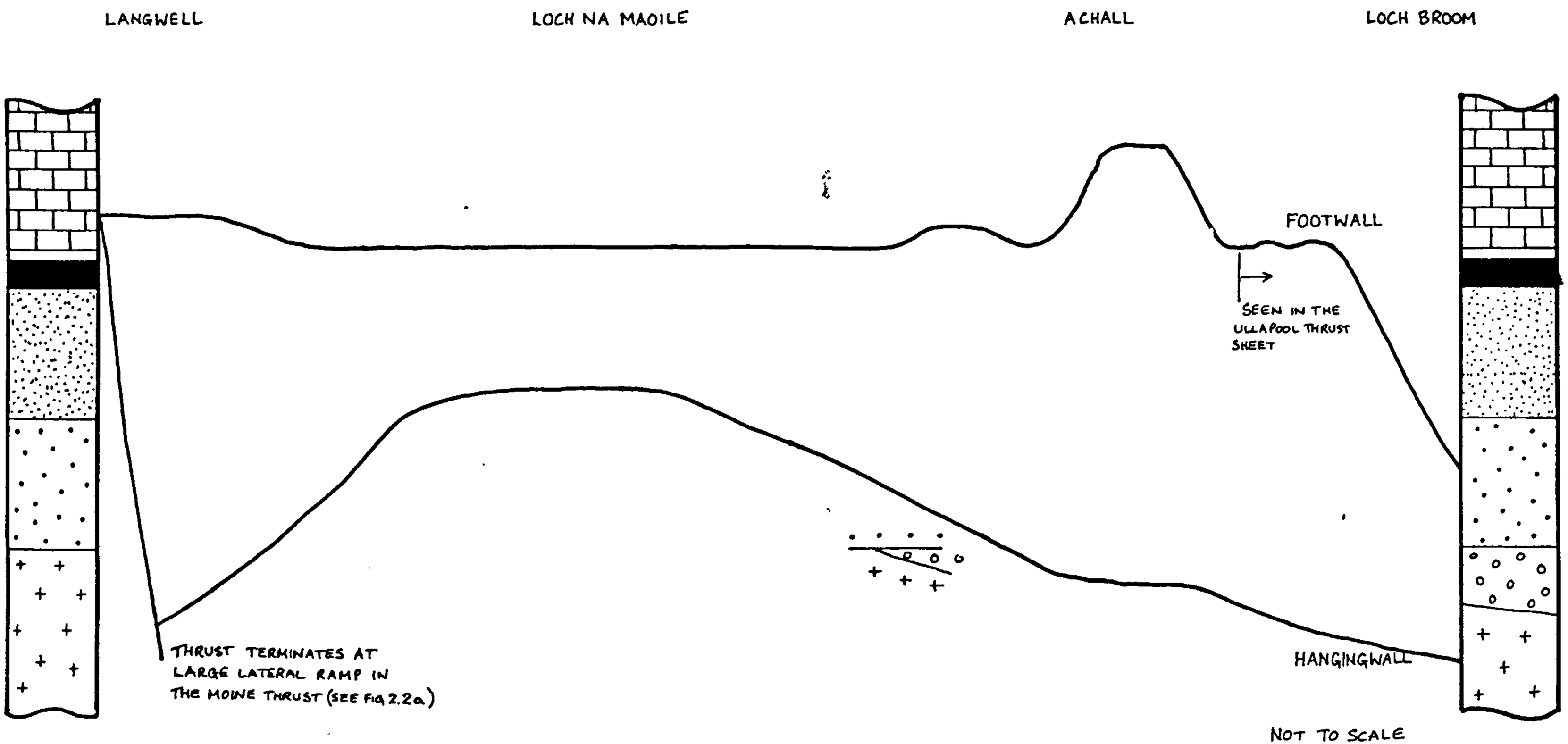

Fig. 2.1.

Stratigraphic separation diagram for the Loch Broom thrust sheet: The hangingwall and the footwall usually start at the same point on the stratigraphic column. However, because prior to movement the Loch Broom thrust terminated against a large lateral ramp in the Moine thrust, the stratigraphic separation is large on the diagram,see fig.2.2. Note the large ramps defined by the hangingwall line. With movement on the Loch Broom thrust large folds developed in the hanging wall.

Fig. 2.2.

A hangingwall sequence diagram illustrates the structural history and geometry of the Loch Broom thrust sheet and Moine thrust by stages from its initiation to the present day geometry. View is down thrust dip, i.e. SE.

a) The Moine thrust ramped laterally from the Lewsian gneiss to at least the Eilean Dubh Member of the Durness Formation. The Loch Broom thrust was initiated along an irregular thrust plane.

b) After movement on the Loch Broom thrust, large folds were developed in the hangingwall, also folding the Moine thrust.

c) Later movement on the Moine thrust cut through the folds and carried two horses of Eilean Dubh Member to rest on the Fucoid Beds and Pipe Rock, demonstrating an extensional geometry for the Moine thrust. See 2.1.1.

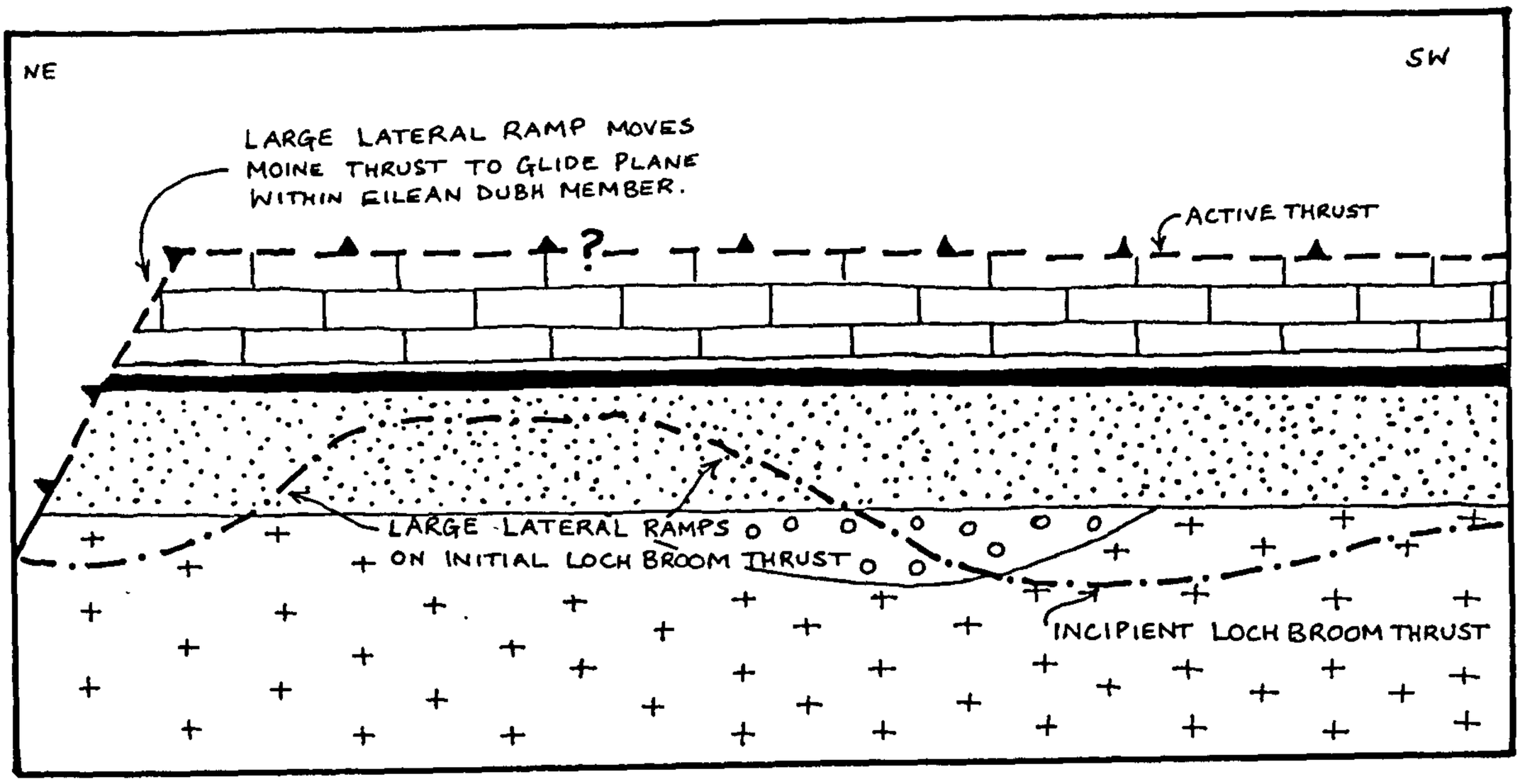
NE
SW
LARGE LATERAL RAMP MOVES MOINE THRUST TO GLIDE PLANE WITHIN EILEAN DUBH MEMBER.
ACTIVE THRUST
?
LARGE LATERAL RAMPS ON INITIAL LOCH BROOM THRUST
INCIPIENT LOCH BROOM THRUST

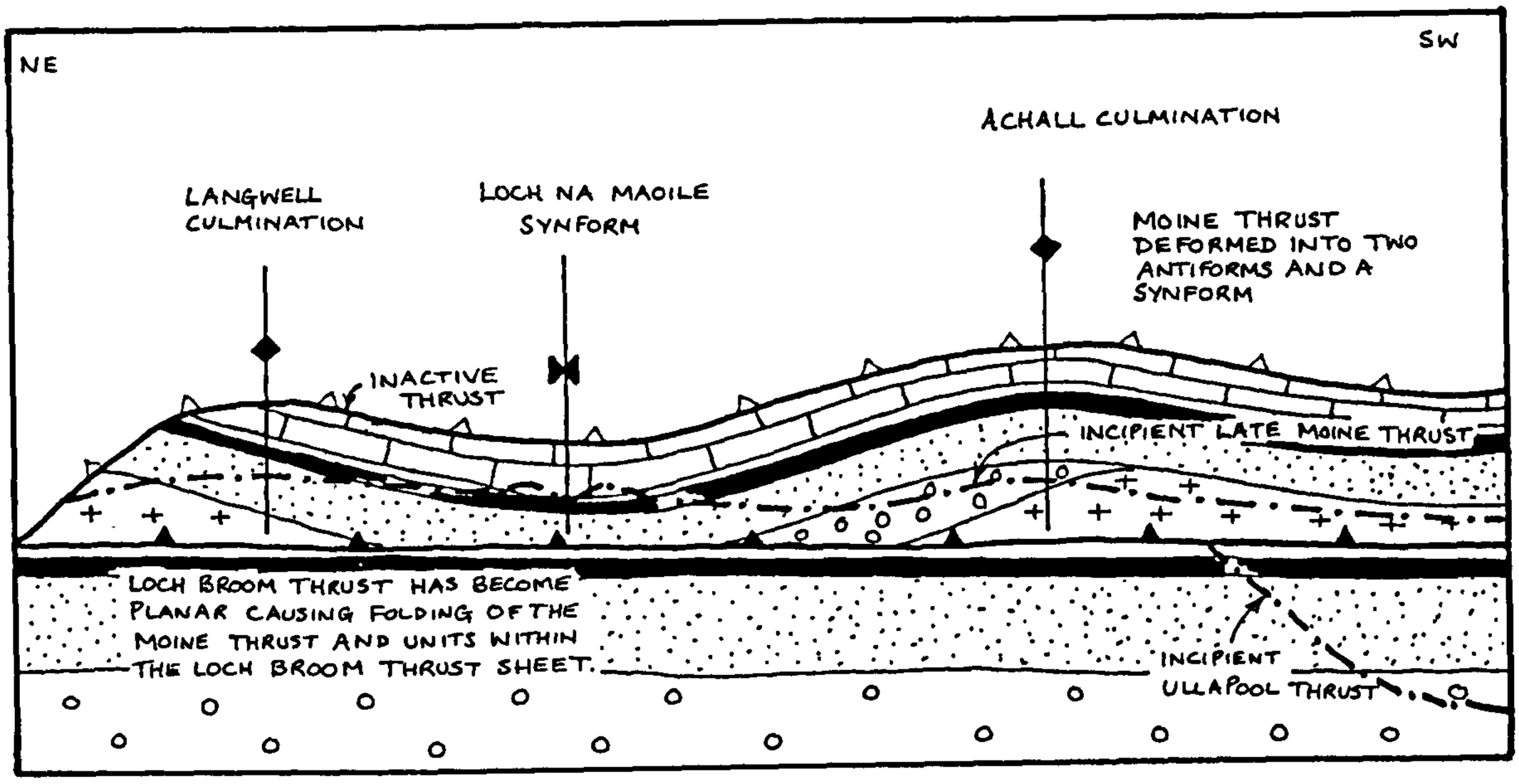
NE
SW
LANGWELL CULMINATION
LOCH NA MAOILE SYNFORM
ACHALL CULMINATION
MOINE THRUST DEFORMED INTO TWO ANTIFORMS AND A SYNFORM
INACTIVE THRUST
INCIPIENT LATE MOINE THRUST
LOCH BROOM THRUST HAS BECOME PLANAR CAUSING FOLDING OF THE MOINE THRUST AND UNITS WITHIN THE LOCH BROOM THRUST SHEET.
INCIPIENT ULLAPOOL THRUST

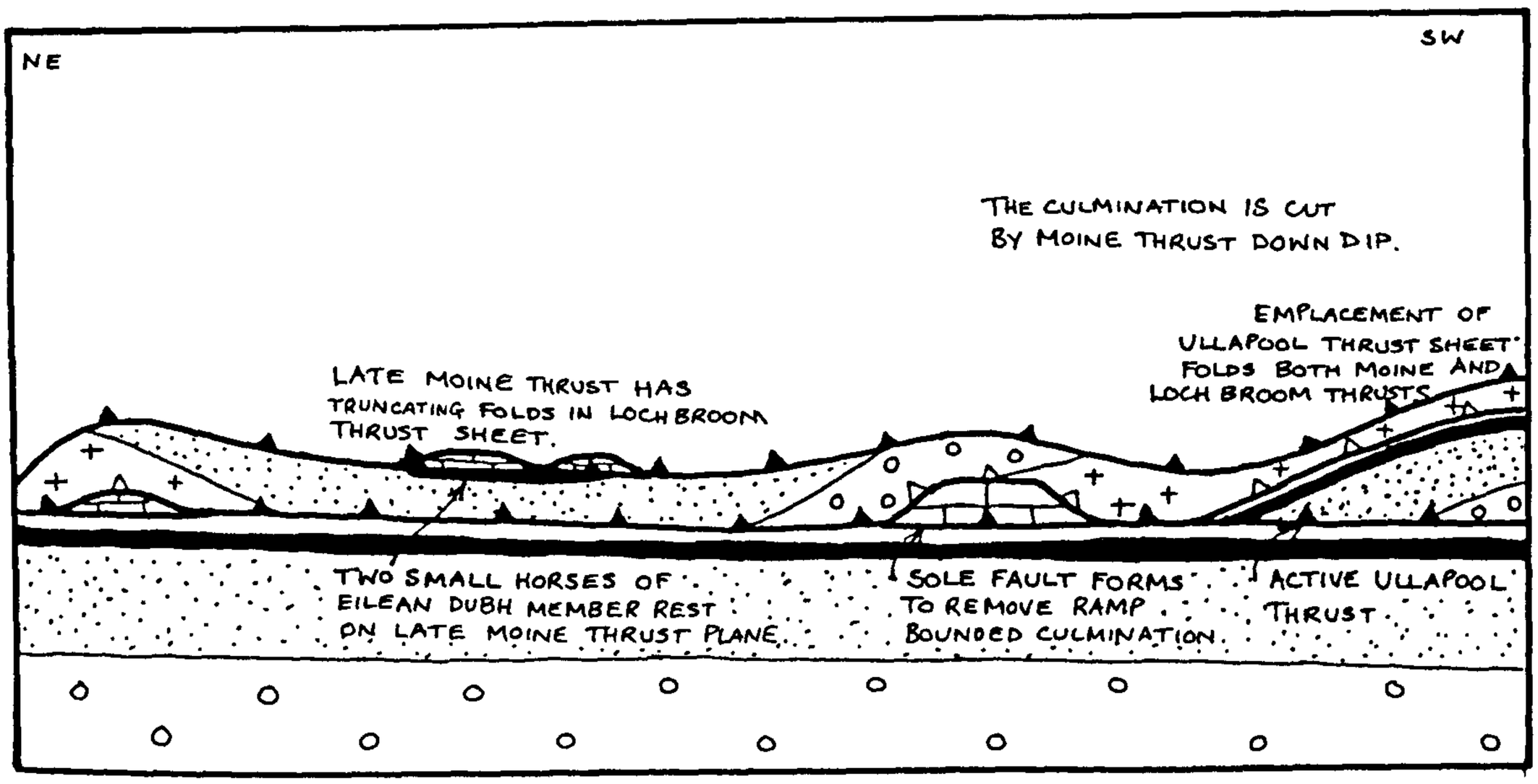
NE
SW
THE CULMINATION IS CUT BY MOINE THRUST DOWN DIP.
EMPLACEMENT OF ULLAPOOL THRUST SHEET FOLDS BOTH MOINE AND LOCH BROOM THRUSTS
LATE MOINE THRUST HAS TRUNCATING FOLDS IN LOCH BROOM THRUST SHEET.
TWO SMALL HORSES OF EILEAN DUBH MEMBER REST ON LATE MOINE THRUST PLANE.
SOLE FAULT FORMS TO REMOVE RAMP BOUNDED CULMINATION.
ACTIVE ULLAPOOL THRUST

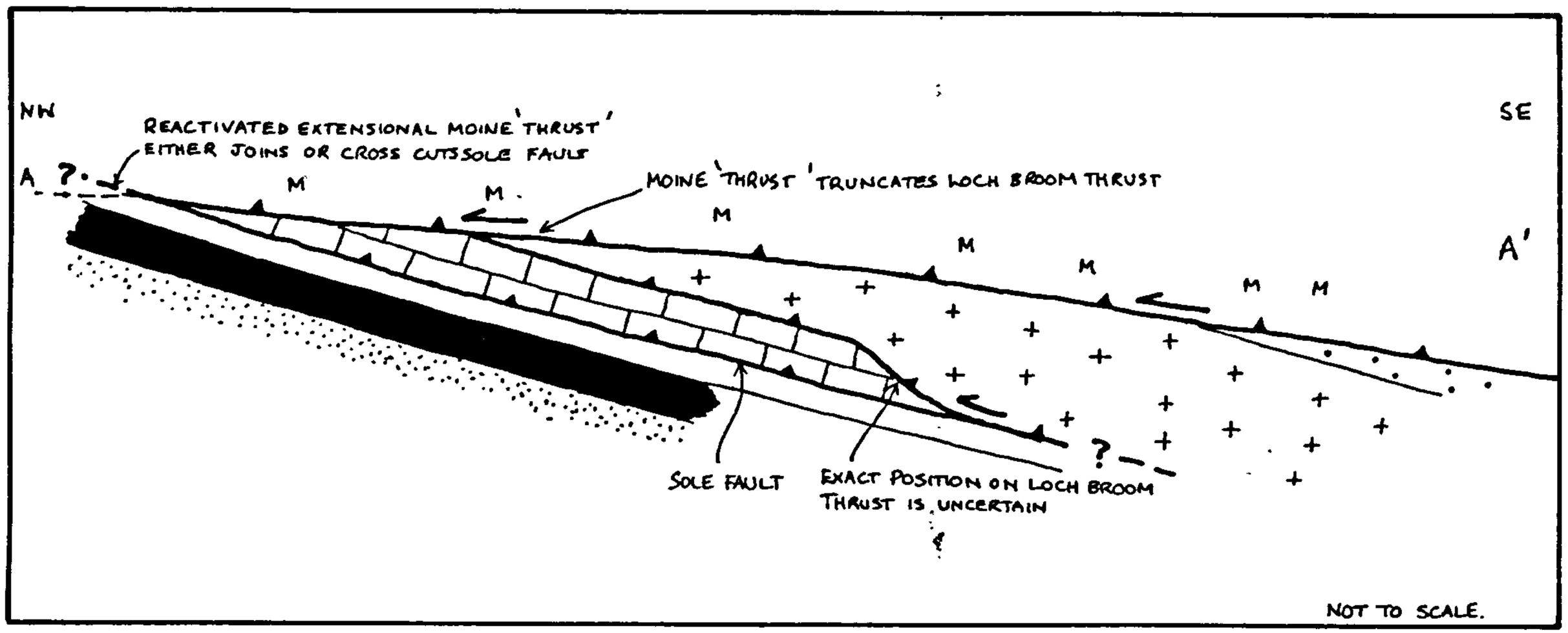

Fig. 2.3.

Restored
Sketch section along the line A-A' on encl. 1. This illustrates the extensional geometry of the reactivated Moine thrust. It may possibly cut across the Sole fault to continue down-cutting onto the foreland, or it may join the Sole fault.

Fig. 2.4.

Diagrammatic section from Elliott & Johnson (1980), to show the disposition of the "Torridonian" rocks in the Foreland and Assynt basins prior to movement on the thrusts. Displacement estimates for the Loch Broom thrust by Elliott & Johnson (op. cit.) are based on the width of the eroded anticline. The original positions of the Langwell and the Achall portions of the Loch Broom thrust sheet are marked. See fig. 2.5 and section 2.3.2.

Fig. 2.5.

Sketch map of the two "Torridonian" basins prior to thrust movement, with the present day thrust front marked. The original thrust front prior to movement on the Loch Broom thrust is also marked, note that it represents a ramp that is oblique to the transport direction. This ramp terminated in the north at the large lateral ramp in the Moine thrust. See fig 2.2a and section 2.3.2

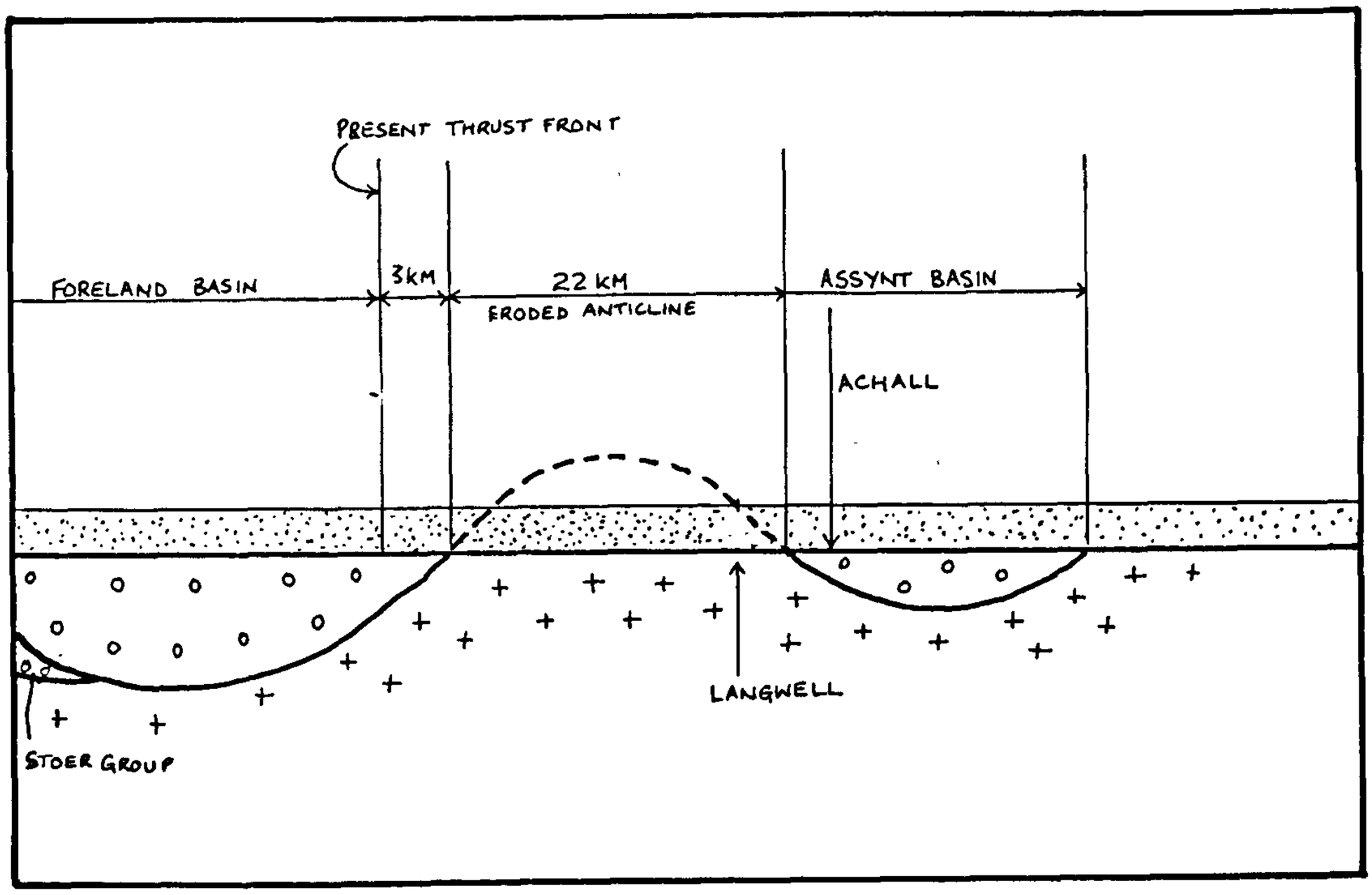
PRESENT THRUST FRONT
FORELAND BASIN
3km
22 km
ERODED ANTICLINE
ASSYNT BASIN
ACHALL
LANGWELL
STOER GROUP

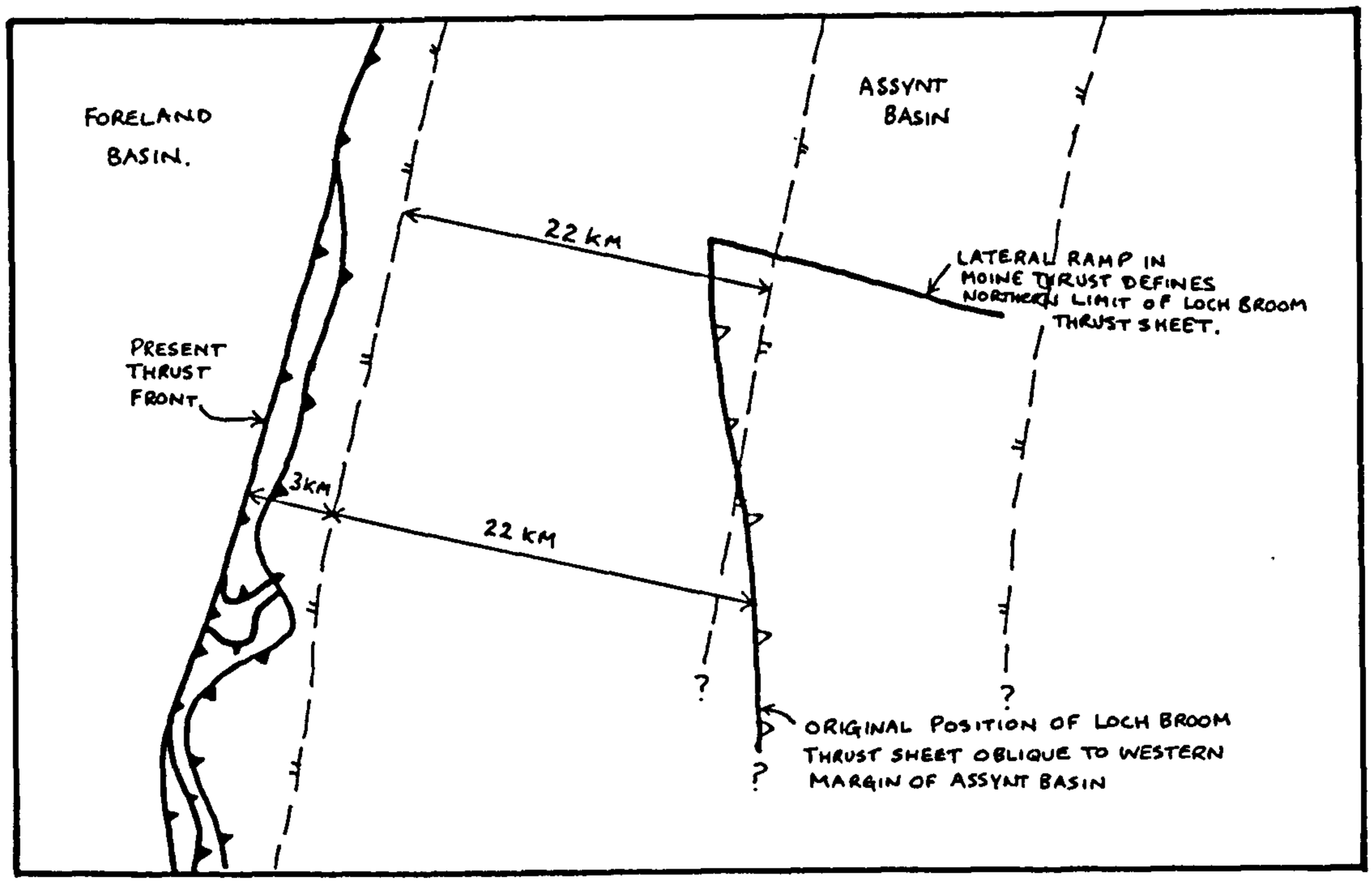
FORELAND BASIN.
ASSYNT BASIN
22 km
LATERAL RAMP IN MOINE THRUST DEFINES NORTHERN LIMIT OF LOCH BROOM THRUST SHEET.
PRESENT THRUST FRONT
3km
22 km
?
?
?
ORIGINAL POSITION OF LOCH BROOM THRUST SHEET OBLIQUE TO WESTERN MARGIN OF ASSYNT BASIN

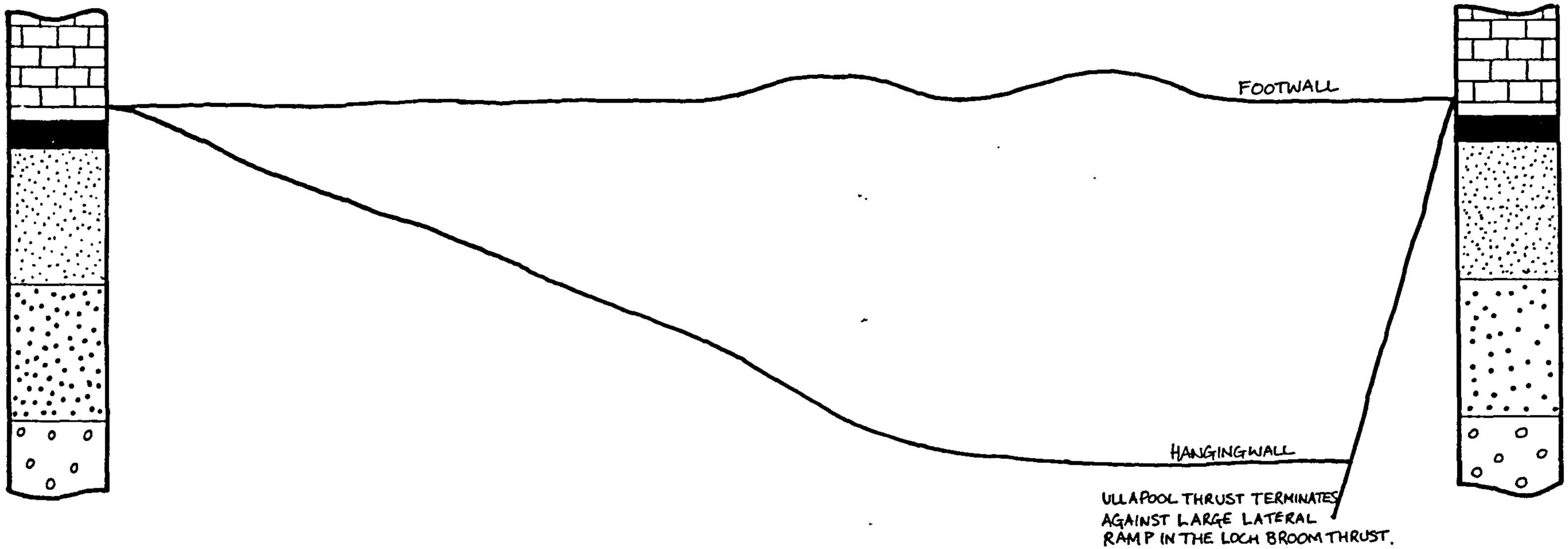

Fig. 2.6.

Stratigraphic separation diagram for the Ullapool thrust sheet: Note that the northern termination is marked by diminishing stratigraphic separation as the displacement decreases. However the southern termination was against a lateral ramp in the Loch Broom thrust. See fig. 2.7 & 2.8.

Fig. 2.7.

Geological map of the Ullapool thrust sheet: The diminishing stratigraphic separation northwards is clearly seen. The bedding dips are a result of rotation during the emplacement of the thrust sheet.

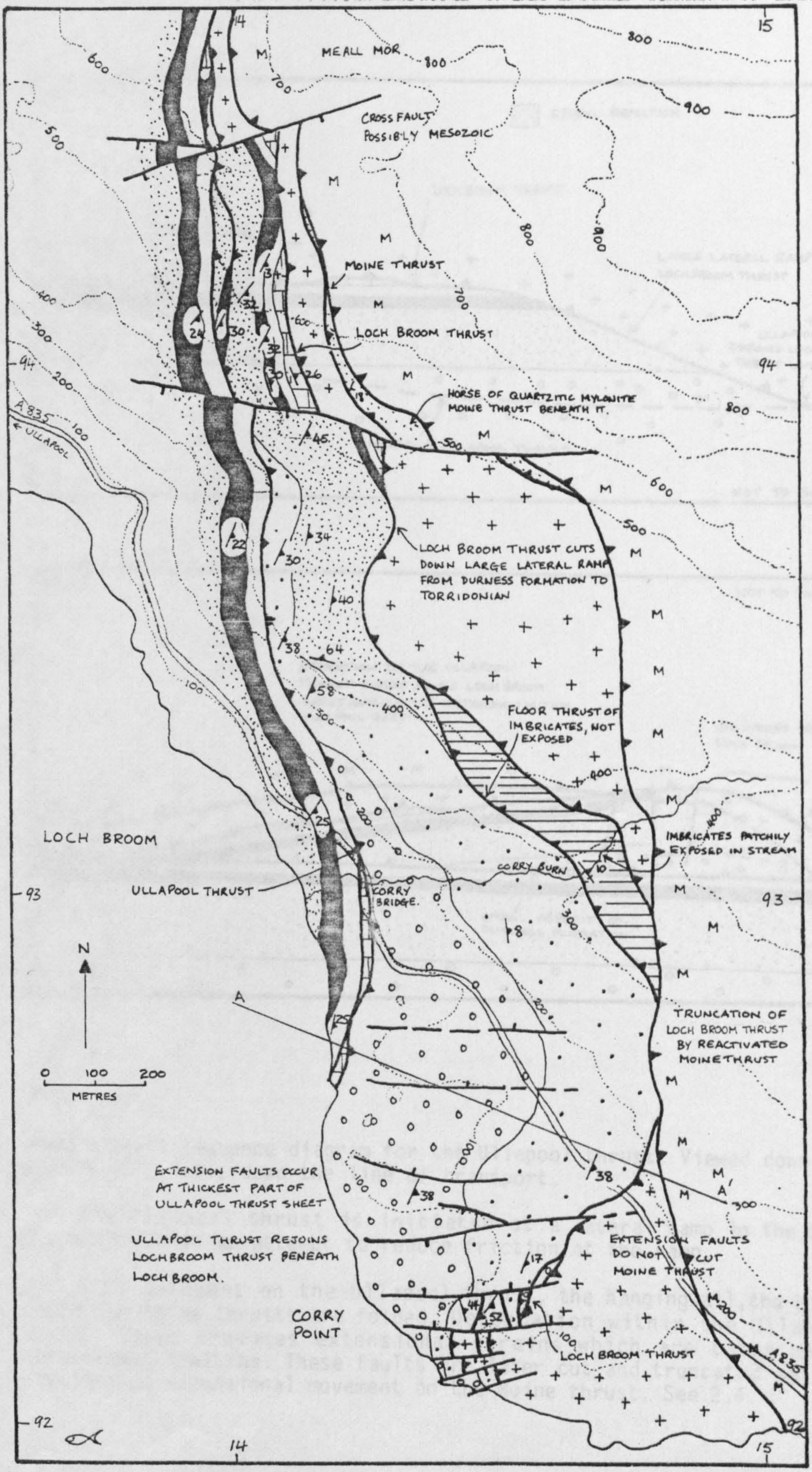
14
15
MEALL MOR
CROSS FAULT POSSIBLY MESOZOIC
MOINE THRUST
LOCH BROOM THRUST
HORSE OF QUARTZITIC MYLONITE MOINE THRUST BENEATH IT.
LOCH BROOM THRUST CUTS DOWN LARGE LATERAL RAMP FROM DURNESS FORMATION TO TORRIDONIAN
FLOOR THRUST OF IMBRICATES, NOT EXPOSED
IMBRICATES PATCHILY EXPOSED IN STREAM
CORRY BURN
CORRY BRIDGE.
ULLAPOOL THRUST
LOCH BROOM
TRUNCATION OF LOCH BROOM THRUST BY REACTIVATED MOINE THRUST
EXTENSION FAULTS OCCUR AT THICKEST PART OF ULLAPOOL THRUST SHEET
ULLAPOOL THRUST REJOINS LOCHBROOM THRUST BENEATH LOCH BROOM.
EXTENSION FAULTS DO NOT CUT MOINE THRUST
CORRY POINT
LOCH BROOM THRUST
A835
ULLAPOOL
A
A'
N
0 100 200
METRES
94
93
92

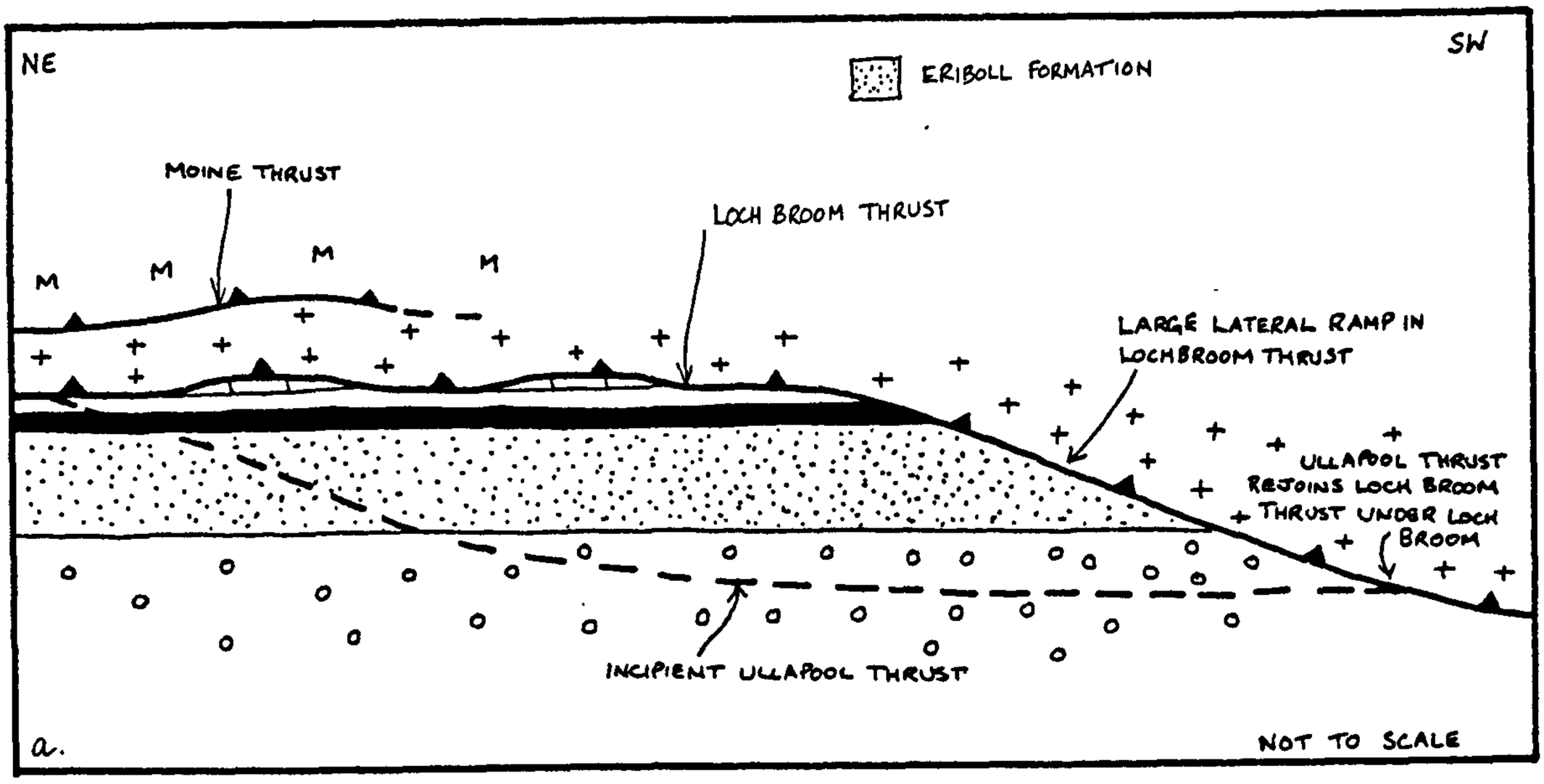

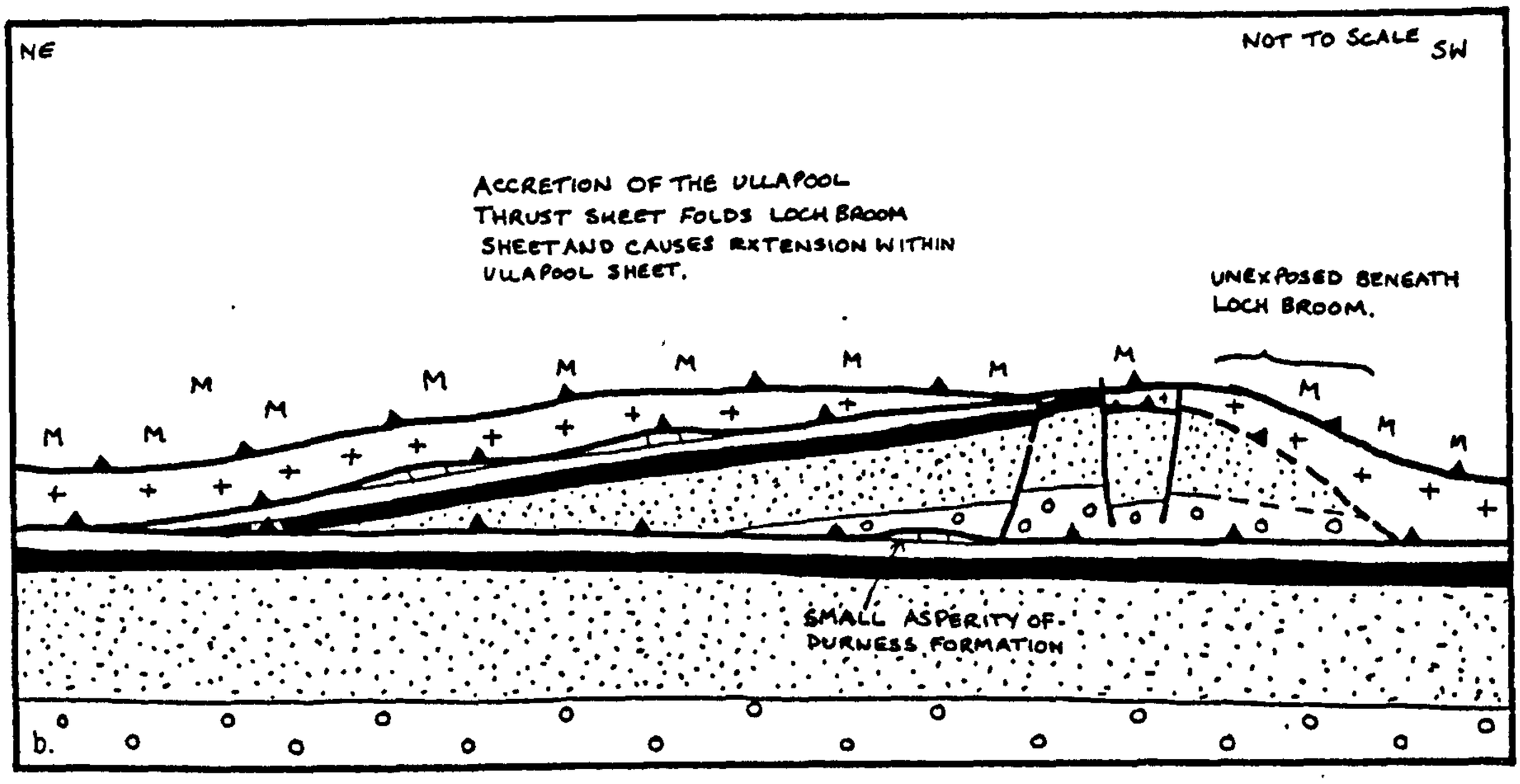

Fig. 2.8.

Hangingwall sequence diagram for the Ullapool thrust. Viewed down the thrust dip, i.e., down the line of transport.

a). The Ullapool thrust is initiated at a lateral ramp in the Loch Broom thrust as an attempt to reduce friction at the ramp.

b). With movement on the Ullapool thrust, the hangingwall, the Loch Broom and Moine thrusts are folded. Deformation within the Ullapool thrust sheet produces extensional strains which are taken up by extensional faulting. These faults are later cut and truncated by the reactivated extensional movement on the Moine thrust. See 2.4.

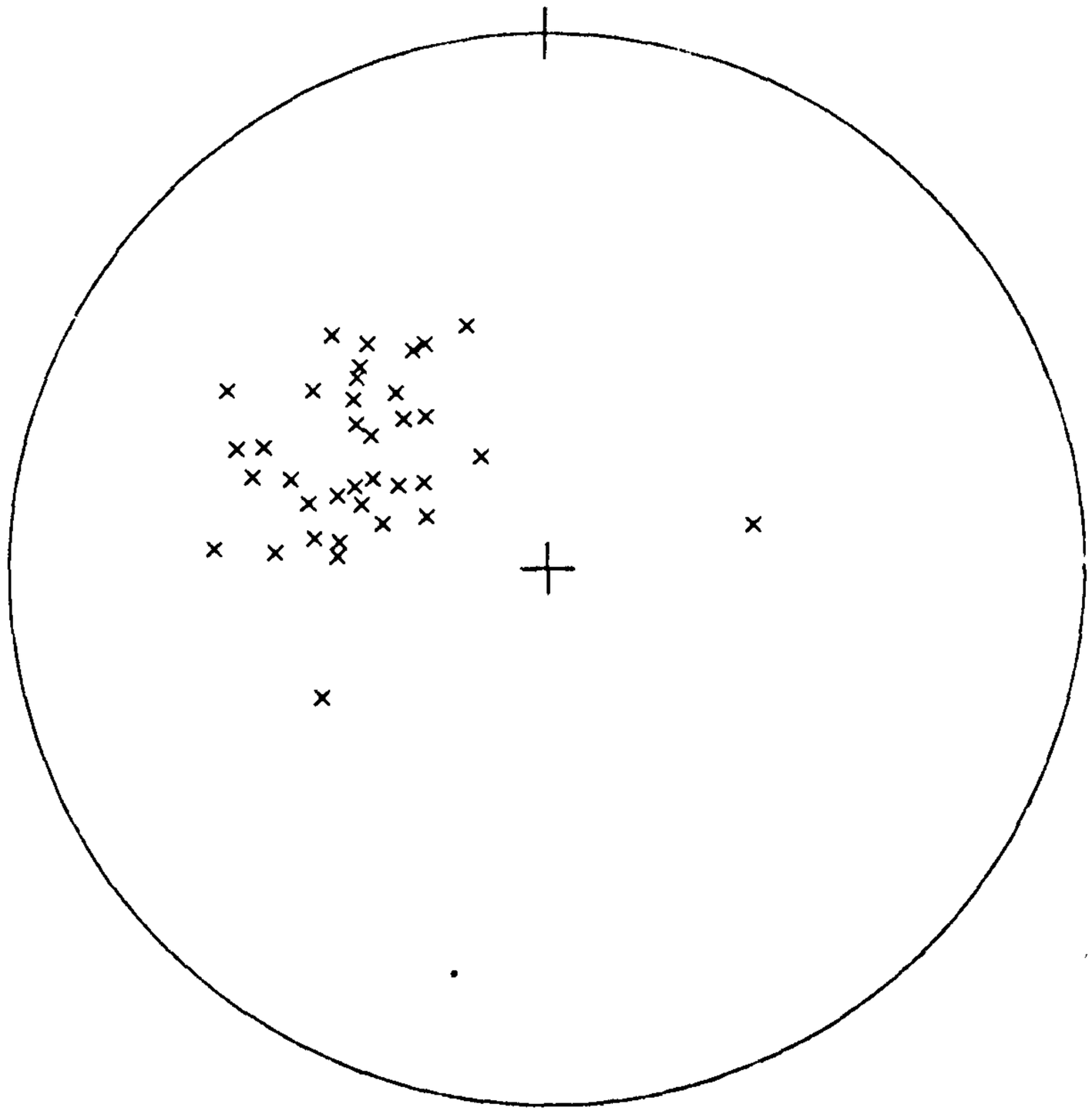

Fig. 2.9.
Equal area
Stereogram of poles to bedding in Sheet IV at Achall. Note the spread of dips as a result of rotation on the extension faults in Sheet IV. Lower hemisphere projection. See 2.5.1.1.

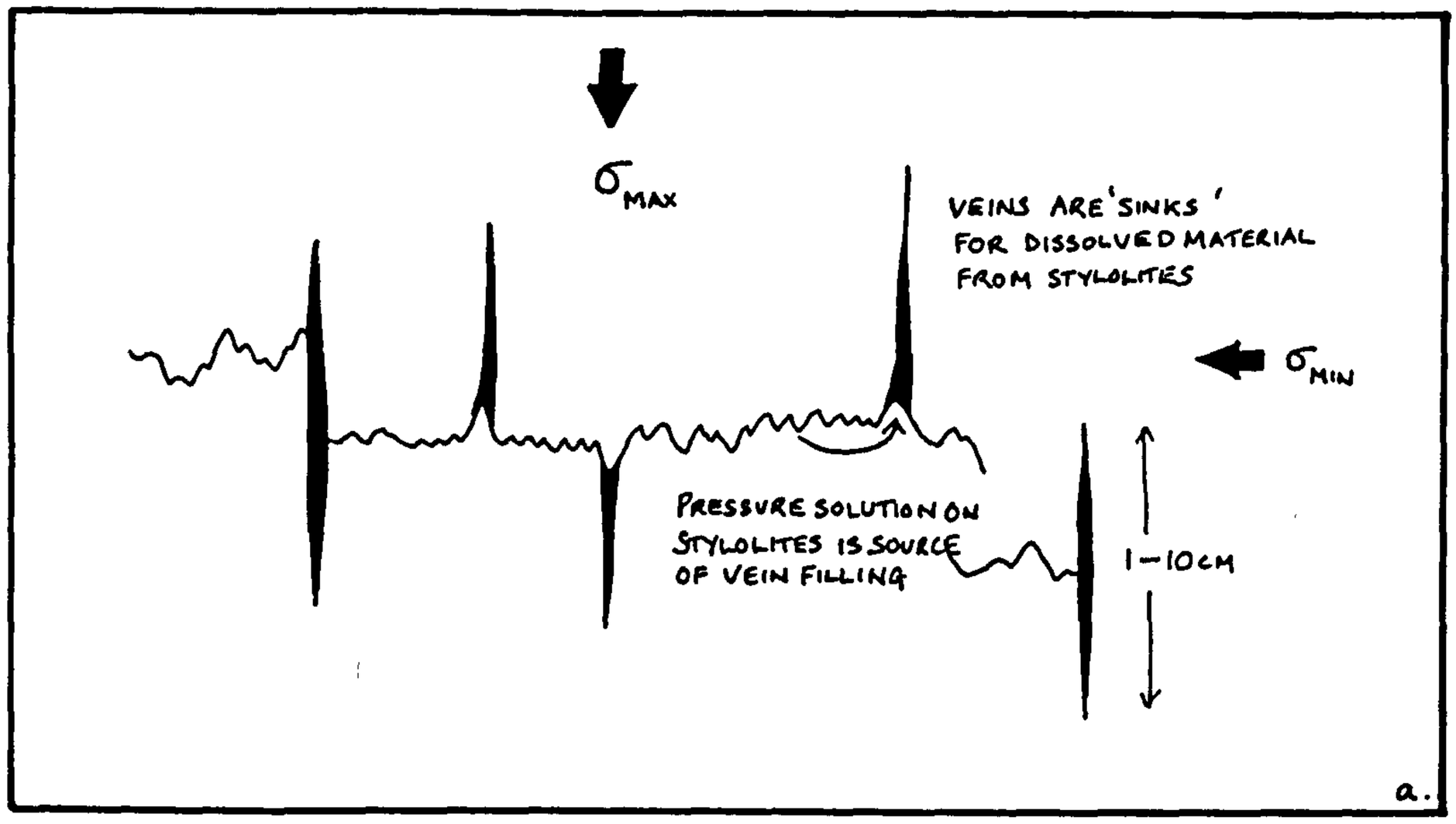

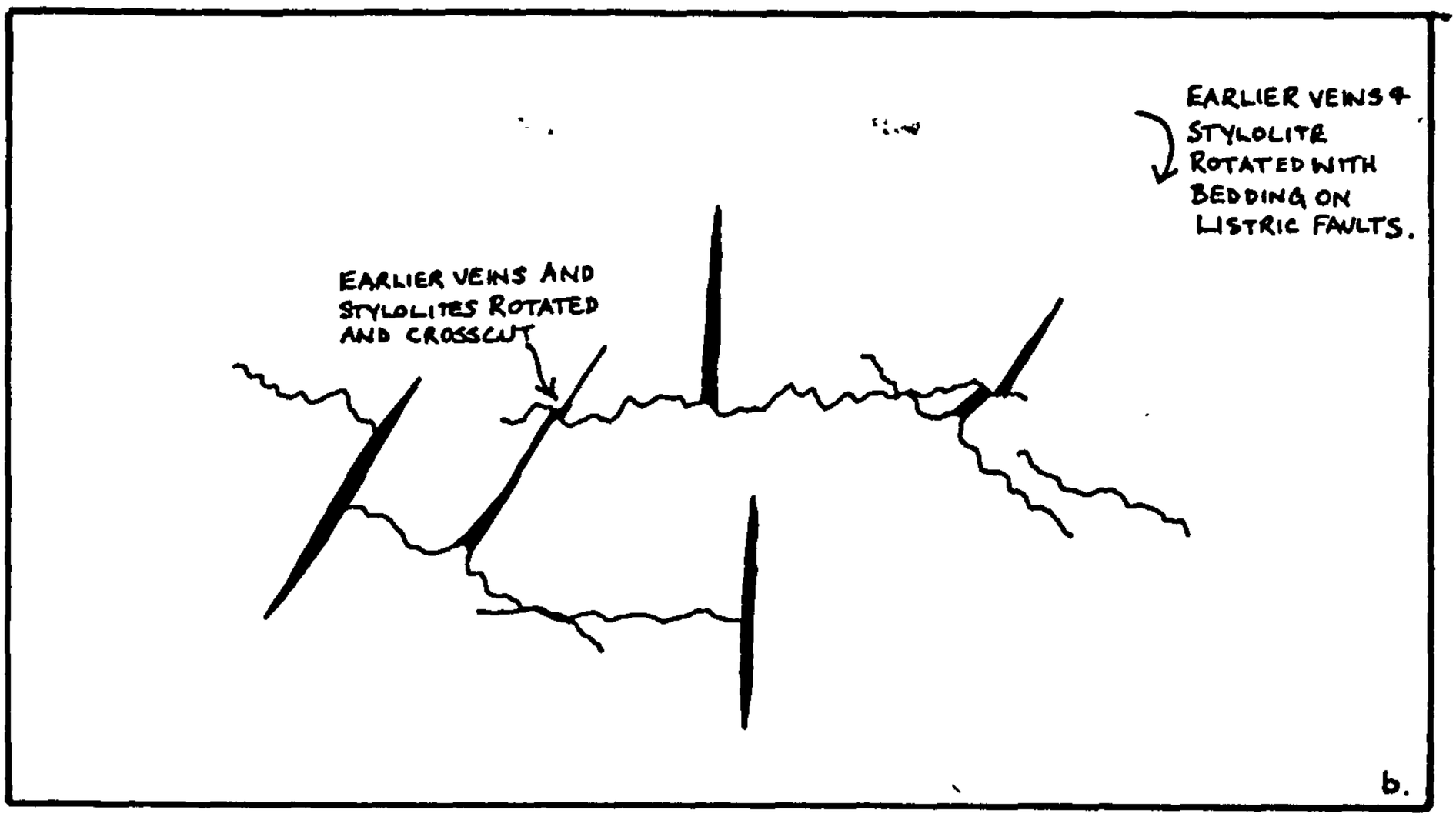

Fig. 2.10.

Diagram to show relationship between tectonic veins and bedding parallel stylolites. These are illustrated with respect to the stress system active during the extensional faulting. Material dissolved by pressure solution along the stylolites is deposited in the veins. With rotation of bedding by movement on the faults, earlier veins and stylolites are also rotated. Later episodes of veining during increments of slip produce cross-cutting relationships. See 2.5.1.1.

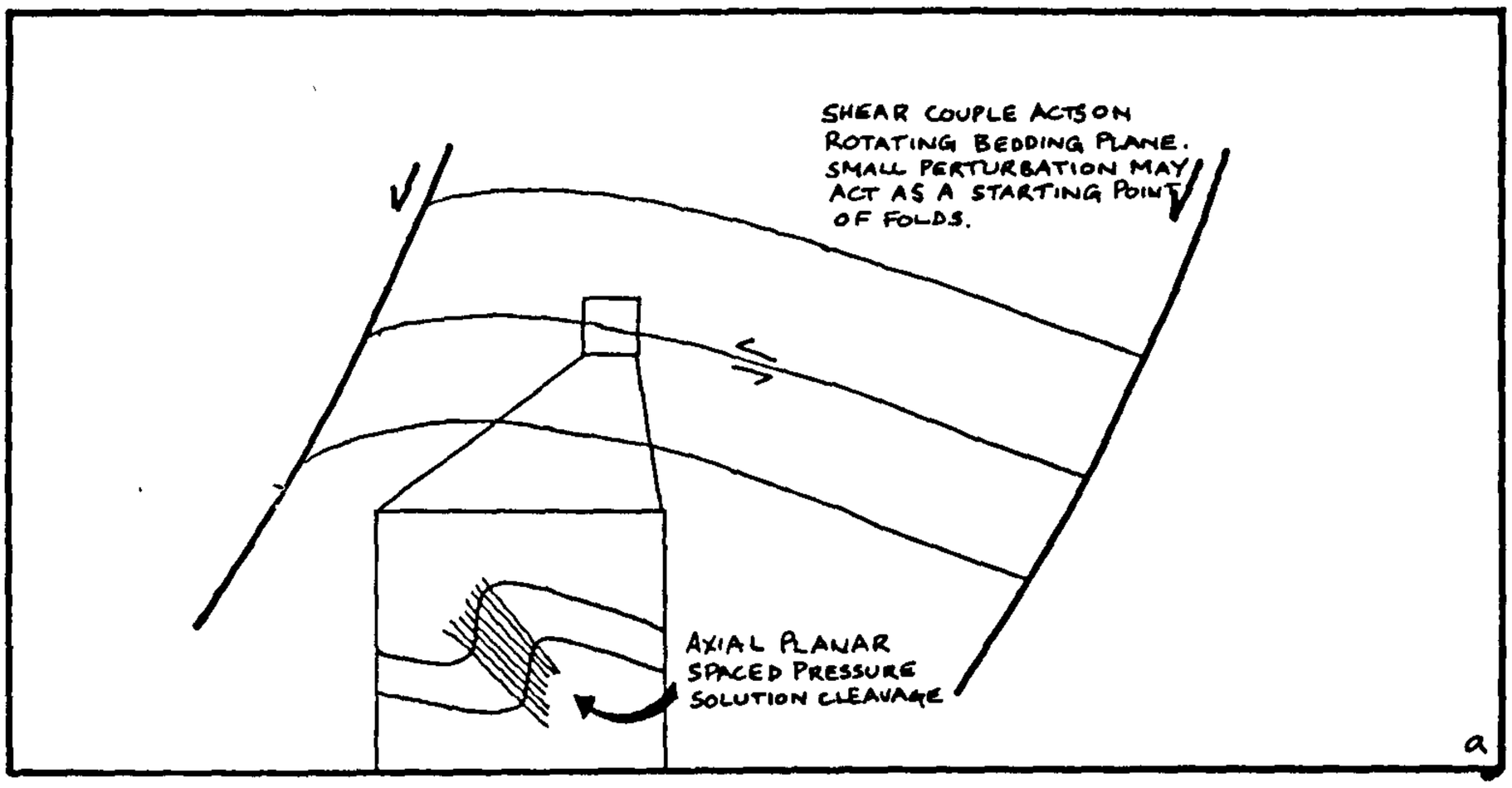

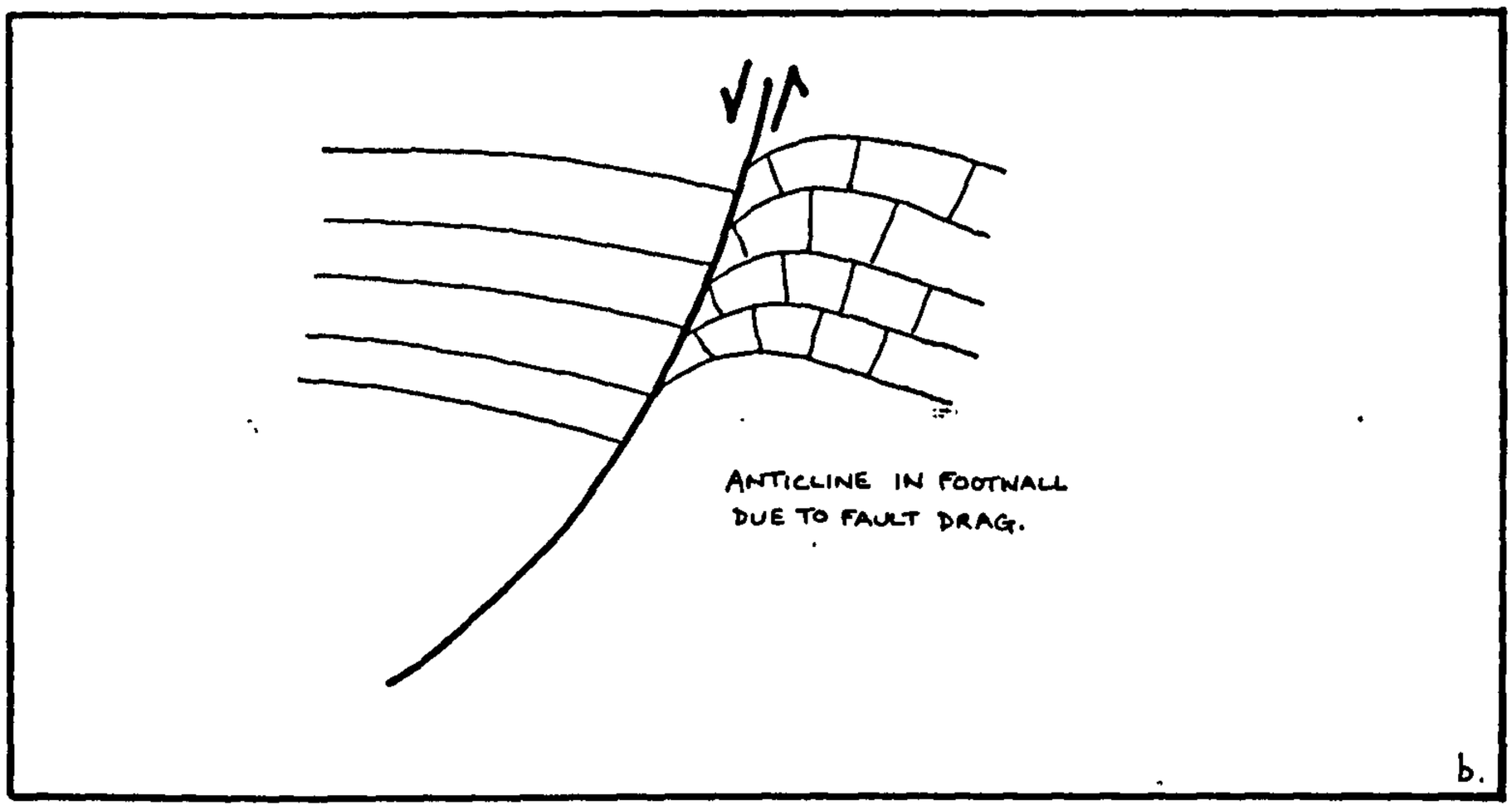

Fig. 2.11.

Sketch diagram to illustrate styles of folding in Sheet IV. See 2.5.1.2.

a). Folds formed by a shear couple acting on the bedding planes during rotation on the extensional faults. The folds may have amplified from a small perturbation.
b). Folds formed by drag on a fault plane.

Fig. 2.12.

Equal area
Stereograms of poles to NE-SW extension faults and tectonic veins.

a). NE-SW extension faults; the spread of the poles is a result of the listric geometry of the faults. Lower hemisphere projection.

b). Tectonic veins which formed synchronously with the faults. The spread of the poles is a result of rotation firstly on the NE-SW extension faults, and secondly on the NW-SE extension faults. Lower hemisphere projection. See 2.5.1.3a.

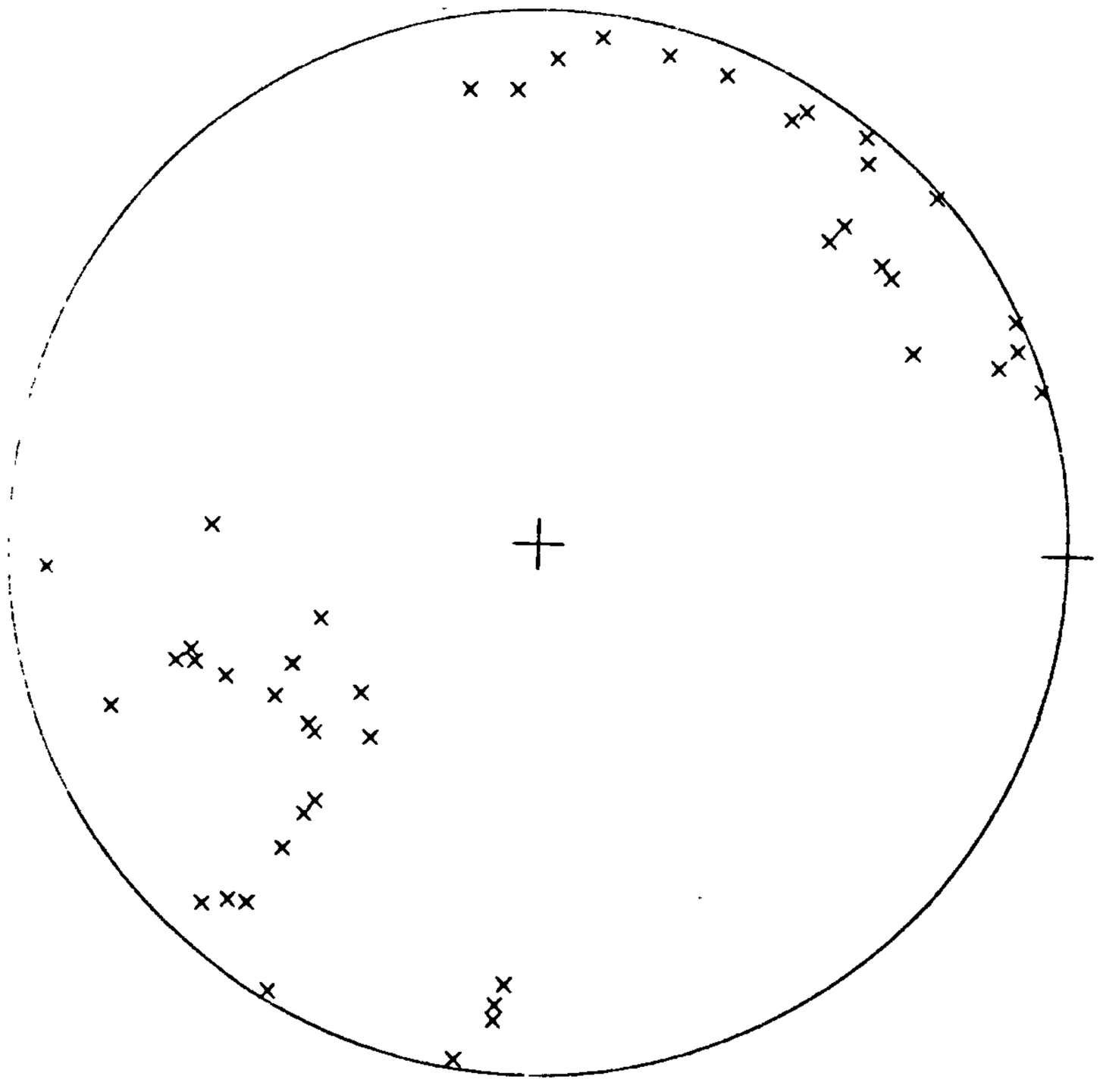

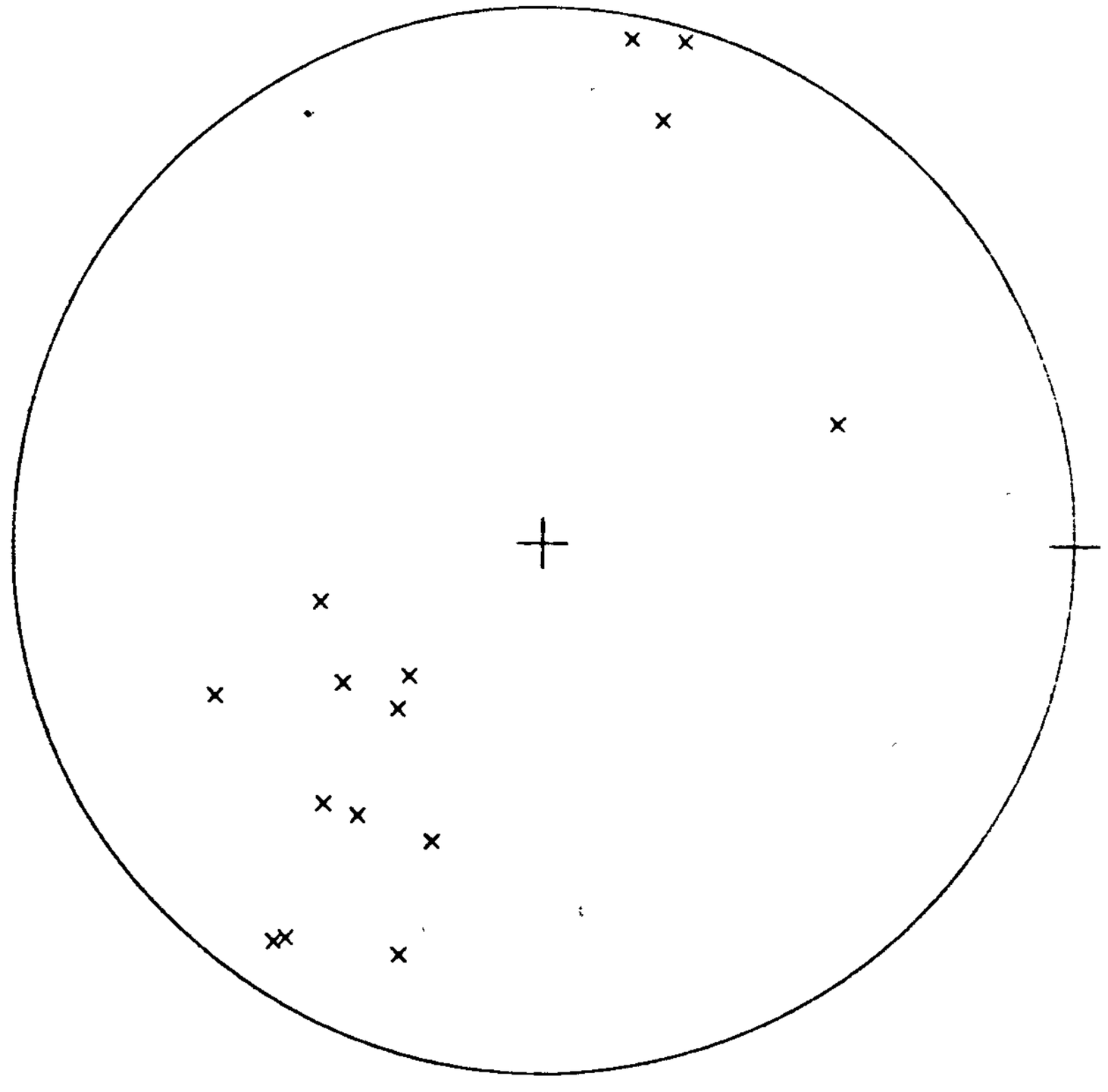

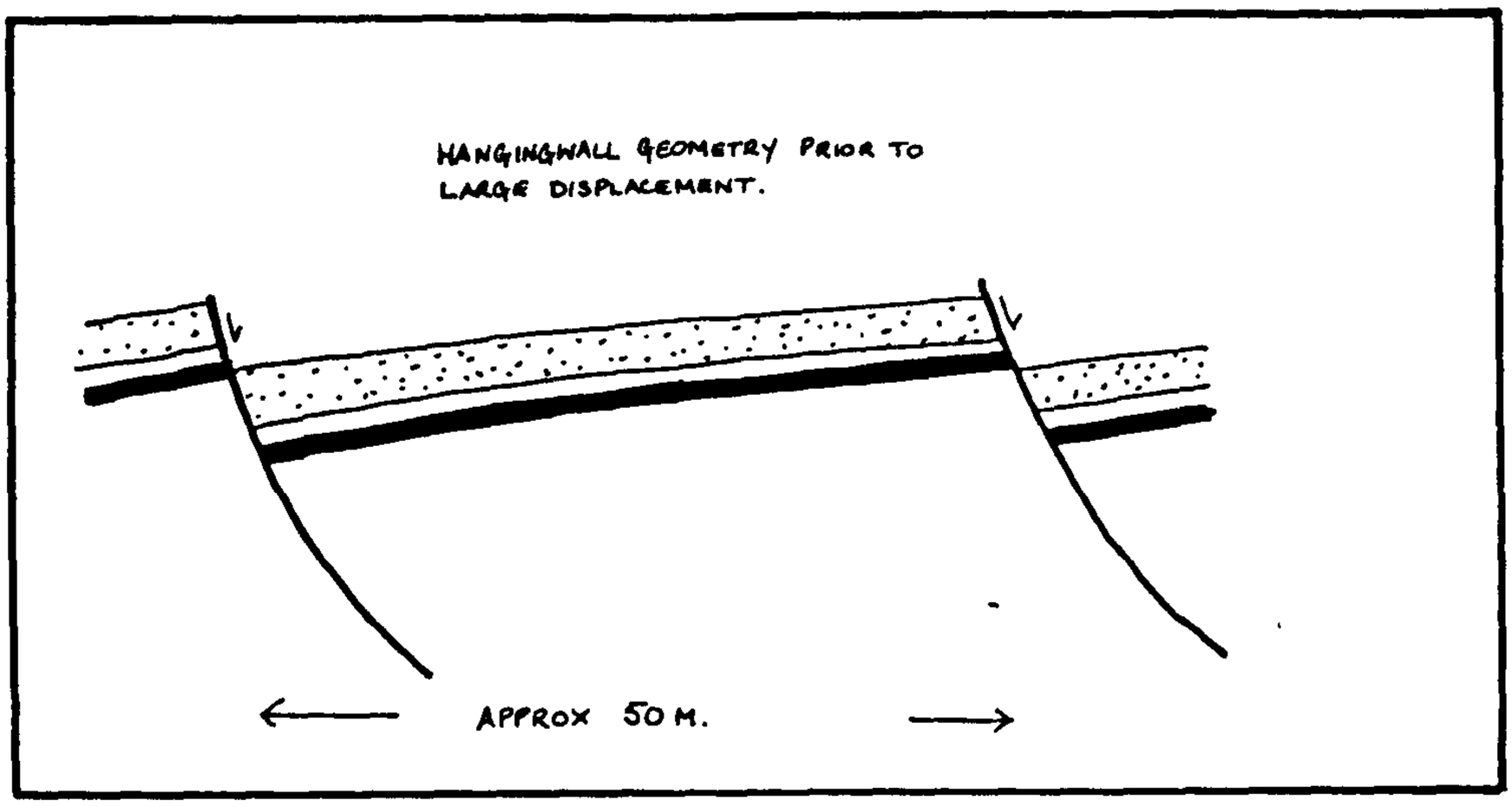

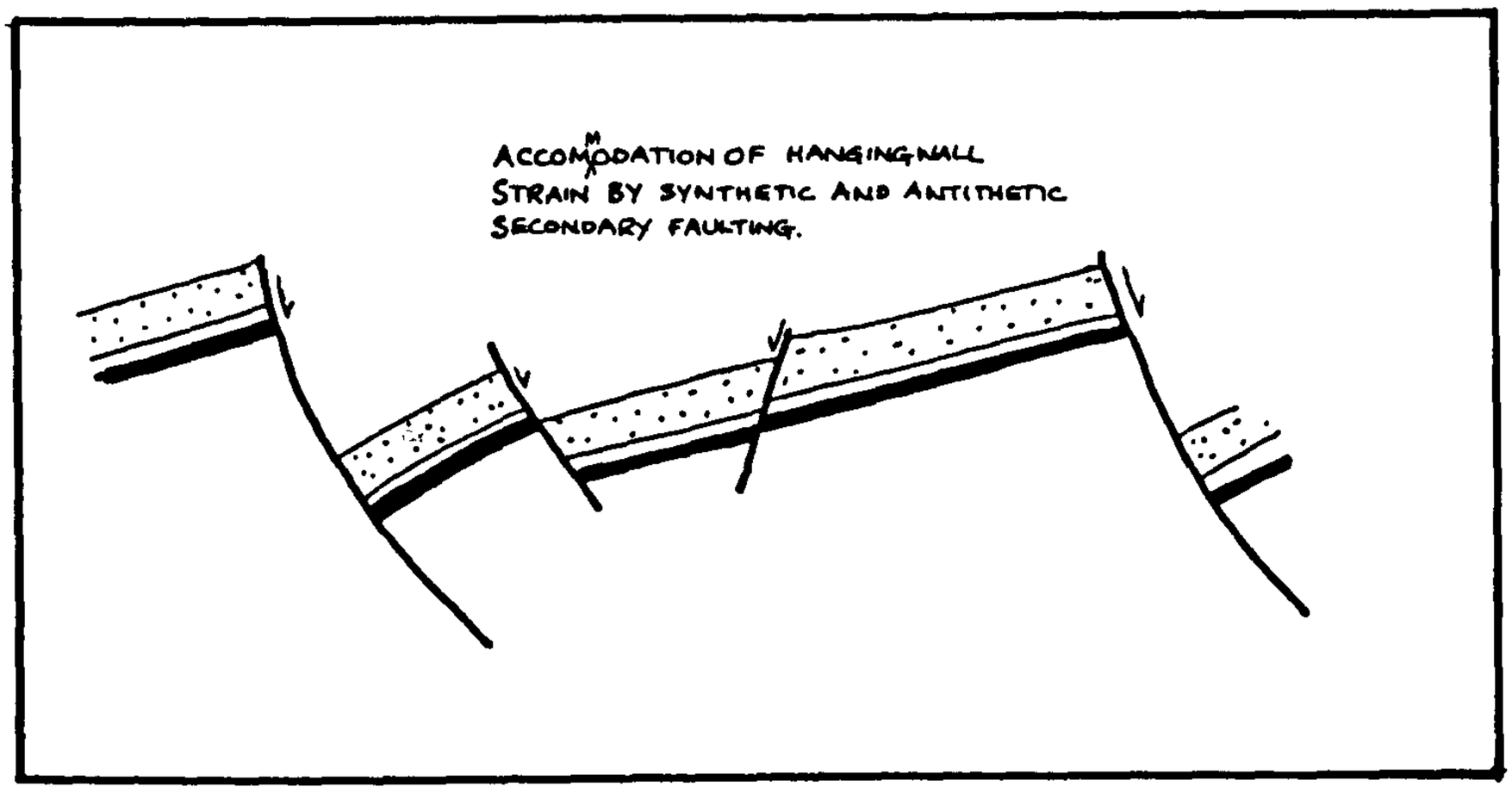

Fig. 2.13.

Sketch diagram to illustrate the development of secondary synthetic and antithetic extension faults. These are a result of hangingwall deformation to accomodate rotation on the first order listric extension faults. See 2.5.1.3a.

Fig. 2.14.

a). Equal area Stereogram of poles to NW-SE extension faults in Sheet IV. Lower hemisphere projection.

b). Equal area Stereogram of poles to tectonic veins which formed concomitantly with the NW-SE extension faults. Lower hemisphere projection.
See 2.5.1.3b.

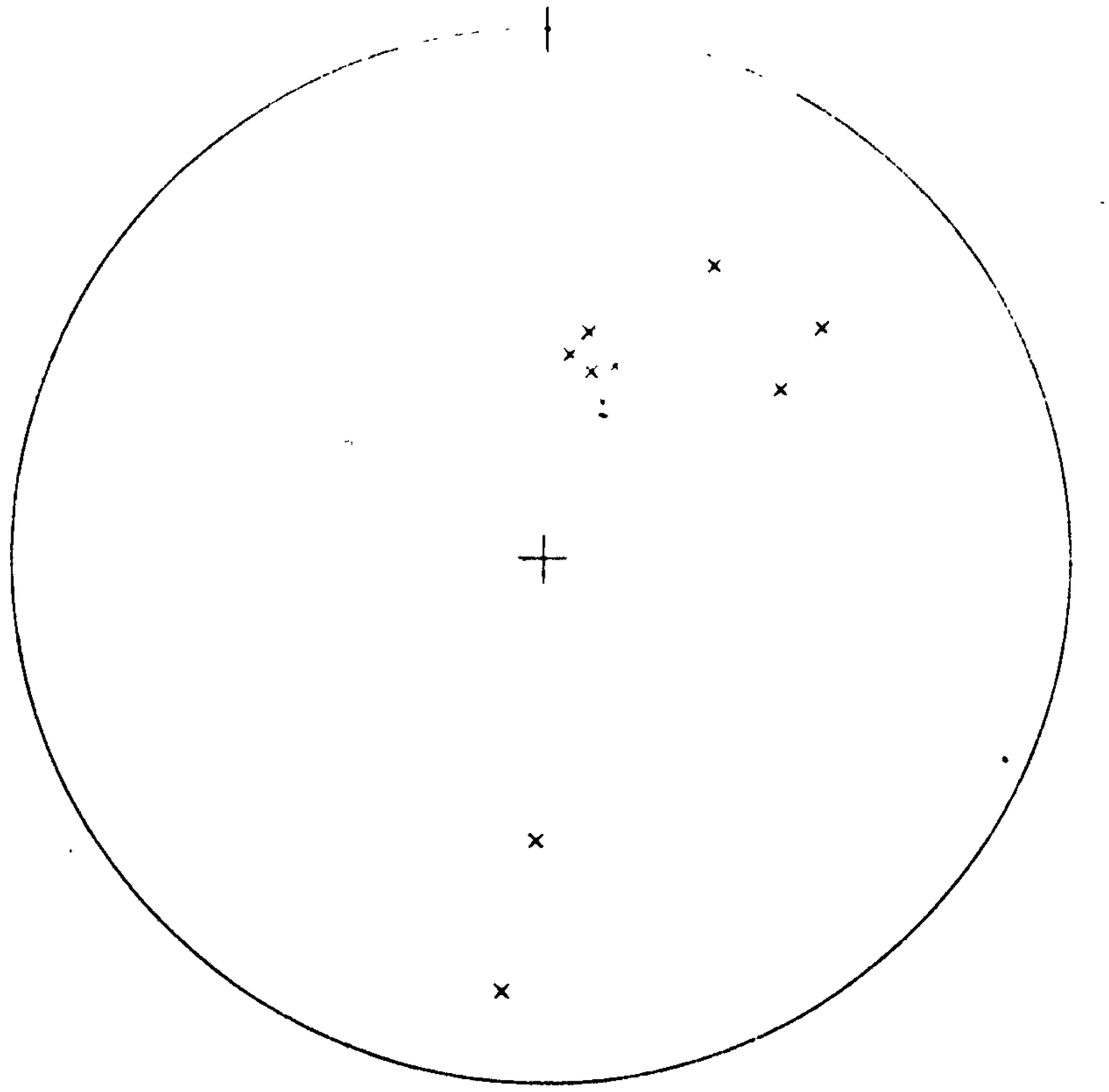

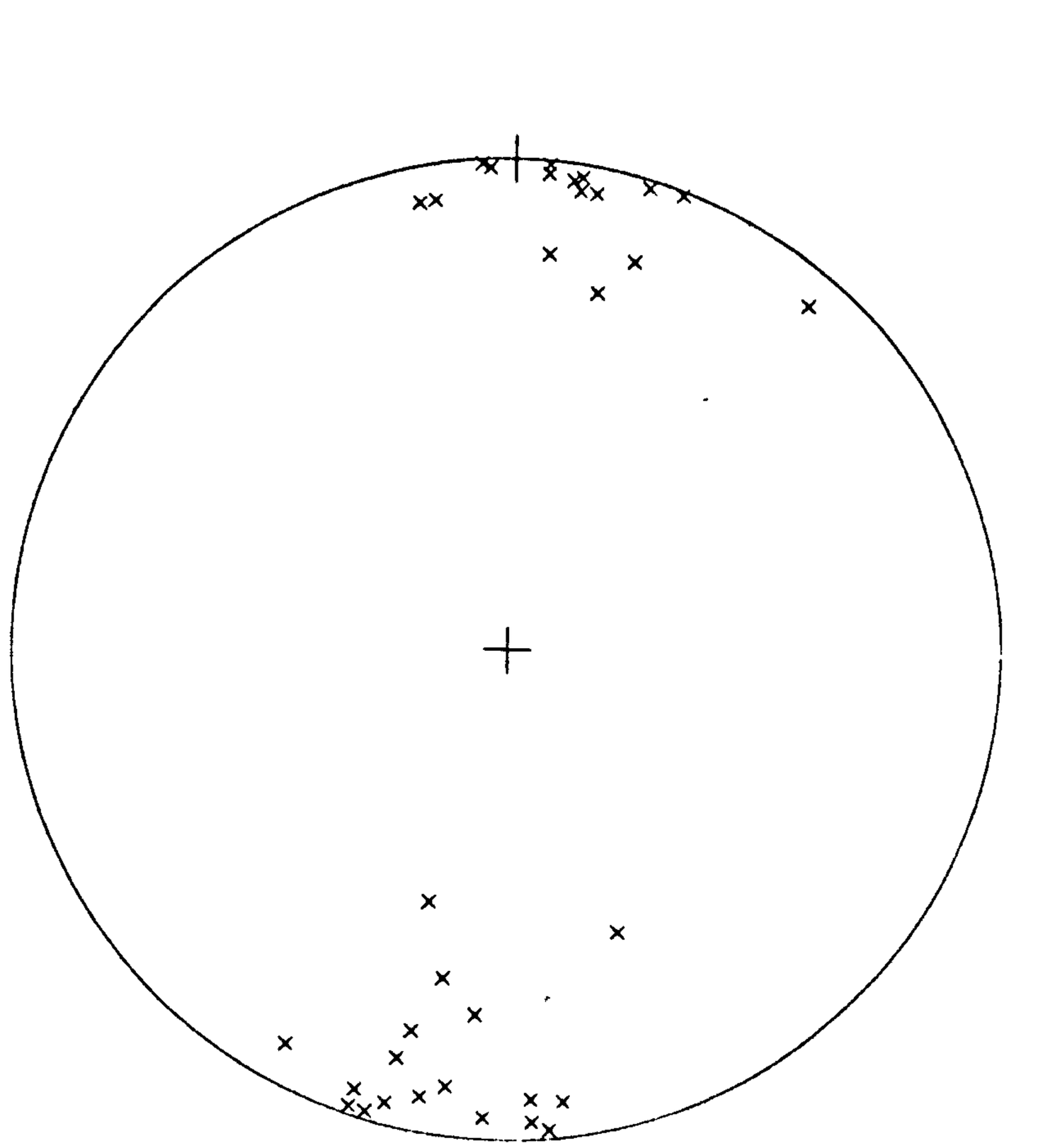

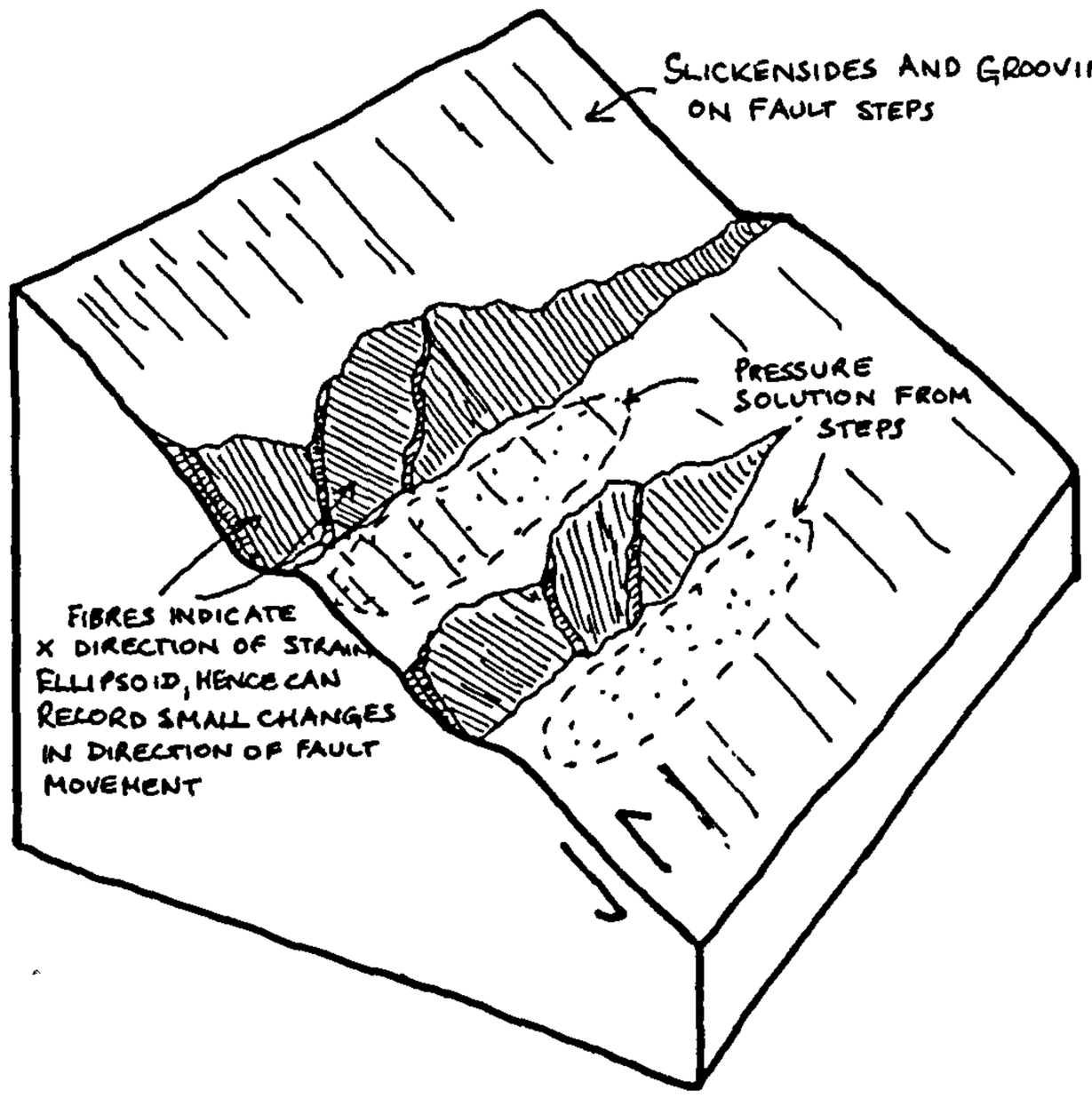

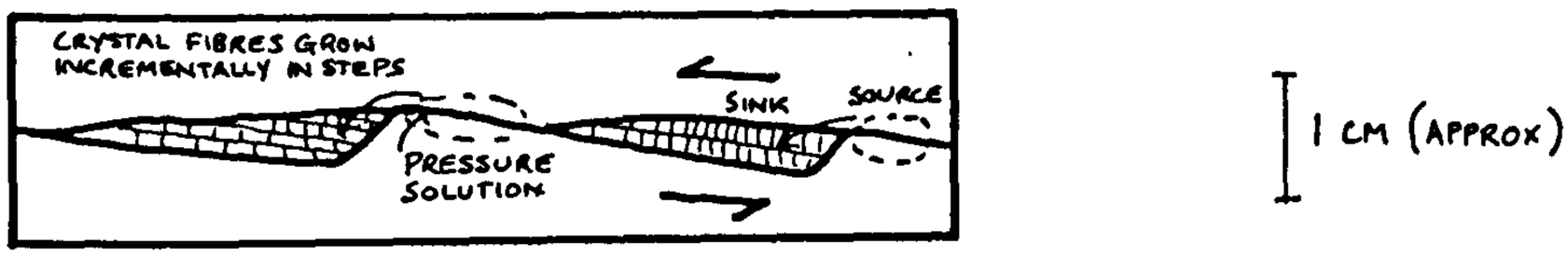

Fig 2.15

Sketch block diagram to show the development of crystal fibre growths at small steps in a fault plane. Crystal fibre growths grow in the lee of the steps, with their long axes representing the X direction of the deformation strain ellipsoid. Any small change in the movement vector of the fault will be reflected in the fibre growths by a change in their orientation. Fibre growths build up incrementally in steps,(see small diagram). Material forming the fibres is removed from the steps by pressure solution. See 2.5.1.3b.

Fig 2.16.

a). Equal area Stereogram of poles to strike slip faults in Sheet IV. Lower hemisphere projection.

b). Equal area Stereogram of the long axes of the crystal fibre growths on the strike slip fault planes. Lower hemisphere projection. See 2.5.1.3c.

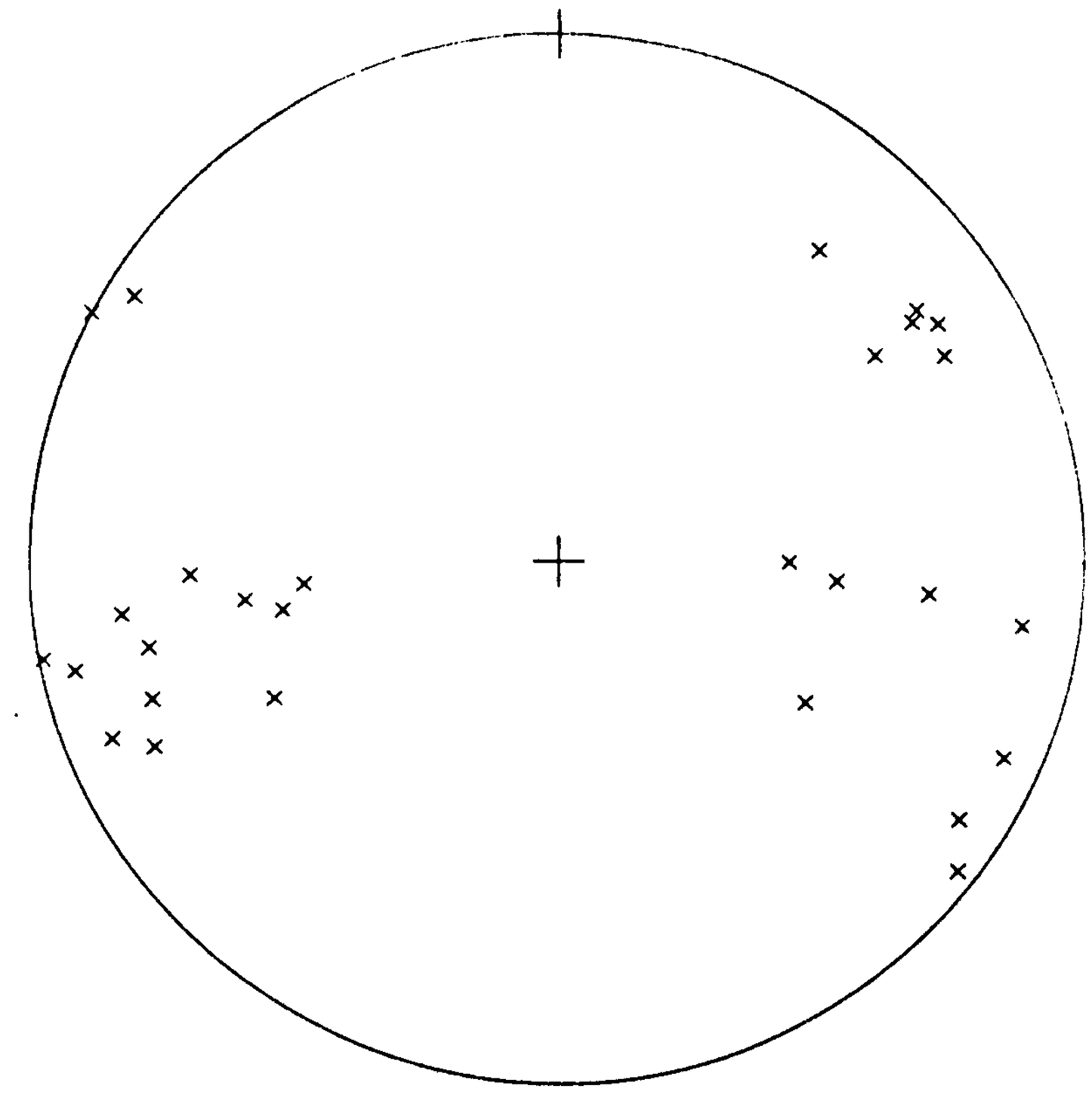

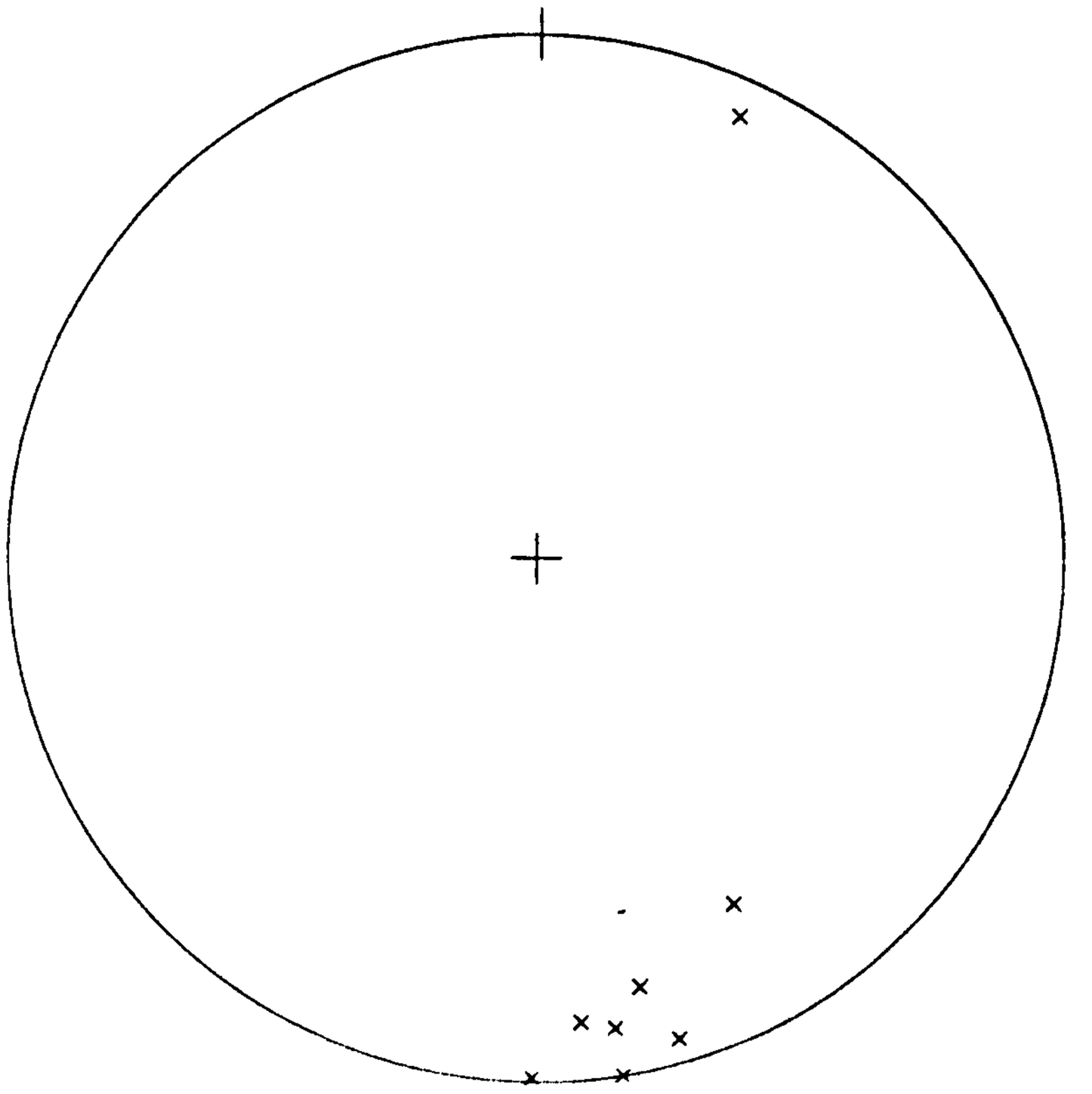

Fig. 2.17.

Diagrams to illustrate the Andersonian relationship between fault geometry and the principal stesses for a). reverse faults, b).extension faults, and c). strike slip faults. $_1$ = maximum principal stess, $_3$ = minimum principal stress. See 2.5.1.3c.

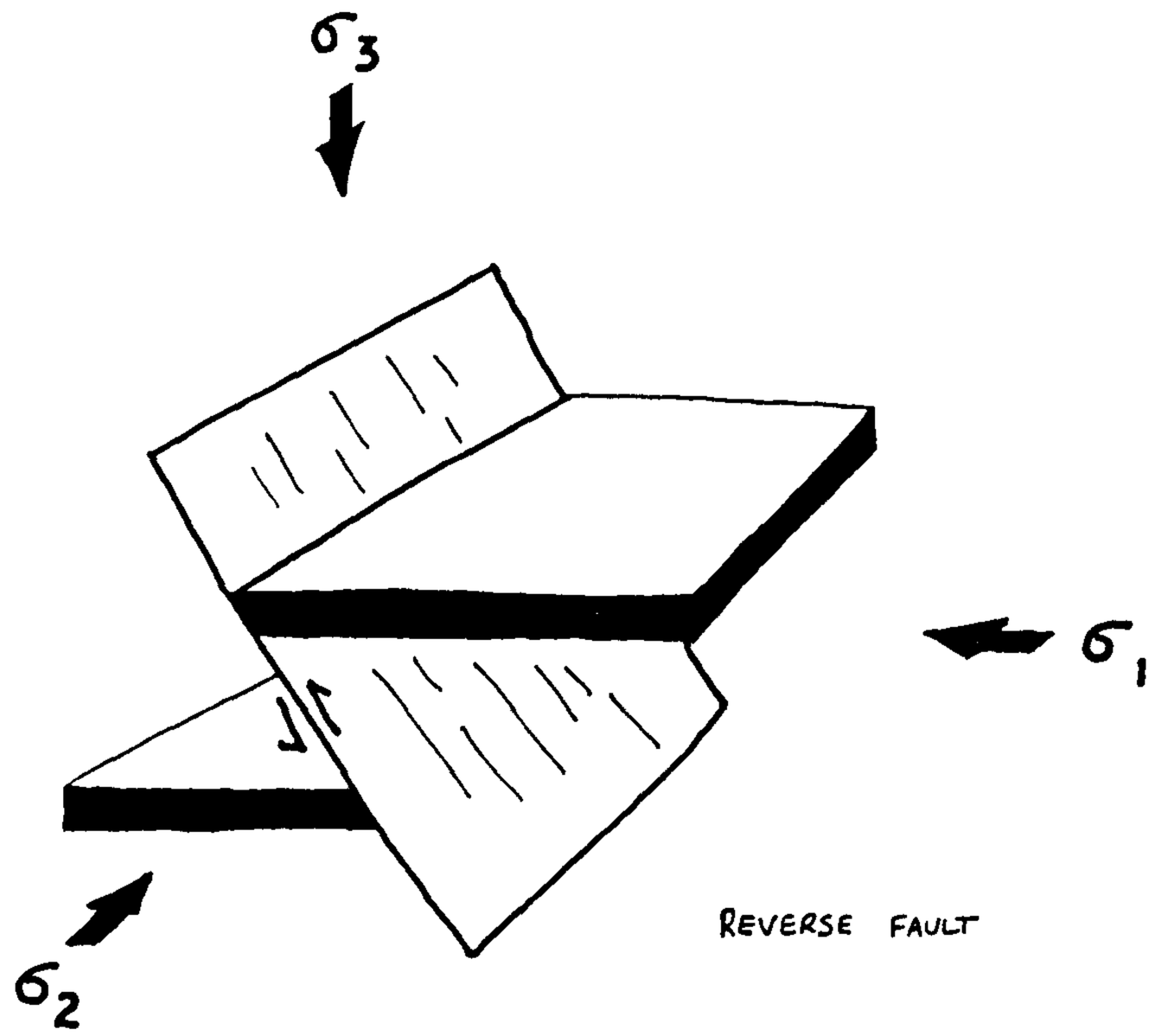

REVERSE FAULT

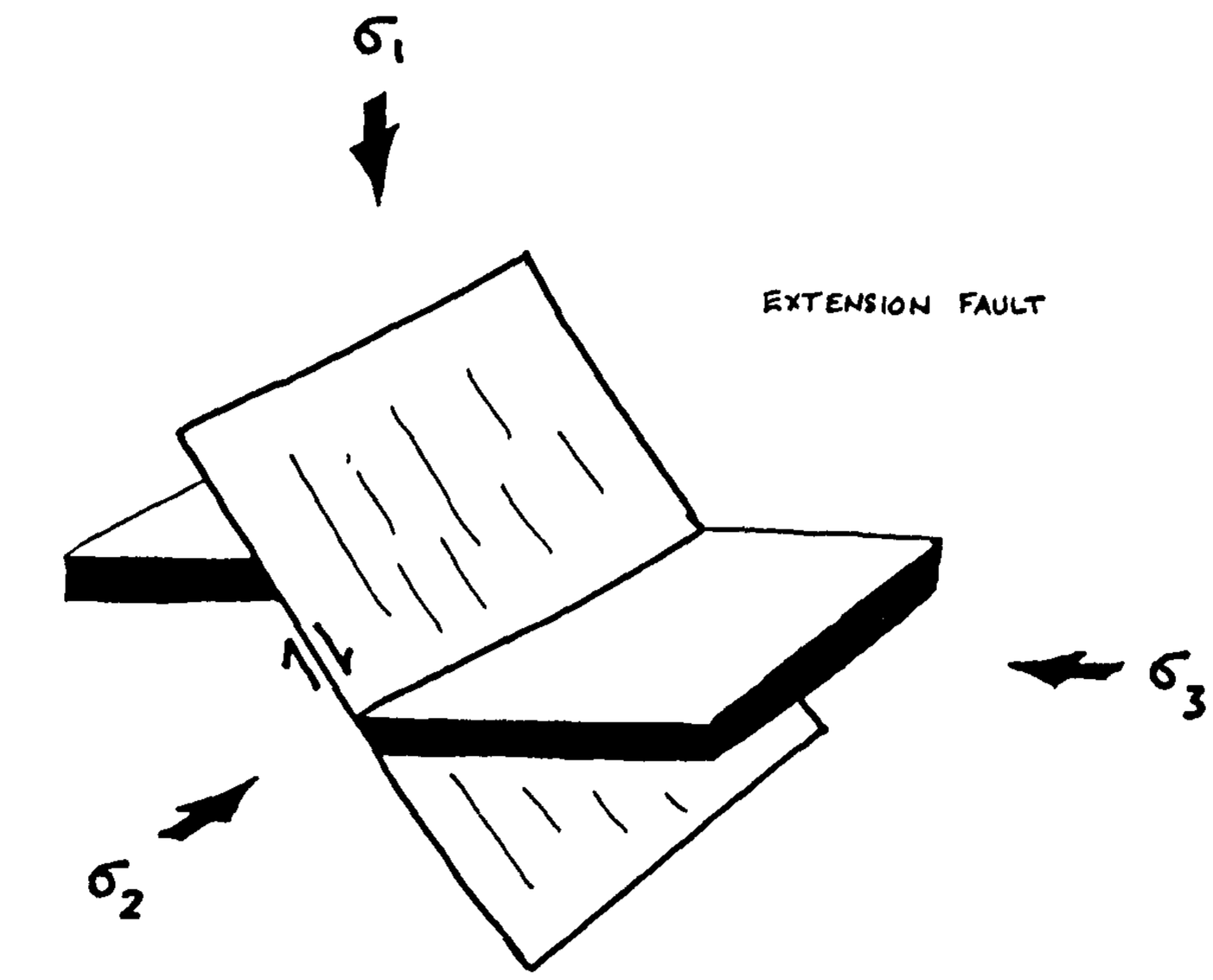

EXTENSION FAULT

STRIKE SLIP FAULT

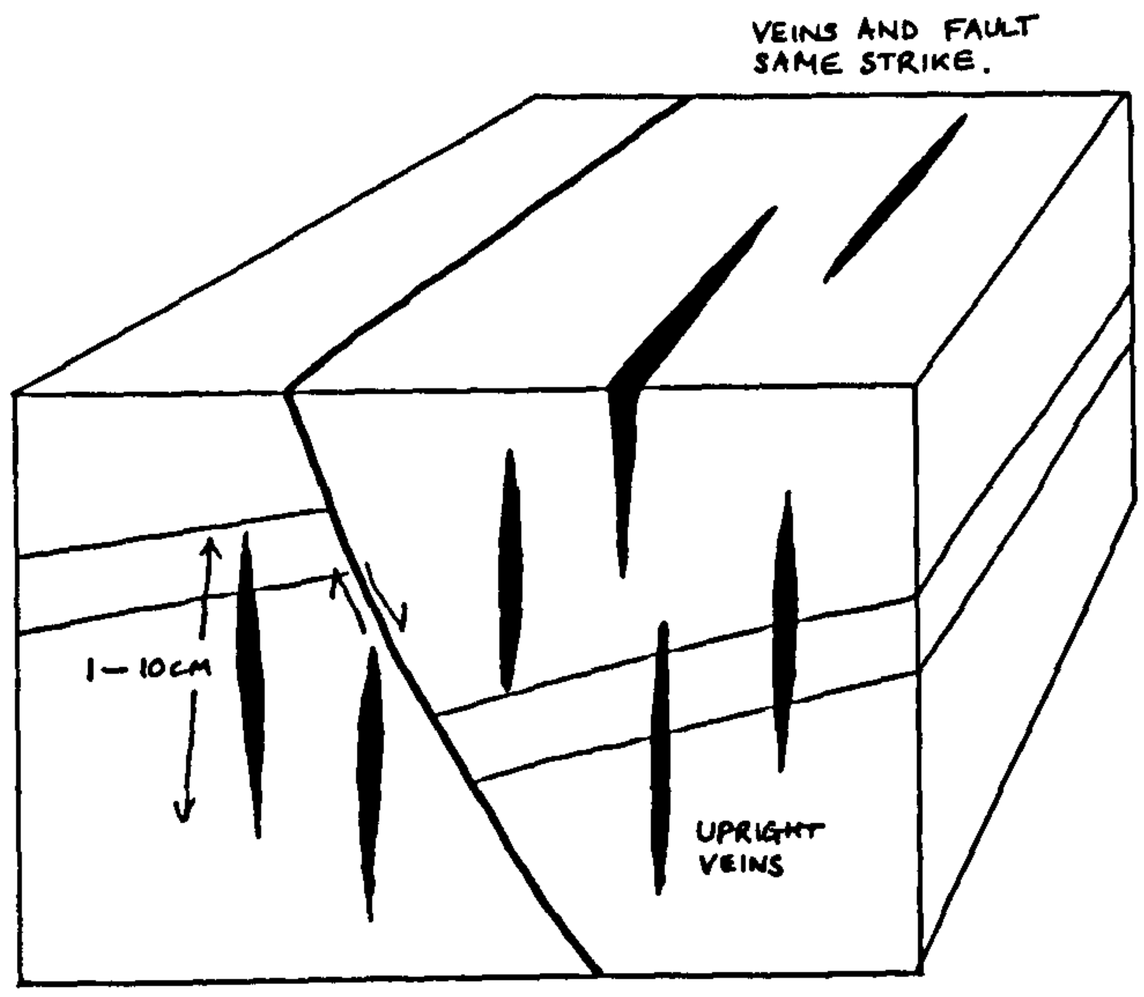

Fig 2.18.

Block diagram to show the geometric relationship between an extension fault and concomitant tectonic veins. Such veins have been interpreted as pre-failure fracture arrays, Sibson (1981). See 2.5.1.4.

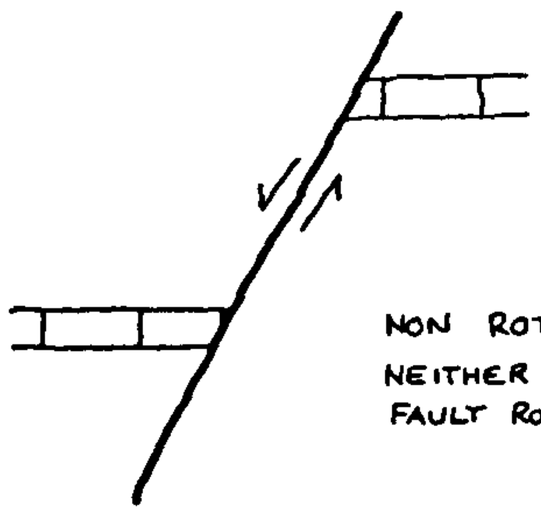

a.

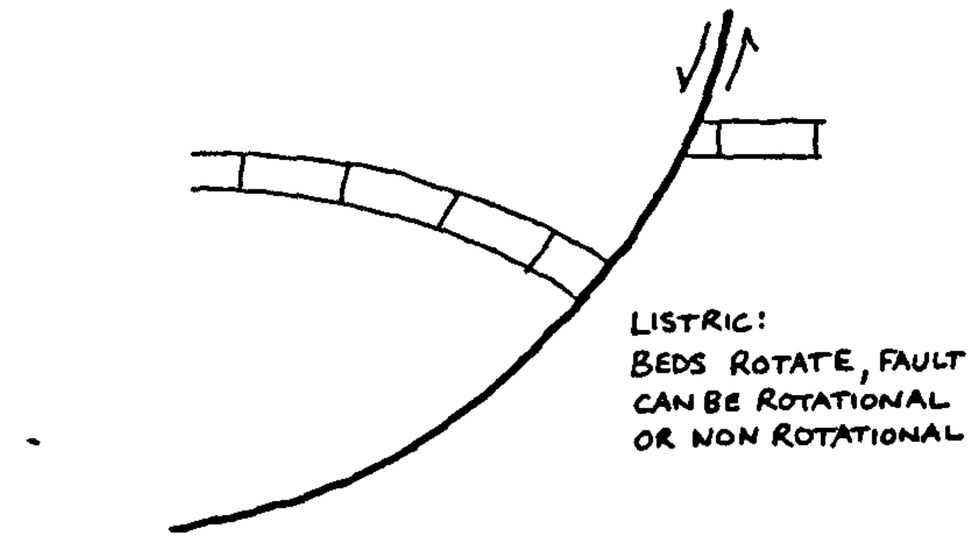

b.

PLANAR ROTATIONAL.

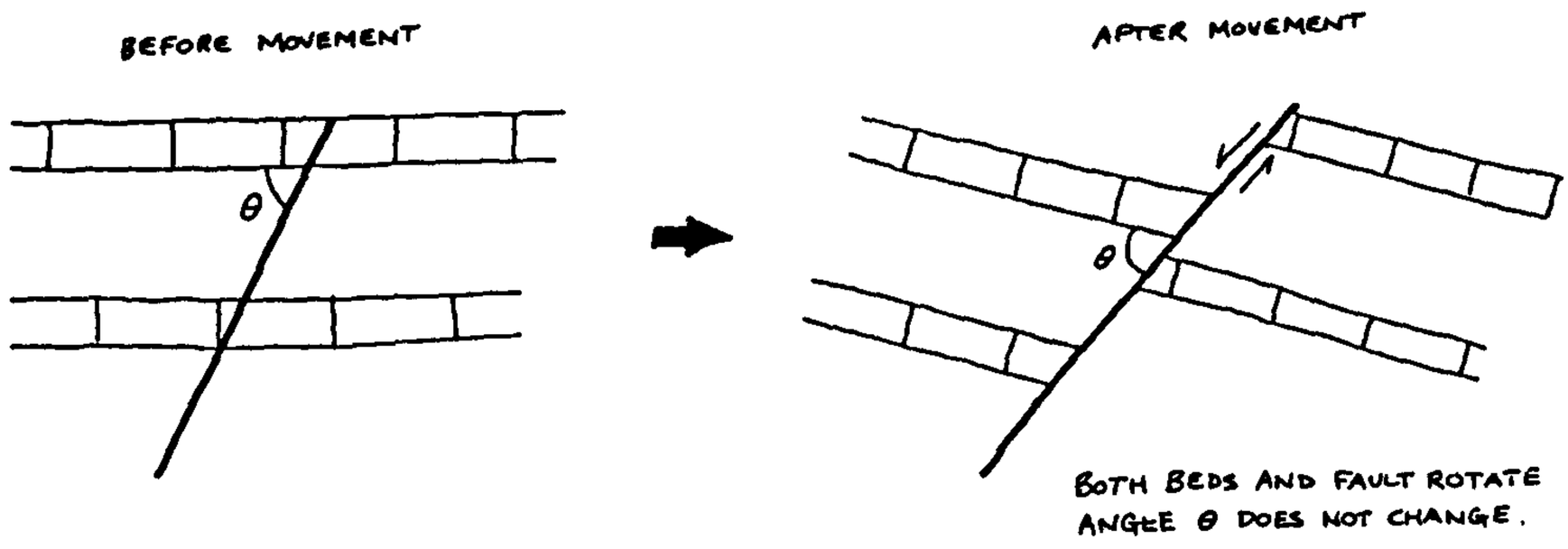

c.

RELATIONSHIP OF FAULT STYLE SEEN AT ACHALL

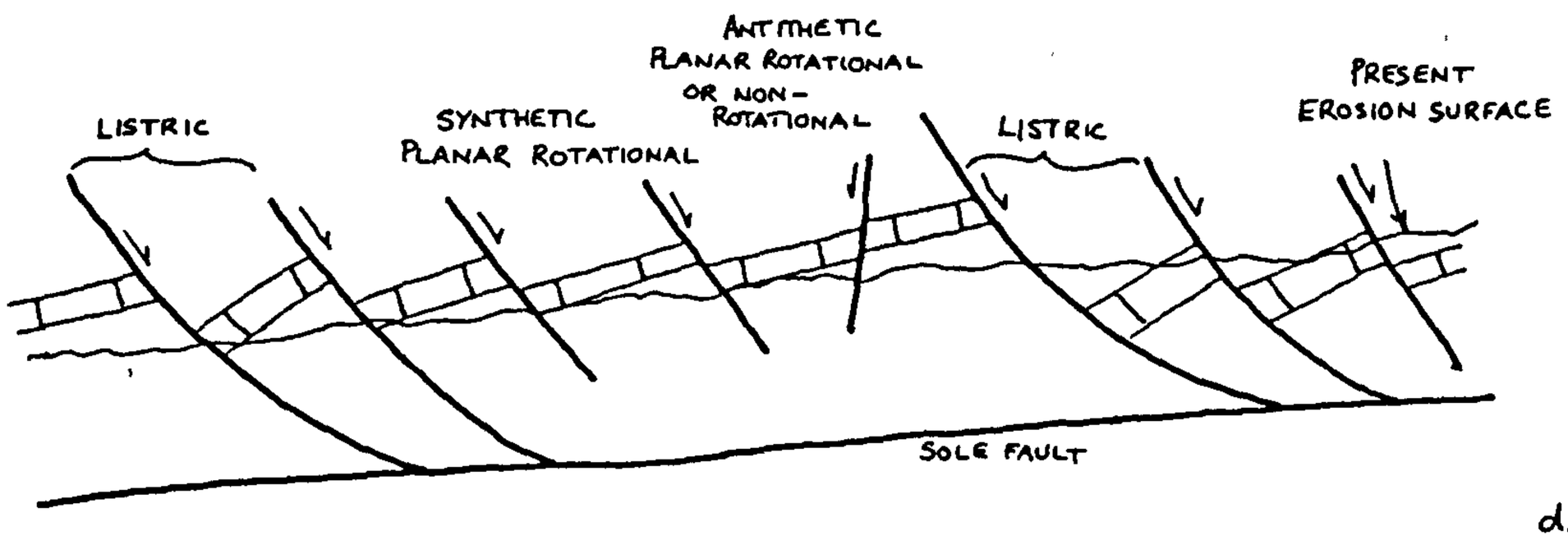

d.

Fig. 2.19.

Sketch diagrams to illustrate the classification of extension faults of Wernicke & Burchfiel (1982), a). non-rotational, b). listric, and c). planar rotational, note that the angle between the fault plane and the bedding remains constant during displacement, hence the fault planes also rotate.

d). sketch diagram to illustrate the most likely relationship between classes of extension faults observed in Sheet IV at Achall, not to scale.
See 2.5.1.5.

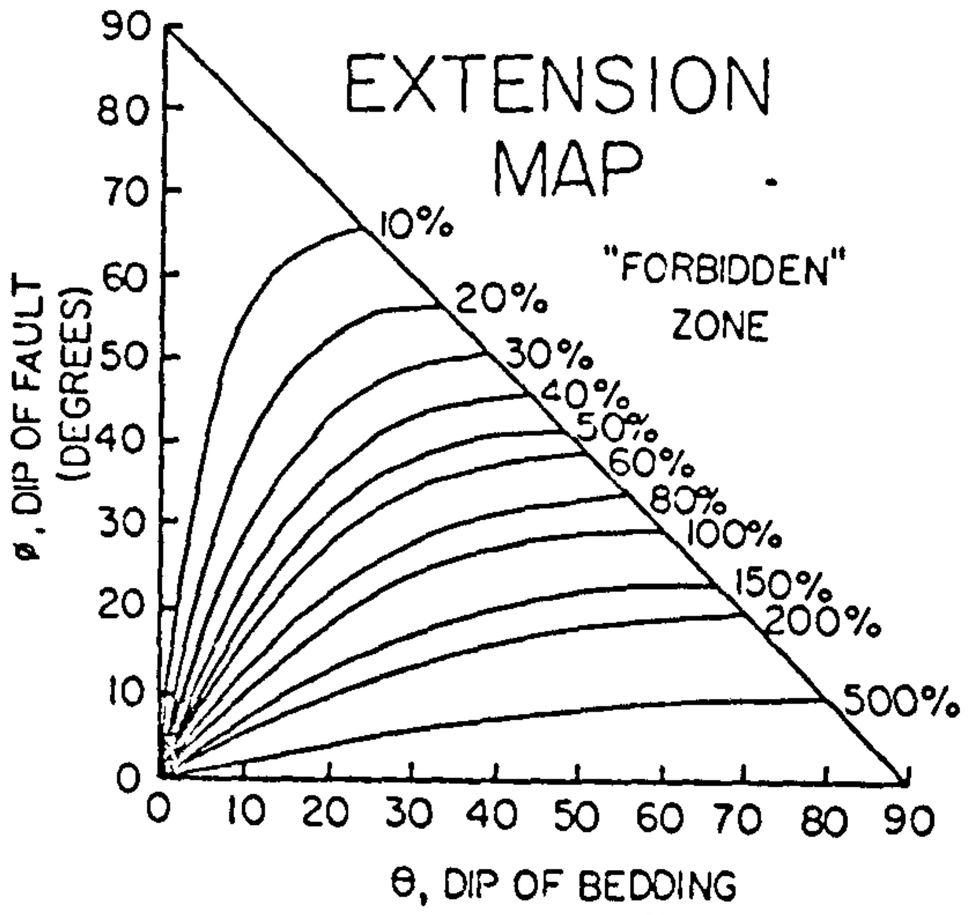

Fig. 2.20.

Extension map from Wernicke & Burchfiel (1982) for planar rotational faults. As the majority of the faults in Sheet IV are planar rotational faults, then the map can give a minimum estimate of extension as it is not possible to produce a restored section. The map gives an approximate estimate of 30% extension in Sheet IV.

Plate.2.1. Periclinal folds within Sheet IV at Creag nam Broc. Note the axial planar pressure solution cleavage. The folds are probably a result of shear stresses acting on the bedding planes during rotation on the listric extension faults.

Plate.2.2. View looking south of the N.E.-S.W. extension faults in the Achall quarry. Note the differential slip across the fault marked A, indicating a listric geometry.

PLATE 2.1

PLATE 2.2

Plate.2.3. View(looking N.N.E)of the N.W.-S.E extension faults in the south facing wall of the Achall quarry.

Plate.2.4. View (looking east) of a N.W -S.E extension fault with a small splay which is markedly listric and is asymptotic to bedding. The splay may indicate that the main fault terminates by branching.

PLATE 2.3

PLATE 2.4

Plate.2.5. View looking north of a strike slip fault cutting and displacing a N.E.-S.W extension fault.

Plate.2.6. En echelon and upright tectonic veins in the Achall quarry. Note that the veins cross-cut an 'inactive' bedding plane, but not the active bedding plane.

PLATE 2.5

PLATE 2.6

Plate.2.7. Massive calcite vein cross-cutting dolomites of the Durness Formation, Sheet IV, Achall quarry.

Plate.2.8. Fibrous calcite/quartz vein cross-cutting dolomite, Sheet IV, Achall. Note that the fibres are curved: this is a result of a slight change in the dilation direction during rotation on the listric extension faults.

Plate.2.9. Upright veins adjacent to an active bedding plane, note that the veins do not cross-cut the active bedding plane but do cross-cut the inactive bedding plane.

PLATE 2.7

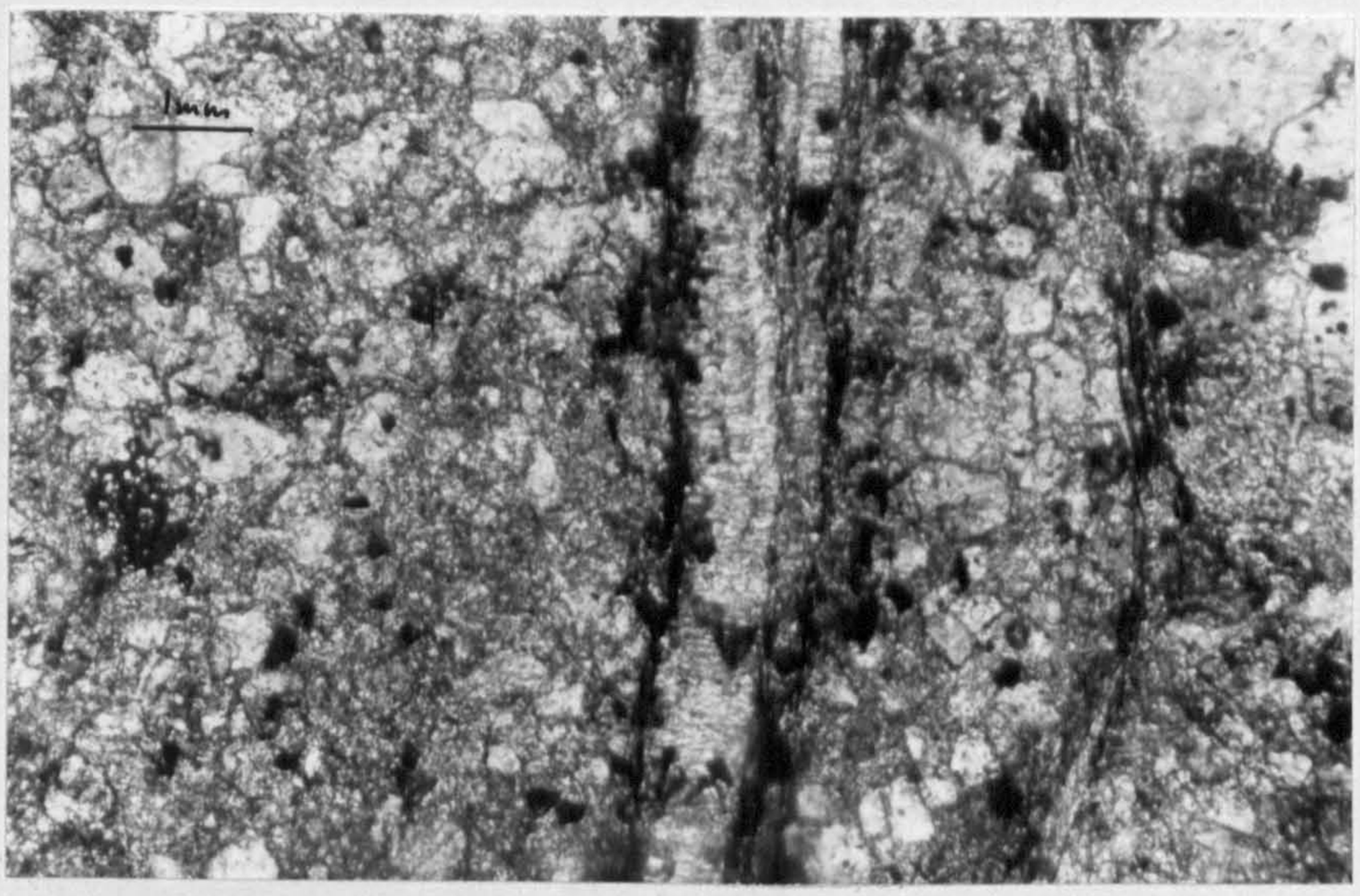

PLATE 2.8

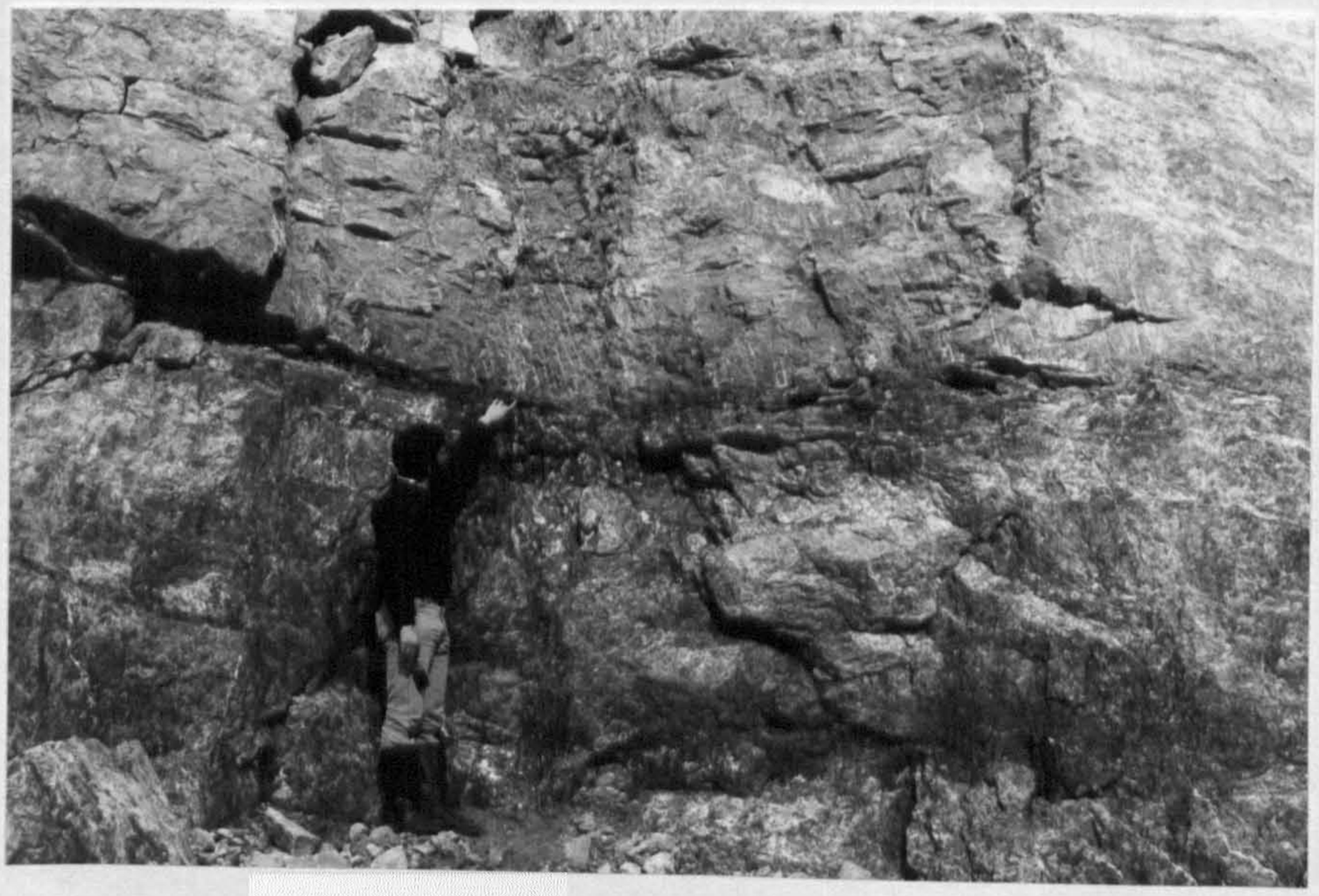

PLATE 2.9

Plate.2.10. Cataclasite, specimen K1, from the Moine thrust at Knockan Crag. Clasts are dolomite (A), Moine mylonite (B), and calcite vein material (C) set in a matrix of very fine grained cataclasite.

Plate.2.11. A crude pressure solution cleavage is developed in high strain areas where two clasts inpinge (arrow).

Plate.2.12. Calcite veins cross-cut the cataclasite. These veins are due to hydraulic fracture after cataclasis during a period when the thrust was inactive and the cataclasite suffered compaction by loading.

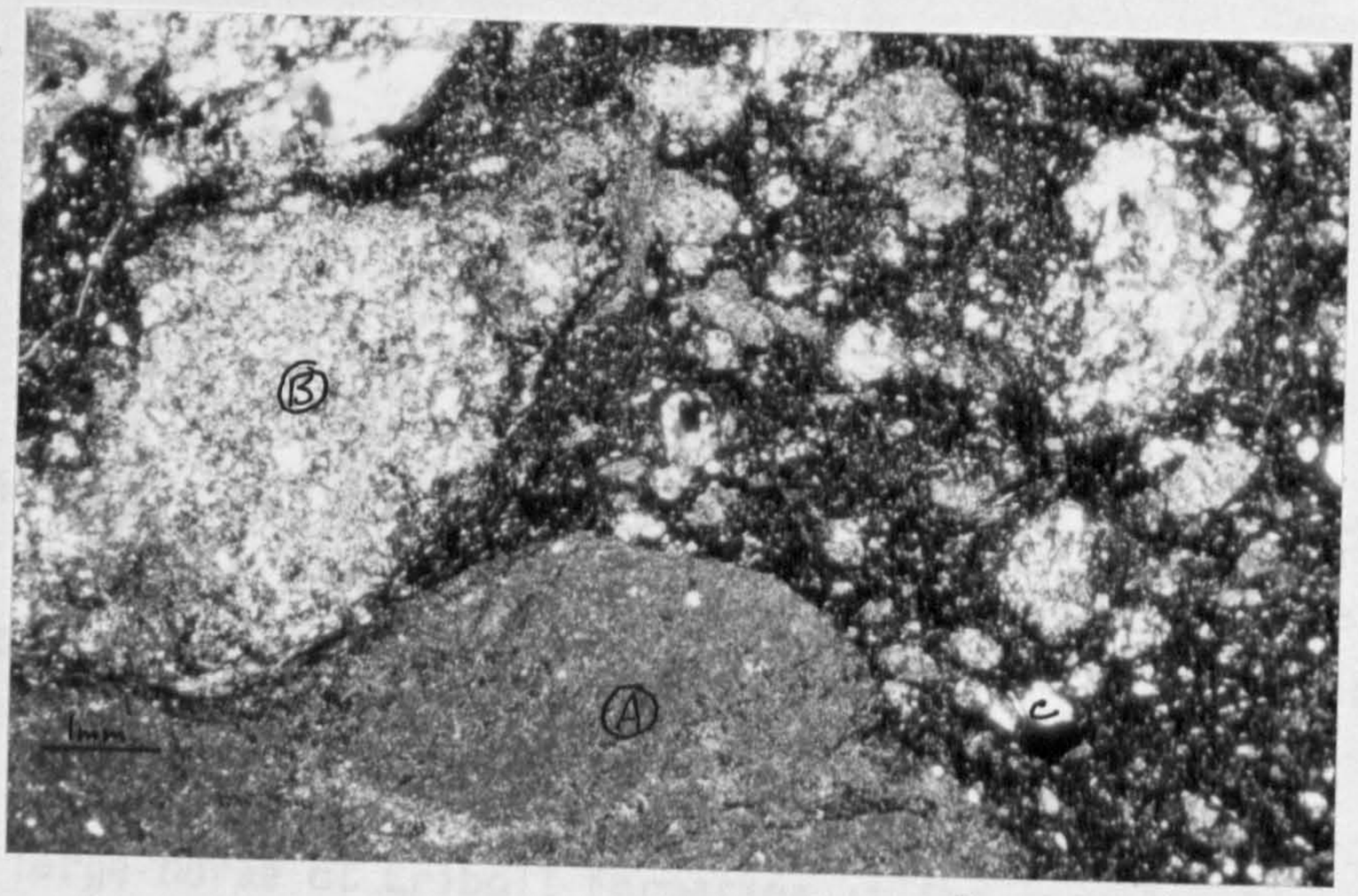

PLATE 2.10

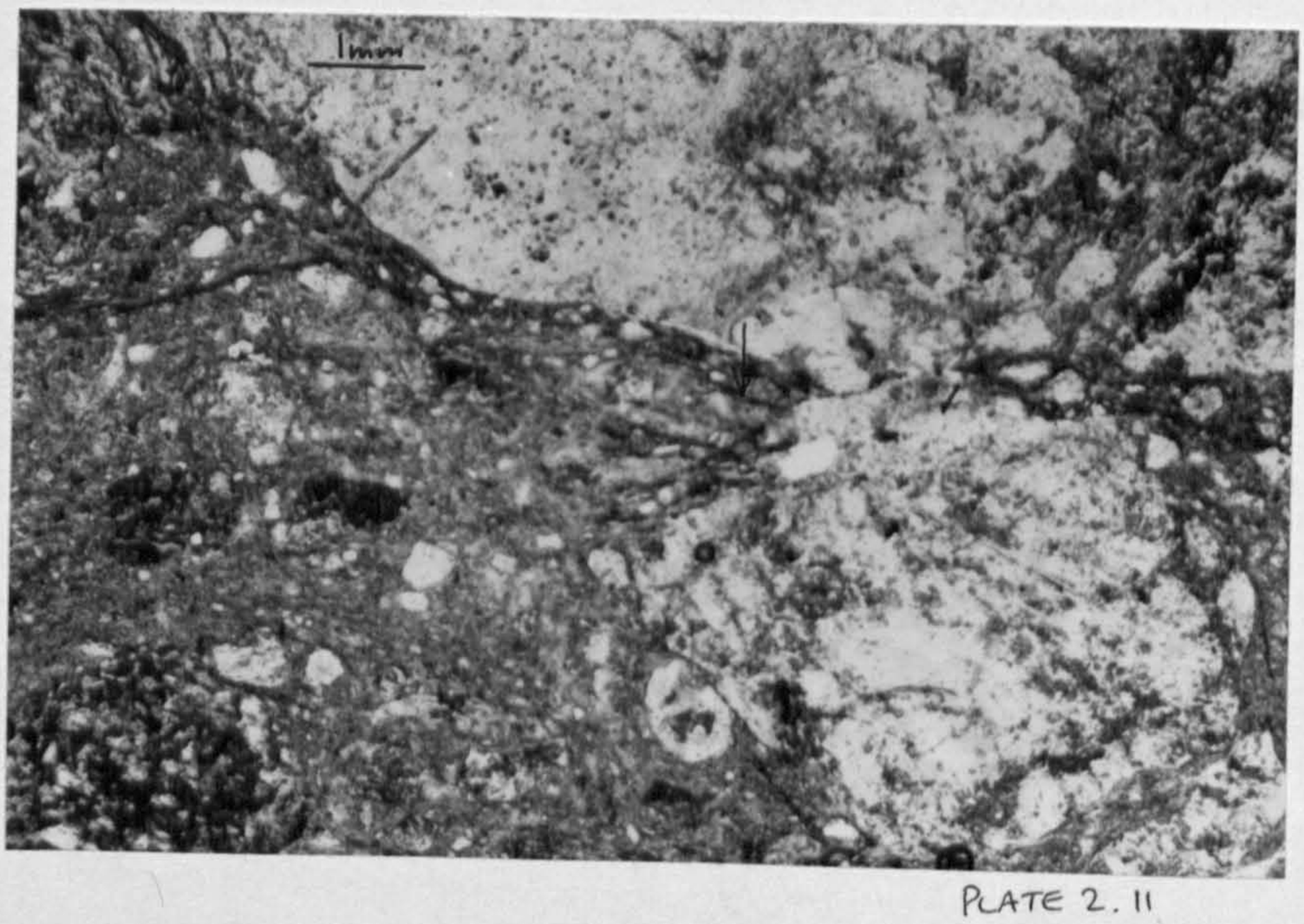

PLATE 2.11

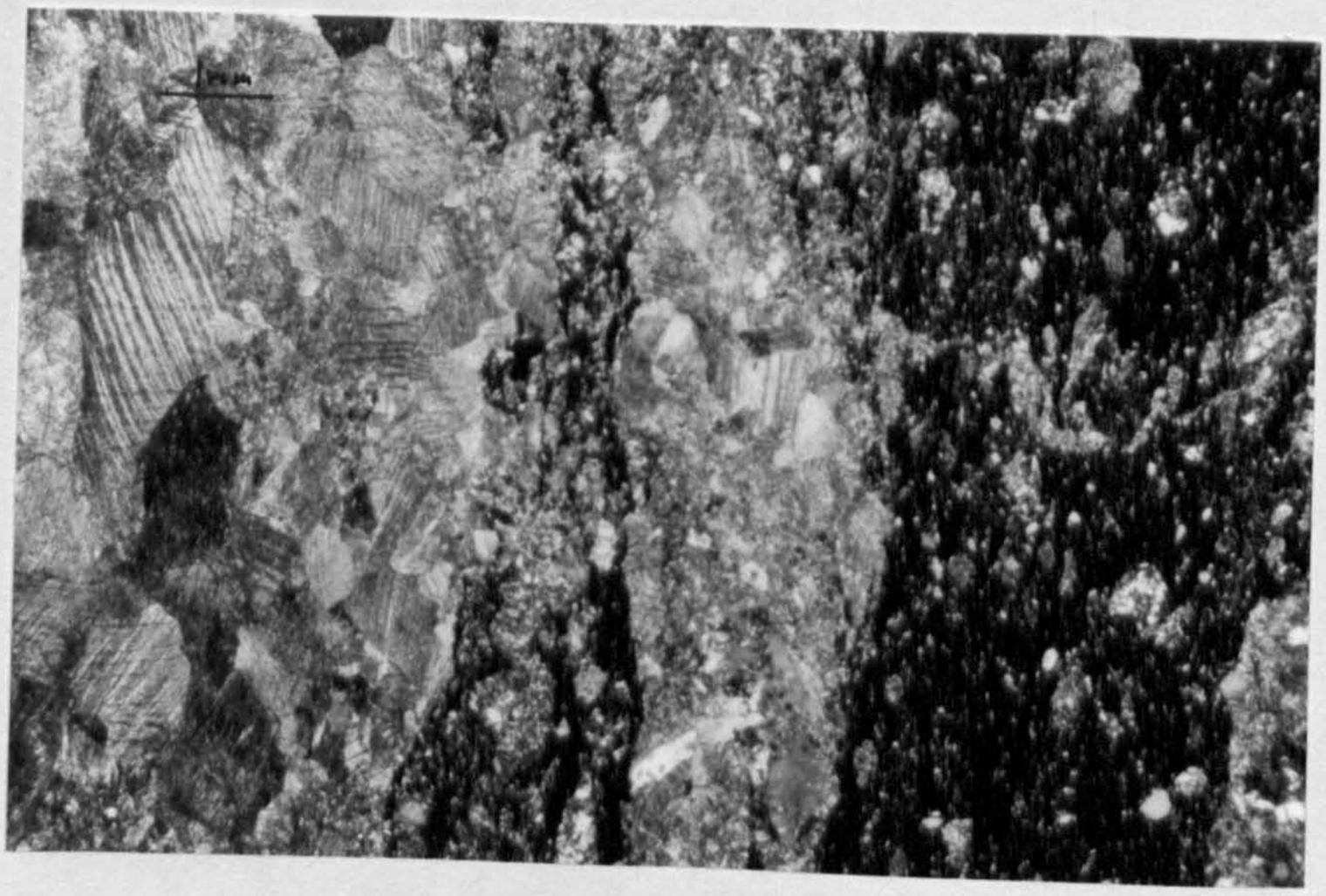

PLATE 2.12

Plate 2.13a. Two small horses of Eriboll Formation are accreted to the hangingwall of the Ullapool thrust sheet (A on plate)at Corry Bridge, GR.NH147925. Note the anastomosing network of fractures in the Torridonian of the hangingwall, defining small horses.

Plate 2.13b. A large horse of Eriboll Formation at the same locality as plate 2.13a. Many of the steep upright fractures have had some strike slip movement on them, presumably due to differential slip movement during accretion.

Plate 2.13c. A cataclasite from the small horses of Eriboll Formation on plate 2.13a. Note reduction in grain size and the lack of an ordered fabric.

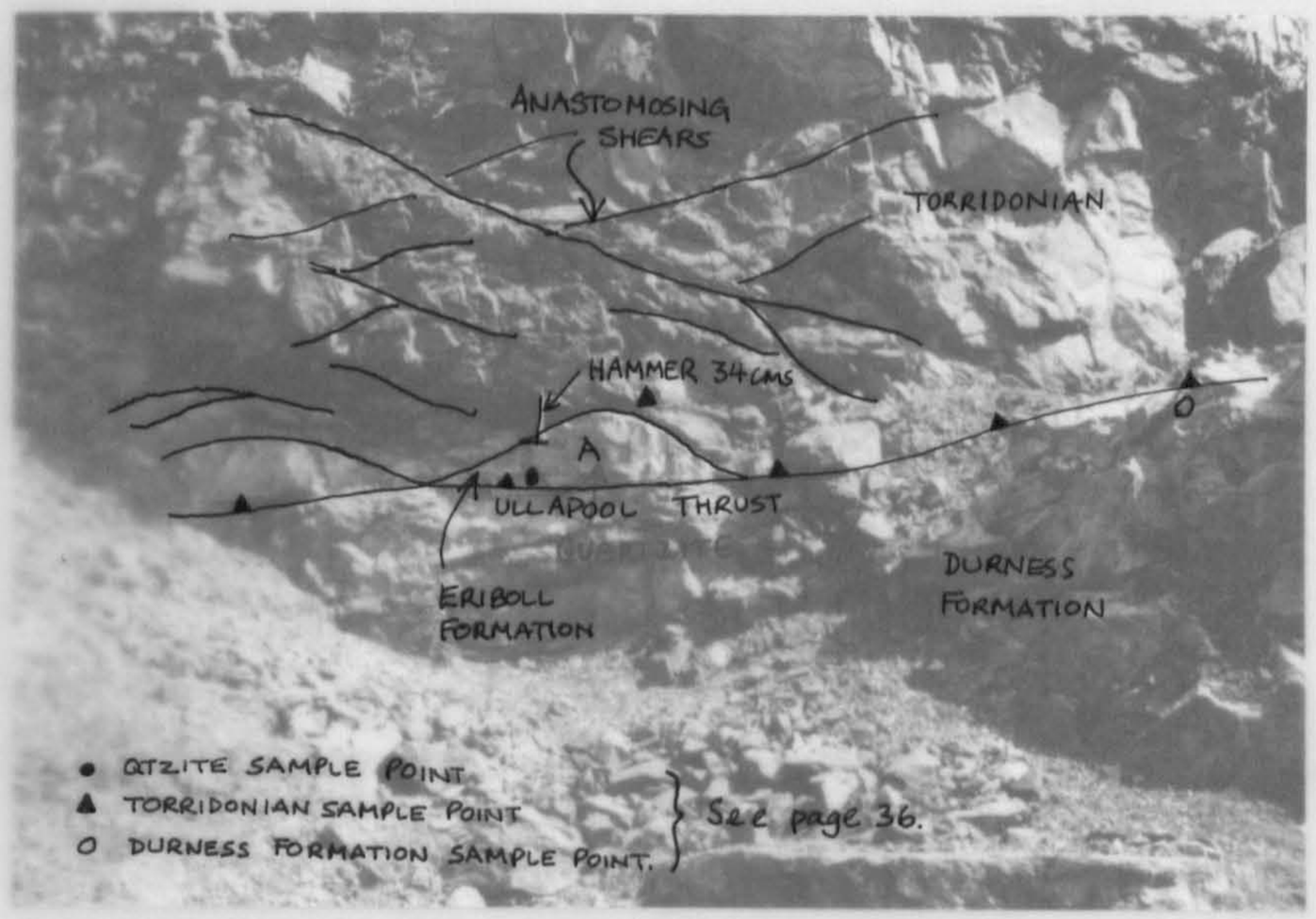

PLATE 2.13a

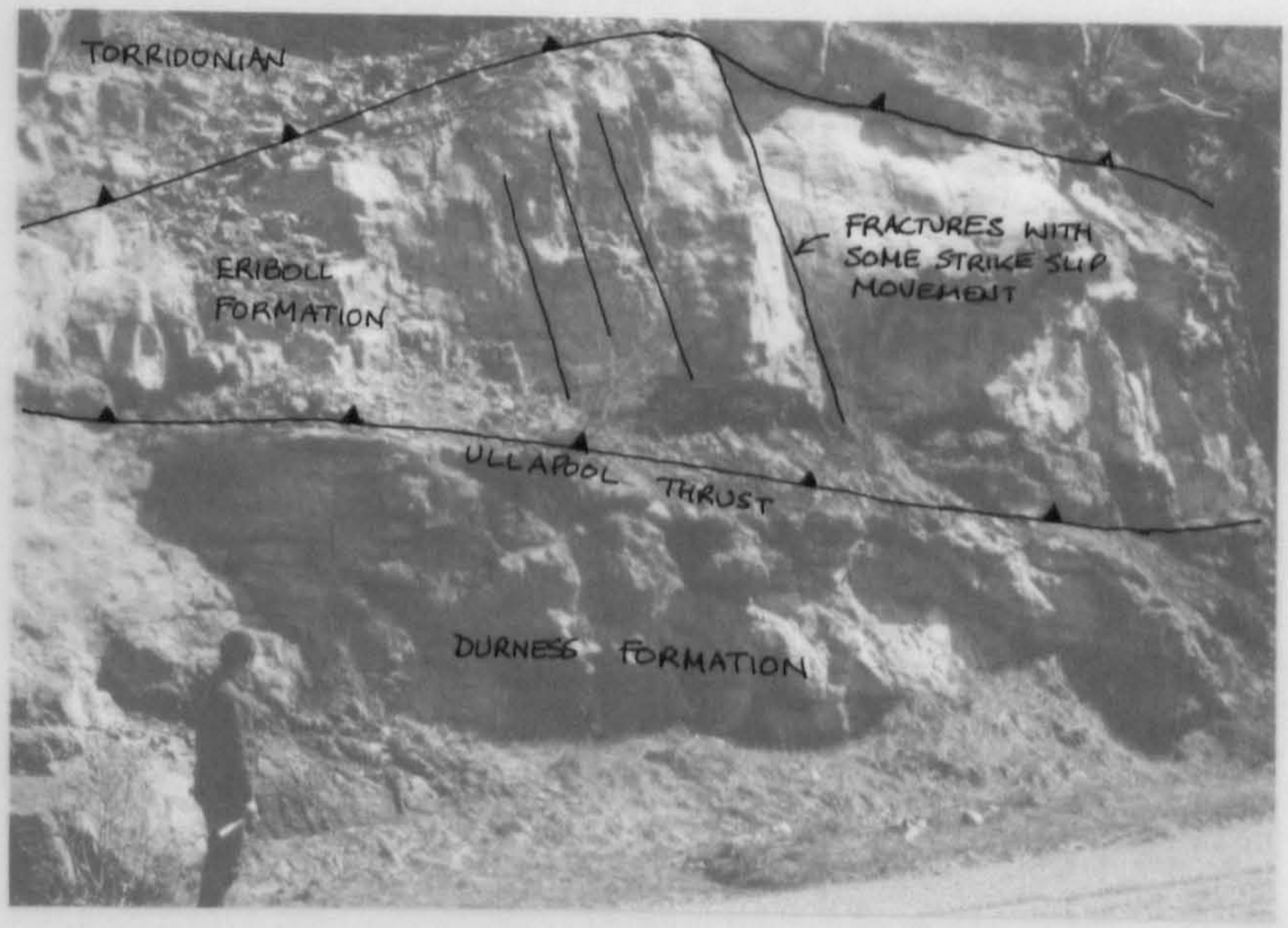

PLATE 2.13b

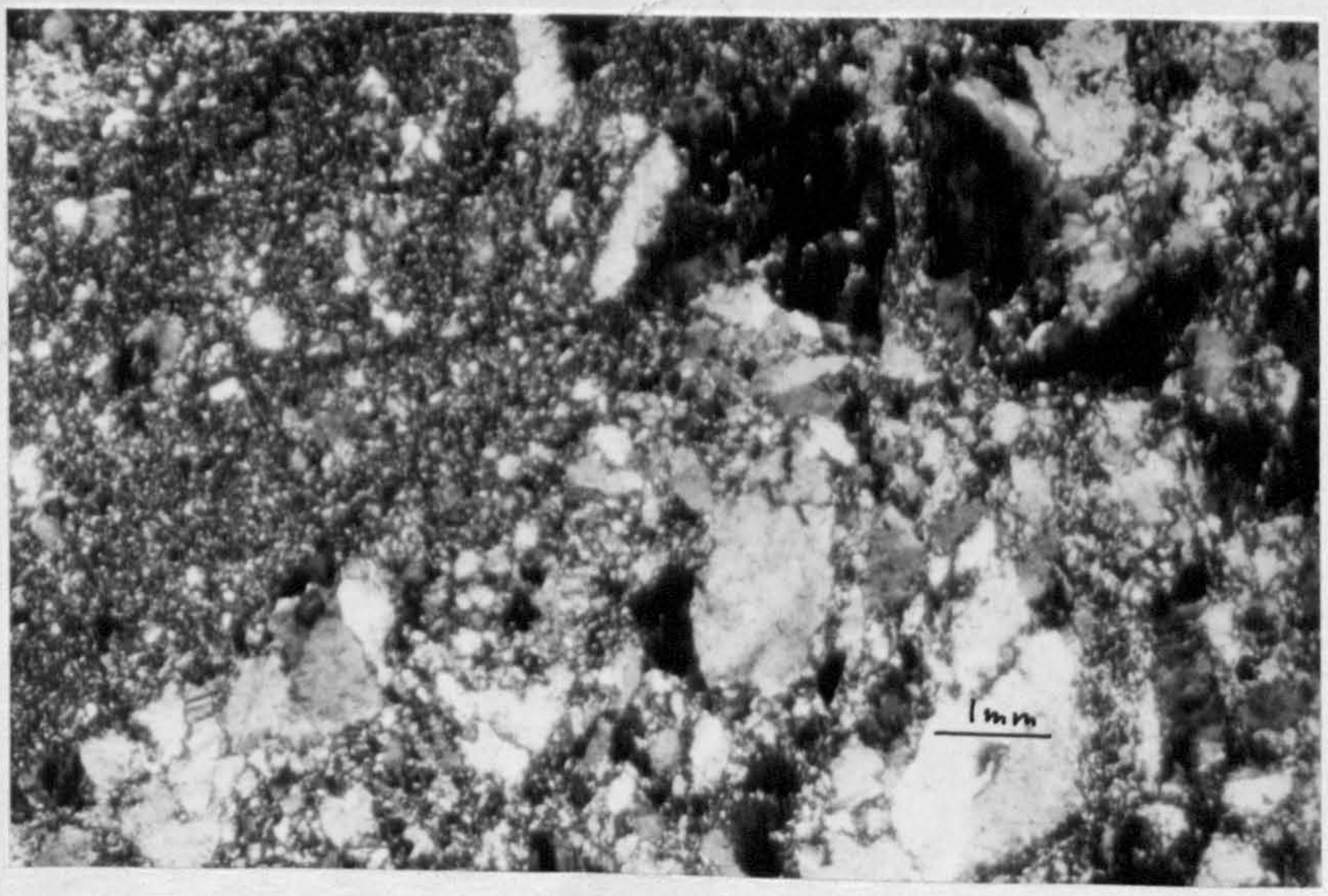

PLATE 2.13c

Plate 2.14. View looking N.W.of the Creag nam Broc fault. Note the extensional geometry with the Torridonian in the hangingwall and the Sheet IV footwall. The fault cuts down section to meet the Sole fault. Specimens shown in Plate 2.15 were collected from(A) marked on the plate. GR. NH148957.

Plate.2.15a-d.

a, thin cataclasite zones cross-cut the dolomites of Sheet IV ca 10m below the Creag nam Broc fault.

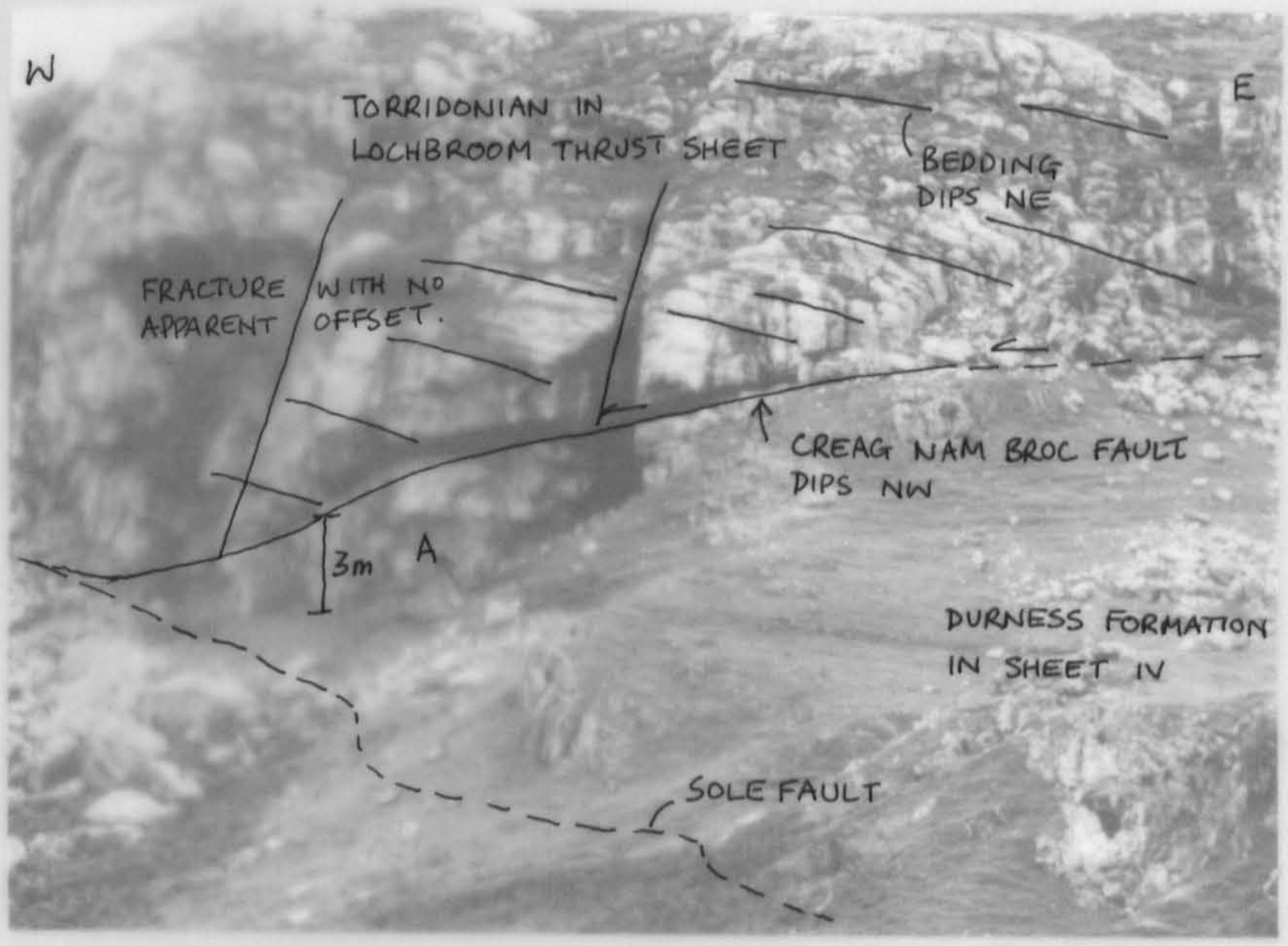

PLATE 2.14

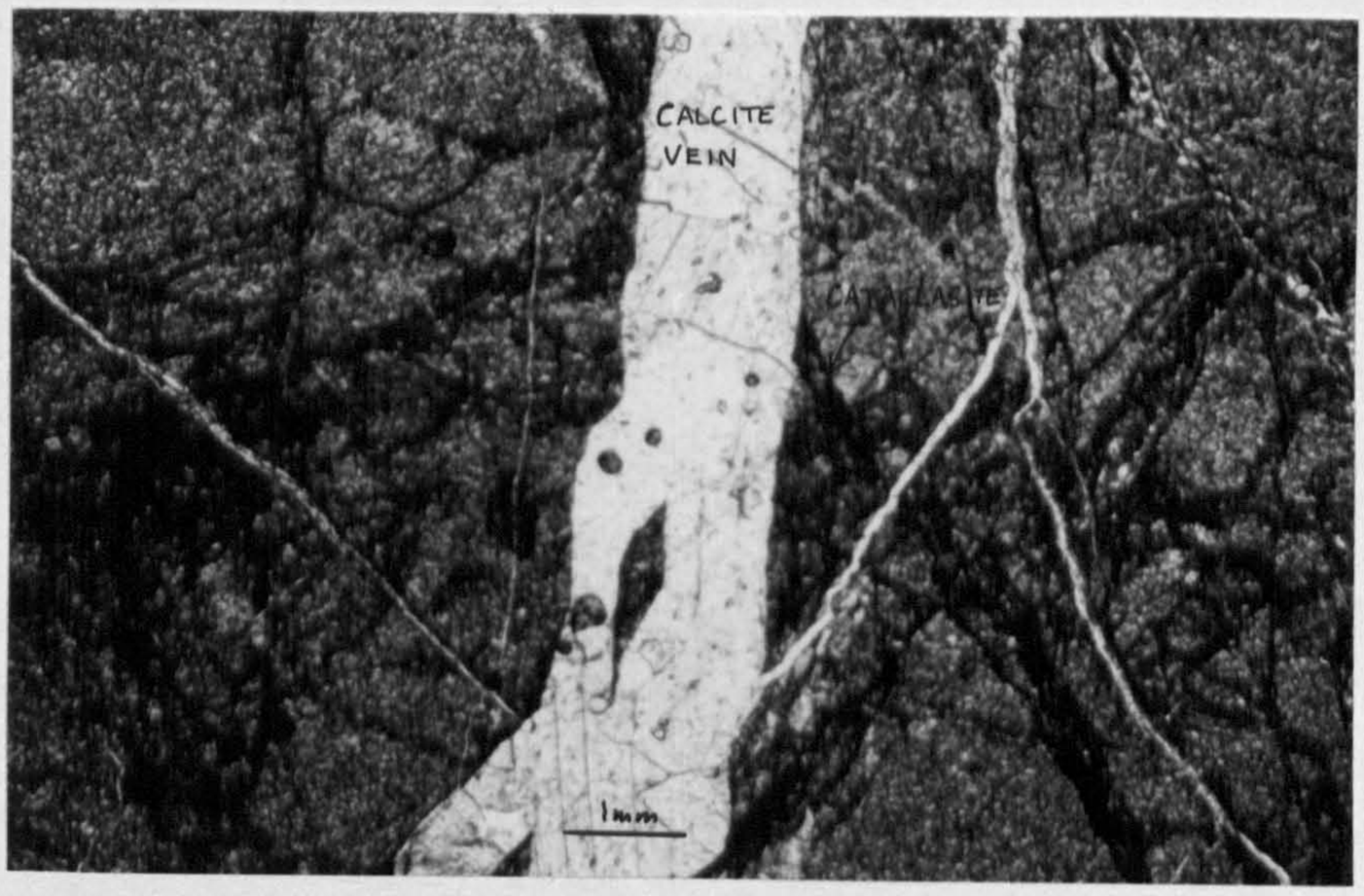

PLATE 2.15a

b Note that calcite veins cross-cut cataclasite zones yet in plate 2.15a, the cataclasite zones cross-cut the veins. This indicates that there is a cyclicity of cataclasis and tectonic veining, see section 2.8.

Plate.2.15c. The dolomite is cut by more cataclasite zones so that it is a microbreccia.This specimen was I m below the fault.

Plate 2.15d. The dolomite at the fault is intensly cataclasised, note the increase in veining.

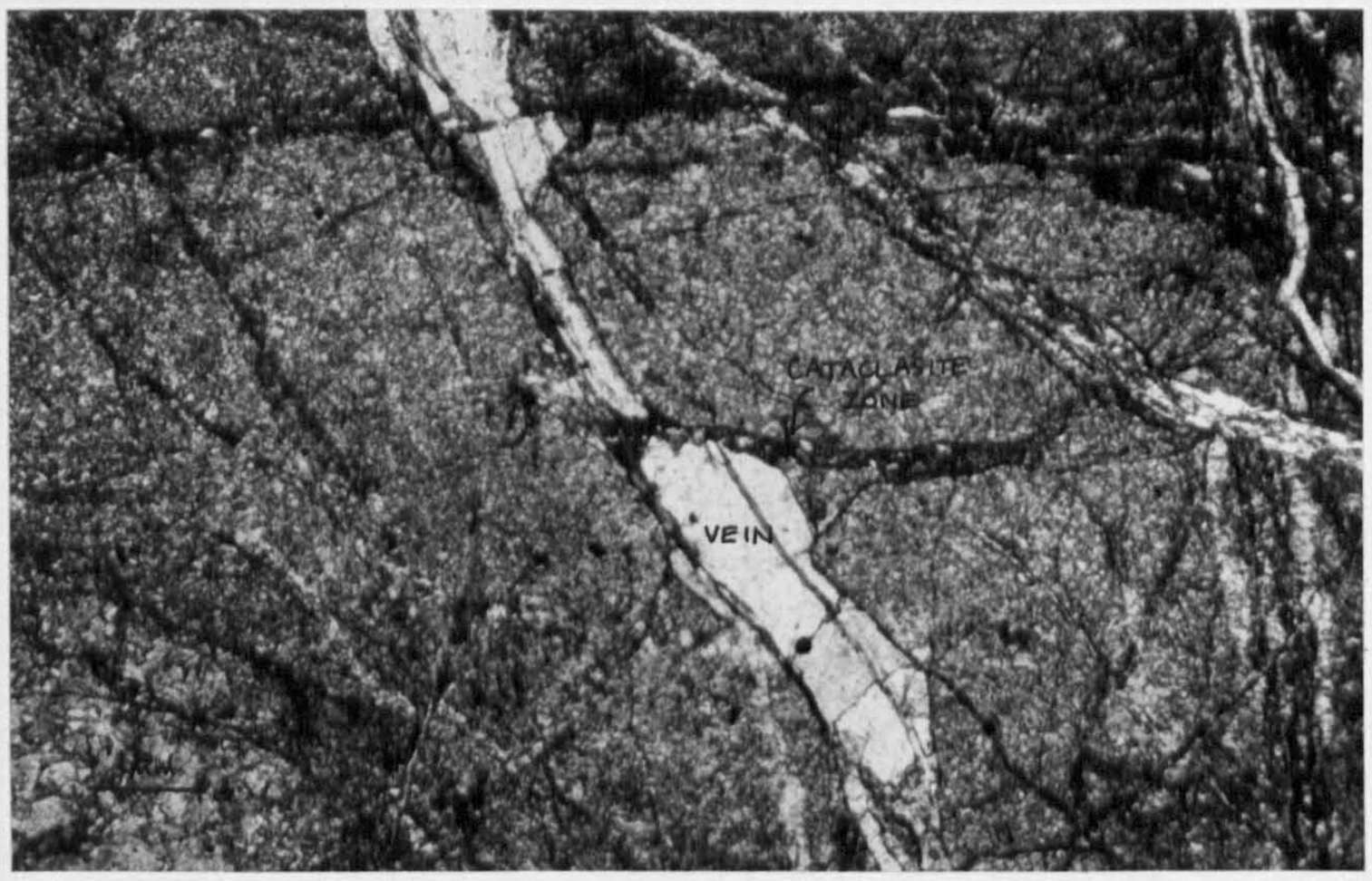

PLATE 2.15b.

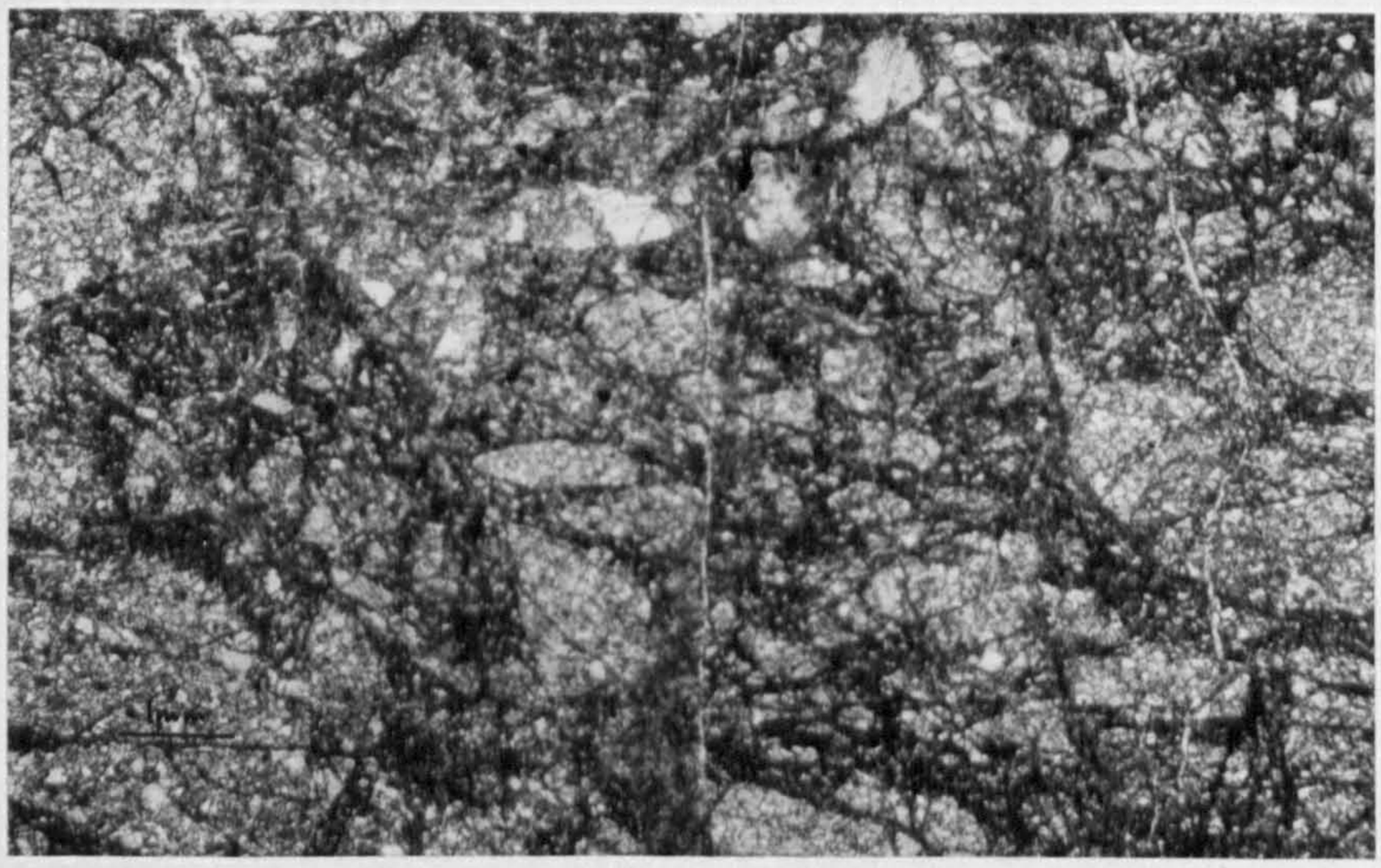

PLATE 2.15c

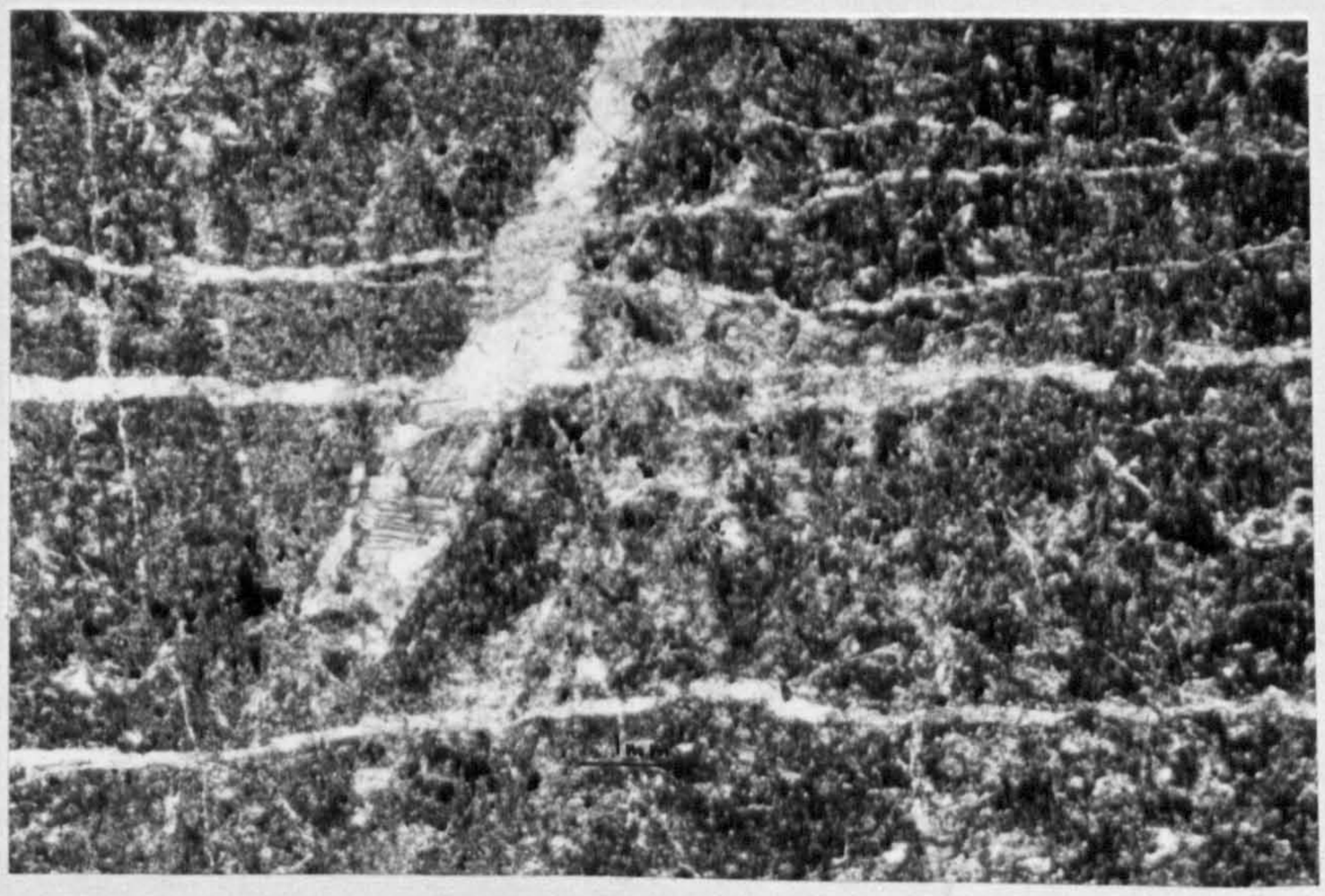

PLATE 2.15d

Plate 2.16. An extensional imbricate complex in Sheet IV near to Knock-an village (GR 213107). The view looks to S.E. Note the listric form of the faults and the occurrence of a small horse. In the Knockan Crag area similar faults join into the Sole fault.

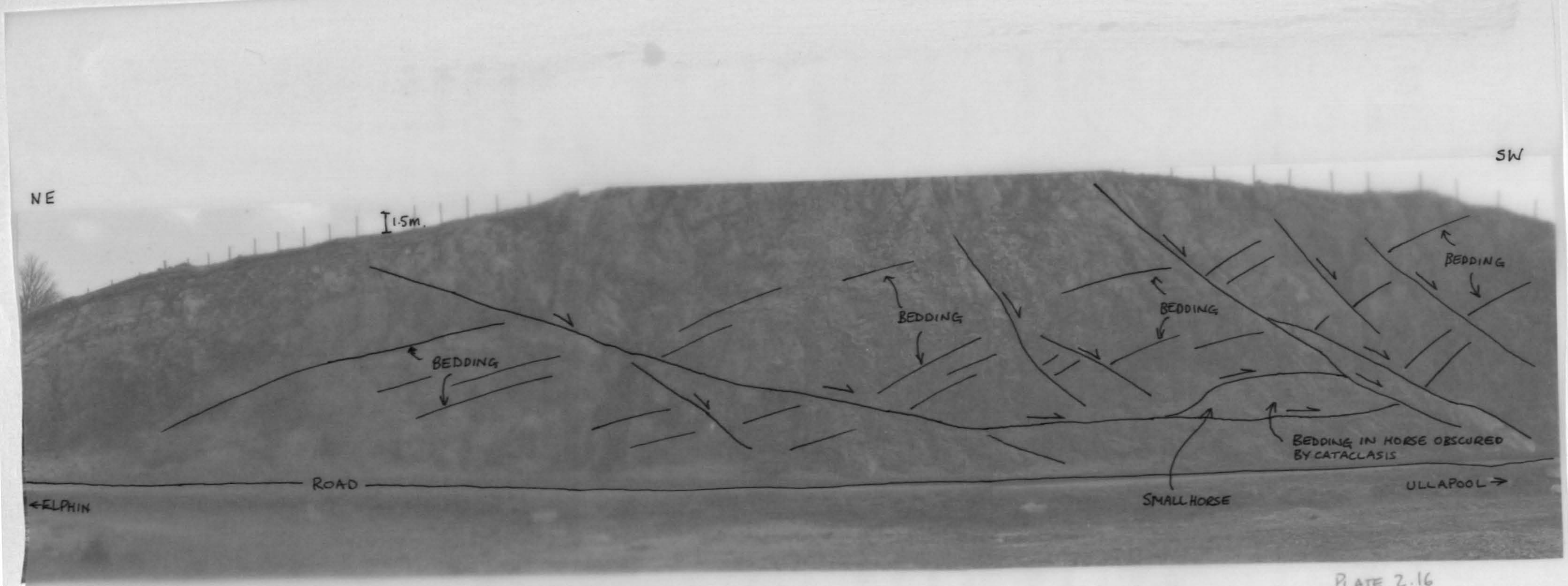
NE
SW
1.5m.
BEDDING
BEDDING
BEDDING
BEDDING
BEDDING IN HORSE OBSCURED BY CATACLASIS
ROAD
←ELPHIN
SMALL HORSE
ULLAPOOL →

PLATE 2.16

CHAPTER 3 INTERNAL DEFORMATION OF THRUST SHEETS, THE DEVELOPMENT AND GEOMETRY OF FOOTWALL DERIVED HORSES.

3.1 INTERNAL DEFORMATION OF THRUST SHEETS.

With movement over footwall irregularities, i.e. ramps or asperities, a thrust sheet must deform to conform to the changes in geometry of the thrust plane. Internal deformation of thrust sheets has been studied in a number of thrust zones and in theoretical studies, and a number of deformation styles have been described:

(i) Thrust faulting - common ramp accommodation structures in thrust sheets are back thrusts, which are antithetic thrusts, i.e. they have a displacement direction opposite to that of the main thrust fault, fig 3.1a. Back thrusts are interpreted as structures resulting from compressive stresses produced when the thrust sheet meets a ramp, and they have been described from a number of thrust belts, Douglas (1950), Jacobeen & Kanes (1974, 1975), Harris & Milici (1977), Serra (1977). Synthetic thrusts, i.e. the displacement direction is the same as the main thrust, also occur, fig 3.1b Jacobeen & Kanes (1975), Serra (1977).

(ii) Extension faulting - Laubscher (1973) interpreted extension faulting within the Helvetic nappes as being in part due to bending stresses. Extension faulting is also reported by Harris & Milici (1977) and Royse et al. (1975) show that extension faulting in thrust sheets is localised above ramps in the Rocky Mountains of the USA, fig 3.2.

(iii) Folding - sometimes the ramp-induced internal stresses in the hanging wall can be accommodated totally by folding, Rich (1934). Anticlines will develop above ramps with wide flat bottomed synclines over flats. Figure 3.3a shows a thrust sheet after some initial movement, with further movement of the thrust the anticline crest migrates onto the flat and the crest is flattened, fig 3.3b. Berger & Johnson (1980) demonstrated that if two competent units were in compression the fold may be initiated prior to movement up the ramp with the result that the forward limb of the anticline may be steepened and possibly overturned, fig 3.4. They interpreted this effect as being due to fault drag on the ramp.

(iv) Theoretical studies by Wiltschko (1979a) show that faulting above ramps is due to bending stresses which are a significant portion of the total stress field. This model predicts both forward and back thrusts above the ramp, with localised extension faulting at the top of the ramp and at its trailing edge, fig 3.5. In a theoretical model Rodgers & Rizer (1981) also predict back and forwards thrust faulting above the ramp.

In the Loch Broom thrust sheet of the Achall valley, the only structures to be seen above the ramp are extension faults orientated NE-SW, The extension faults do not occur at the apex of the ramp, (i.e. where the ramp changes geometry to become a flat) as described by Laubscher (1973) and Royse et al. (1975) but they are present directly above the ramp itself. The extension faults occur in the area of the thrust sheet where compressive stresses are active and hence thrust faults would be expected, Wiltschko (1979a).

The faults have a comparable orientation to the NE-SW faults described in section 2.5.1.3a., which displace the Loch Broom thrust. The faults occur above the ramp itself, rather than at the apex of the ramp,so therefore cannot have been formed by internal deformation

caused by movement of the Loch Broom thrust sheet over the ramp. I interpret the extension faults as having formed initially when the Loch Broom thrust sheet was emplaced on the Durness Formation; these then propagated up into the Loch Broom thrust sheet when the Loch Broom thrust became inactive and the Sole fault was active, see section 4.4 and fig 3.6.

3.1.1. Deformation of the Loch Broom thrust sheet due to the accretion of footwall horses.

The hangingwall of a thrust sheet must be deformed in order to contain a footwall horse which has been accreted onto it. Figure 3.7a is a hangingwall sequence diagram of a thrust sheet prior to the accretion of a horse. A line marker is shown in the hangingwall, and with accretion of a horse the thrust plane and thrust sheet with marker will be extended to accommodate the horse, fig 3.7b. Extension could occur by small-scale normal faulting, fig 3.7c, or by fracturing and veining. The veins that occur in the Loch Broom thrust sheet indicate that locally fluid pressures were high enough to induce a tensile hydraulic fracture, Sibson (1981), see section 4.1.1.

With the accretion of further horses to the same point in the hanging wall, i.e. beneath an existing horse, further extension can take place, fig 3.8. Sequential plucking of horses from a ramp may produce this effect. In fig 3.8a,b, horse A is produced from low down the ramp and horses B and C from successively higher portions of the ramp. If a number of horses are accreted in this manner the hanging wall will undergo a large extension parallel to lateral edges of the horses, and a drop fault may form, fig 3.8c, Butler (1982a).

Accretion of horses at adjacent hanging wall sites produces a more complex hanging wall deformation history, fig 3.9. Parts of a hanging wall which were previously in extension during an earlier accretion, may be in compression during a later accretion, Butler (1982b), fig 3.9a,b. Folds which plunge NE in the Torridon Group of the Loch Broom sheet, at locality A on encl.3., and within Fucoid Beds of the horse at B on encl.3, were formed as a result of multiple accretion which caused complex deformation patterns in the hanging wall.

3.1.2. Internal deformation of the Ullapool thrust sheet.

The Ullapool thrust sheet can be viewed as a large horse accreted beneath the Loch Broom thrust. Examination of the hanging wall sequence diagram for the Loch Broom thrust sheet,fig 3.10, shows that the Ullapool thrust sheet originated beneath a long lateral ramp. The geometry of the Ullapool thrust is fully described in section.2.4.

Figure 3.10 is a hangingwall sequence diagram to demonstrate the development of the internal geometry within the Ullapool thrust sheet.In figure 3.10a the incipient position of the Ullapool thrust is marked, the lithologies of the incipient thrust sheet are part of an undisturbed foreland sequence. With movement on the Ullapool thrust both the Loch Broom thrust and the internal bedding of the Ullapool thrust sheet are deformed, fig 3.10b; they are folded into a large warp, with its maximum amplitude above Corry Point, fig 3.11. From figure 3.10 a & b it is clear that the Ullapool thrust sheet is lens shaped both along strike and also up and down the transport direction of the Ullapool thrust,fig.3.12. With the accretion of the Ullapool thrust sheet, both the Loch Broom thrust and bedding have extended in length both along strike and down dip. The extension will be greatest at the crest of the large warp, fig 3.10b and fig.3.12.. The Ullapool thrust sheet has accommodated this extension

by faulting at its thickest part which is sited between Corry Point and Corry Bridge, fig.3.11. Because the extension is both down dip and along strike, extension faults will develop both parallel and normal to the slip direction. The extension faults cut the Loch Broom thrust, see figs.3.11 and 3.10b.

During the development of the warp minor bedding plane slip has occurred with the development of some cataclasis, which is especially noticeable at the boundary between Pipe Rock Member and the Fucoid Bed Member of the An-t-Sron Formation.

The orientation of the extension faults is similar to that of the late cross faults, see fig.3.11, and could perhaps be similarly interpreted. However, the extension faults in the Ullapool thrust sheet produce marked escarpments, fig 3.11. These do not cross the outcrop of the Ullapool thrust near Corry Point, implying that the faults do not cut the thrust, furthermore they are only developed at the crest of the warp, where extension is expected to be greatest. Therefore I interpret the extension faults as being the result of local extensional strains caused by the change in bedding geometry when the Ullapool thrust sheet was emplaced.

3.2. THE DEVELOPMENT AND GEOMETRY OF FOOTWALL-DERIVED HORSES.

A horse is a volume of rock completely bound by fault surfaces, Dennis (1967). Horses are often lensoid in shape and are surrounded by branch lines, (which are lines at the intersection of thrust planes), on the major thrust surface, Boyer & Elliott (1982), fig 3.13, and can vary in size from <1 m in strike length, up to thrust sheet dimensions, such as the Loch Broom thrust sheet, and the Glencoul thrust sheet where strike length is commonly >10 km, Elliott & Johnson (1980).

Horses are produced in order to reduce the friction on the thrust plane. Increase in friction is caused by increase in shear stress and normal stress acting on the fault, according to the relationship, Price (1966).,

$$\tau = \mu \cdot \sigma_n \ldots\ldots 3.1$$

where τ is the shear stress, σ_n the normal stress acting upon the thrust plane and μ is the coefficient of friction.

Both τ and σ_n can be increased by a change in the angle between the thrust plane and the maximum principal stress line according to the equations, fig 3.14

$$\sigma_n = \sigma_{max} \cdot \sin^2\theta \qquad \ldots\ldots 3.2$$

$$\tau = \sigma_{max} \cdot \cos\theta \cdot \sin\theta . \qquad \ldots\ldots 3.3$$

It follows that any change in geometry of the thrust plane causes a change in τ and σ_n, and hence friction. Thrust planes commonly have a staircase trajectory through a stratigraphy, with long flats parallel to bedding and short steep ramps, Rich (1934). At these ramps friction will be increased, and horses will be 'plucked off' in an attempt to smooth out the ramp, Serra (1977), Engelder (1979). Asperities are undulations on thrust planes cause a similar increase in friction, and the asperity may be removed to form a horse, Engelder (1979).

A change in the physical nature of a lithology or fault plane, for example due to induration, facies change, deformation, etc, causes a change in the coefficient of friction and in consequence horses may form in an anastomosing network, see section 3.2.3.

Each of the horse formation mechanisms above need to be discussed in turn, as each produces a unique geometry.

3.2.1. Derivation and geometry of horses derived from ramps.

Before describing the geometry of horses from ramps it is relevant to discuss the origin of ramp themselves.

3.2.1.1a. The origin of ramps.

It is well known that thrusts prefer to glide along 'easy flats' where the friction to be overcome is least. These planes of weakness can have several forms:-

(i) A zone of high pore fluid pressure, Hubbert & Rubey (1959), Gretener (1972, 1981).

(ii) A shale horizon or other 'weak' rock, Kehle (1970), Chapple (1978), Wiltschko (1979b).

(iii)A horizontal stress concentration, where large lateral stresses are concentrated in thick competent beds, the reason why this occurs is unknown. However, it has been used to explain the occurrance of thrust planes within thick carbonates rather than shale horizons in Nevada U.S.A., Burchfiel et al (1982).

Should the physical properties of a 'weak' layer change laterally (along the layer) and it becomes 'less weak' then obviously it will not be such a viable glide horizon. Lateral changes in a layer can occur in several ways:-

(i) A change in the state of pore fluid pressure from a high pressure area to a low pressure area, will induce strengthening of the glide plane, with concomitant increase in the normal stress; i.e. a decrease in the effective normal stress, according to the relationship-

$$\sigma_n' = \sigma_n - P \quad \ldots\ldots \quad 3.4$$

where σ_n' is the effective normal stress, and p is the pore fluid pressure. If a number of planes of weakness are operative then they could become connected by a system of ramps so as to develop a through-going fault plane, Gretener (1981), fig.3.15a.

(ii) A lateral facies change in the glide horizon perhaps a shale layer lensing out or biostratigraphic changes in carbonates, can cause the physical properties of the layer to change and a ramp can form, Elliott (1976a).

(iii) Pre-existing faults and palaeotopography cause abrupt lateral changes in glide horizons. Pre-existing faults may provide a link between the displaced glide horizons, and can be reactivated as ramps, Jacobeen & Kanes (1974, 1975), Davies (1982), fig 3.15b. Fossil hills could provide a situation similar to the pre-existing faults and cause ramping, fig 3.15c, Barton (1978), Jacobeen & Kanes (1974, 1975).

(iv) Footwall deformation by folding and thickening prior to thrust propagation would cause strengthening of the lithologies. Short-steep limbs of folds are commonly thrust out and folds could act as 'stress risers' which initiate ramps, Fischer & Coward (1982), Coward & Potts (1983), fig 3.15d.

(v) Igneous intrusions and accompanying metamorphic aureoles can act as sites for ramps as they force an abrupt lateral change in the glide plane. The Assynt Alkaline Suite, Parsons (1979), was in part responsible for the formation of the Assynt culmination, Elliott & Johnson (1980).

3.2.1.2. Geometry of footwall horses from ramps.

Accepting the concept that thrusts always cut-up section in the direction of transport, Dahlstrom (1970), Elliott (1976a), it follows that horses derived from footwall ramps will be stratigraphically older than their footwall, and either stratigraphically younger or the same age as the hanging wall. Assuming that the rocks had not been deformed extensively before the thrusting, then it is impossible for horses of lithologies younger than the footwall to be developed.

Figure 3.16a,b shows the development of internal geometry in a ramp-derived horse and illustrates a ramp cutting through a simple undeformed stratigraphy, with an incipient horse marked, fig 3.16a. After movement the horse is accreted into the hangingwall, and displaced up the thrust zone, fig.3.16b. During the accretion and movement, the internal bedding geometry will rotate so that bedding should dip towards the foreland. i.e. a foreland dipping horse, and bedding will be right way up.

Figure 3.17a shows a more complex ramp, cutting through a folded footwall, with an incipient horse marked. After movement and accretion, the internal geometry of the horse will be rotated from its original orientation so that the bedding will dip steeply towards the hinterland and the bedding will be inverted, i.e. a hindward dipping horse, fig.3.17b.

During accretion and transport, the horse will inevitably be internally deformed by fracturing and cataclasis. This is the case in some of the horses of Pipe Rock Member at Achall; encl.3 show the relationships of the quartzite horses to the Loch Broom thrust in the Achall Valley. They appear to be a single horse

displaced by the extension faults of Sheet IV. Bedding is commonly obscured by fracturing though at C on encl.3, the bedding is vertical and using pipes as way-up markers appears to young to the west. From the criteria given above the quartzite horse is a hindward dipping horse, and the original ramp must have formed in a folded footwall.

The large horse of quartzite that outcrops near to Knockan village, encl.2, has been deformed by extensional faulting during the formation of Sheet IV. The roof thrust is the Moine thrust, which truncates the extension faults . Previously this body of quartzite was interpreted as a klippen of the Ben More thrust sheet, Peach et al, (1907), Elliott & Johnson (1980), however, I interpret it as a simple quartzite horse accreted to the Moine thrust.

The internal bedding of the horse is gently warped but the general dip is to the south-east, encl. 2, and pipes at GR.211096 show that the bedding is right way up. This is contrary to the interpretation of Elliott & Johnson (1980) who advocated that the quartzites of the horse were inverted, on the basis that the Pipe Rock Member appeared to dip beneath the Basal Quartzite Member. The contact between the two is now interpreted as a steep extension fault. The horse is right way up and hindward dipping, so does not fit readily in the classification of ramp related horses. It is possibly derived from a large asperity, see below, section 3.2.2.

3.3.2. Footwall horses derived from asperities.

Thrust planes are often undulating, the undulations being referred to as asperities, which will have a locking effect on the fault zone and will tend to be sheared off in order to facilitate movement, Engelder (1979). Ramps are a form of asperity, but asperities can also occur on the long flats, thus down-cutting can occur in the direction of transport at the leading edge of the asperity, contrary to the thrusting 'rules' of Dahlstrom (1970) and Elliott (1976a), fig.3.19.

The stratigraphy within horses which are derived from asperities can be older than, the same age as or can have elements younger than the footwall rocks. On encl.3, horse D consists of the An-t-Sron Formation and some Durness Formation, while the footwall of the Loch Broom thrust is the Salterella Grit Member of the An-t-Sron Formation. Because the Durness Formation is present in the horse, and is stratigraphically younger than the footwall, it follows that the horse is unlikely to have been derived from a ramp. The internal geometry of the horse is hindward dipping and right way up. This is due to rotation of bedding by imbricate thrusting, and the horse is in effect a small contractional duplex. If no internal deformation occurs then the internal geometry could remain unchanged from that which existed prior to thrusting. Indeed, if the footwall has not been deformed prior to thrusting then asperity derived horses can never be foreland dipping, or inverted.

Along both the Loch Broom and Ullapool thrusts are strings of Durness Formation horses resting upon a footwall of An-t-Sron Formation, encl.1. There is no stratigraphic separation across the floor thrust of the horses, but internally, bedding is often steeply hindward-dipping suggesting rotation either by thrusting or extensional listric faulting. The Achall Sheet IV is in effect a large asperity horse similar to the small Durness Formation horses. With further movement and transport to higher levels in the thrust zone, the asperity-derived horses will be emplaced onto a stratigraphically younger footwall, and the only distinction between them and ramp derived horses will be the internal bedding geometry The horses of Durness Formation are asperity-derived horses in the process of accretion, or newly accreted onto the hanging wall. Returning now to the Knockan quartzite horse it is evident from its internal geometry (hindward dipping, right way up) that they are asperity-derived from a thrust 'flat', not from a ramp as in the case of the Achall quartzite horses.

Horse E on encl.3, is an anomaly in that it is a horse of the Eilean Dubh Member of the Durness Formation, resting directly upon a footwall of An-t-Sron Formation. The internal geometry is hindward facing and right way up. The Loch Broom thrust must have accreted this horse whilst moving over the Achall Sheet IV, and it could either be derived from an asperity on top of Sheet IV, or accreted from the leading edge of Sheet IV by the Creag nam Broc fault, which emplaced the horse to its present position, fig 3.20. The implication is that any horse of a stratigraphically younger age than either its hanging wall or its footwall indicates downcutting in the direction of transport by a thrust, i.e. extensional displacement.

3.2.3. Horse development from anastomosing thrust zones.

The Ullapool thrust is the only thrust which consists of a zone of anastomosing fractures, plates 2.13a,b. These fractures define pods, which are horses and are commonly less than 1 m in length. The hanging wall is mainly composed of Torridon Group arkoses with horses of quartzite immediately adjacent to the footwall of Durness Formation, plate 2.14. The anastomosing occurs on all scales from the outcrop scale to the microscopic. Anastomosing networks can develop by several ways, Engelder (1974, 1979), Aydin & Johnson (1978), House and Gray (1982):-

(i) As a fracture deforms the rock, a field of work hardening will exist around the propagating fracture and results in the strengthening of the rock within that field. Continuing deformation will now be more difficult, and the deformation will shift to undeformed host rock, and a lens of the work hardened rock is removed, Engelder (1979), Fig 3.21a.

(ii) If a fracture becomes indurated either by its own fault rock product or a vein filling, then depending upon the strength and coefficient of friction of the host rock, the fault-fill may be the stronger. Hence with continuing deformation the fault will shift to the weaker host rock, fig 3.21b. This mechanism requires that movement along an individual fracture is episodic to allow induration, and may be indicative of a stick-slip seismic fault.

(iii) If a thrust plane is continuously forming irregular surfaces the irregularities will lock until the differential stress rises high enough for them to be sheared off as horses, Engelder (1979), fig 3.21c.

The effect of any one of these deformation mechanisms is to change the friction within the zone both in time and space, and hence cause the fault to lock. To continue deformation of the fault zone, reactivation is achieved by shifting the deformation into the weaker host rock.

The Ullapool thrust shows evidence that both mechanisms (ii) and (iii) were active. The fractures surrounding the horses on the thrust are filled by a layer of cataclasite. Cataclasite also occurs as small <10cm horses; this suggests that the thrust was deforming by mechanism (ii). The horses of 'Torridonian' rocks and quartzite indicate that the Ullapool thrust was continually forming an irregular fracture plane, along which the irregularities (asperities) were subsequently sheared off; thus indicating that mechanism (iii) was also active The thrust is shown in plate 2.14. It is irregular with incursions into the underlying Durness Formation. With further movement the Durness Formation would become accreted onto the main thrust zone. The two quartzite horses are accreted asperities from deeper in the thrust zone where quartzite constituted the footwall, hence a horse stratigraphy can be built up as the thrust sheet moves

up dip. The Ullapool thrust originated in the Torridon Group which is the oldest unit in the thrust sheet. When movement occurred, the thrust climbed section up to the quartzites of the Eriboll Formation and then up to its present level. The horses in the anastomosing fault zone will young both stratigraphically and structurally downwards towards the active thrust plane, fig 3.22.

All horses in the anastomosing Ullapool thrust zone show intense cataclastic fabrics, see section 2.7.2., and original bedding has been obliterated.

3.2.4. Horse stacking.

The outcrop pattern west of Creag nam Broc on encl.3, shows a complex arrangement of horses accreted beneath the Loch Broom thrust. The horse 'stratigraphy' is best illustrated by using a hanging wall sequence diagram, fig 3.23a-d. This shows an evolutionary sequence:-

a. The Loch Broom thrust has ramped into the Pipe Rock Member of the Eriboll Formation, and one large and two small horses have been accreted. Evidence from the large horse (C on encl.3) shows these horses to be hindward-dipping, inverted horses derived from a folded footwall. See section 3.2.1.2, pg 50

b. The thrust climbed up section to the top of the Pipe Rock Member, but an asperity formed which included all of the An-t-Sron Formation and a part of the Durness Formation. This asperity was accreted to the hanging wall and was detached. Internal deformation occurred with imbricate reverse faulting, see encl.3. The horse is hindward dipping but right way up.

c-d. Before the Creag nam Broc fault had formed the Loch Broom thrust climbed up into the Eilean Dubh Member of Sheet IV. A horse of Eilean Dubh Member was accreted from the Creag nam Broc fault and was emplaced to its present position by the Creag nam Broc fault which dropped the Loch Broom thrust to the top of the An-t-Sron Formation. The horse is hindward dipping and right way up.

At each accretion, the hanging wall is deformed to accommodate the horse. With successive accretion of horses it can be seen from fig 3.23c that folding is likely to occur in the already accreted horses. Comparable deformation due to horse accretion has also been described in the Eriboll area, Butler (1982b).

3.3. CONCLUSIONS.

Horses which are derived from the footwall of thrust sheets can be classifed by their geometry. Three divisions have been established, fig.3.24.:-

(i) Ramp related horses - these are foreland-dipping and right way up or hindward-facing and inverted depending upon the original geometry of the ramp. They are always stratigraphically older than or the same age as the footwall rocks.

(ii) Asperity related horses - these are hindward-dipping and right way up and may incorporate rocks which are stratigraphically younger than the footwall.

(iii) Horses from anastomosing thrust zones - these produce horses which exhibit intense internal deformation so that original bedding is obliterated.

Fig.3.1. Deformation of a thrust sheet at a ramp-

(a) Back thrusts may form as a result of compressive stresses produced when a thrust sheet moves against a ramp.

(b) Synthetic splay thrusts may also form above a ramp, again as a result of compressive stresses.

Fig.3.2.

Extension faults occur in the thrust sheets at the apex of the ramp: these commonly form as a response to bending stresses within the thrust sheet as it moves from the ramp onto the flat.

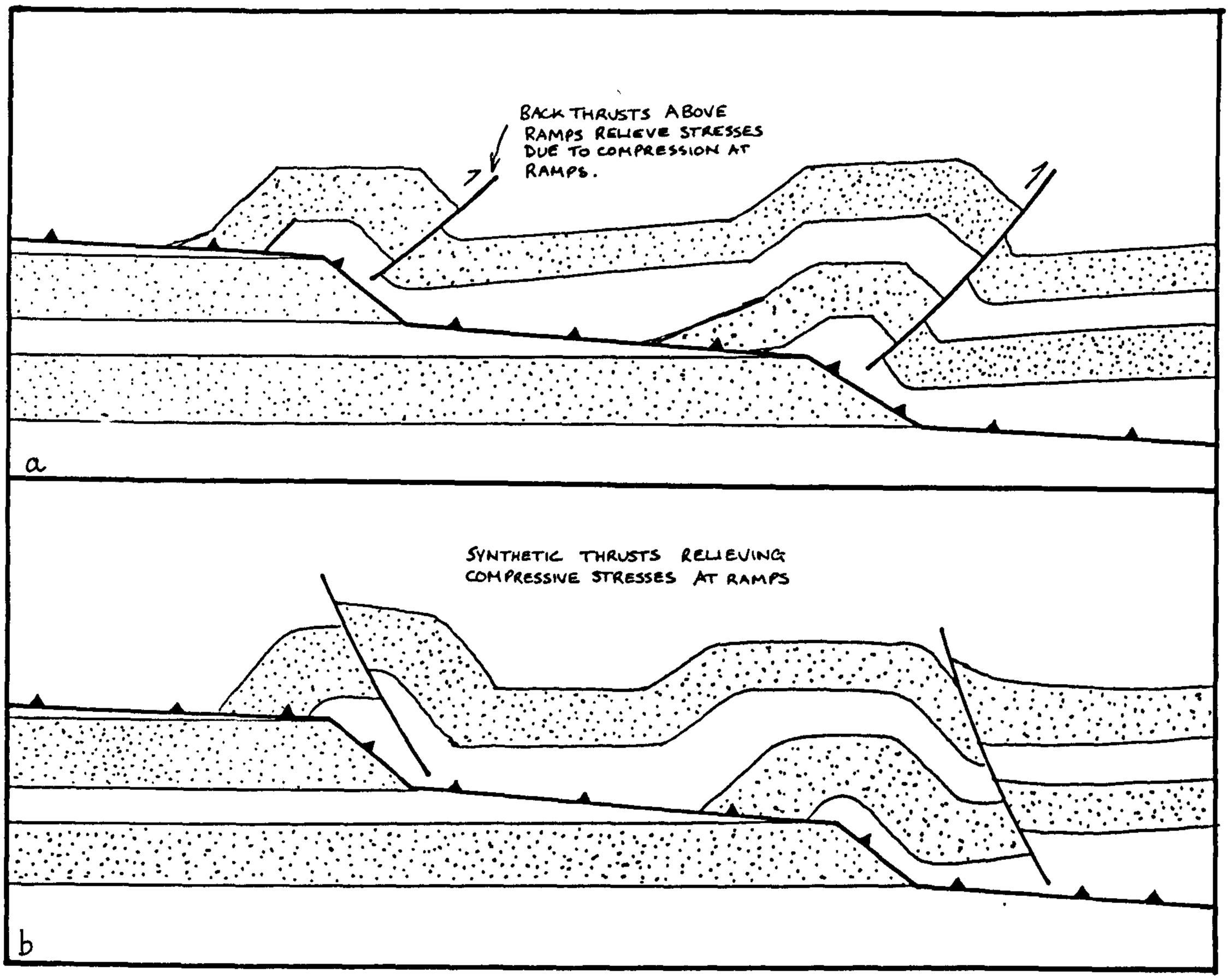
BACK THRUSTS ABOVE RAMPS RELIEVE STRESSES DUE TO COMPRESSION AT RAMPS.
a
SYNTHETIC THRUSTS RELIEVING COMPRESSIVE STRESSES AT RAMPS
b
EXTENSION FAULTS DEVELOP AT THE APEX OF RAMPS AS A RESULT OF EXTENSIONAL STRAINS WHICH DEVELOP AS THRUST SHEET MOVES FROM RAMP TO FLAT.
C

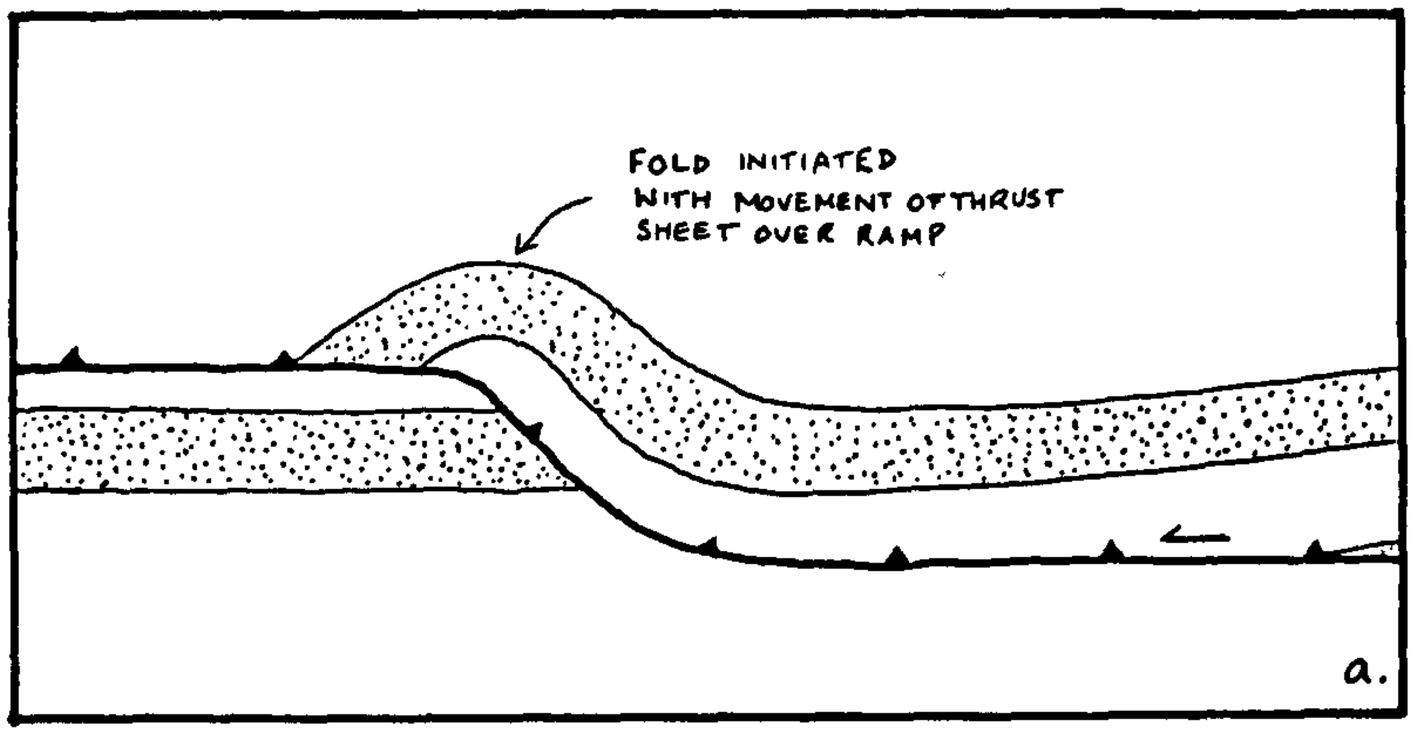

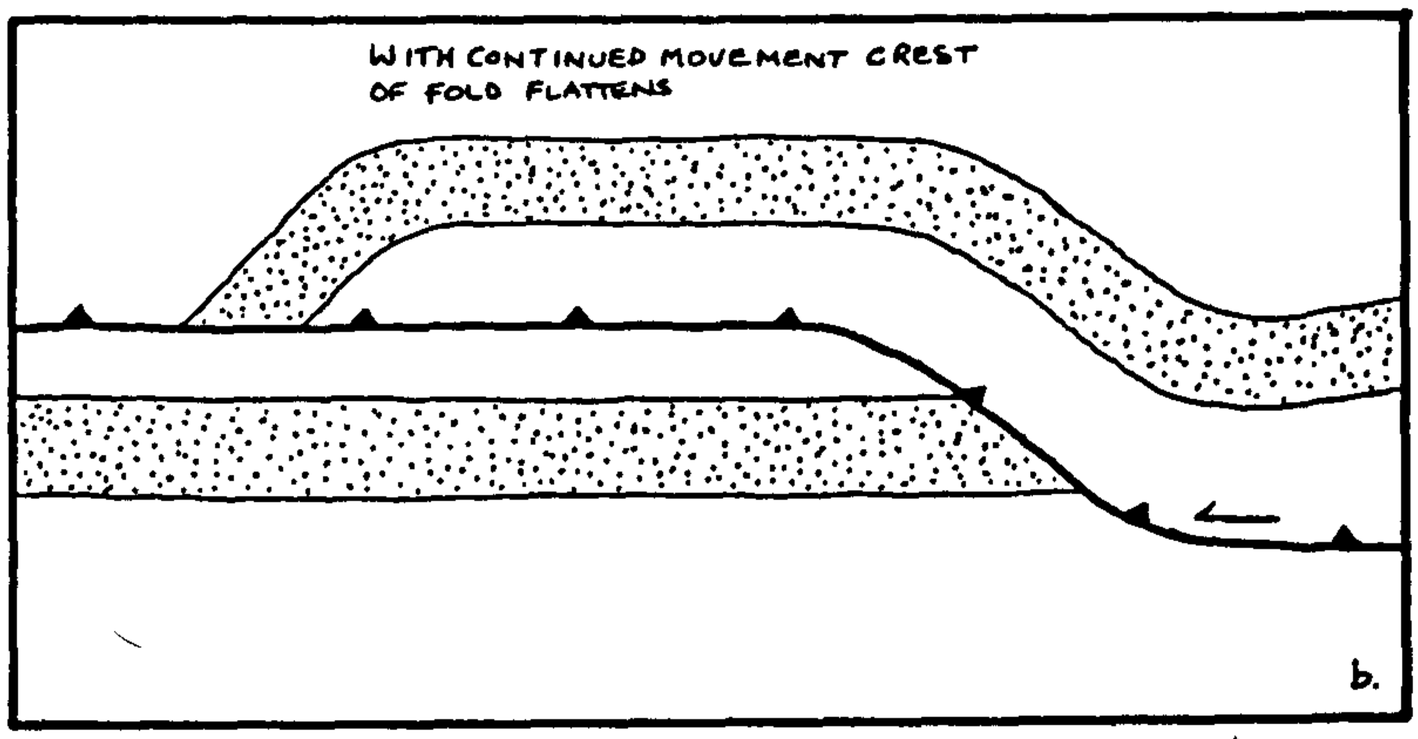

Fig.3.3.

The ramp-induced internal deformation of the thrust sheet can be totally accommodated by folding: in (a) a thrust is shown soon after some initial movement, with continuing motion the fold crest flattens (b).

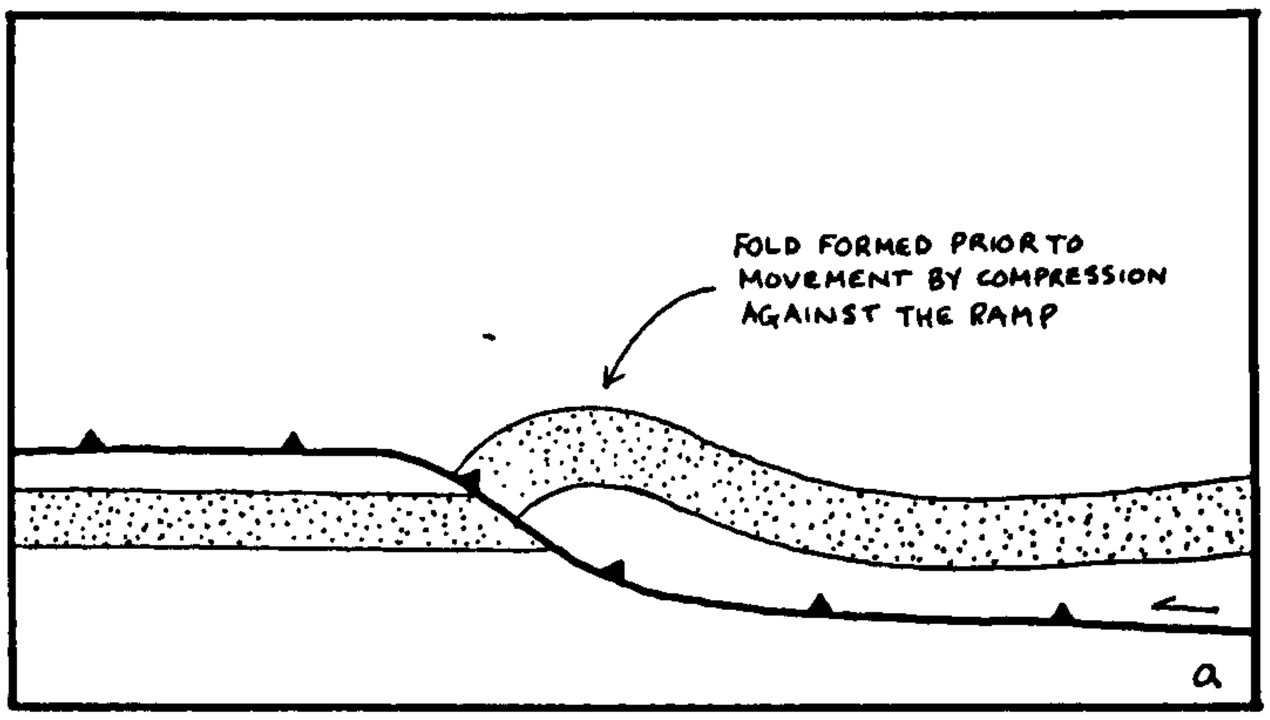

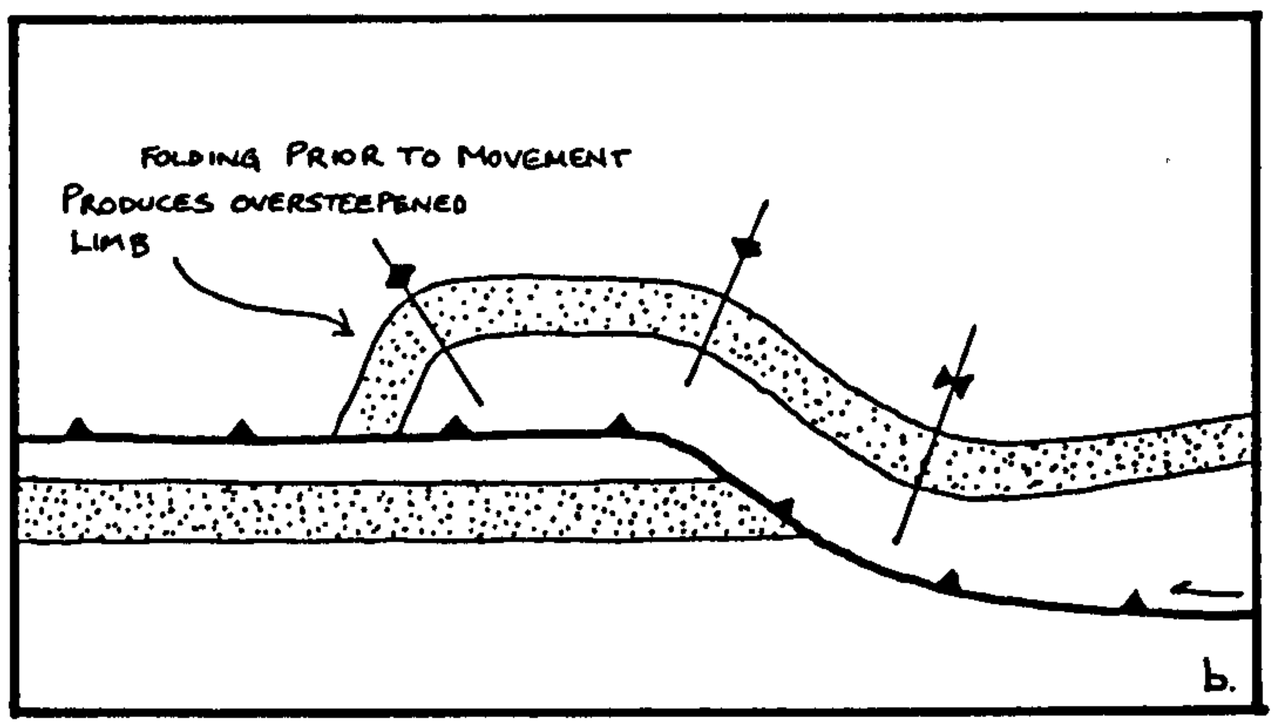

Fig.3.4.

A fold may develop in the competent units prior to movement up the ramp. With movement onto the upper flat the fold limb becomes oversteepened, and in some cases may become overturned, Berger& Johnson (1980).

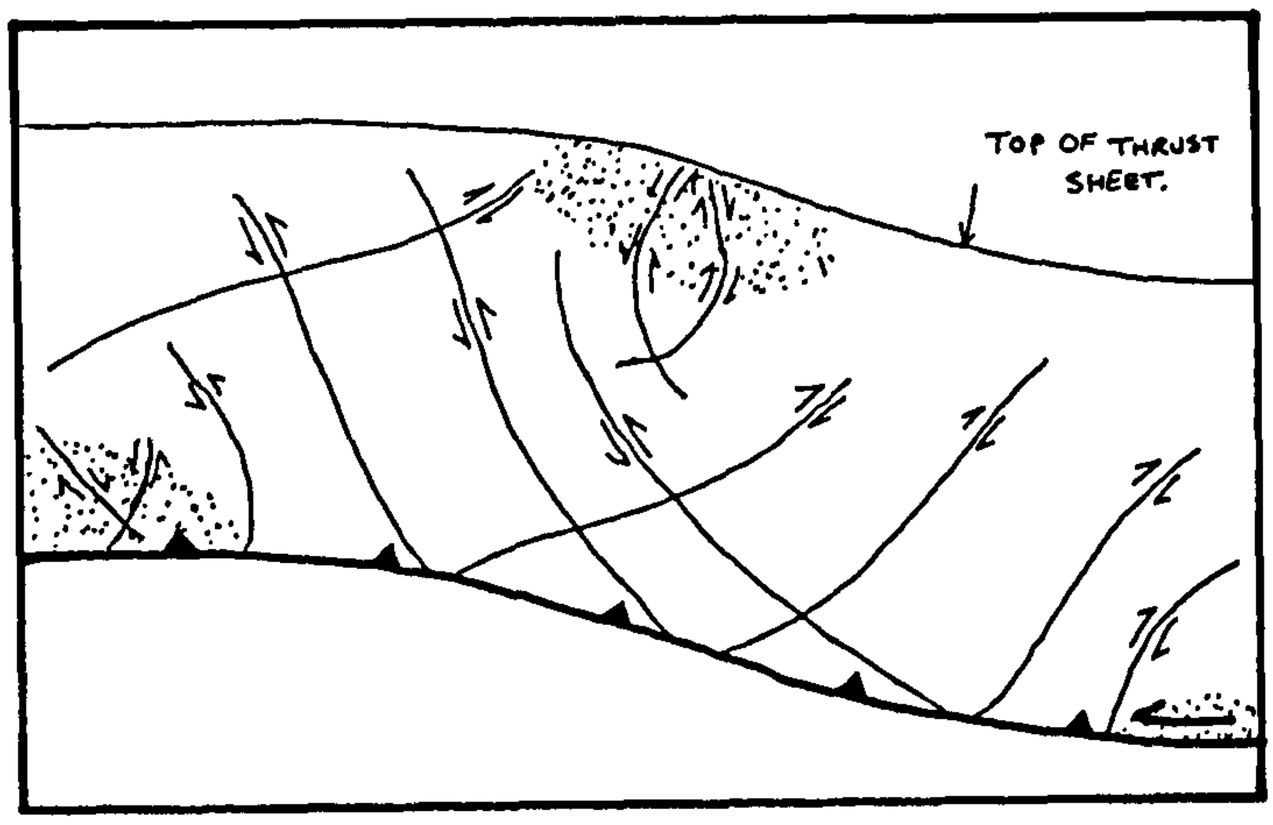

Fig.3.5.

Possible fault orientations in a thrust sheet at a ramp, predicted by theoretical analysis. The stippled areas are where the stresses are tensile. Note the position at the apex of the ramp, from Wiltschko (1979a).

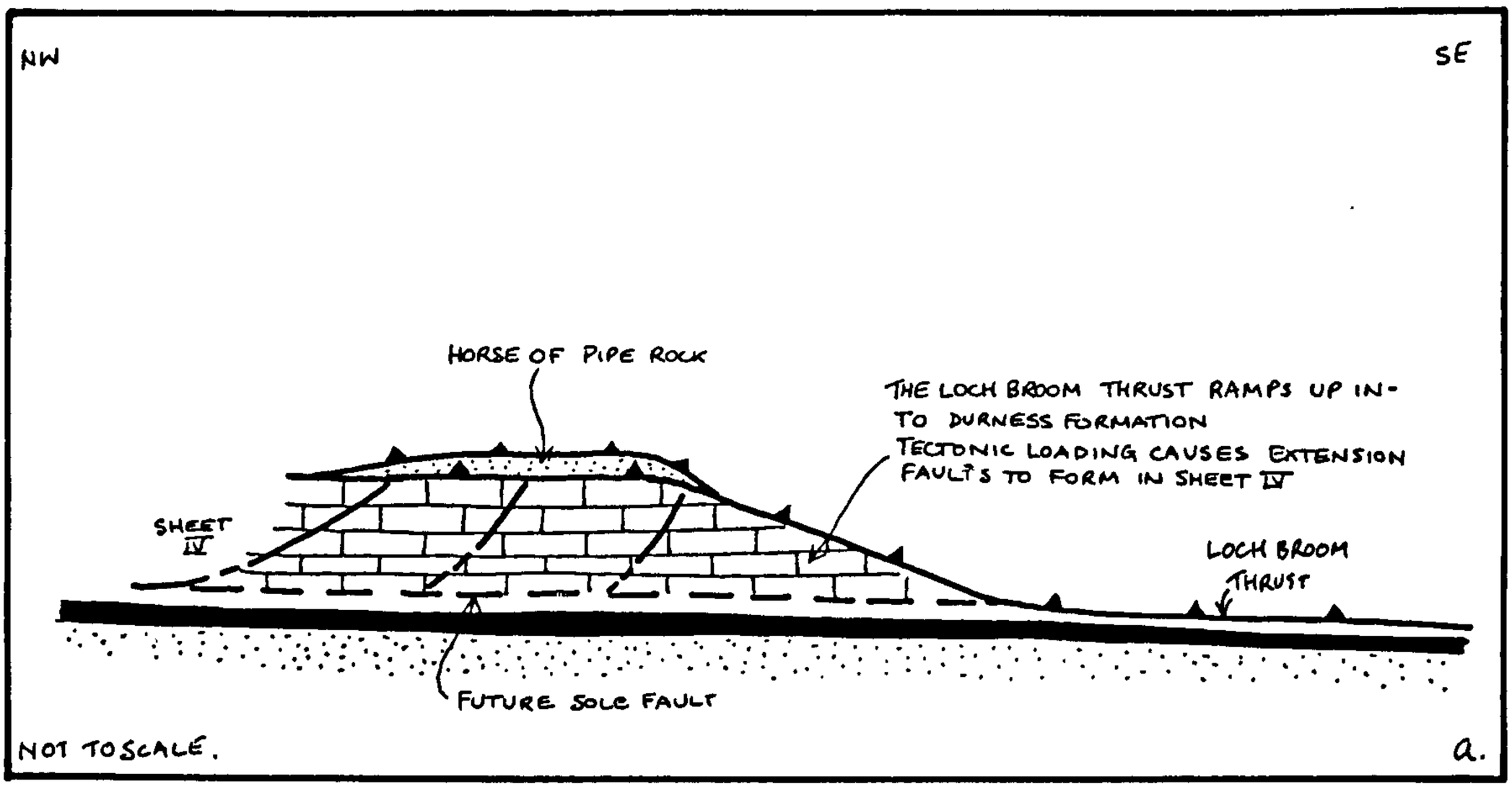

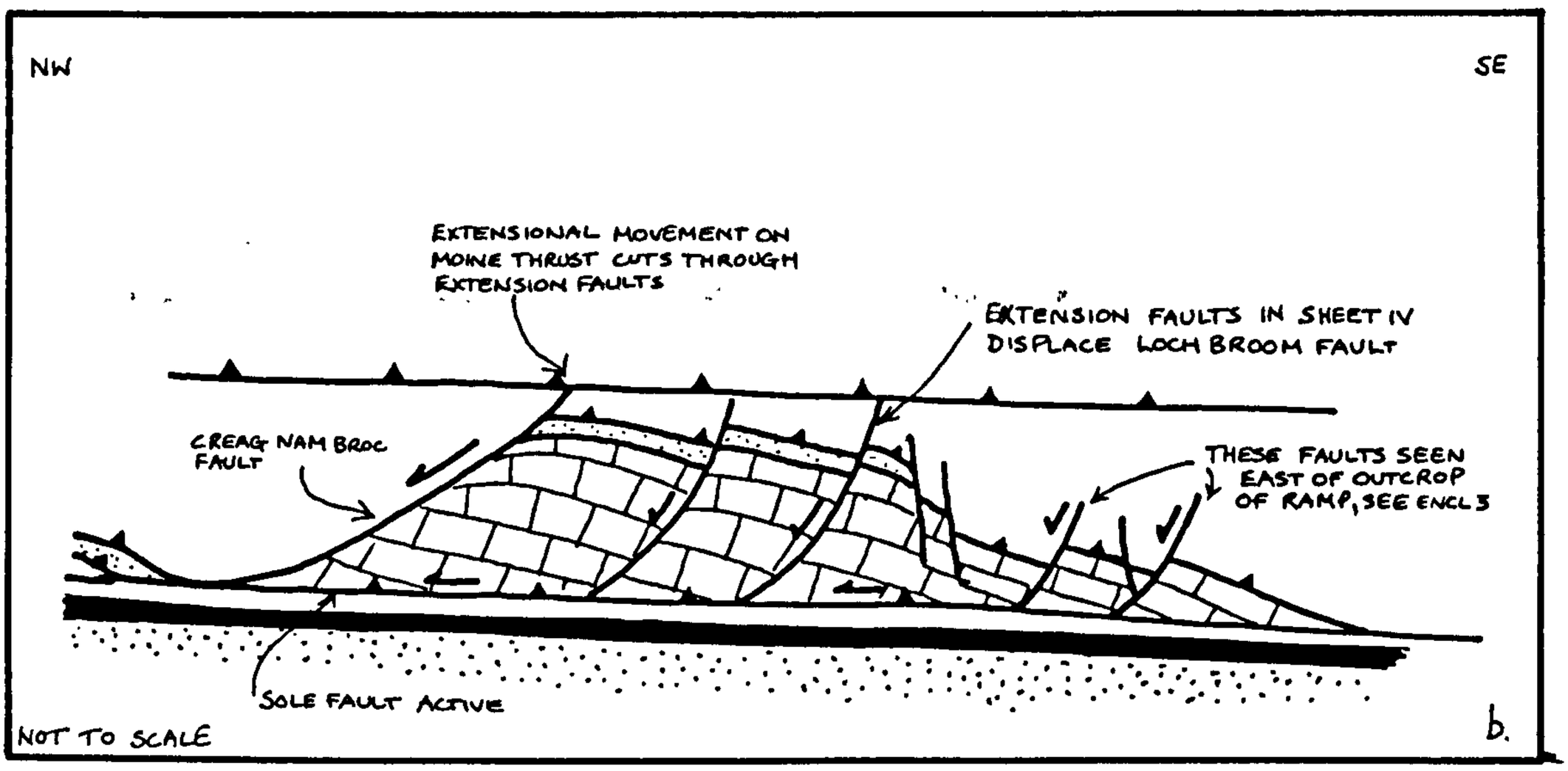

Fig. 3.6.

A hangingwall sequence diagram to show the development of extension above the ramp in the Loch Broom thrust. These occur where compressive stresses would be expected. The faults are interpreted as NW-SE orientated extension faults of Sheet IV which have propogated up into the Loch Broom thrust sheet.

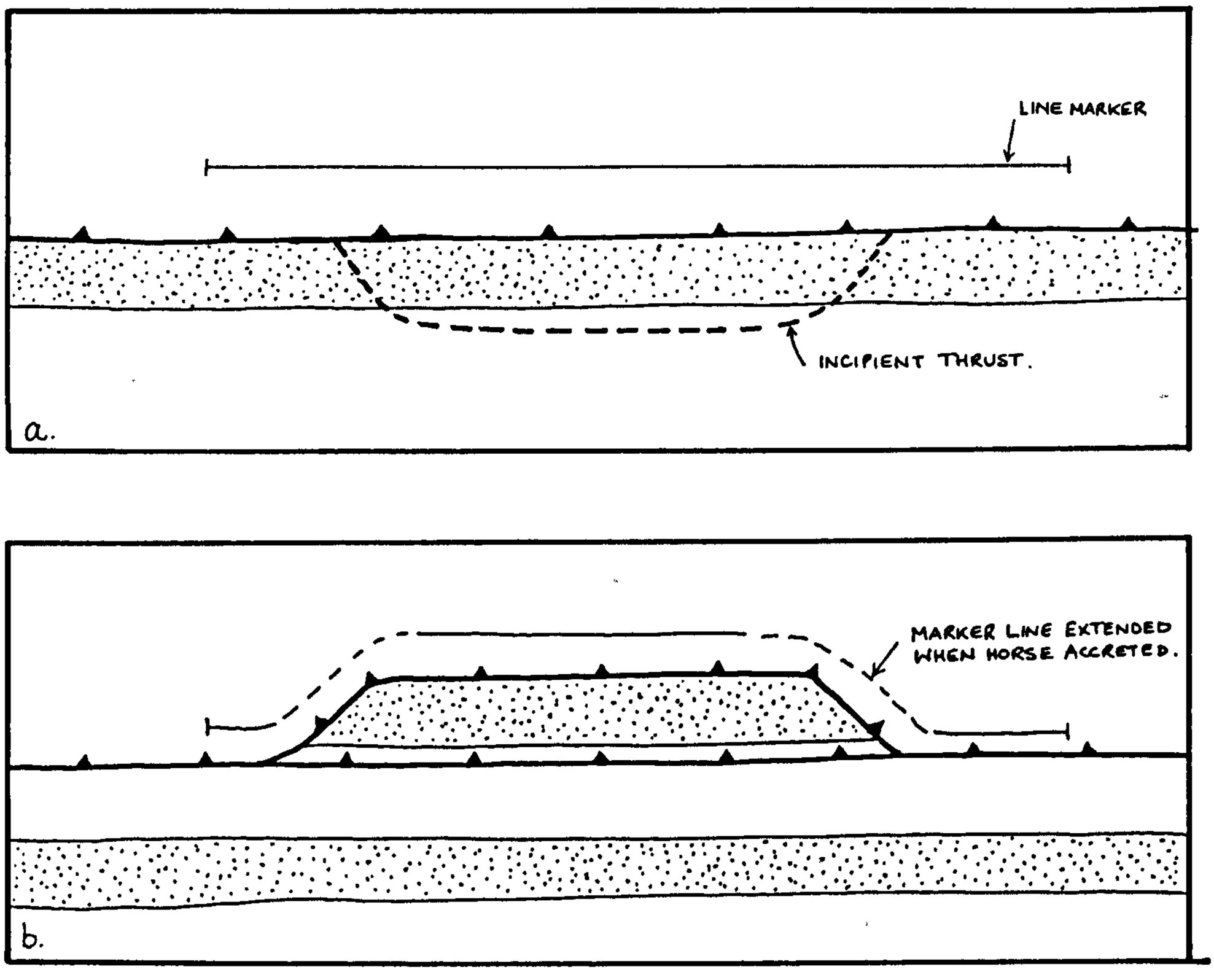

Fig.3.7.

A hanging wall sequence diagram to illustrate the accretion of a horse and the resulting deformation of the hangingwall. (a) shows a thrust prior to accreting the horse. (b) with accretion the thrust and the hangingwall are folded and extended. This extension may be taken up by extension faults (c).

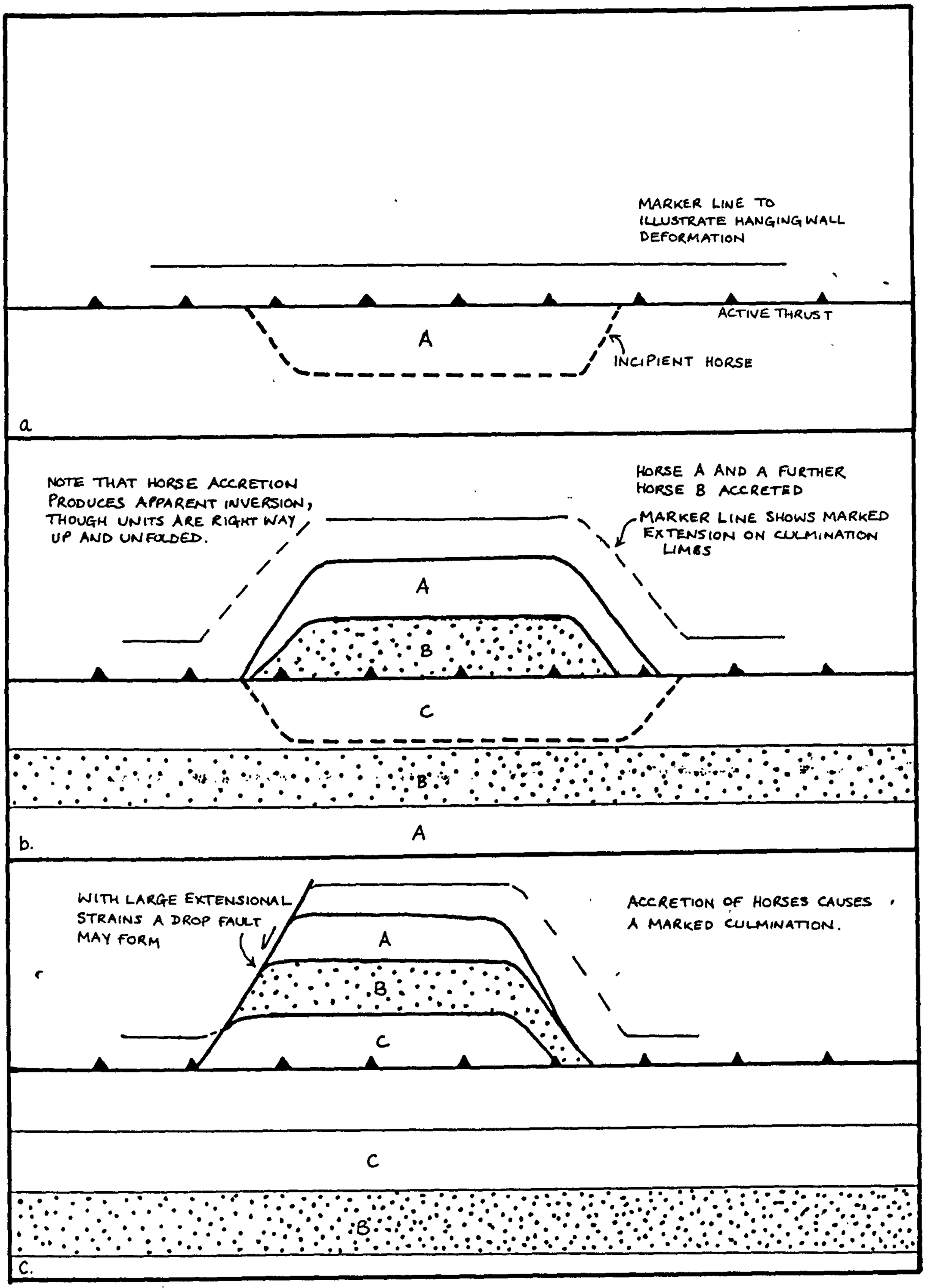

Fig.3.8.

A hangingwall sequence diagram to illustrate the sequential accretion of horses onto a thrust sheet. With each successive accretion, the hangingwall becomes more extended, (a,b) which may eventually lead to the formation of a drop fault, (c).

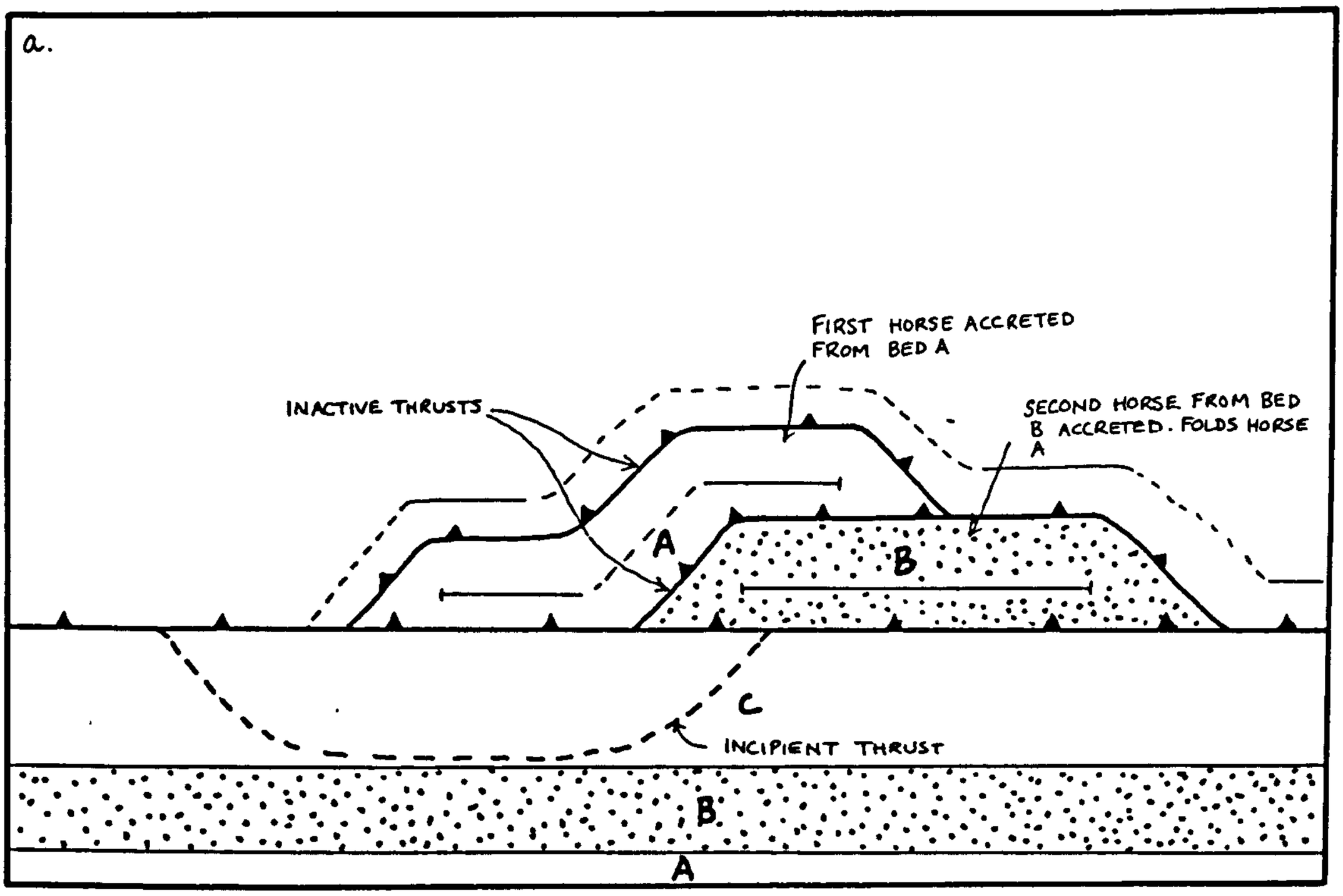

Fig.3.9.

Accretion of horses to adjacent hangingwall sites can produce a complex hangingwall deformation. This hangingwall seqence diagram shows that successive accretions causes folding of horses and extension in the hangingwall, (a). Further accretion, (b), can cause folding in areas of the hangingwall which were previously in extension.

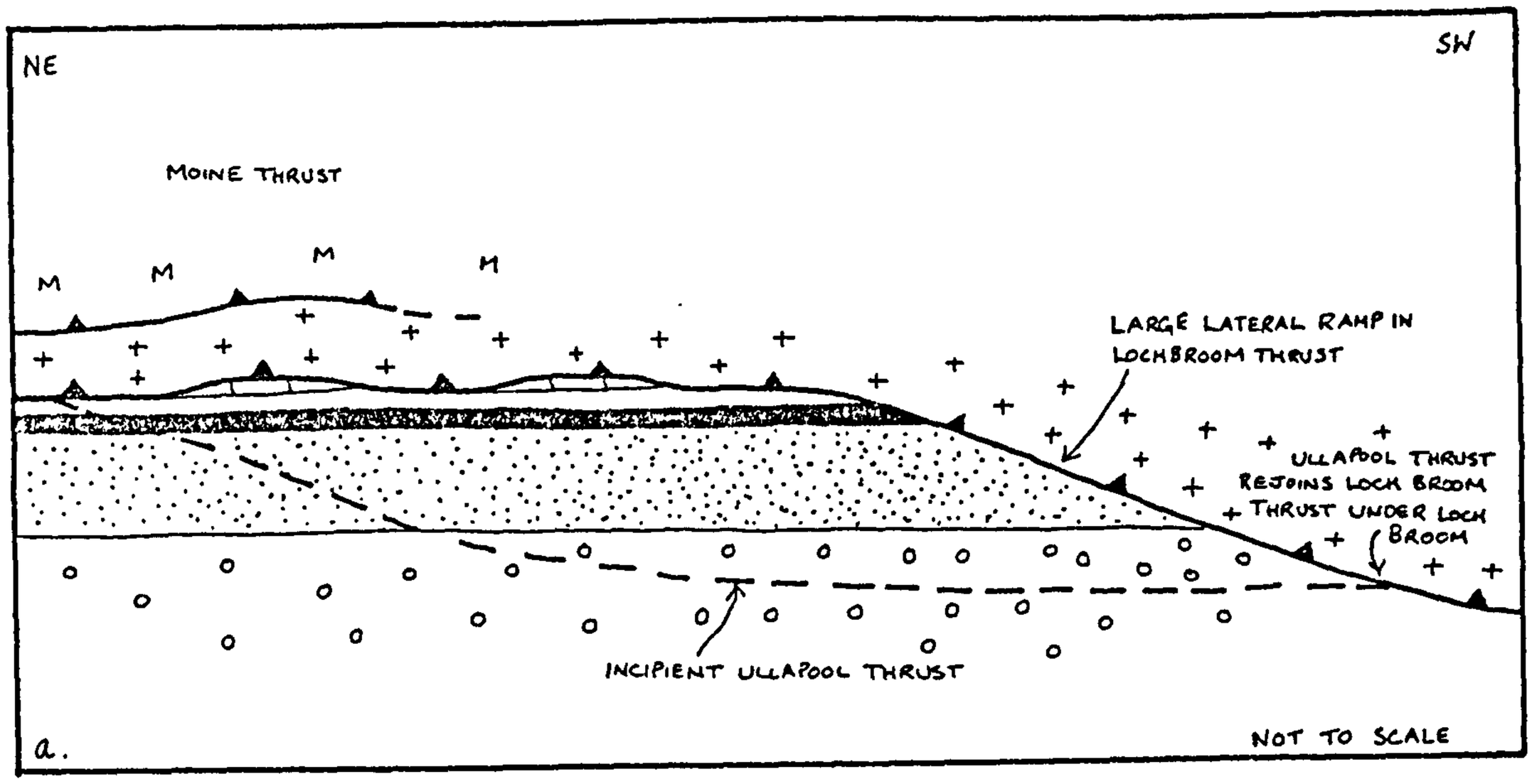

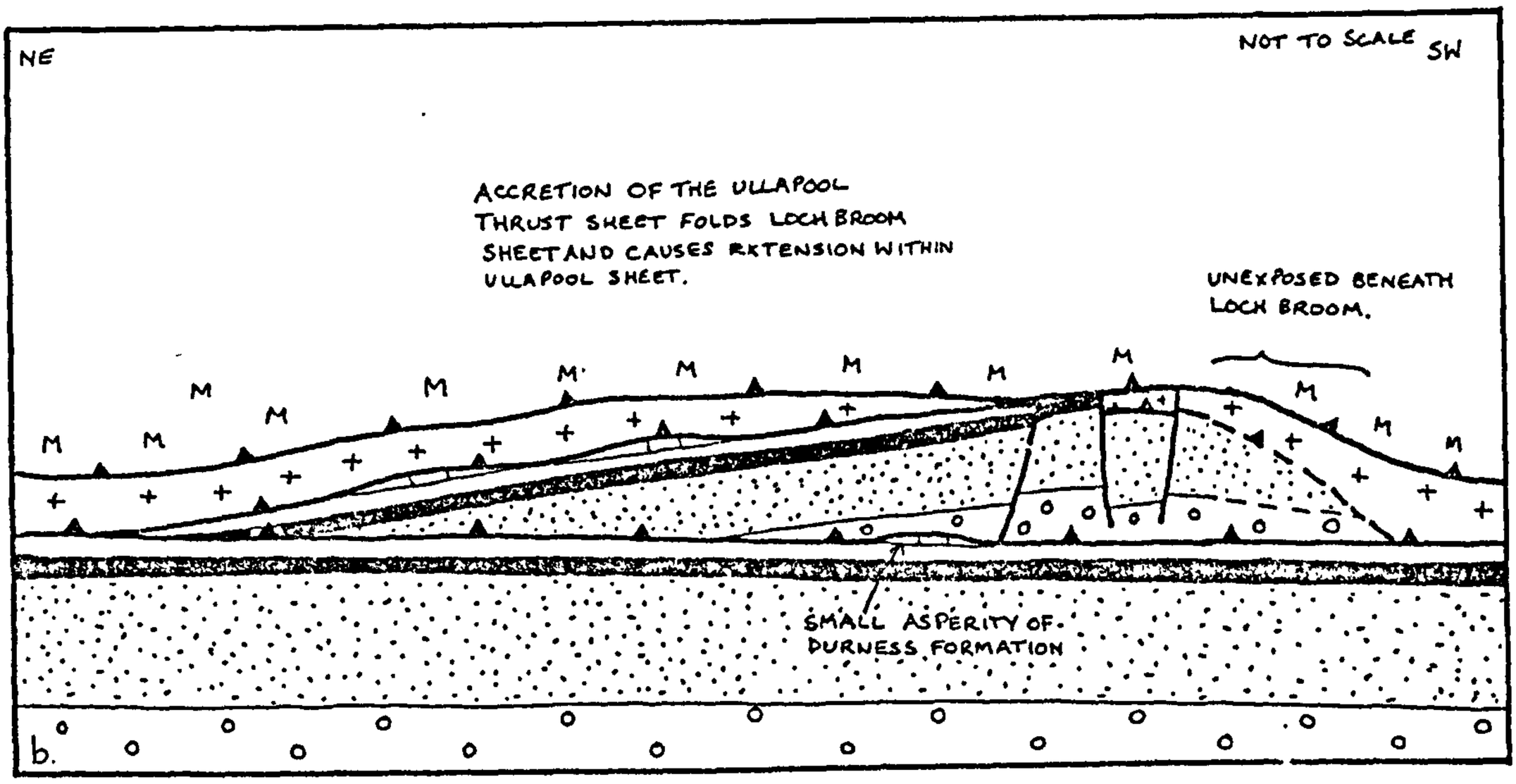

Fig.3.10.

Hangingwall sequence diagram to demonstrate the development ot the internal geometry of the Ullapool thrust sheet. The thrust sheet initiated at a large lateral ramp in the Loch Broom thrust, (a). With movement the thrust sheet was deformed into a large warp, with extension occurring at the crest.This extension was accommodated by extension faulting both in the strike and dip directions of the thrust sheet.

Fig.3.11.

Geological map of the Ullapool thrust sheet. Note the situation of the extension faults at the thickest part of the thrust sheet.

MEALL MOR

CROSS FAULT POSSIBLY MESOZOIC

MOINE THRUST

LOCH BROOM THRUST

HORSE OF QUARTZITIC MYLONITE MOINE THRUST BENEATH IT.

LOCH BROOM THRUST CUTS DOWN LARGE LATERAL RAMP FROM DURNESS FORMATION TO TORRIDONIAN

FLOOR THRUST OF IMBRICATES, NOT EXPOSED

IMBRICATES PATCHILY EXPOSED IN STREAM

TRUNCATION OF LOCH BROOM THRUST BY REACTIVATED MOINE THRUST

EXTENSION FAULTS DO NOT CUT MOINE THRUST

LOCH BROOM THRUST

EXTENSION FAULTS OCCUR AT THICKEST PART OF ULLAPOOL THRUST SHEET

ULLAPOOL THRUST REJOINS LOCH BROOM THRUST BENEATH LOCH BROOM.

LOCH BROOM

ULLAPOOL THRUST

CORRY BURN

CORRY BRIDGE.

CORRY POINT

ULLAPOOL

A835

N

0 100 200

METRES

Fig.3.12.

Cross section along the line A-A' on fig.3.11, parallel to the tectonic transport direction. Note the lens shape of the thrust sheet. The Ullapool sheet is a large horse plucked from a lateral ramp in the Loch Broom thrust. The late extensional movement on the Moine thrust truncates the Loch Broom thrust.

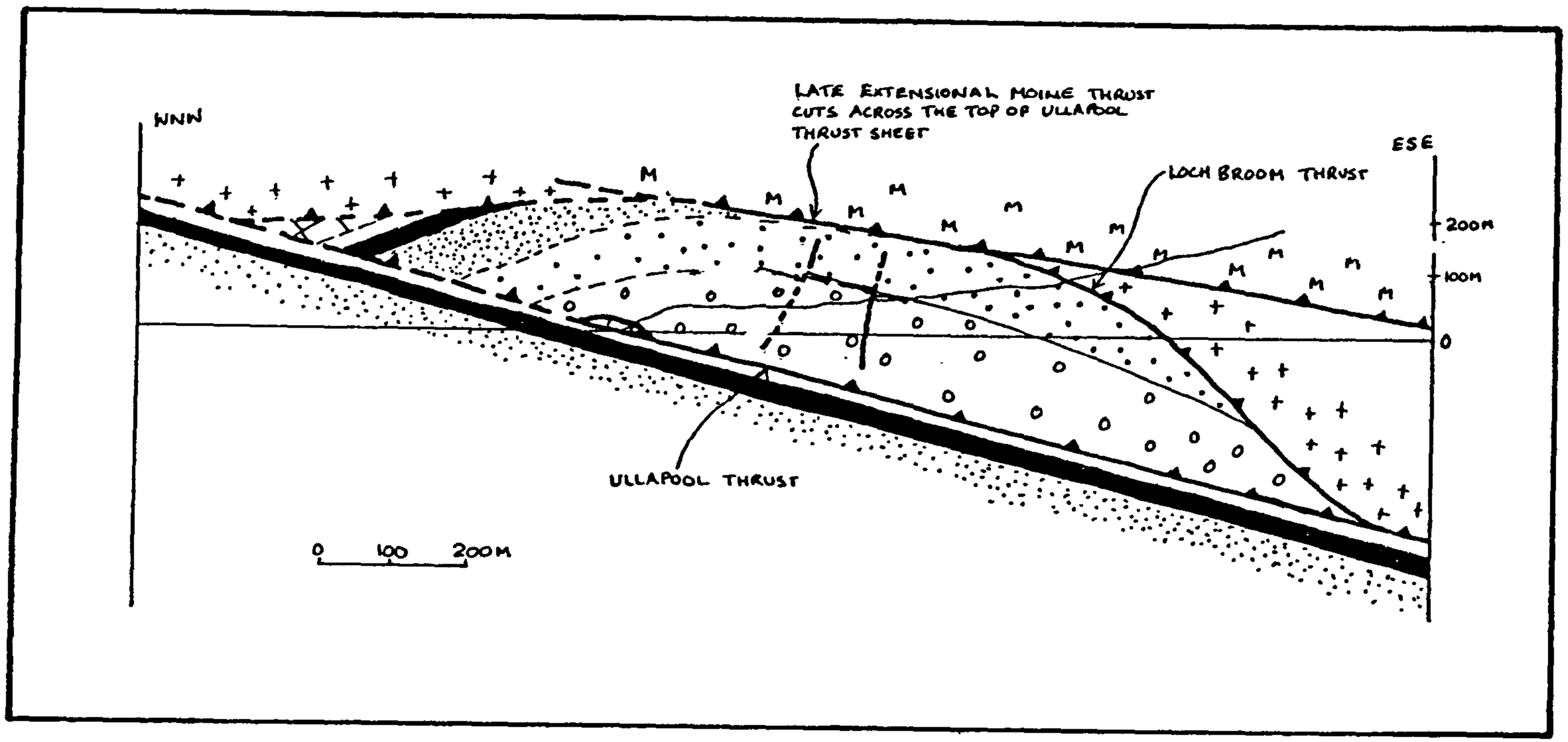
WNW
LATE EXTENSIONAL MOINE THRUST
CUTS ACROSS THE TOP OF ULLAPOOL
THRUST SHEET
ESE
LOCH BROOM THRUST
200M
100M
0
ULLAPOOL THRUST
0 100 200M

Fig.3.13.

Diagram to show the shape of a horse; the bounding fault planes meet the main thrust plane at a branch line, these line surround the horse. Horses are often lensoid in shape, the section X-X' shows a typical cross section. After Boyer & Elliott.(1982)

Fig.3.14.

Diagram to show the ralationship between the principal stresses and a thrust plane. An increase in the angle θ causes an increase in the normal stress σ_n and hence also τ, friction on the thrust plane will also rise.

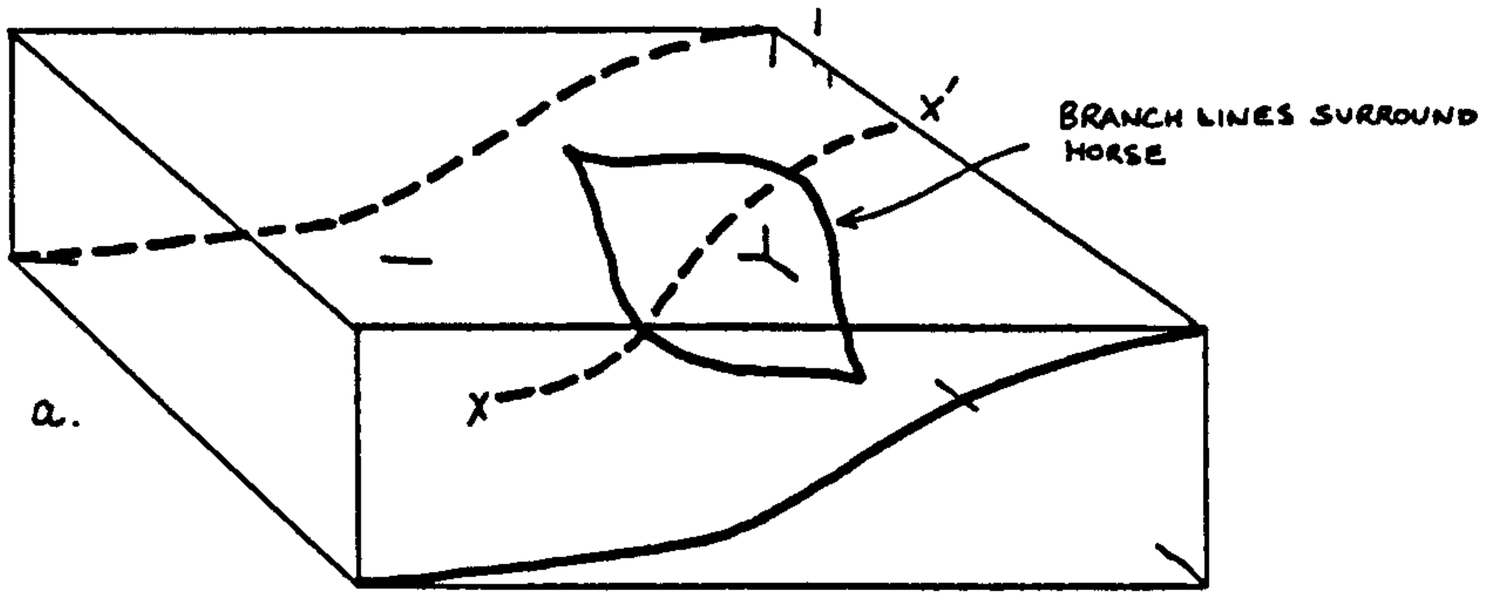
a.
X
X'
BRANCH LINES SURROUND HORSE

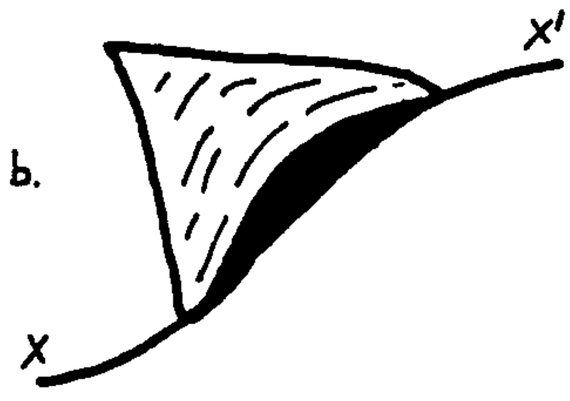
b.
X
X'

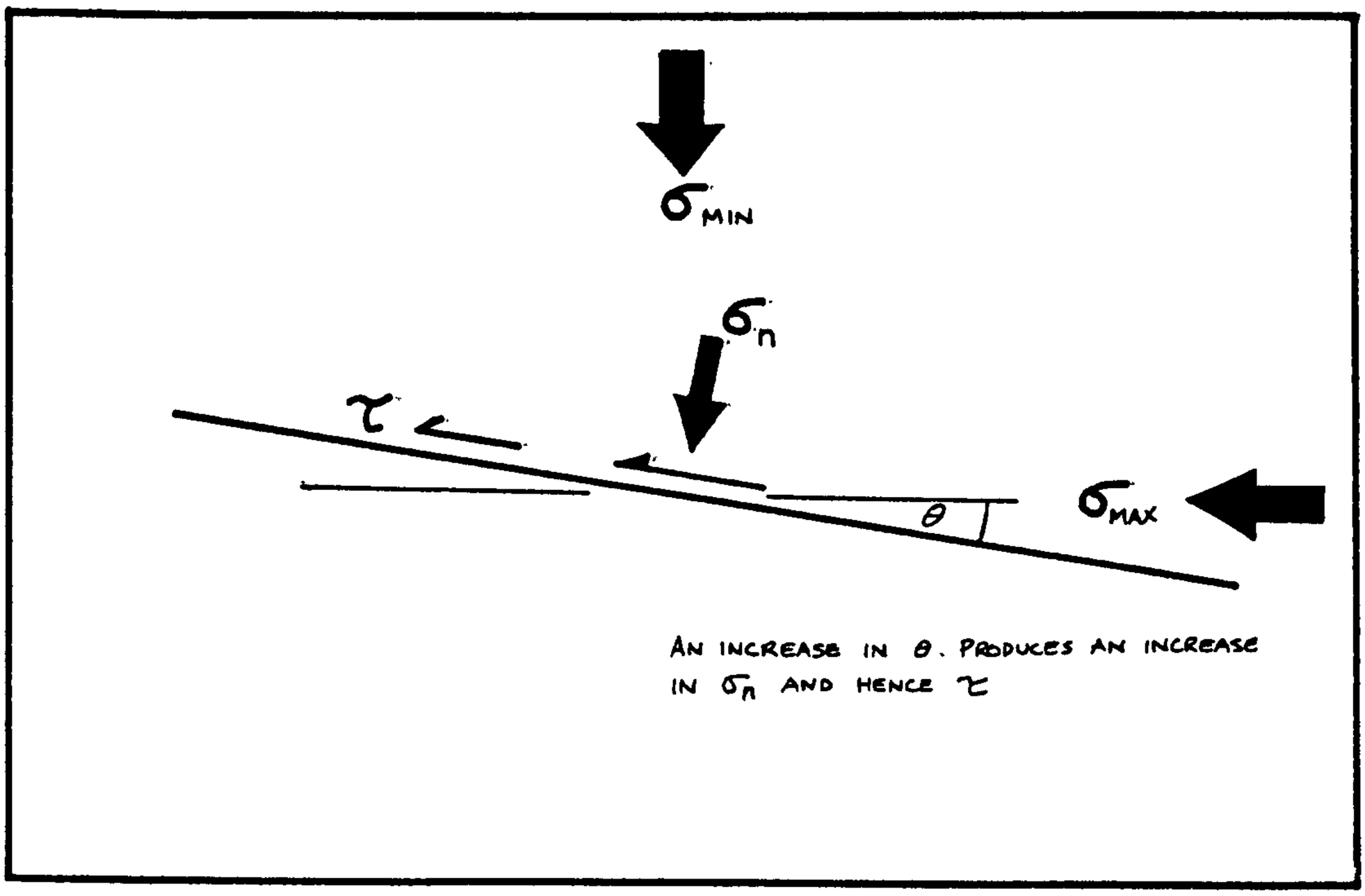
σ_{MIN}
σ_n
τ
θ
σ_{MAX}
AN INCREASE IN θ. PRODUCES AN INCREASE IN σ_n AND HENCE τ

Fig.3.15.

Diagrams to show the formation of ramps as a result of lateral changes in their glide plane.

(a) Ramps may form as links connecting planes of high pore fluid pressure.

(b) Old extension faults which have previously displaced the glide horizon may become reactivated as thrust ramps.

(c) Fossil hills may provide a similar situation to old extension faults

(d) Folding may occur prior to thrusting, thickening the layers. The short steep limbs of folds are commonly thrust out and are often sites of ramps.

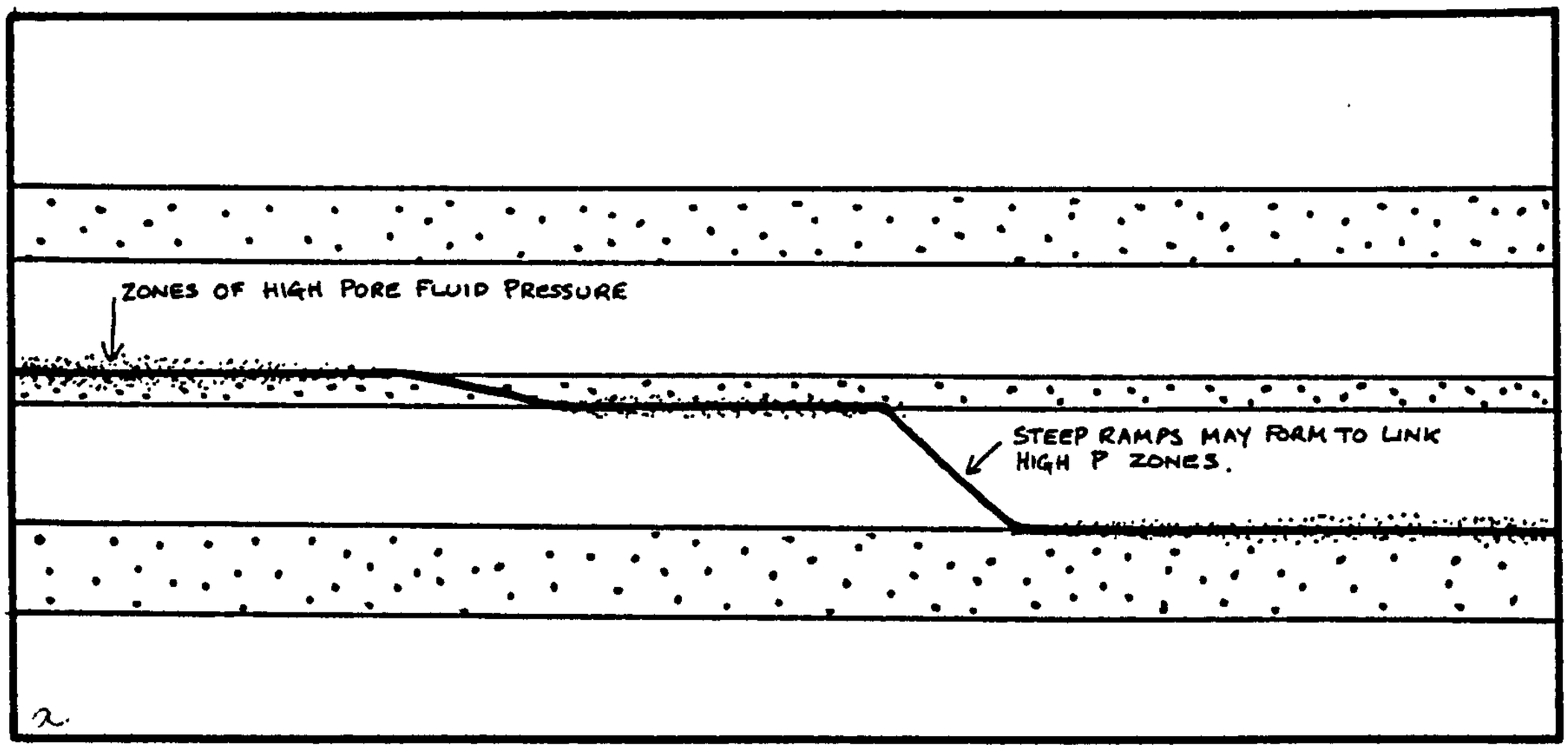
ZONES OF HIGH PORE FLUID PRESSURE
STEEP RAMPS MAY FORM TO LINK HIGH P ZONES.
a.

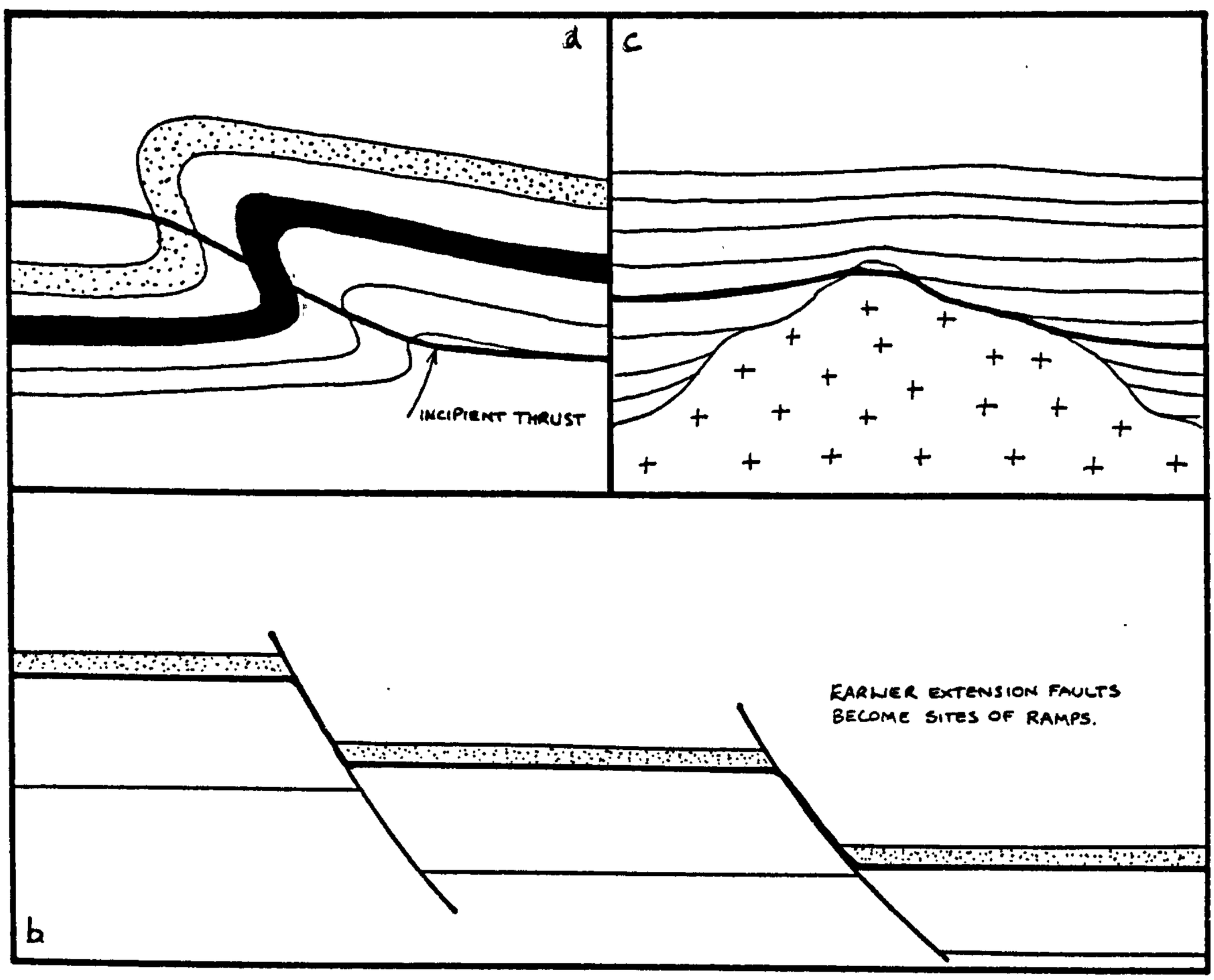
d
c
INCIPIENT THRUST
EARLIER EXTENSION FAULTS BECOME SITES OF RAMPS.
b

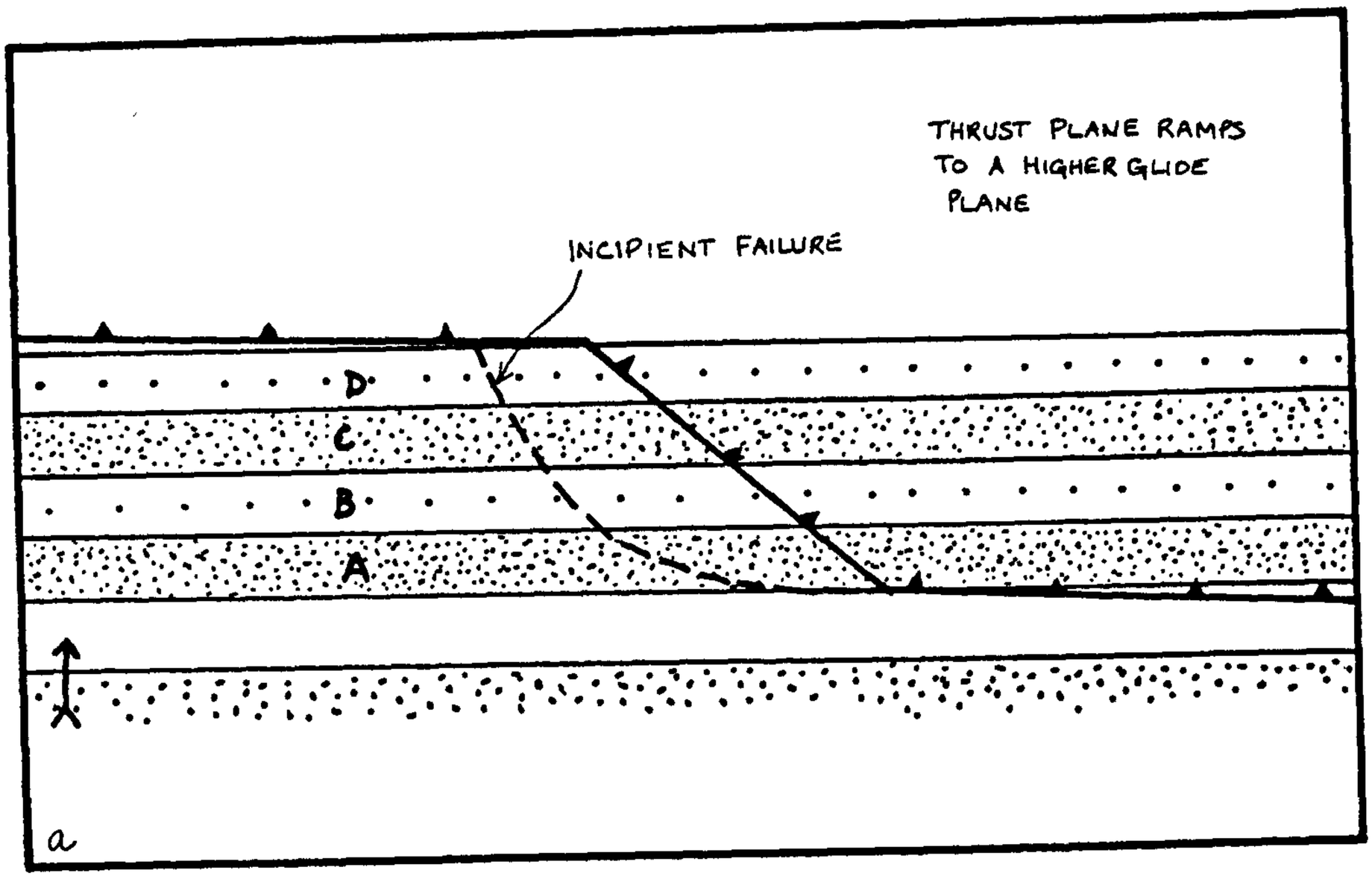

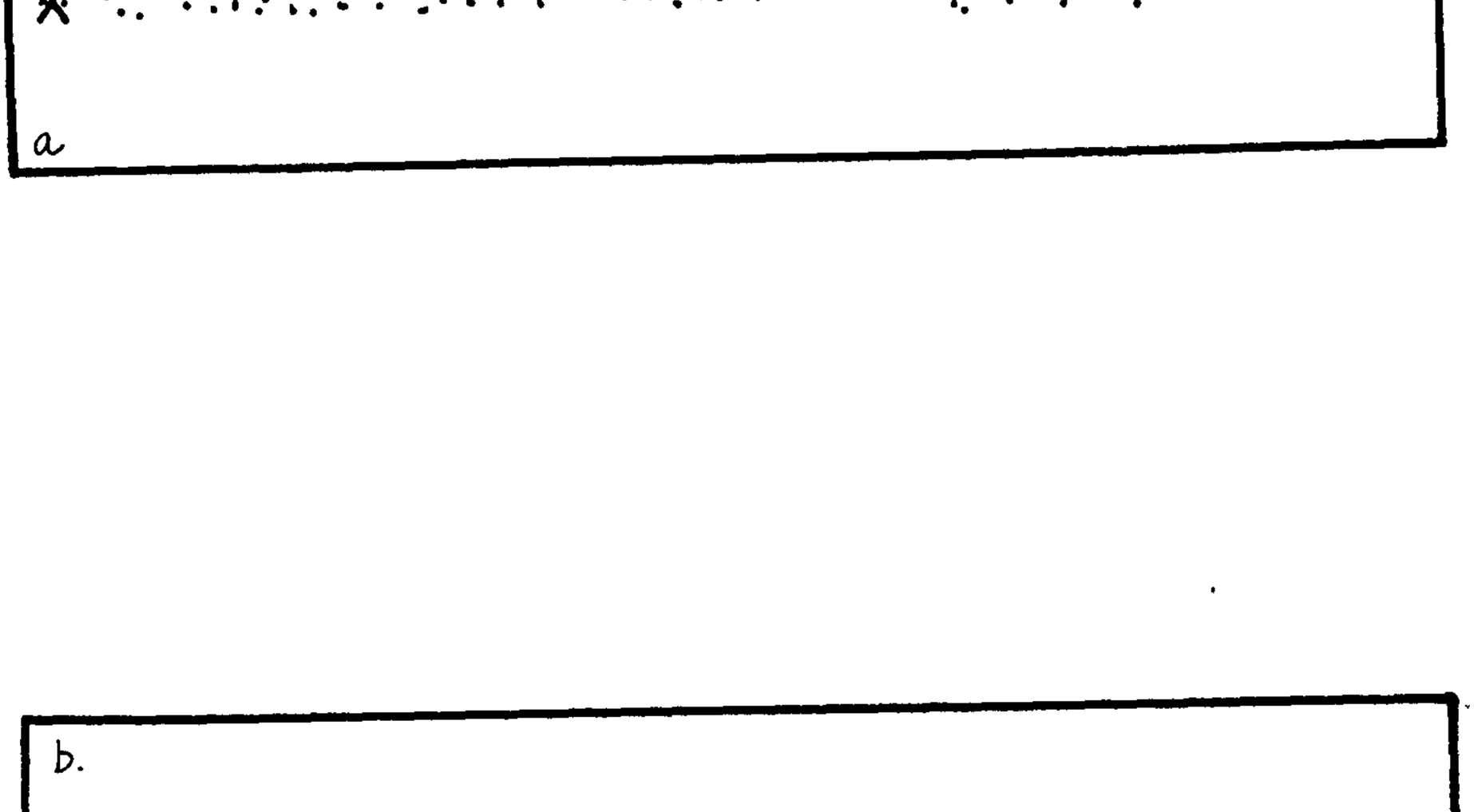

Fig.3.16.

Two diagrams to show the geometry of a horse that is formed from a simple ramp.

(a) The footwall is undeformed, and the incipient fracture is shown.

(b) With accretion and movement over the ramp, the bedding rotates to become foreland dipping and right way up.

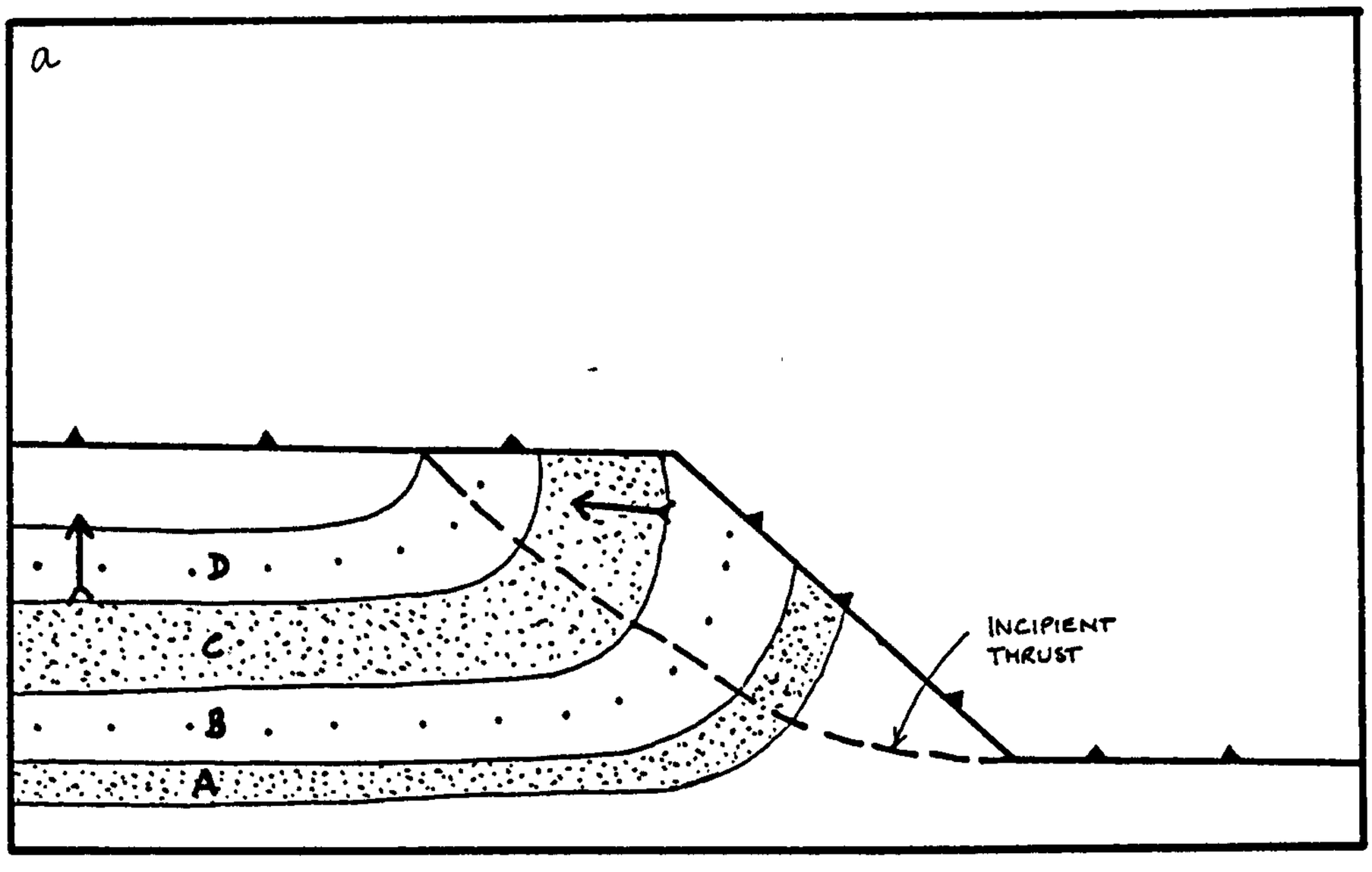

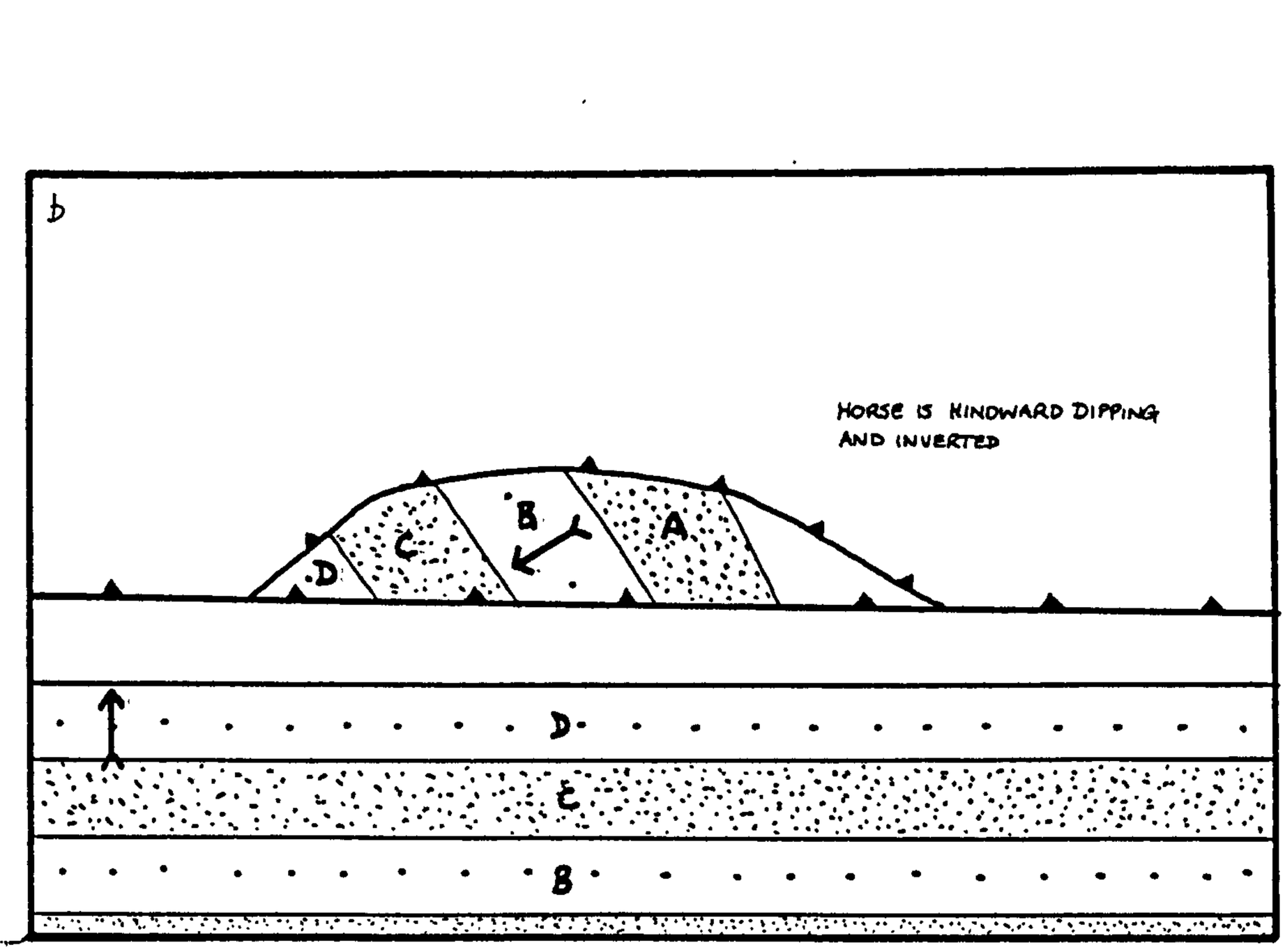

Fig.3.17

Two diagrams to show the geometry of a horse derived from a ramp which cuts through a folded footwall.

(a) Geometry before movement.

(b) After accretion and movement up the ramp, and the bedding is rotated to become hindward dipping and inverted.

Fig.3.19.

Cross section drawn along a line parallel to the transport direction of an aperity. Note that at the leading edge of an asperity the thrust cuts down section in transport direction.

Fig.3.20.

Diagrammatic cross section through the horses at Creag nam Broc to show the geometry of horse E. Horse E was either derived from an asperity whose original position wsa on the top of Sheet IV, or it was was plucked off of Sheet IV by movement on the Creag man Broc fault, which then moved the horse to its present position.

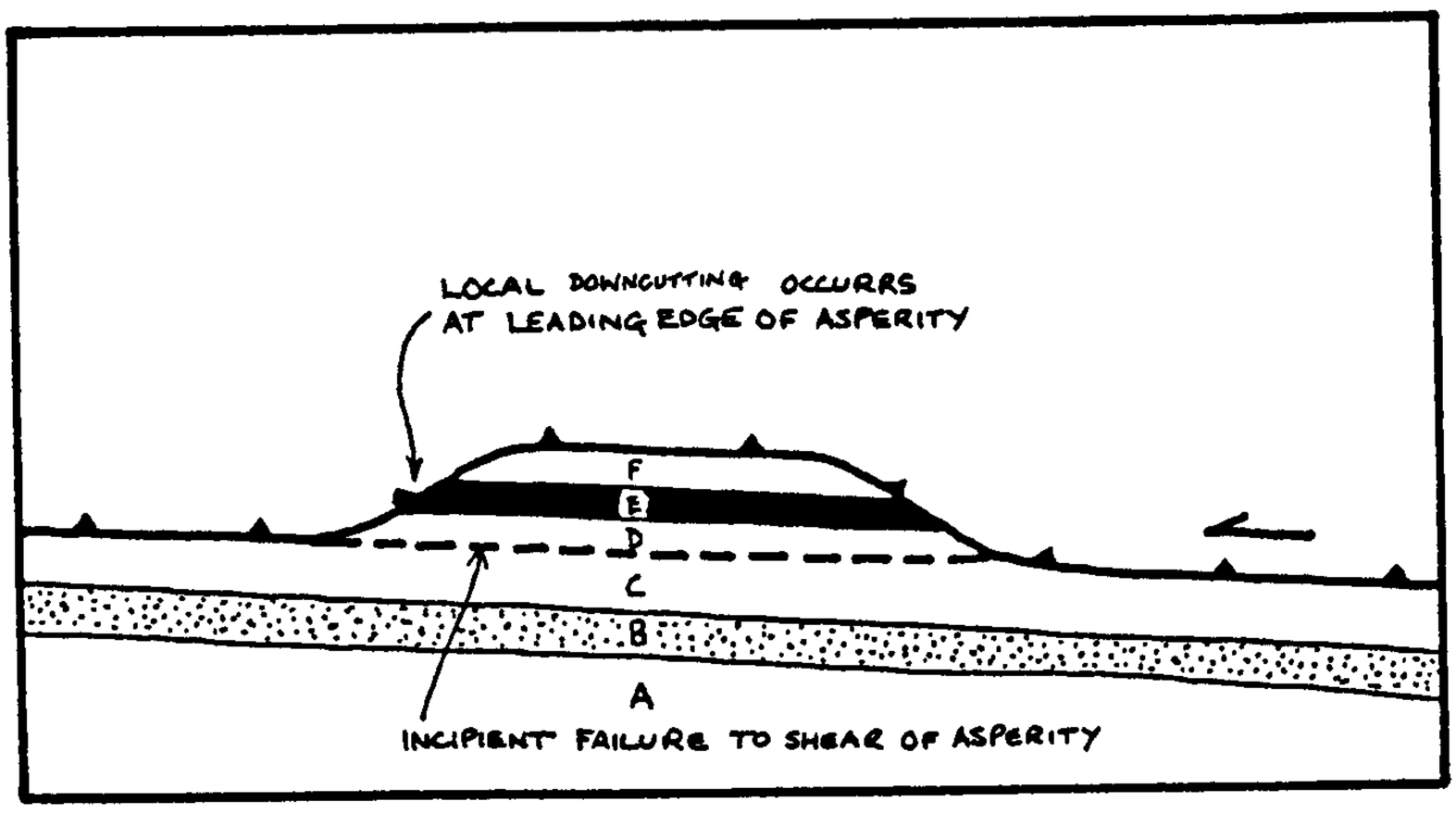
LOCAL DOWNCUTTING OCCURRS
AT LEADING EDGE OF ASPERITY
F
E
D
C
B
A
INCIPIENT FAILURE TO SHEAR OF ASPERITY

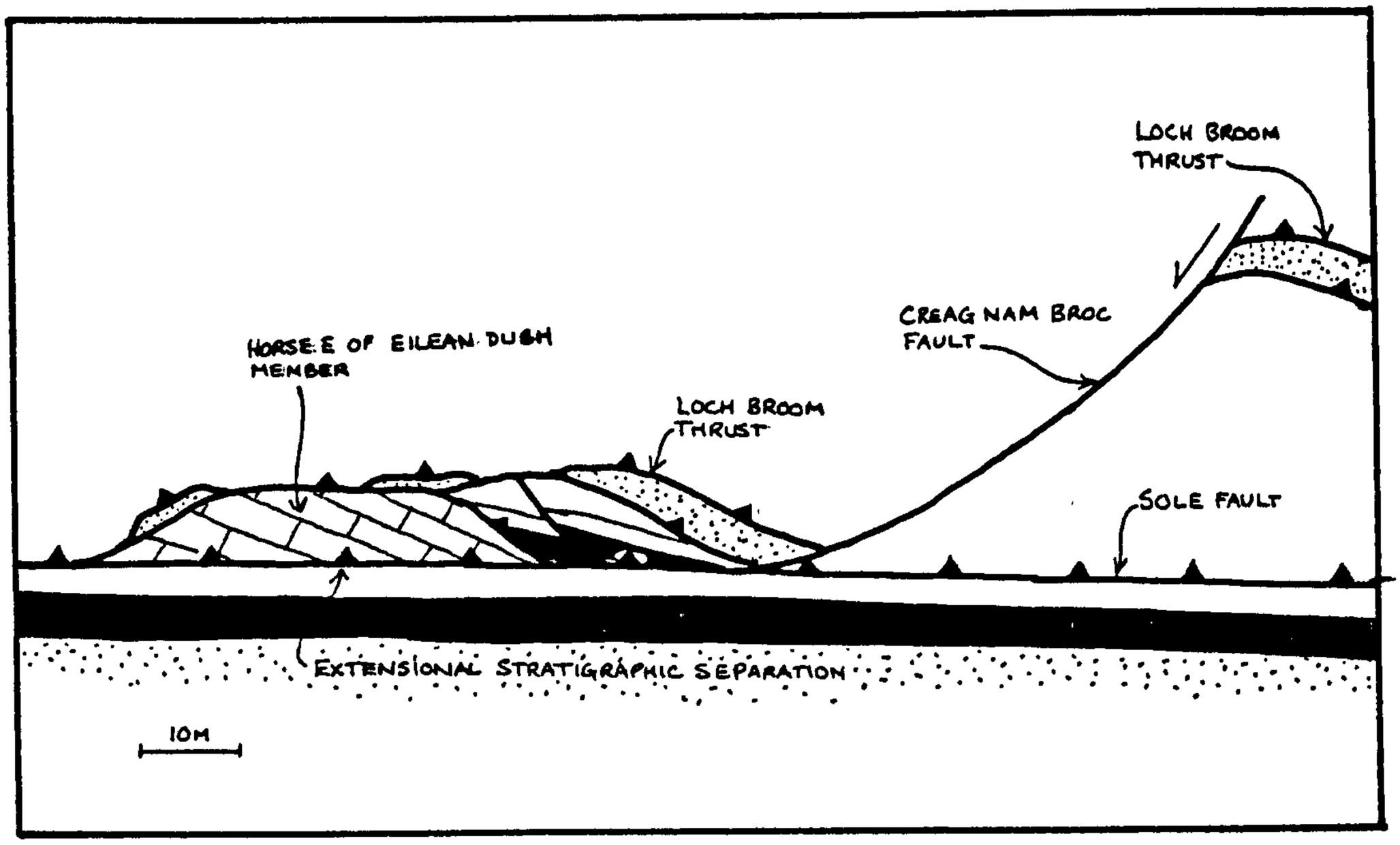
LOCH BROOM
THRUST
CREAG NAM BROC
FAULT
HORSE E OF EILEAN DUBH
MEMBER
LOCH BROOM
THRUST
SOLE FAULT
EXTENSIONAL STRATIGRAPHIC SEPARATION
10M

Fig.3.21.

Diagrams to illustrate the formation of horses from an anastomosing thrust zone-

(a) As a fracture deforms the rock a field of work hardening develops around it, and which strengthens the fracture. Continuing deformation will then shift the deformation to the weaker host rock, and a lens of the work hardened rock removed.

(b) A fault plane may become indurated by its own fault rock or vein. The deformation may then shift to the host rock. Small horses of fault rock may form.

(c) If a thrust is continually forming an irregular fracture, then the irregularities will be sheared off as horses.

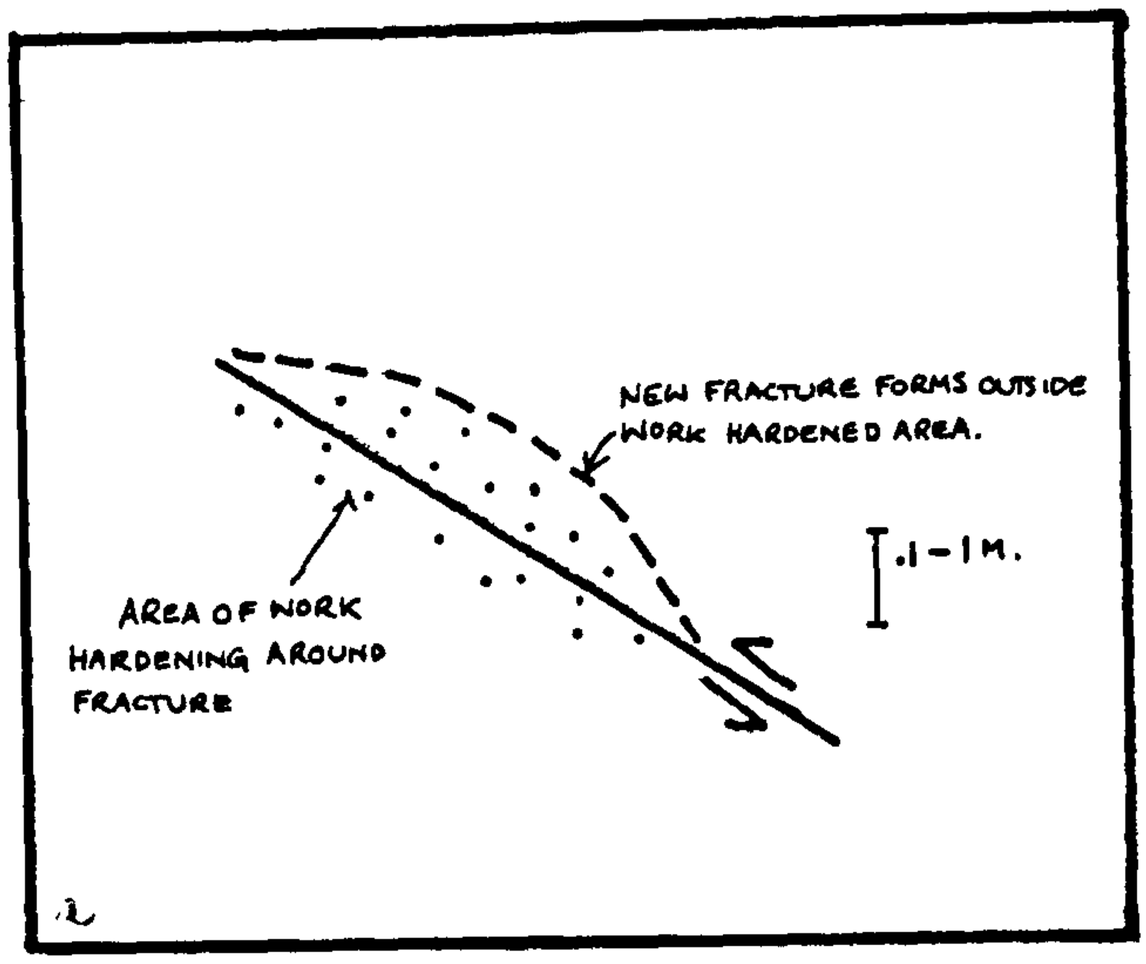
NEW FRACTURE FORMS OUTSIDE WORK HARDENED AREA.
.1 - 1 M.
AREA OF WORK HARDENING AROUND FRACTURE

a.

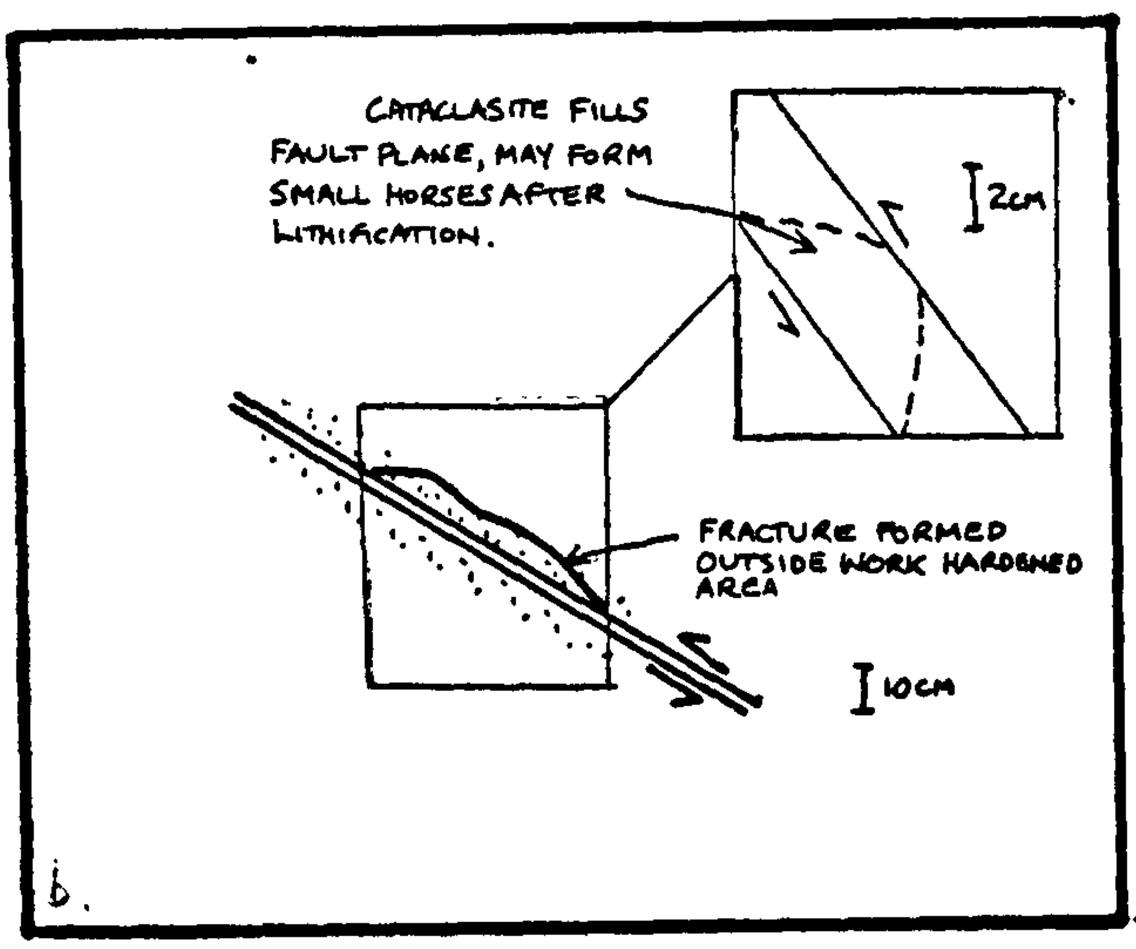
CATACLASITE FILLS FAULT PLANE, MAY FORM SMALL HORSES AFTER LITHIFICATION.
2cm
FRACTURE FORMED OUTSIDE WORK HARDENED AREA
10cm

b.

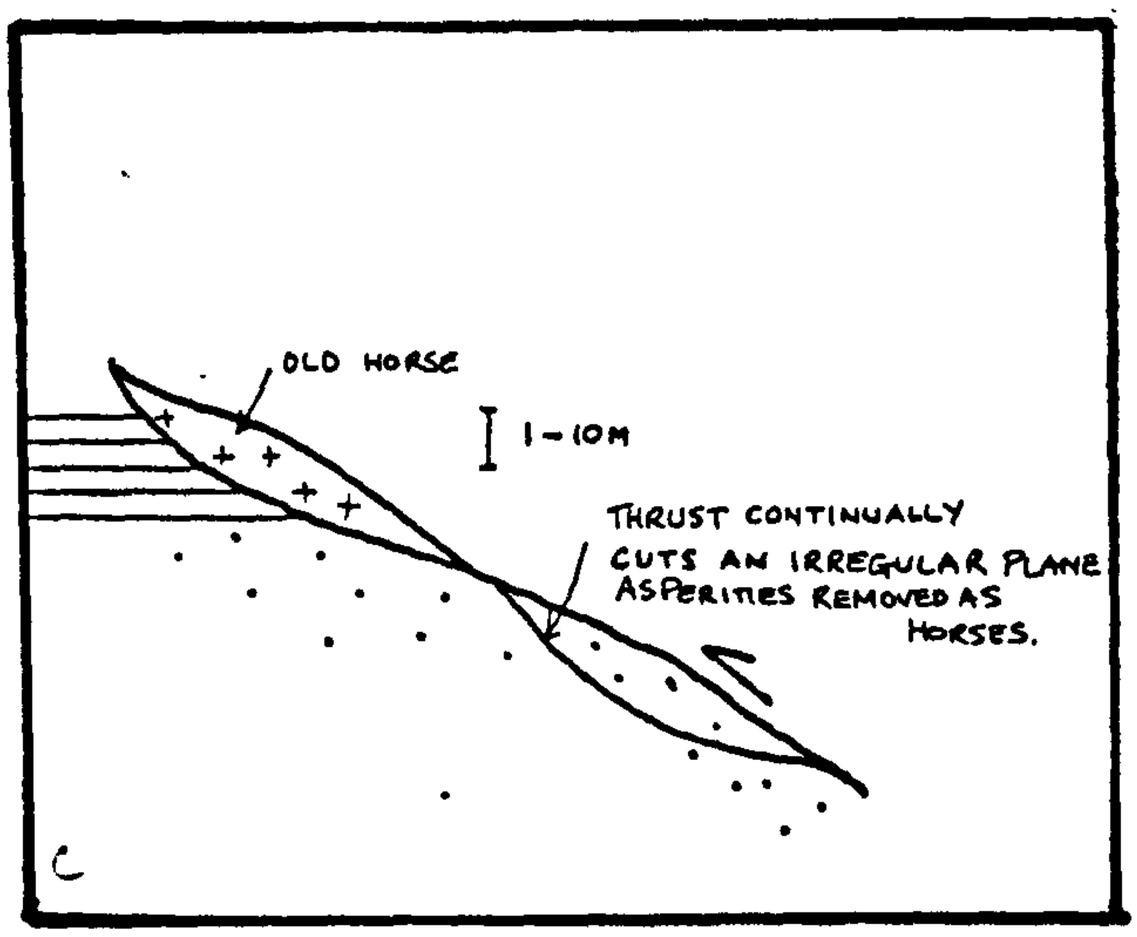
OLD HORSE
1 - 10M
THRUST CONTINUALLY CUTS AN IRREGULAR PLANE ASPERITIES REMOVED AS HORSES.

c

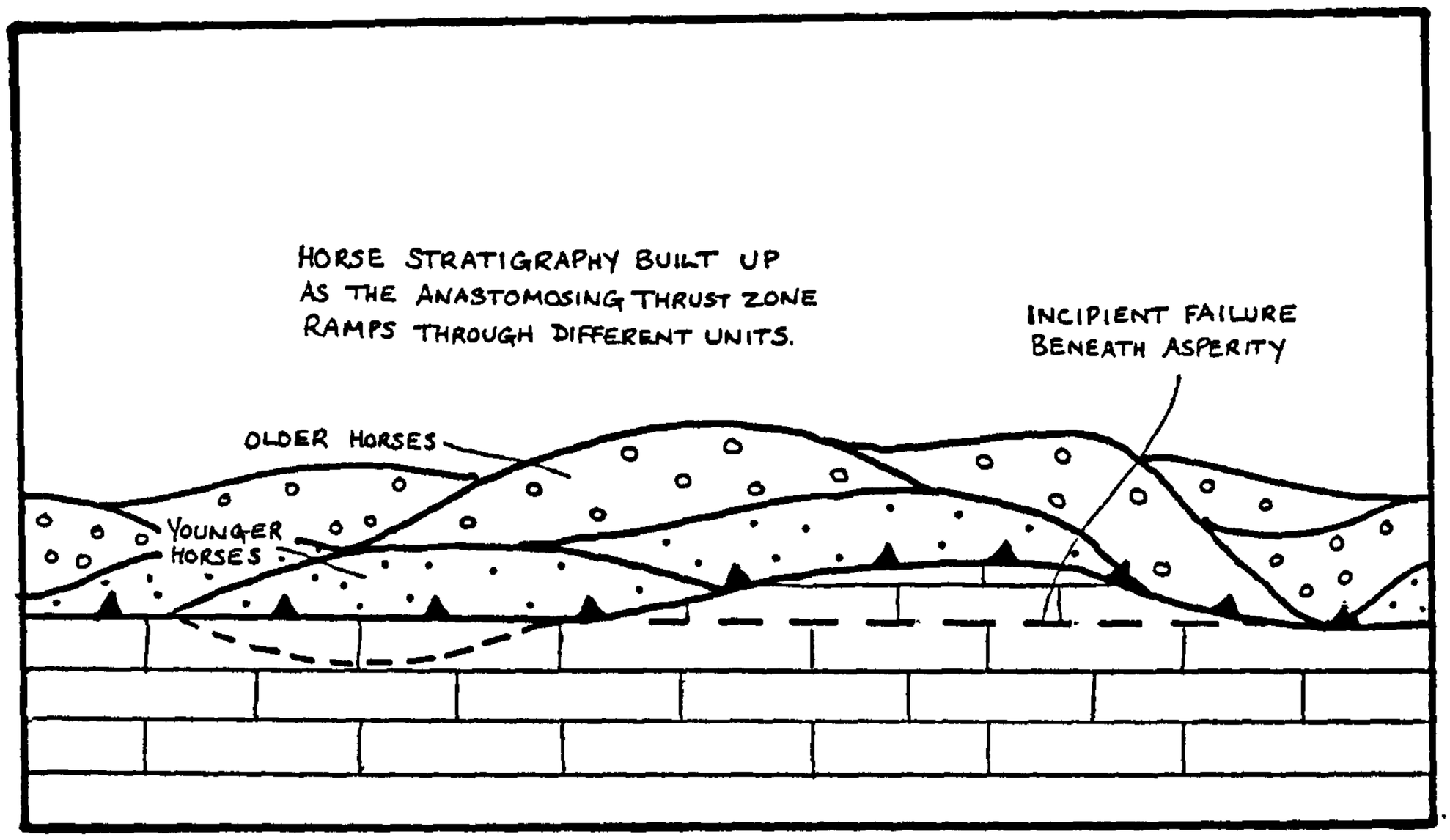

Fig.3.22.

Sketch diagram to show the development of a horse 'stratigraphy' from an anastomosing thrust zone. As the thrust is always picking up asperities from the footwall, these horses will be stratigraphically older away from the thrust.

Fig.3.23.

A hangingwall sequence diagram viewed down the transport direction, to illustrate horse stacking at Creag nam Broc.

(a) The Loch Broom thrust has ramped into the Pipe Rock Member and accreted horses from the ramp.

(b) An asperity formed, which contains An-t-Sron Formation and Durness Formation, has become detached and accreted, and folded the older horses.

(c) The Loch Broom thrust then ramped up to the Eilean Dubh Member at the top of Sheet IV. Horse E was then accreted either as an asperity from the top of Sheet IV or, it was plucked off of Sheet IV by the Creag nam Broc fault, which then emplaced it to its present position.

(d) The accretion of horse E folded the other horses. This diagram shows the present geometry of the horses.

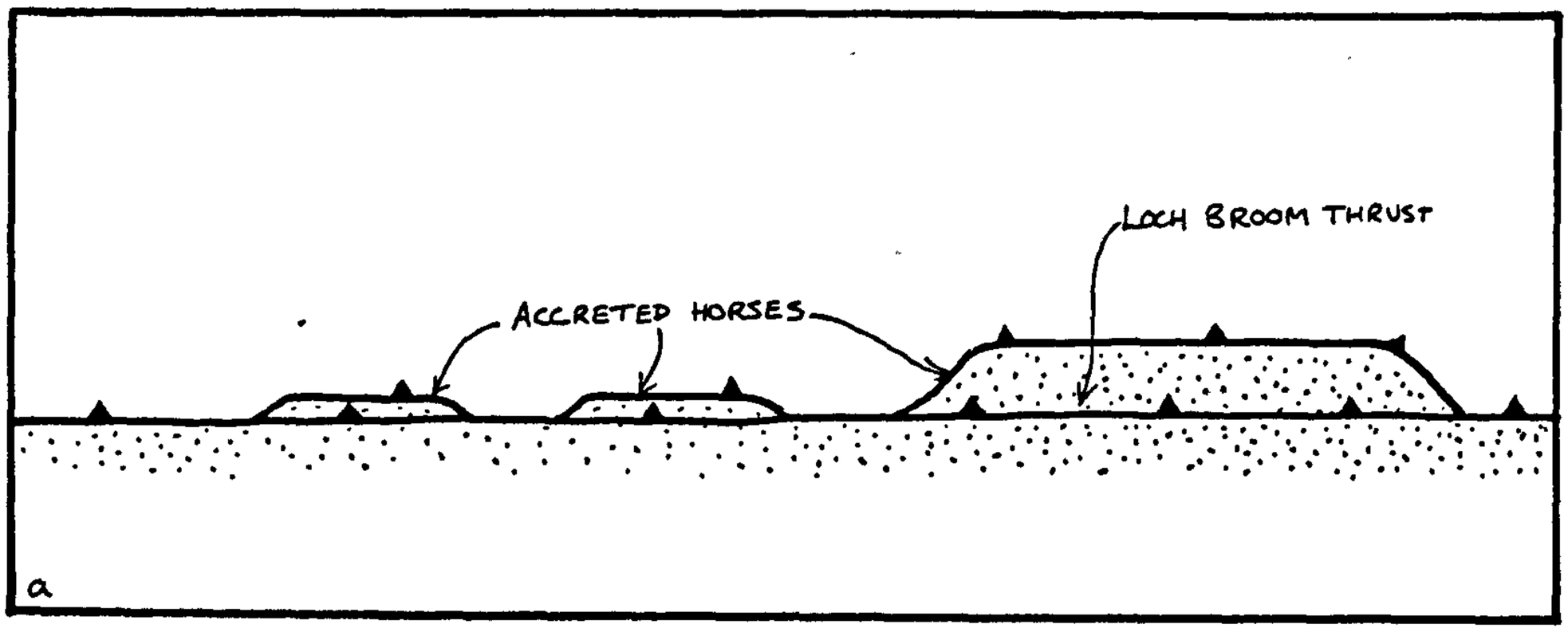
LOCH BROOM THRUST
ACCRETED HORSES
a

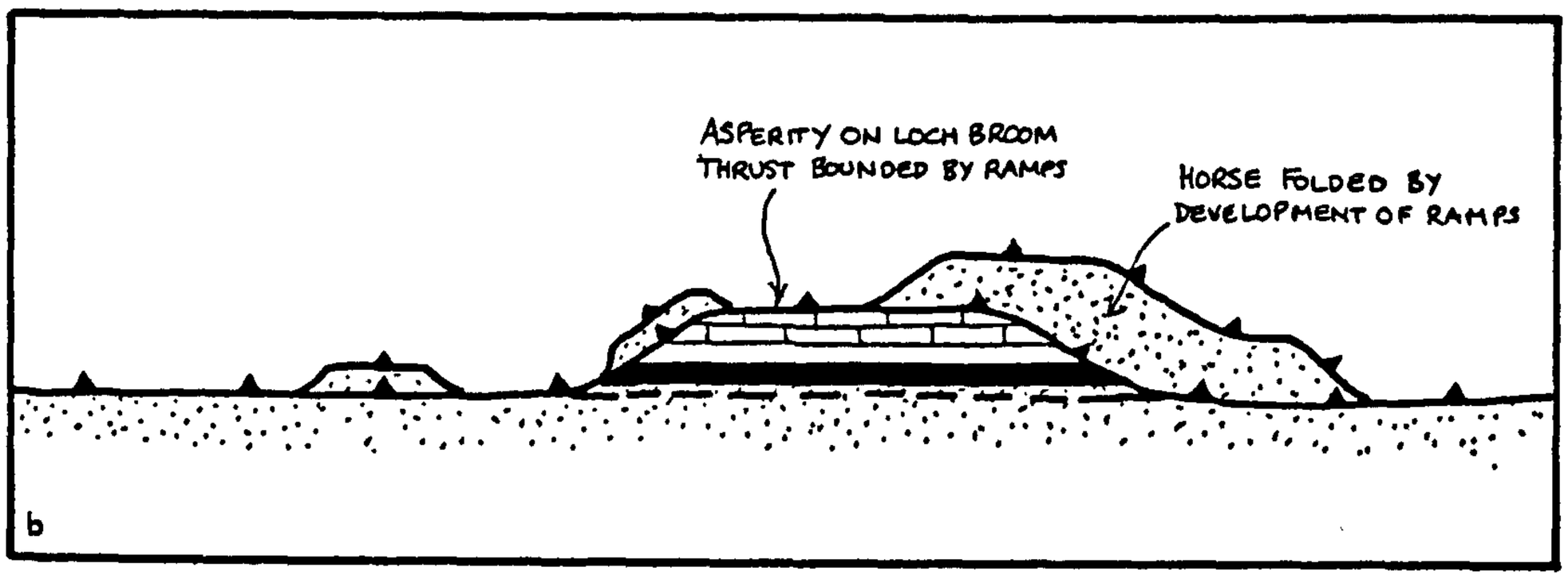
ASPERITY ON LOCH BROOM THRUST BOUNDED BY RAMPS
HORSE FOLDED BY DEVELOPMENT OF RAMPS
b

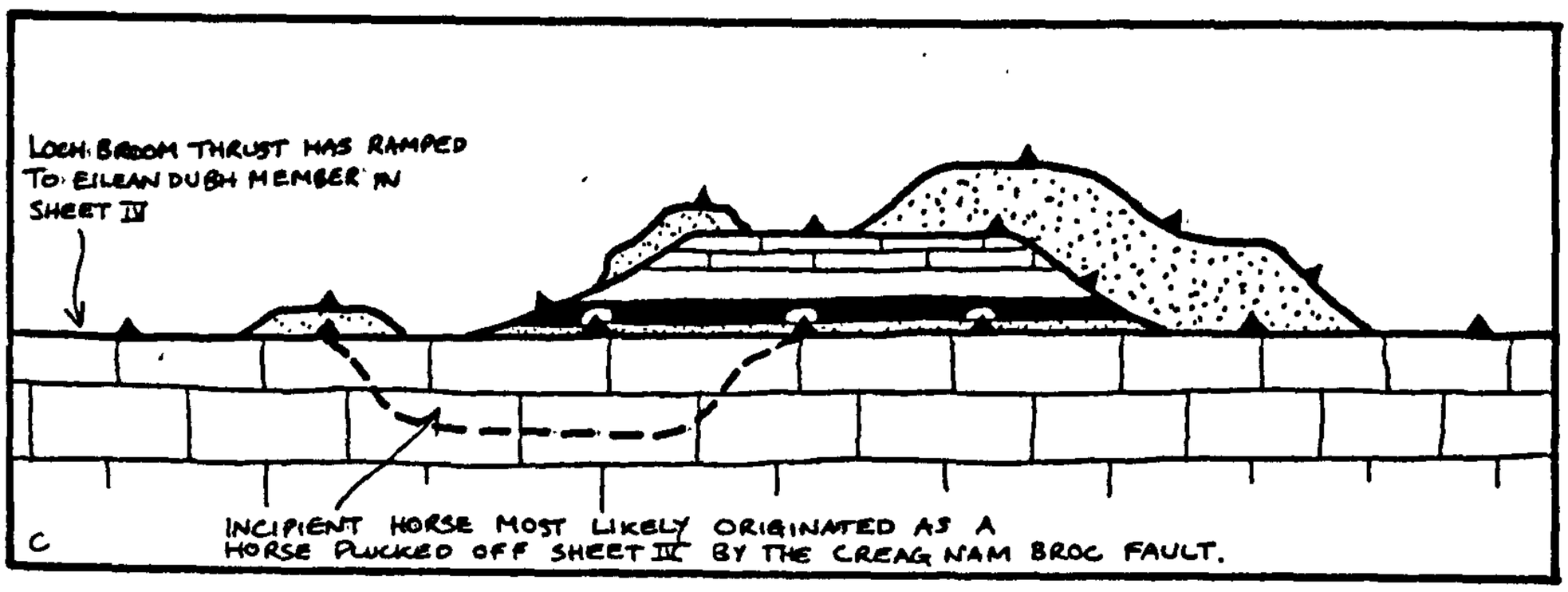
LOCH BROOM THRUST HAS RAMPED TO EILEAN DUBH MEMBER IN SHEET IV
INCIPIENT HORSE MOST LIKELY ORIGINATED AS A HORSE PLUCKED OFF SHEET III BY THE CREAG NAM BROC FAULT.
C

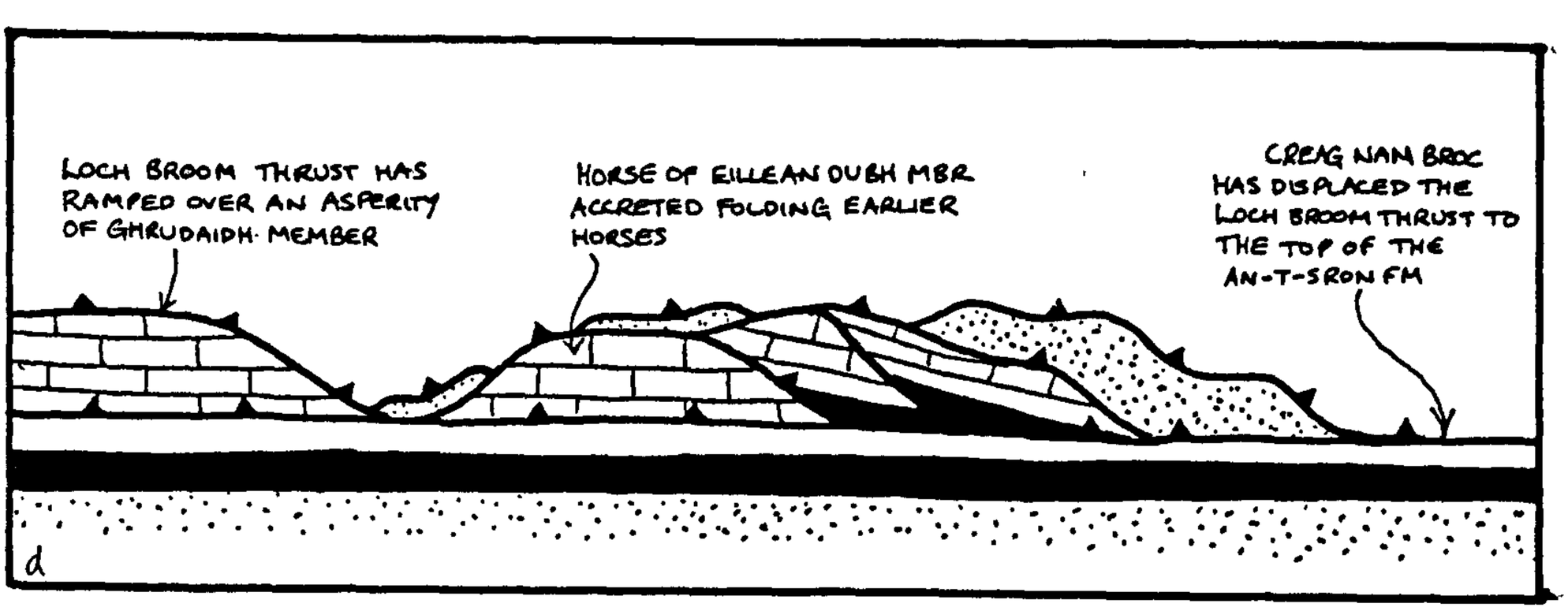
LOCH BROOM THRUST HAS RAMPED OVER AN ASPERITY OF GHRUDAIDH MEMBER
HORSE OF EILLEAN DUBH MBR ACCRETED FOLDING EARLIER HORSES
CREAG NAM BROC HAS DISPLACED THE LOCH BROOM THRUST TO THE TOP OF THE AN-T-SRON FM
d

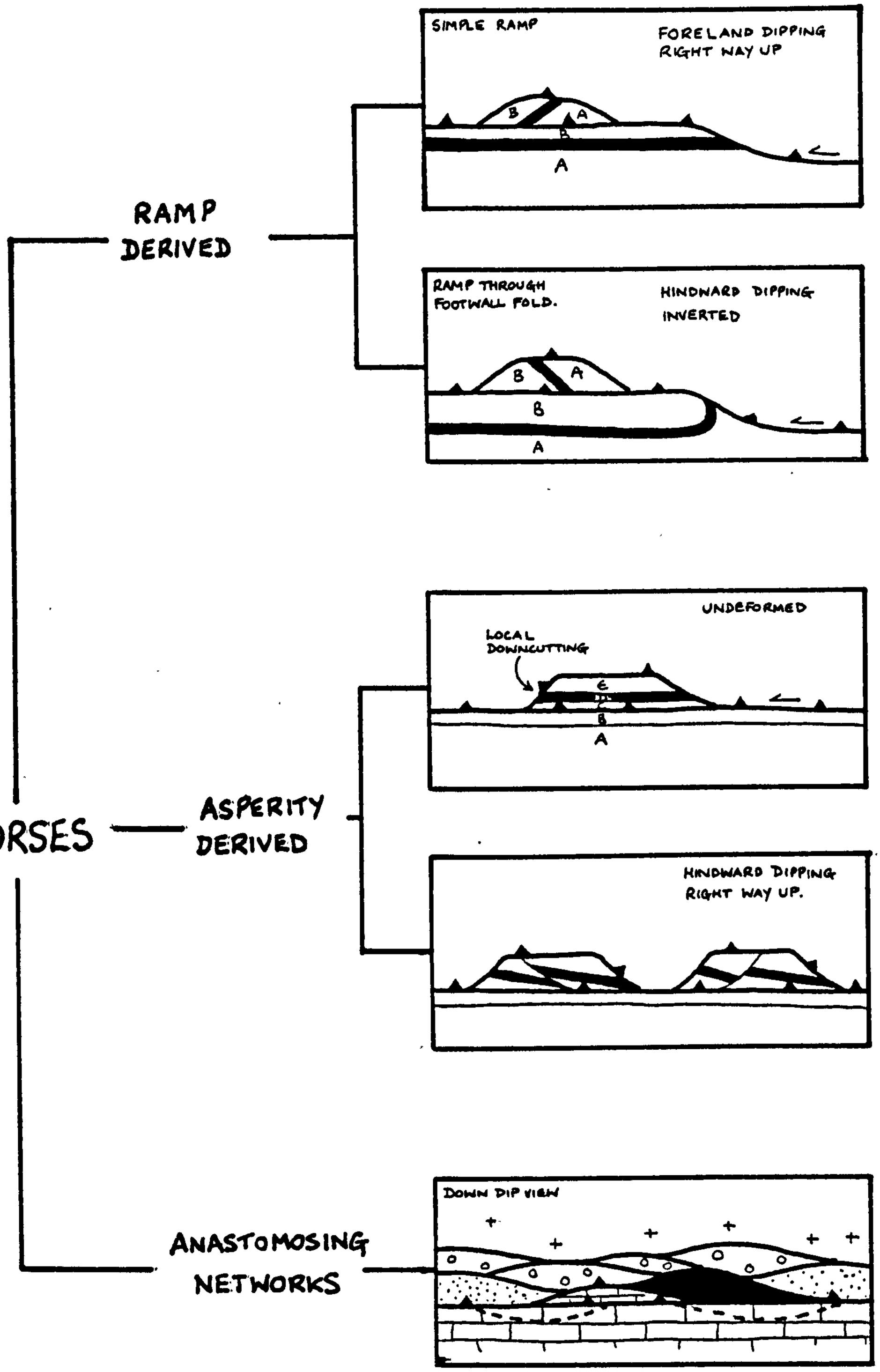

Fig.3.24.

Diagram of the classification of horses. Horses can be divided into three main groups, (i) horses derived from ramps, (ii) horses derived from asperities and (iii) horses derived from anastomosing thrust zones. Each group produces distinct geometries.

CHAPTER 4. THE FORMATION OF EXTENSIONAL STRUCTURES DURING TECTONIC LOADING BY A THICK THRUST SHEET.

4.1. INTRODUCTION.

Extension faults have been described from different thrust belts by a number of authors, Bally et al. (1966), Dahlstrom (1970), Elliott (1976a), Wiltschko (1979b, 1981), Coward (1982, 1983), Elliott and Johnson (1980), Coward and Kim (1981), and can have a number of different origins;

i) Late-stage extension: the faults either cross-cut the thrust zone, Dahlstrom (1970) or are post-thrusting relaxation faults. The latter are listric extension faults which 'bottom out' on pre-existing thrust planes and have been interpreted as post thrusting gravity structures as a result of back-sliding, Bally et al. (1966), Gretener (1972, 1977), Price (1973), Elliott (1976a), Royse et al. (1975).

ii) Stress deviation within a thrust sheet caused by movement of the thrust sheet over footwall irregularities, e.g. ramps. Depending upon the geometry of the irregularity some areas of the thrust sheet will be in compression others in extension. Where internal stresses are extensional the thrust sheet may be deformed by extension faulting. This has been noted in both theoretical studies, Elliott (1976), Wiltschko (1979a, 1981), and field studies, Jacobeen & Kames (1974, 1975), Elliott & Johnson (1980), Coward and Kim (1981).

iii) Gravity gliding and landslide-type surge zones, Pierce (1973), Coward (1982, 1983), Fischer & Coward (1982).

Recent mapping by the author shows that at both Knockan and Achall, extension faulting is the major tectonic style within Sheet IV ,see 2.5, and a new model for the development of the extension faults is developed as the faults do not fall into the above categories on several points.

Firstly, extension faulting is syn-thrusting, as the faults cut the Loch Broom thrust but are truncated themselves by the late movement on the Moine thrust, see 2.2.1, which precludes them being post-thrusting faults. Secondly, the extension faults are not due to stress deviation caused by movement of Sheet IV over any footwall ramps. There is no stratigraphic separation across the Sole fault, and so no movement over footwall ramps. The Durness Formation is the highest stratigraphic unit present and is the footwall of ramps in the Loch Broom thrust, fig. 4.1. Thirdly, at Achall the leading ramp of the extensional complex is the Creag nam Broc fault which is an extension fault, and no thrust faults occur within Sheet IV therefore the Sheet IV itself is not a surge zone type structure. However, the Creag nam Broc fault is possibly the trailing edge of a surge zone in the Loch Broom thrust sheet, with its frontal parts eroded away, (the area of small horses which outcrop just to the NW of Creag nam Broc, encl.3, is not a contractional duplex, but a succession of stacked horses, see 3.2.4.). At Knockan, thrust faults and folds do sporadically occur, but their field relations with the extension structures are unclear due to poor exposure. The folds and thrusts may be interpreted either as:-

i) contractional parts of surge zones in which the extension faults make up the extensional trailing edge, Coward (1983), see 2.6.

ii) a contractional duplex developed prior to the formation of the extension faults.

iii) accommodation structures in the extension fault complex.

Boyer & Elliott (1982) have described geometrically comparable structures to the extension faults in Sheet IV termed foreland dipping duplexes, as the faults within the duplexes dip towards the foreland, i.e. in the direction of transport. These structures place older rocks onto younger and are developed by the collapse of a footwall ramp, fig. 4.2. Depending upon the original geometrical relationship

between the footwall bedding planes and the ramp, the internal geometries are either right way up if the footwall is undeformed, fig. 4.2a, or inverted if the footwall is folded, fig. 4.2b, but they are always forwards facing. However, the extension duplex at Achall differs from the Boyer & Elliott (1982) classification, in that, although the majority of faults are foreland dipping, the internal geometry of bedding is right way up but backwards facing, i.e. towards the hinterland, fig. 4.2c.

Clearly the extension faults within the Achall and Knockan Sheet IV do not fit into the classifications given above. To explain the faults a new model has been evolved which considers the mechanical effects of tectonic loading on footwall rocks, and the effects of high pore fluid pressures caused by the loading. Firstly it is necessary to briefly outline fracture theory and the role of pore fluid pressure, and how high pore fluid pressures are generated and maintained. Secondly to describe the evidence for tectonic loading from Achall and Knockan, and thirdly to develop the model itself.

4.1.1. Pore fluid pressure and hydraulic fracture.

Porous sedimentary rocks are normally saturated with fluid under pressure to constitute a rock-fluid stress system. Pore fluid pressure (P) is often used in conjunction with the vertical stress σ_z to which it is related by the ratio (vertical stress is the overburden stress)

$$\lambda = \frac{P}{\sigma_z} \qquad \ldots 4.1$$

The hydraulic head of pressure in connected pores and fractures is given by

$$P = Pw\ g\ z \qquad \ldots 4.2$$

where Pw = 1 and is the density of water, g is the gravitational acceleration and z the depth. In a normal equilibrium condition, with the density of sedimentary rocks being in the range 2.3-2.5, λ has an approximate value of 0.4.

With the accumulation of sediments and their compaction due to loading, the fluid in the pores will try to escape as the pores begin to close. However, it may not be able escape easily and the fluid has to bear a greater portion of the load and the fluid pressure will rise. High fluid pressures are often termed abnormal fluid pressures, which is misleading as they are probably the norm in most thick sedimentary sequences. In the Gulf Coast area of the U.S.A. this has long been established and $\lambda = 0.8$ has often been recorded, Dickinson (1953), Gretener (1977).

Pore fluid pressure has a drastic effect on tectonic stress, to which it is related by the law of effective stress, first used in soil mechanics by Terzaghi (1950) and more importantly and with great impact by Hubbert & Rubey (1959). The law of effective stress is given by

$$\sigma' = \sigma - p \qquad \ldots 4.3$$

where σ' is the effective stress, σ is the tectonic or total stress, and p is the pore pressure.

The appliance of the law of effective stress to the formation of fractures leads to the obvious conclusion that a rise in pore fluid pressures causes a reduction of tectonic stress needed to initiate failure. Figure 4.3a illustrates this point using Mohr circles; Circle A lies within the stability field. i.e. non-fracturing, and represents stresses in a dry rock, with a pore fluid pressure the circle is moved to the left by P to circle B and represents the effective stresses, circle B touches the failure envelope and fracture can occur. From a different viewpoint the pore fluid pressure has reduced the strength of the rock. In order to produce extension fracture or hydraulic fracture σ_3 must move in to the tensile field of the Mohr circle diagram, fig.4.3b, and the pore fluid pressure must exceed or equal the tensile strength of the rock according to the relationship.

Experimental work has shown that the law of effective stress is applicable to most sedimentary rocks Brace, (1968), Price (1966), Jaeger & Cook (1976), even when porosities are less than 0.1%, Brace & Martin (1968).

Recent work has shown that hydraulic fracture is a common occurrence in most rocks and often results in the formation of tectonic veins arrays, Beach (1975, 1977, 1980), Price (1975, 1977), Phillips (1972), Sibson (1981) and Shearman et al. (1972), and jointing, Secor (1965, 1968), Fyfe et al. (1978).

4.1.2 Shear failure.

Shear failure will occur when the differential stress $\Delta\sigma$ is greater than four times the tensile strength of the rock, To, or

$$\Delta\sigma > 4To \quad ...4.4$$

and when the maximum effective stress σ'_1, is more than three times the tensile strength of the rock, or

$$\sigma_1 > 3To \quad ...4.5$$

Secor (1965, 1968), Price (1966), Fyfe et al. (1978), see fig..4.5a.

In the compressional field, shear failure is governed by a frictional criterion in the Coulomb form,

$$\tau = C + \mu \sigma_n \quad ...4.6$$

where C is the cohesive strength of the rock, u is the coefficient of friction where u = tan Ø, the angle of friction, and σ_n is the effective normal stress. The optimum angle of the fault to the maximum principal stress is given by

$$\theta = 45° - \frac{\emptyset}{2} \quad ...4.7$$

a reasonable value of μ = 0.75, Sibson (1974, 1981), which gives values for Ø of 37° and hence θ = 27°. Faults often occur in conjugate sets, with the maximum principal stress, σ_1, bisecting the acute angle between the faults. Therefore, if σ_1 is acting vertically, i.e. a loading situation, then faults will develop with angles of ±27° from σ_1, fig. 4.4.

4.1.3. Tensile failure.

For tensile failure to occur, the minimum principal stress σ_3, must decrease to zero, which is equal to the tensile strength of the rock so that

$$P > \sigma_3 + To \quad \text{or} \quad -To = \sigma_3 - P$$

Tensile failure occurs at low differential stresses where

$$\Delta\sigma < 4T \quad ...4.8$$

Secor (1965, 1968), Price (1966, 1977), Fyfe et al. (1978), Watts (1983) and where

$$\sigma_3 = -To \text{ and } \sigma_1 < 3To \quad ...4.9$$

On a Mohr circle diagram fig. 4.5a, for tensile failure to occur the circle can only touch the failure envelope on the negative side of the τ axis. Tensile failure is governed by the Griffiths failure criterion, Secor (1965), Watts (1983)-

$$\tau^2 - 4To.\sigma_n - 4To^2 = 0 \quad ... \ 4.10$$

and the failure envelope curves towards the σ_n axis as in fig. 4.5a.

With failure, tensile fractures will form parallel to σ_1 but perpendicular to σ_3. Where pore fluid pressure is the cause of the decrease of σ_3 to -To, then failure is one of hydraulic fracture (or hydro-fracture), fig. 4.5b.

4.1.4. Simultaneous shear failure and hydraulic fracture.

Recent work by Sibson (1977, 1981) and Sibson et al. (1975) show that shear faulting and hydraulic fracturing can occur simultaneously. Sibson (1981) showed that vertical tectonic veins and normal extension faults were intimately related and were formed in the same stress field. The veins commonly consist of hydrothermal minerals which have grown in from the walls towards a median parting, and often show evidence of repeated opening and build-up of minerals in the vein: this implies that the fluid flow into the vein was intermittent, Durney & Ramsay (1973), Sibson (1981).

But simultaneous shear failure and hydraulic fracture appears to contravene the stress conditions discussed earlier. Fig. 4.6a is a Mohr circle drawn so that shear failure occurs, i.e. the circle touches the failure envelope to the right of the τ axis, and $\Delta\sigma > 4T$ but $\Delta\sigma < 5.7T$, σ_3 still lies to the left of the τ axis, so that the minimum principal effective stress is still tensile, i.e. negative. This is the critical stress condition for simultaneous shear failure and hydraulic fracture, fig.4.7b. Sibson (1981) showed that the critical differential stress occurs when

$$\Delta\sigma = 4C - 3To \quad ...4.11$$

when $\mu = 0.75$. Above this critical stress only shear failure can occur, as σ_3 on the Mohr circle will move to the right of the τ axis.

Later in section 4.4.3 this concept is applied to the dolomites of Sheet IV in the Achall valley to estimate the upper limit of differential stress operative at the time of tectonic loading.

4.2. ABNORMAL FLUID PRESSURE GENERATION: TECTONIC LOADING.

4.2.1. Tectonic loading.

In order for abnormal fluid pressures to be developed and maintained, fluid flow must be inhibited or sealed, both laterally and vertically. Both Dickinson (1953) and Magara (1975b) used the term isolation, which implies that the sealing in of fluids is absolute, and there is zero fluid flow. Isolation is unrealistic in most rock columns and Gretener (1977) introduced the term 'restriction', this implies that although some fluid flow is possible it is too slow to allow equilibrium conditions to exist.

Rapid loading is the most likely mechanism for generating abnormal fluid pressure, and is based on the concept that the application of an external load on to a porous rock system causes a rise in pore fluid pressure. This rise is caused by the restriction to fluid flow caused by the decrease in pore size under the external load. The resulting pore fluid pressure may be permanent or transient. Sedimentary loading can cause overpressuring with loading rates of 10^{-1}mm-yr^{-1}, this is well documented in Dickinson (1953), Hubbert & Rubey (1959), Dickey (1976), Fertl (1976).

The emplacement of thick thrust sheets along thrust faults is a case of rapid tectonic loading. Displacement rates of 1-10 cm/yr cause loading rates of mm/yr, Gretener (1981), which in geological terms is instantaneous. The deformation of undisturbed foreland by the emplacement of large thrust sheets can be divided into two stages.

i) a pre-faulting stage, during which the lateral stress components build up to the point of failure. If this lateral stress build up is fast enough, fluid pressure may rise to abnormal levels.

ii) a post-faulting stage, during which the thrust sheet is displaced along the thrust fault for great distances. During this stage active tectonic loading occurs as the thick thrust sheet is emplaced over the undisturbed footwall. Abnormal fluid pressures will occur in those parts of the overridden sequence where restriction to fluid flow prevails. It is this stage in which we are interested in this chapter.

4.2.2. Aquathermal pressuring and phase changes.

Aquathermal pressuring occurs when wet sediments are heated due to burial, Barker (1972), Magara (1975a, b), Norris & Henley (1976). Burial along thermal gradients greater than 12°C/km, leads to thermal expansion of restricted fluids, and because of the restriction to fluid flow, the fluid pressure will rise. Barker (1972) calculated that the pore fluid pressure may rise 15b per 1°C rise in temperature. For pure loading alone to produce a fluid pressure equivalent to the overburden pressure, i.e. $\lambda = 1$, the formation would have to be isolated from the time of deposition; clearly this is unlikely, Gretener (1977). However, as burial by loading and temperature increase are inseparable, aquathermal pressuring could enhance fluid pressures to values which approach the overburden stress. There must be a time lag between the loading and the resultant thermal effect, and as a rapid tectonic loading is virtually instantaneous, aquathermal pressuring may not have any effect until the later stages of the thrust sheet emplacement and post-thrust-sheet emplacement.

In Chapter 6 it is advocated that the loading of the footwall by the Moine thrust sheet caused temperatures in the footwall to rise to 275° (Upper Zeolite) facies immediately below the Moine thrust. Although the original temperatures of the footwall can only be guessed at, the temperature rise would probably have caused aquathermal pressuring in the footwall sequence to enhance abnormal fluid pressure due to loading.

The effect on fluid pressures by the montmorillonite-illite transformation has been investigated in recent years, Magara (1975a). The concept is based on the observation that bound clay water has a higher density than pore fluids, and that the conversion from montmorillonite to illite has to be accompanied by either a volume or pressure change in the bound fluids, and fluid is generated in situ. Although this process is still little known, it may be a contributing factor to abnormal fluid pressures.

4.3. THE EVIDENCE FOR HIGH PORE FLUID PRESSURES IN SHEET IV.

In section 2.5. the geometry of the tectonic veins and extension faults in Glen Achall was described. Tectonic veins have been studied extensively in recent years, Beach (1977, 1980), Latjai (1977), Sibson (1981), and it is now accepted that the veins are formed by hydraulic fracture. A prerequisite for hydraulic fracture is pore fluid pressures greater than the hydrostatic pressure, i.e. $\lambda = 0.4$, see section 4.1.1.

Within Sheet IV in Glen Achall tectonic veins are well developed (section 2.5.1.4.) and are related to extension faults which are associated with detachment on the Sole fault. These veins testify that high pore fluid pressures existed in Sheet IV at the time of thrusting. Apart from areas close to the Loch Broom Thrust, veins are uncommon in the Loch Broom thrust sheet, suggesting that either;

i) the tensile strength of the gneisses and 'Torridonian' arkoses in the Loch Broom thrust was high enough to prevent hydraulic fracture from occurring, and allowed only shear failure, or

ii) high pore fluid pressure may never have existed as fluid may have been able to flow through the thrust sheet.

(iii) fluids may have been absent in the Lewisian gneisses and Torridonian rocks.

The first option seems unlikely as hydraulic fractures do occur near to the Creag nam Broc fault and the Loch Broom thrust. Therefore, it seems likely that high pore fluid pressures never existed within the Loch Broom sheet and fluids could flow through it, with local areas of high pore fluid pressure near to the major thrust and faults.

The above implies that the Loch Broom thrust plane provided the restriction to fluid flow which allowed high pore fuid pressures to build up in Sheet IV. In section 2.7, evidence is described that shows that the cataclasites on the major thrust planes develop by alternations of cataclasis, when the cataclasite was porous and permeable, and long periods of induration when the cataclasite was impermeable. During the periods of induration the cataclasite could have restricted the fluid flow. At the time of loading, Sheet IV in Glen Achall was bound by a dorsal ramp and two lateral ramps of the Loch Broom thrust, the fault plane of which is marked by a cataclasite 1-5 cm thick, see fig. 4.1. The cataclasite on the ramps would have provided good vertical and lateral restrictions to fluid flow and allowed pure fluid pressure to build up within Sheet IV. With the movement on the Creag nam Broc fault, section 4.5.1, fluid flow out from Sheet IV was then further restricted. In section 2.8 it is also advocated that faults are only channelways for fluid flow when they are active, i.e. undergoing pre-failure dilatancy and failure. With fluid flow up the Loch Broom thrust/Sole fault system,fluids would be added to Sheet IV, thus any major losses of fluid from Sheet IV during activity on the Loch Broom thrust and Sole fault, would be replaced by fluids moving up the thrust system. Once movement had ceased and induration of the cataclasites was occurring, the fluid flow would then be restricted, and a high pore fluid pressure could build up.

4.3.1. Porosity and permeability of the Durness Formation during tectonic loading.

The dolomites of the Durness Formation at the present day are extensively dolomitised with minor calcification and silicification, Swett (1969). This process must have occurred either prior to faulting or syn-faulting as the cataclasites disrupt the diagenetic fabric of the dolomites. How the Zeolite facies metamorphism described in Chapter 6 affected the dolomites is unclear so it is assumed that the dolomites had a diagenetic fabric prior to thrusting. The original thickness of the Cambro-Ordovician sequence is unknown, so it is assumed that no significant sedimentary loading had taken place and all loading effects are taken as being due to rapid tectonic loading.

The porosity of a dolomite with a diagenetic fabric can range between 5-30%, with permeabilities of between 10^{-2}-10^{-15} Darcies, Fyfe et al. (1978) but this will be dependent upon the diagenetic history and the confining pressure. With the rapid loading by a 10km thrust sheet, porosities would rapidly decrease, even when using conservative estimates of the original porosity of ~5%. The dolomite is now totally recrystallised when studied in thin section, and porosities for recrystallised dolomites are <1%, Fyfe et al.(1978). Therefore it is assumed that the porosity of the Durness Formation dolomites was between 1% and 5%. Does this change the tectonic loading model by affecting the pore pressure history? The answer must be no, as rocks with porosities of <1% even as low as 0.1% still obey the law of effective stress, which is fundamental for hydraulic fracture, Brace & Martin.(1968). This concept is further backed up by occurrences of hydraulic fractures, i.e. veins, in Upper Greenschist metamorphic rocks, where porosities could be as low as 0.1%, Ramsay (1980).

With failure, and the formation of hydraulic fractures, a 'fracture porosity' is developed, and with migration of fluids into the fractures there will be a sharp drop in the ambient pore fluid pressure. However, with fluid flow into fault system during dilatancy and continued loading, pore fluid pressure would continue to rise. In detail pore fluid pressure will vary with transient fracture porosities, but in general will continue to rise with the tectonic loading.

4.4 A MODEL FOR THE DEVELOPMENT OF EXTENSION FAULT SYSTEMS IN SHEET IV.

The model for the development of the extension fault systems, the geometry of which is described in Chapter 2, is built up by considering the formation of the extension structures asa result of gravitational tectonic loading. The loading was caused by movement of thrust sheets in the Moine thrust zone onto an undisturbed sedimentary foreland sequence. Price (1974) described fracture patterns formed in undeformed sediments by loading and burial , and the accompanying subsidence and downwarp in terms of the stresses and pore fluid pressures. A similar approach is adopted, by considering possible stress systems and pore fluid pressures which may be developed in a sedimentary sequence which is tectonically loaded. Before developing the model there are a number of factors which need to be assessed.

4.4.1. Orientation of the principal stresses.

Following the Andersonian relationship between fault geometry and stresses, Anderson (1951), the orientation of the principal stresses with respect to the fault are shown in fig.4.7. Within Sheet IV, two sets of extension faults were developed, a NE-SW set cross-cut by a NW-SE set. This indicates that during the course of fault development, the minimum and intermediate principal stresses changed their orientation. As the NW-SE faults cross-cut and displace the NE-SW faults, then the first formed set of faults must be the NE-SW set. Therefore, prior to the development of the faults, at the onset of tectonic loading the minimum principal stress, σ_x, must have been orientated at 90° to the strike of the NE-SW set, i.e. parallel to the transport direction of the thrust sheets, NW-SE. The intermediate stress, σ_y, acted parallel to the strike of the thrust sheet, and the maximum principal stress, σ_z, acted vertically and was the loading stress component.

4.4.2. Magnitude of the overburden stress.

The magnitude of the overburden stress, i.e. σ_z, is the easiest to deduce and is expressed as

$$\sigma_z = p.g.z \quad ...4.12$$

where p is the mean density of the rocks, g is the gravitational acceleration, and z is the depth, which for tectonic loading will equal the thickness of the overlying thrust sheet. It is assumed that the maximum thrust sheet thickness was 10 km. This assumption is not implausable and can be reasonably constrained by the structures displayed. All the faults show evidence of brittle-frictional behaviour described fully in section 2.5. This indicates that deformation occurred above the brittle-ductile transition zone in the Earth's crust. This zone divides that part of the crust which deforms in an elastic-brittle manner, where large strains cannot be absorbed by crystal plasticity, and a deeper zone where major rock constituents can deform by crystal plasticity and the deformation behaviour is termed quasi-plastic. Quartz is by far the most important mineral constituent of rocks, and penetrative crystallographic fabrics do not appear until Lower Greenschist facies is attained, Spry (1969), along the isotherm in the range 250-300°C where $P_{load} = P_{H2O}$, Turner 1968). This suggests that the zone dividing brittle deformation from quasi-plastic deformation occurs broadly between 10-15km deep, Sibson (1977).

The development of pressure solution cleavage in the rare folds, and the crystal fibre growth on fault planes indicate that pressure solution processes were operating and suggests depths of 5-10km for their formation, Elliott (1976b).

The rocks of the overlying thrust sheets are gneisses, arkoses, quartzites and schists with an assumed average density of $2.6 gm/cm^3$. It is necessary to use effective stresses as the model takes into account pore pressure, so that the effective overburden stress σ_z', is

$$\sigma_z' = p.g.z - p \quad ...4.13$$

where p is the pore pressure.

4.4.3. Estimation of differential stress.

Differential stress is the least constrained variable in the Earth's crust. There have been two main approaches in tackling the problem

i) laboratory testing and direct measurements in the Earth's crust and

ii) palaeopiezometry using dislocation density, subgrain size, and recrystallised grain size.

Hanks (1977) reviewed differential stress magnitudes and argued that a lower bound of 1kb in the vicinity of faults is required. This figure was derived from a number of experiments on frictional resistance to sliding on a wide variety of rock surfaces, and implied that ambient differential stresses of kilobars are common in the Earth's crust and upper Mantle.

By using direct measurements, (usually strain relief or hydraulic fracturing), McGarr & Gay (1978) demonstrated that differential stress increased with depth from less than 100b in the top few hundred meters up to 200-500b for below 1km. Deeper measurement down to 5km showed that there is little or no significant increase in these values.

Recent research in palaeopiezometry has shown that the dislocation density, sub-grain size, and recrystallised grain size in rocks which have undergone intra-crystalline deformation, i.e. dislocation flow, are dependent on differential stress and are related to temperature and strain rate through a flow law, Twiss (1977), White (1979a, b), Weathers et al. (1979), Christie & Ord (1980), Etheridge & Wilkie (1981). Stresses estimated from the microstructures are dependent on several factors;

i) the choice of substructure development

ii) the choice of flow parameters and

iii) the introduction of a second phase, e.g. mica, can restrict equilibration in recrystallised grains and consequently affect stress estimates.

A range of stress estimations, all from ductile shear zones, have been produced and range from 100-1500 bars with the majority below 500 bars. White (1979b) and Weathers et al. (1979) have produced differential stress estimates from mylonitic quartzites in the Moine thrust zone and range from 450-560 bars from recrystallised grain size and 1000-2000 bars from dislocation densities. The discrepancy between the two estimates can be explained by the fact that dislocation densities are greatly affected by slight later deformation, whereas recrystallised grain size records the highest differential stress attained and is not easily affected by a later deformation.

In the dolomites of Sheet IV no mylonites are developed, and hence differential stresses cannot be estimated from microstructural parameters. Two methods were used to estimate differential stress

i) the analysis of calcite and dolomite twin lamellae, Jamison and Spang (1976)
ii) the occurrence of natural veins and extension faults which can provide an upper bound of differential stress, and simultaneous shear and tension fractures can give a further limit to differential stress estimates.

The second method is important as it allows an estimation of differential stress using natural structures which are common and well researched.

4.4.3.1. Estimation of differential stress from the analysis of Calcite and Dolomite twin lamellae.

Jamison and Spang (1976) showed that, assuming an infinite number of possible crystal orientations, it is possible to determine the percentage of grains that have a given value of the resolved shear stress coefficient S_1 on one, two and three twin sets, and that this is related to differential stress by the equation

$$t_r = S_1 . \Delta\sigma$$

where t_r is the resolved shear stress for twin gliding, S_1 is the resolved shear stress coefficient and $\Delta\sigma$ is the differential stress. Jamison and Spang (1976) developed the method for carbonates with randomly orientated grains, which were deformed in an irrotational, uniaxial stress field, i.e. the carbonates are essentially undeformed and $\sigma_2 \approx \sigma_3$. The method also assumes that all twinning can be observed in thin sections, and occurs only in theoretically possible orientations which in calcite are the e $\{0\bar{1}2\}$ twin planes and in dolomite the f $\{02\bar{2}1\}$ twin planes. Friedman and Heard (1974) found that twinning can be time-dependent in that the number of twin grains and number of twin sets increased with the duration of loading at a constant differential stress, hence the twin analysis method may overestimate the magnitude of differential stress. Also if a sample has been deformed in a rotational stress field or in several distinct stress fields, an overestimation of differential stress will result. Further if $\sigma_2 - \sigma_3$ becomes significant in relation to $\sigma_1 - \sigma_3$, i.e. $\sigma_2 \neq \sigma_3$ then the estimate will be inaccurate, and result in an overestimate; but the technique, in these circumstances, will be a first approximation of $\Delta\sigma$. Jamison and Spang (1976) applied the method to six samples of experimentally deformed Indiana Limestone, where the stress conditions were known, and found that by using the maximum number of twins developed in any one grain, the stress estimates differed from the experimental values by no more than 21%. They then applied the method to naturally deformed samples from the McConnell thrust plate in the Front Ranges of the Canadian Rocky Mountains.

The samples used in this study were collected from the Sheet IV dolomites from Achall, (sample Nos A3, A5, A6, A7, A8 and A14) and Knockan (sample Nos K3, K4 and E9). There is no preferred orientation fabrics in the dolomites, and it is certain that they were undeformed prior to thrusting, as no pre-thrusting structures exist. Twins were measured in two groups

(See Encl 3 for location)

(See Encl 2 for locations.)

i) from the grains in the groundmass of the rock which are predominantly dolomite and

ii) from vein crystals in the tectonic veins which are predominantly calcite. These veins were formed during tectonic loading, so that the twins will have formed under the differential stress at the time of loading.

Values for t_r are taken as 100 b for calcite and 500 b for dolomite, Jamison & Spang (1976). The assumptions inherent in the method are all reasonable for the Sheet IV dolomites and calcite veins; σ_2 is unlikely to be that much greater than σ_3 as $\sigma_1 - \sigma_2$ is sufficient enough to cause extensional shear failure, see 4.4.4, and the assumed stress system is approximately uniaxial during loading.

Table 4.1 shows the differential stress estimates from the samples collected, and it is immediately obvious that the dolomite in the groundmass gives $\Delta\sigma$ of $\sim$1300 b whilst the calcite of the tectonic veins gives a $\Delta\sigma \sim$ 540 b. It is certain that the veins have experienced a loading deformation only, thus $\Delta\sigma \sim$ 540 b seems reasonable in the light of the assumptions above. However, the high values of $\Delta\sigma \sim$ 1300 b for the dolomite groundmass is more problematical in its interpretation. Earlier, section 4.2.1, it was suggested that the footwall deformation could be divided into two deformation components. Firstly, a compressional deformation prior to and during the thrust initiation where σ_1 acted horizontally and secondly, a loading deformation during the translation of the thrust sheet, where σ_1 acted vertically and the footwall underwent tectonic loading. As the tectonic veins cut across dolomite which were already twinned at the time of veining, the stress system must have been active earlier than that which produced the loading deformation. I interpret the earlier deformation of the dolomite as a result of compressional deformation, i.e. σ_1 is horizontal, prior to and during the initiation of the thrust fault, in this case the Loch Broom thrust. The high figure of in the dolomites should be treated with some caution, as the dolomites have been affected by two independent stress systems, so the $\Delta\sigma \sim$ 1300 b value is a probable overestimate. For the purpose of the tectonic loading model, the relevant value of $\Delta\sigma \sim$ 540 b is used, as the veins are a product of that tectonic loading.

	1 TWIN SET		2 TWIN SET		3 TWIN SET	
SPECIMEN	S_1	$\Delta\sigma$ (bar)	S_1	$\Delta\sigma$ (bar)	S_1	$\Delta\sigma$ (bar)
DOLOMITE A5	0.14	3571	0.33	1515	0.35	1428
DOLOMITE A7	0.37	1351	0.42	1190	-	-
DOLOMITE A3	0.36	1388	0.39	1282	-	-
DOLOMITE A6	0.36	1388	0.37	1351	-	-
DOLOMITE A14	0.45	1111	0.29	1724	-	-
DOLOMITE A4	0.375	1333	0.44	1136	-	-
DOLOMITE K4	0.325	1538	0.38	1315	-	-
DOLOMITE E9	0.41	1219	-	-	-	-
CALCITE VEIN E9	0.32	312	0.19	526	-	-
CALCITE VEIN K3	0.32	312	0.18	555	-	-

Table 4.1 Table of S_1 and $\Delta\sigma$ for 1, 2 and 3 twin sets. Values of τ_r for calcite and dolomite of 100 bar and 500 bar respectively were used.

4.4.3.2. Estimation of differential stress from natural extension fractures and veins.*

From observations of experimental rock mechanics and theoretical studies it is well known that there is a simple relationship between differential stress, $\Delta\sigma$, and the tensile strength of a rock, T_o, to produce a fracture in shear and tensile failure modes, see 4.12 and 4.1.3, Price (1966), Jaegar & Cook (1976). For shear failure the relationship is

$$\Delta\sigma > 4To$$

for tensile failure

$$\Delta\sigma < 4To$$

and for the condition where simultaneous shear failure and tensile failure occur, e.g. normal faulting and concomittant veining, Sibson (1981)

$$\Delta\sigma = 4C - 3To$$

or

$\Delta\sigma < 5.7To$ but $\Delta\sigma > 4To$, see fig. 4.7b

There is now a reasonable source of tensile strength data available, for most common rock types, Lama & Vutukuri (1978). Thus from a simple observation of the failure mode of fracturing in natural fracture systems, and a knowledge of available tensile strength data, it is possible to estimate upper and lower bounds of $\Delta\sigma$. Before applying this concept to the dolomites of Sheet IV, a further factor

* Note: Since originally writing this section, concurrent work by Etheridge (1983) was bought to the author's attention, in which similar conclusions regarding stress estimations were reached and introduced me to the importance of static fatigue and stress corrosion.

should be considered. It is known that in a wide variety of materials, time dependent fracture growth occurs at $\Delta\sigma$ less than the critical value for failure, and this is known as subcritical crack growth, or static fatigue, see Atkinson (1982) for review. This process is commonly attributed to a chemical reaction between the solid material and a corrosive fluid filling the fracture at the fracture tip, and is known as stress corrosion. However, the details of stress corrosion are still not fully explained and more than one process may be active, Atkinson (1982). Tensile strength may be reduced by as much as 50% by subcritical crack growth, hence reducing the necessary to produce failure, Atkinson (1982).

The failure mode in the dolomites of Sheet IV is simultaneous shear failure and hydraulic fracture hence

$\Delta\sigma$ >4To but <5.7To

The tensile strength of wet dolomite ranges from 100-150 b, Price (pers com 1982), Lama & Vutukuri (1978). The value of 100 b will be used to allow for any static fatigue effects and for convenience; this gives a value for $\Delta\sigma$ of between 400 b- 570 b which is in agreement with the values obtained for loading by the calcite twin analysis. For the two fault sets to occur in Sheet IV $\sigma_1 - \sigma_2$ must also have been <570 b and as σ_2 and σ_3 interchanged and produced extension faults $\sigma_2 - \sigma_3$ must be relatively small. For the model I will use a value of $\sigma_1 - \sigma_3$ ($\Delta\sigma$) of 500 b and $\sigma_1 - \sigma_2$ a value of 450 b.

The values of $\Delta\sigma$ estimated by the twin analysis and the natural fractures is consistent with in situ stress measurement of McGarr & Gay (1978) of 200-500 b, and values obtained from ductile shear zones of 450-550 b from recrystallised grain size palaeopiezometry, White (1979b), Weathers et al. (1979). In summary, it is clear that simple observations of the failure mode of natural fractures and vein arrays can be powerful tools in estimating differential stresses active in the Earth's crust, and that they agree consistently with established techniques.

4.4.4. <u>The development of the fault systems with loading: Application of the tectonic loading model</u>.

Table 4.2 shows the stress values of σ_x, σ_y, σ_z, and P used for the model based on the criteria discussed in the previous two sections, and Table 4.4 shows various values of pore pressure and effective stresses obtained by varying the value of λ at depths of 5 km and 10 km. From these values the effective stresses were calculated and fig. 4.8 a, b are plots of effective stress versus λ, assuming that at the onset of loading, λ = 0.4, the hydrostatic stress, see 4.1.1. From these figures it is clear that with a 5 km thick load as soon as the pore pressure had risen to values where λ=.65, failure could occur as $\sigma_x - p = -To$. Moreover, if pore fluid pressure were to continue to rise to values where λ = 0.7-0.8, failure could occur when $\sigma_y - p = -To$, hence two sets of fractures are possible. With increase in the load to 10 km, λ has to reach values of ~.75 for σ_x and >.8 for σ_y to initiate failure. It is necessary to point out that the values and stresses given above are only necessary to cause failure, however further slip on existing fractures will occur at lower values and stresses. This is because only the cohesion across the fault plane needs to be overcome to enable further slip, according to the relationship

$$\tau = C + u\,\sigma_n \ldots$$

Figure 4.9 is a schematic graph which illustrates the changes in σ_x, σ_y, σ_z and p through the time of loading. σ_z increases linearly as loading continues, σ_x and σ_y increase at a slower rate. The slight curvature in the paths of σ_x and σ_y is due to the change in the Young's modulus and Poisson's ratio as the formations are loaded. This effect will be more pronounced in footwalls of relatively uncompacted rocks, as the Young's modulus and Poisson's ratio change as the rock compacts. The effect will be less pronounced with already compacted footwall formations, Price (1974).

	σ_x	σ_y	σ_z
5 km	800	850	1300
10 km	2100	2150	2600

Table 4.2 Value of principal stresses used to calculate effective stresses.

λ	σ_z'(bars)	P(bars)	σ_x'(bars)
0.5	650	650	50
0.6	520	780	20
0.7	390	910	-110
0.8	260	1040	
0.9	130	1170	

Effective stress for σ_z' and σ_x' at 5 km depth.

λ	σ_z'(bars)	P(bars)	σ_x'(bars)
0.4	1560	1040	1060
0.5	1300	1300	800
0.6	1040	1560	540
0.7	780	1820	280
0.8	500	2100	0
0.9	260	2340	-240

Effective stress for σ_z' and σ_x' at 10 km depth.

Table 4.3 Values of effective stress calculated for varying values of P given a known overburden stress, σ_z.

With a load of 5 km, when λ =.6 5, failure occurs, A on fig. 4.9, as σ_x is the least principal stress, fractures form which strike NE-SW parallel to the strike of the thrust belt, with concommitant veining, fig. 4.10. Thus, even a moderate increase in pore fluid pressures can cause faulting and veining given the correct conditions. With the relief of the 'tectonic' stress σ_x (not the effective stress), σ_x will approach the value of the pore pressure, and σ_y becomes the least principal stress, σ_x will again start to increase until σ_x - p reaches the threshold condition, B on fig. 4.9, to cause further sliding, then once again σ_x approaches the value of p and the cycle is repeated. This cycle of events indicates that movement on the faults is episodic which is supported by field evidence; multilayers of crystal fibre growths occur on exposed fault planes, which show that episodic fault movement had taken place, see 2.5.1.3.

Once failure has occurred with σ_x as the least principal stress, σ_x then becomes the intermediate principal stress and σ_y the least principal stress. It has already been noted that when λ reaches values of 0.75-0.85 at depths greater than 5 km, failure can occur, C on fig.4.9. With failure σ_y will approach the value of the pore pressure and with continued loading σ_y will increase until σ_y - p reaches the threshold condition to cause further slip, D on fig.4.9. The faults and concommitant veins which form strike NW-SE and will cross-cut the NE-SW orientated faults and veins, fig. 4.10. After each successive episode of slip, σ_x and σ_y alternate as the least principal stress. Movement can only take place on one set of faults at any one time as the displacement vectors for each set of faults have a different orientation, for movement to occur on two different sets of faults simultaneously, the displacement vectors need to have the same orientation, Jackson & McKenzie (1983).

At each movement of the faults, upright hydraulic fractures and veins form, see section 2.5.1.3; in this section it is established that the faults are listric in form. Movement on these faults caused rotation of bedding, so that veins formed during earlier increments of slip can be rotated and cross-cut by the veins associated with later

increments of slip. Further, any hydraulic fractures which formed during the earlier increment of slip were also rotated, and thus became suitably orientated for slip to occur, fig.4.12. Angelier & Colletta (1983) describe similar geometries in a number of extensional regimes. Several of the smaller faults with displacement of <1 m may have been originated in this way.

Neither set of extension faults displace the Sole fault, but curve into and join it, this indicates that either:-

i) the extension faults are syn-movement on the Sole fault, or

ii) the extension faults are post-movement on the Sole fault, and the already existent Sole fault acted as a weak horizon for the extension faults to flatten into.

There is no clear field evidence to suggest that either option is correct, however, I will assume a combination of both options. The extension faults displace the Loch Broom thrust. Therefore, the extension faults must have been operative after movement on the Loch Broom thrust had ceased and thrusting displacement transferred to the Sole fault. However, the extension faults do not displace the Moine thrust which has cut across the faults during its later extensional movement, see 2.2.1.

This model provides a good mechanism for the formation of extensional faults beneath major thrust sheets, however, the tectonic loading cannot account for the formation of the strike slip faults described in 2.5.1.3c. A development to the model is put forward to account for the strike-slip faults by considering the effects of erosion and possibly uplift on the thrust sheet.

4.4.5. Formation of strike slip faults and reactivation of extension faults during the erosion and uplift of the thrust sheet.

If Andersonian stress/fault relationships are valid, the strike slip faults must have formed in a different stress system than the extension faults. To form the extension faults σ_1 acted vertically in a loading capacity, whilst for the strike slip faults, σ_1 must have acted horizontally. As the strike slip faults have a general N-S trend then σ_1 must have acted sub-parallel to the strike of the thrust zone, see 2.5.1.3c.

In thrust systems, strike slip faults commonly separate areas of a thrust sheet which are moving at different slip rates, Boyer & Elliott (1982). Strike slip faults can also be developed in areas of extensional tectonics, again reflecting differential slip on the main fault, Bally et al. (1981), Jackson & McKenzie (1983). This type of strike-slip fault is therefore sychronous with thrusting or extension. The strike slip faults in Sheet IV at Glen Achall can be confidently excluded from this category as;

i) the strike slip faults displace both sets of extension faults. They are therefore post-extension

ii) some of the N.E-S.W extension faults have been reactivated as strike slip faults. This occurs where the orientation of the extension faults has deviated from the mean orientation towards an orientation where strike-slip displacement is convenient and because it is easier to cause slip on already existing faults than to initiate new faults.

iii) the orientation and consistent displacement relationships of the strike slip faults suggest a compressional stress field, where the overburden stress, σ_z, is the intermediate principal stress, and σ_y the maximum principal stress.

The approach adopted to account for the strike slip faults considers the effect of erosion and removal of overburden on the stress configuration, and is based on theoretical work by Price (1974) which studies the effect of uplift and erosion on sedimentary rocks in a hypothetical basin and the fractures which form. Price (op cit) considers two models

i) parallel uplift without change in the dip of bedding, and

ii) non-parallel uplift, where the dip of the bedding in the basin changes.

In most sedimentary basins the latter is the case, but in the case of a thrust sheet, uplift may be occurring or movement on the thrust may have ceased and only erosion is active. The case of erosion of the thrust sheet and no movement on the thrust is equivalent to parallel uplift as there is no change in the dip of bedding.

In Glen Achall displacement on the Sole fault is small, see section 2.5, therefore movement on the Sole fault/Loch Broom thrust system must have ceased shortly after the formation of the Sole fault. Erosion of the thrust sheet pile after thrusting would result in a decreasing overburden stress σ_z, also the late extensional movement on the Moine thrust which occurred later than movement on the Sole fault , see section 2.2.1., would have thinned the thrust sheet pile. The removal of overburden whether by erosion or tectonic thinning by late extensional movement on the Moine thrust is equivalent to parallel uplift.

Removal of overburden would produce a linear decrease in the overburden stress, σ_z. But because the physical parameters, Poisson's ratio (m) and Young's modulus, E, are not constant but change with depth, the lateral stresses σ_x and σ_y would display a non-linear decrease, and at a slower rate than σ_z, thus lateral stresses may not equilibrate with depth causing high lateral stresses at shallow depths, Price (1966, 1974). Indeed this can often lead to the magnitude of the intermediate lateral stress being greater than the overburden stress.

Figure 4.13 is a schematic graph of the relationship between stress and depth in an uplift/erosion situation. Because the inactive thrust planes acted as fluid flow restrictors, pore fluid pressure is unlikely to decrease rapidly. Thus it is reasonable to suggest that during the first stages of erosion the pore pressure does not decrease so rapidly as the lateral stresses σ_x and σ_y. The situation could arise where $\sigma_x - p$ becomes large enough to cause further slip on the NE-SW set of faults or if $\sigma_x - p = -To$ and $\sigma_1 - \sigma_3 < 4To$, cause hydraulic fractures to form and σ_x will increase to the value of p. With further slip or failure σ_x now becomes the intermediate principal stress, fig. 4.13. Likewise, when $\sigma_y - p$ reaches a certain value, further slip can occur on the NW-SE set of faults and σ_y will increase to the value of p. With further slip on the faults and/or initiation of hydraulic fractures, the fluid may be able to escape more easily and the pore fluid pressure will drop off more rapidly. Now as a result of erosion the lateral stress may decrease less rapidly than the pore pressure and eventually become greater than σ_z, which then becomes the intermediate principal stress. If σ_y reaches the stage where $\sigma_1 > 3\ \sigma_3$ and $\sigma_1 - \sigma_3 > 4To$, shear failure can occur with σ_y active as σ_1 fig. 4.13, causing strike-slip faults to form, and causing reactivation of favourably orientated extension faults as strike slip faults, fig. 4.14.

The erosion model does provide a neat way of altering the stress configuration to cause strike slip failure, but it is impossible to quantify accurately as little is known about the timing of the late extensional movement on the Moine thrust. Extension contributes to the removal of the overburden by thinning the nappe pile. Thus the erosion model is a qualitative but viable explanation of the strike slip faults.

4.5. DISCUSSION.

4.5.1. The Creag nam Broc fault.

Previous workers have interpreted the Loch Broom thrust at Glen Achall as a folded thrust, developed by deformation of the thrust during the formation of an underlying imbricate duplex, Peach et al. (1907), Elliott & Johnson (1980). However, the geometry of the Creag nam Broc fault, its footwall and hangingwall, suggests otherwise. Figure . 4.15a is a diagrammatic section across the Creag nam Broc fault to illustrate its geometry. In the footwall the fault clearly cuts down section from the Eilean Dubh Member to the Ghrudaidh Member, further, in the Eilean Dubh Member a drag fold is developed which is consistent with an extensional fault. If the Creag nam Broc fault were a part of a folded Loch Broom thrust then the hangingwall geometry could be expected to be comparable to the geometry shown in fig. 4.15b with bedding in the Torridonian rocks dipping to the NW. However, this is not so, as the bedding dips to the NE-E, fig. 4.15a, which is consistent with rotation on a listric extension fault.

The Creag nam Broc fault is clearly a listric extension fault, plate 2.14, and post-dates the Loch Broom thrust as it displaces the thrust from its glide horizon in the Eilean Dubh Member down to the top of the An-t-Sron Formation. The orientation of the Creag nam Broc fault is the same as the NE-SW faults and is considered to have been formed at the same time as a result of the loading induced high pore fluid pressures.

4.5.2. Footwall deformation at thrust ramps.

The extension structures seen in Sheet IV at Achall and Knockan are only developed beneath ramps, under which are the dolomites of the Durness Formation, which act in a mechanically isotropic manner. Where a footwall ramp contains other members of the Cambro-Ordovician sequence the deformation in the footwall has been by compressive folding and thrusting, with development of contractional duplexes, Peach et al (1907), Bailey (1935), Elliott & Johnson (1980), Butler (1982b), Coward (1982). These contractional duplexes are notably developed at Glencoul [GR 263303], and Inchnadamph, north east of Loch Assynt. The rock units in these contractional duplexes behaved in a mechanically anisotropic manner. It is now known that anisotropy reduces the compressive strength of a rock unit, hence an anisotropic rock sequence is more likely to fail than an isotropic unit, Jaeger & Cook (1976). It has already been suggested that the emplacement of thrust sheets can be divided into two stages;

i) a compressional stage prior to and during initiation and failure of the thrust sheet,

ii) a translation stage where the thrust sheet is emplaced and the main deformation in the footwall is one of gravitational loading by the weight of the thrust sheet

The contractional duplexes would have formed during stage (i). In the dolomites of Sheet IV stage (i) is marked by the twinning in the dolomite groundmass. The twin analysis shows that differential stress during this stage was of the order of 1kb and the isotropic dolomites with their high compressive strength were only locally deformed.

With the beginning of stage (ii), fluid pressure would rise and the extension faults in Sheet IV would develop. These may also develop in contraction duplexes if fluid pressure reaches sufficiently high levels. At Glencoul extension structures appear to be rare, however, immediately below the Glencoul thrust, the Durness Formation

contains numerous vertical veins indicative of hydraulic fracture with σ_1 acting vertically, i.e. a loading situation. In section 2.7, it is advocated that movement on thrusts in the brittle field is episodic and can be divided into a short cataclastic phase and a long inactive phase where loading was important. At Glencoul this may explain the occurrence of upright hydraulic fractures and veins adjacent to the thrust plane, plate 4.1.

At Knockan, see section 2.6 , both compressional structures and extensional structures occur, although the relationship between the compressional folds and thrusts and the extension faults is vague. Coward (1983) has recently suggested that the extension faults are the dorsal faults of small surge zones, however, encl.2 shows that folds occur within the area of extension faults. In Coward's (op cit) surge zone, contraction structures should be separate from the extension faults at the leading edge of the surge zone.. Further Coward (op cit) has interpreted many of the faults as thrust faults in a large duplex, this can be demonstrated in a number of cases not to be so as:-

i) several of the extension faults cut through the quartzite horses and their extensional geometry is without doubt.

ii) several fault traces can be followed to the Knockan Cliffs [GR 196099] where faults are extension listric faults.

iii) the predominant 'family' of small scale structures are small extension faults, upright tectonic veins, and horizontal stylolites, indicating that a loading stress system was dominant.

From this evidence and the spatially limited distribution of folds and thrusts, I favour an interpretation of these folds as either

i) a limited response to the compressive stage of thrusting in specifically weak areas, perhaps caused by a higher than average pore fluid pressure, see section 2.5,or

ii) accommodation structures developed during the extension faulting.

4.6. CONCLUSIONS.

The footwall deformation of rocks caused by gravitational loading as a result of the emplacement of thick thrust sheets has been given little or no attention in the literature. The extension faults within Sheet IV were first developed as a response to loading by the Loch Broom/Moine thrust system. At the time of loading, Sheet IV was part of an undetached footwall ramp complex. This deformation produced a family of extension structures i.e. listric faults, hydraulic fractures, upright tectonic veins and bedding-parallel stylolites within the Durness Formation, the presence of which indicates that high pore fluid pressures were active. It is shown by the use of a stress model that high pore fluid pressures were necessary to cause extension parallel to the strike of the thrust belt. Stresses were calculated for loading at 5 km, and a total loading depth of 10 km, and differential stresses were estimated by twin analysis of calcite crystals in veins and dolomite of the groundmass, and by the simple observation of the rock failure mode combined with a knowledge of the tensile strength of the rock. This simple but powerful tool enables a field geologist to estimate differential stress, if he knows or can estimate physical parameters from structures in the rocks. The model is then extended to take into account the erosion and uplift of the thrust sheet, and provides a reasonable explanation for the occurrence of the strike slip faults and indicates that reactivation of the extension faults was probable.

The model could be refined if more were known about the isostatic responses of loading by thrust sheets, and could perhaps explain regional fault geometries seen in the foreland of thrust belts. This would be a worthwhile topic for future research.

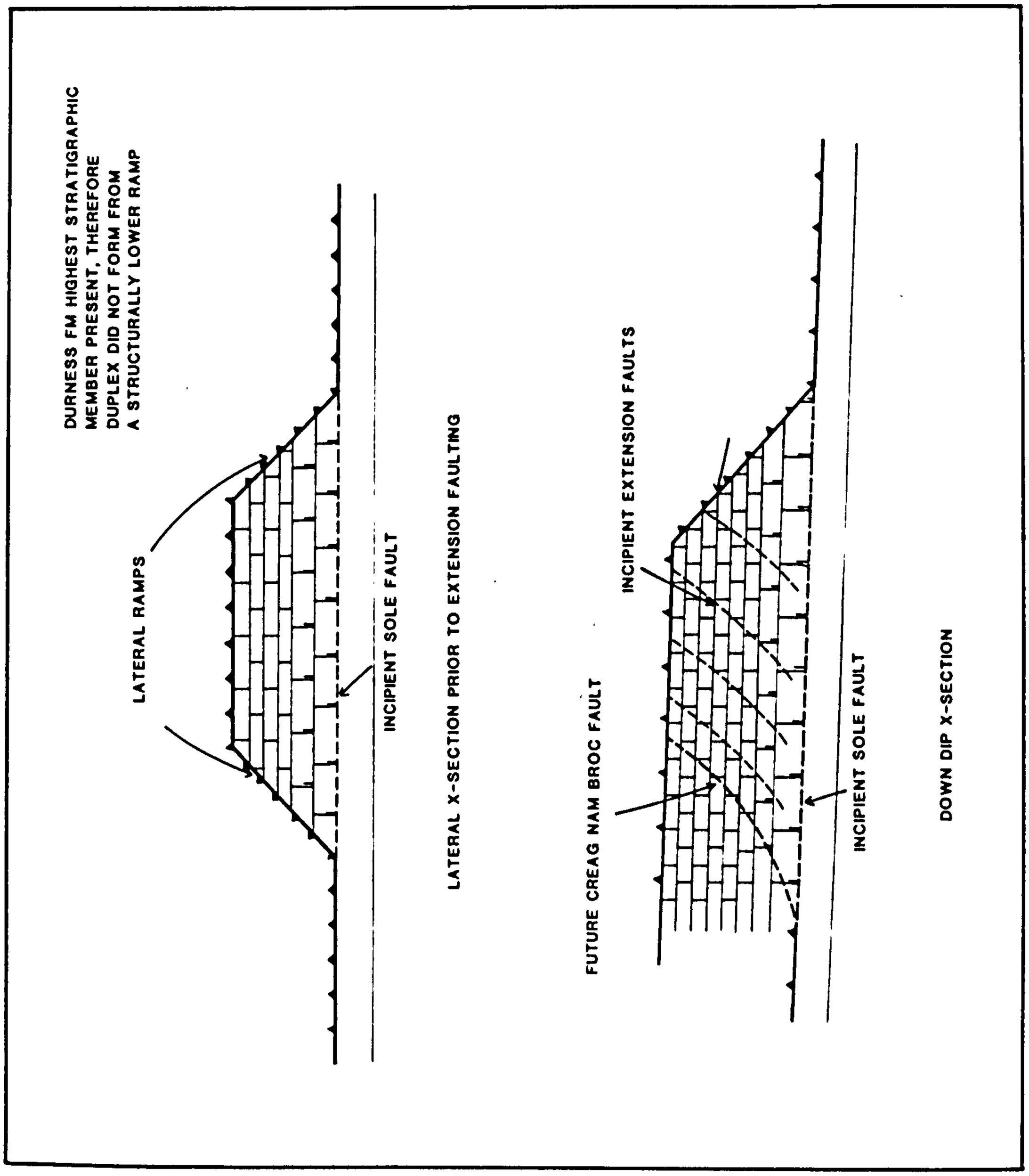

Fig.4.1.

Schematic diagram to show the geometry of Sheet IV prior to movement on the extension faults. Sheet IV comprises of Durness Formation and it is bounded by ramps. It is a large asperity.

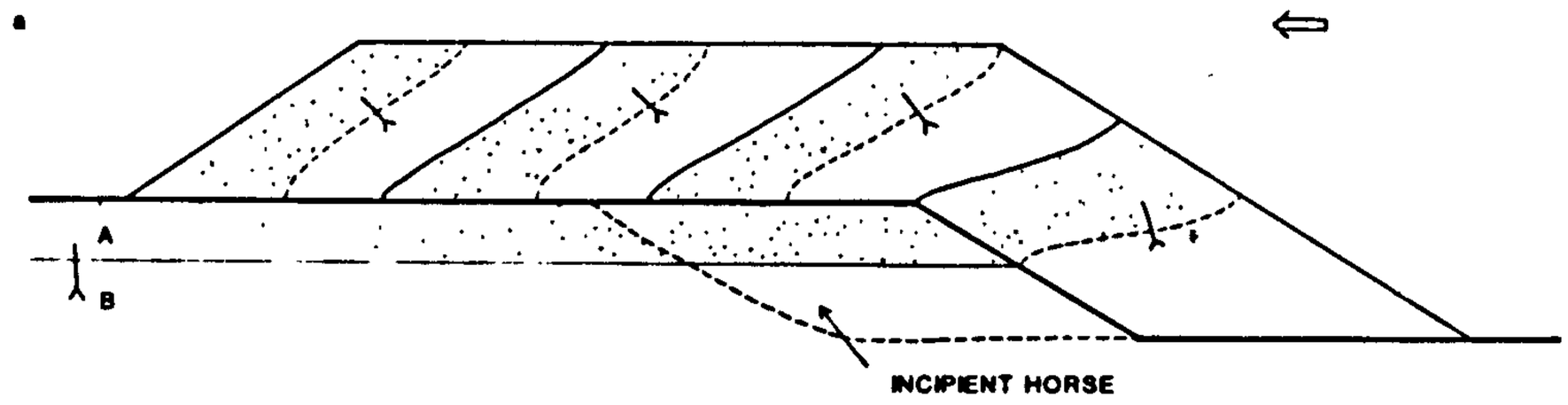

FOREWARDS FACING, FORELAND DIPPING DUPLEXES (FROM BOYER & ELLIOTT 1982)

a. RIGHT WAY UP b. INVERTED

FORELAND DIPPING DUPLEX BUT BACKWARDS FACING

Fig.4.2.

Figures 4.2a and 4.2b show foreland dipping duplexes, i.e. the faults dip towards the foreland, from Boyer & Elliott (1982): these duplexes are derived from ramps and are always forward facing. However, fig.4.2c which shows Sheet IV which is also foreland dipping but hindward facing, i.e. the bedding dips towards the hinterland.

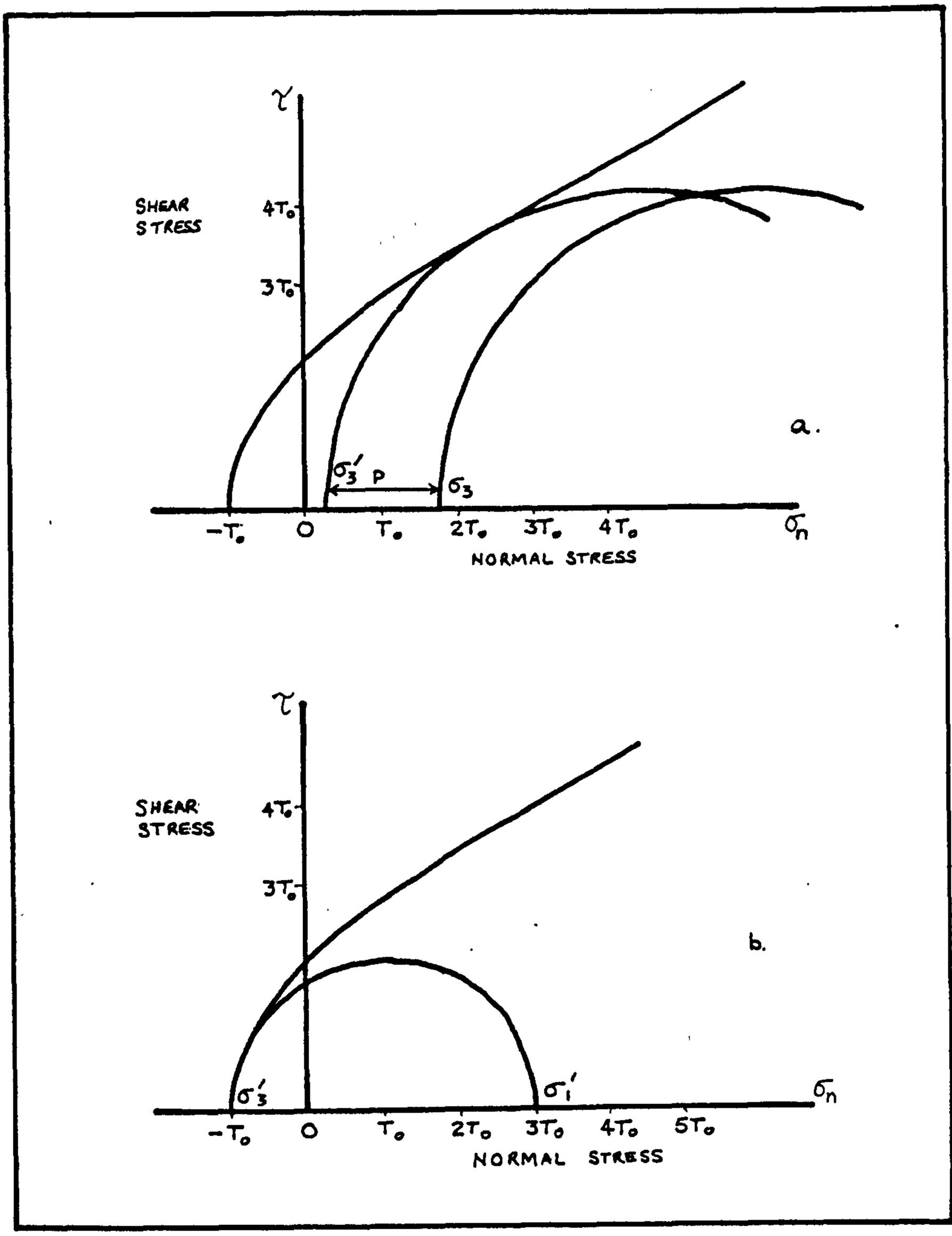

Fig.4.3.

Fig.4.3a- A Mohr circle diagram to show the stress conditions to show the effect of pore fluid pressure on the stress circle. The σ_3 point on the normal stress axis moves to the left to σ_3'.

Fig.4.3b- A Mohr circle diagram to show the stress conditions for hydraulic fracture. Hydraulic fracture occurs when $\sigma_3' = -T_0$.

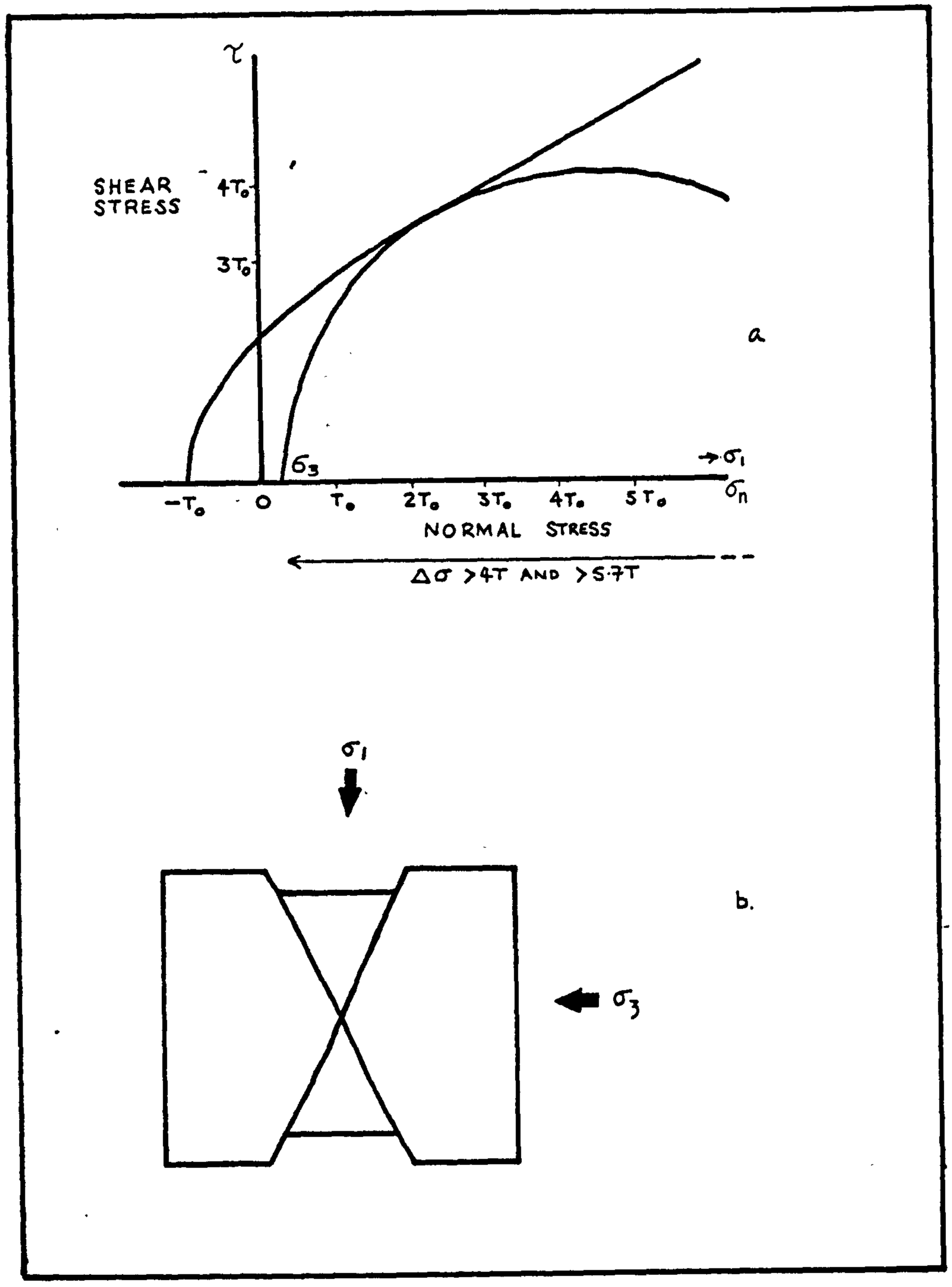

Fig.4.4.

Fig.4.4a is a Mohr circle diagram to show the stress conditions for shear failure. Note that σ_3 is in the compressive field of the diagram to the right of the shear stress axis, and that $\Delta\sigma > 4T_o$. This stress condition will cause shear failure only, fig.4.4b.

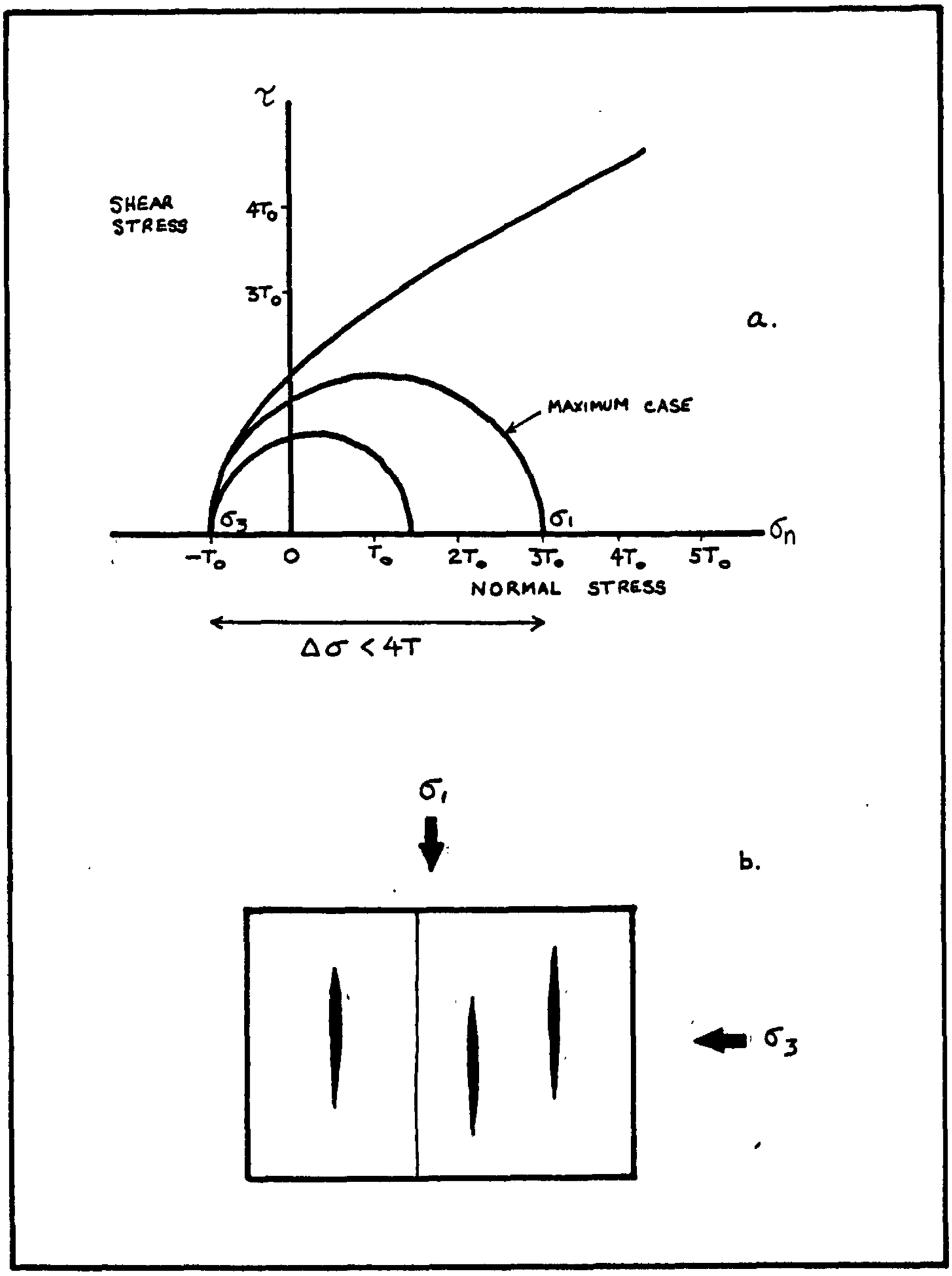

Fig.4.5.

Fig.4.5a is a Mohr circle diagram to show the stress condition for hydraulic fracture, note that $\Delta\sigma < 4T_0$ and that σ_3 lies in the tension field. The largest circle is the maximum case for hydraulic fracture. Fig.4.5b shows the resulting structures.

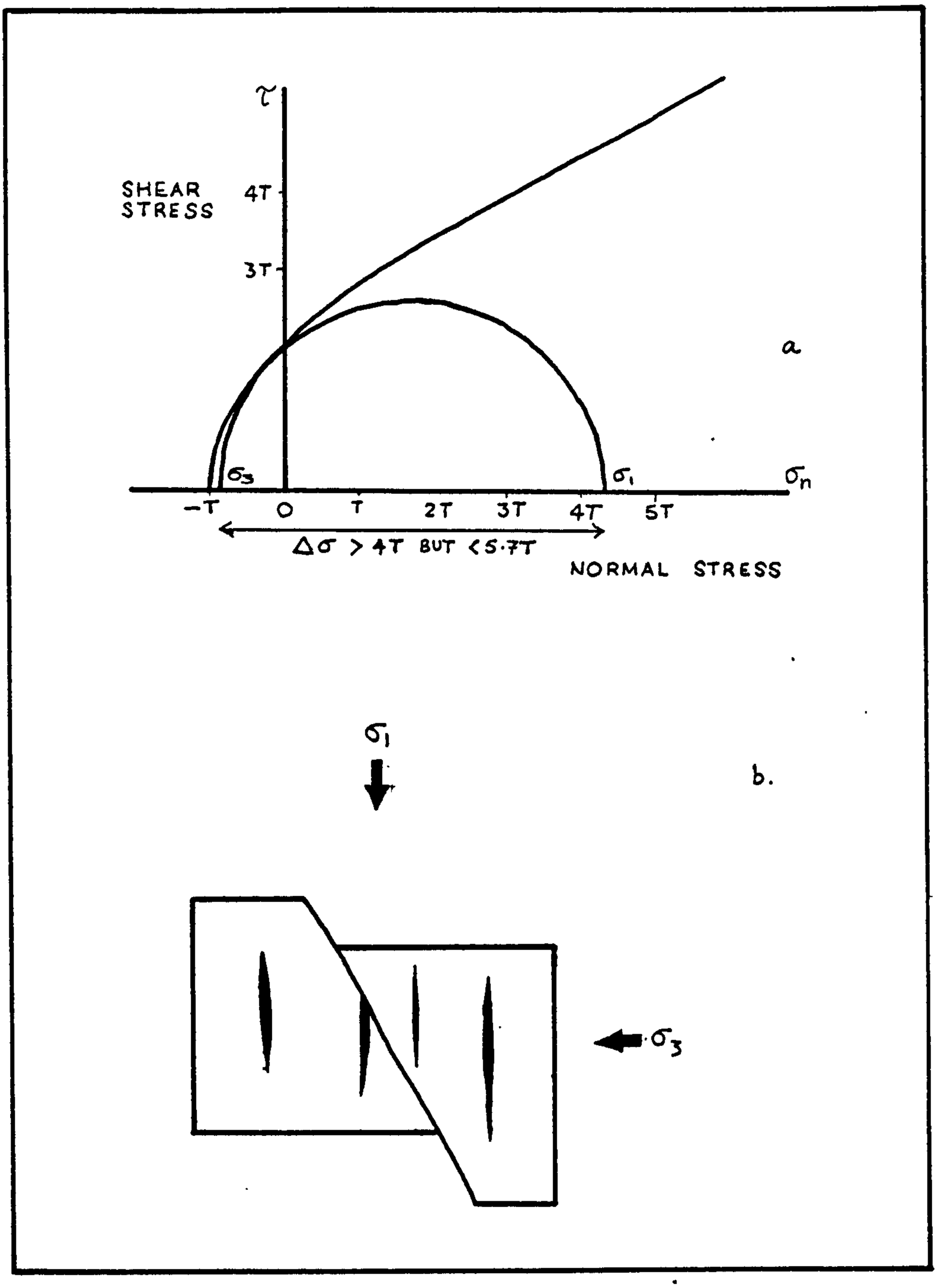

Fig.4.6

Fig.4.6a is a Mohr circle diagram to show the stress condition for simultaneous shear failure and hydraulic fracture. Note that $\Delta\sigma > 4T_o$ but $< 5.7T_o$. Fig.4.6b shows the resulting structures, note that the veins are not displaced by the fault but form off of the fault, these are termed feather veins.

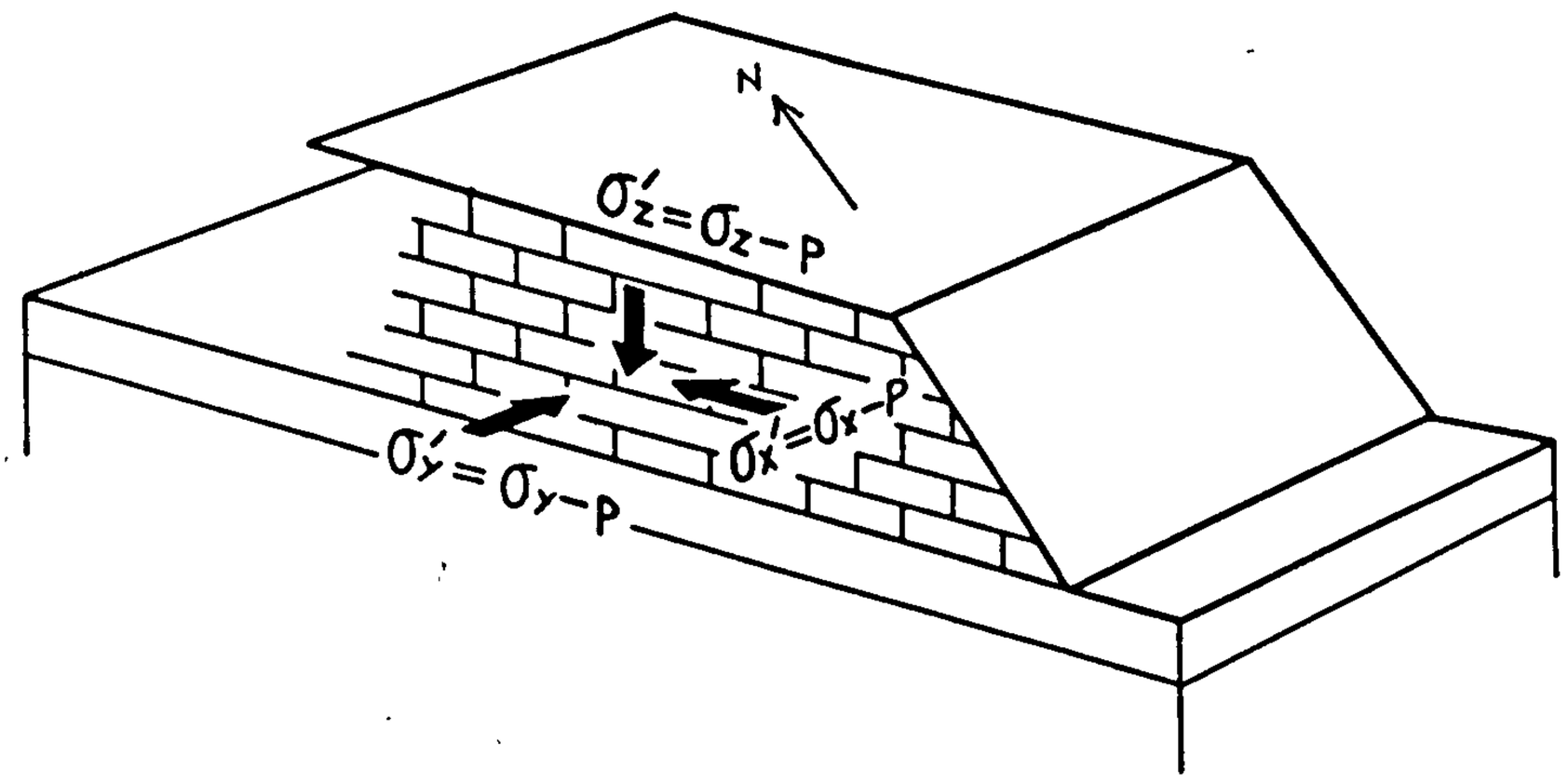

Fig.4.7.

Sketch block diagram to show the orientation of the principal effective stresses within Sheet IV.

Fig.4.8.

Graphs of λ against σ'. In fig.4.8a the overburden is 5km thick, note that λ =0.65-7 in order to cause failure, with σ_x as σ_3, but would need to rise to λ= 0.7-0.8 to cause failure with $\sigma_y = \sigma_3$. In fig.4.8b the overburden is 10km thick, λ has to rise to 0.85 for failure with $\sigma_x = \sigma_3$ and 0.9 when $\sigma_y = \sigma_3$.

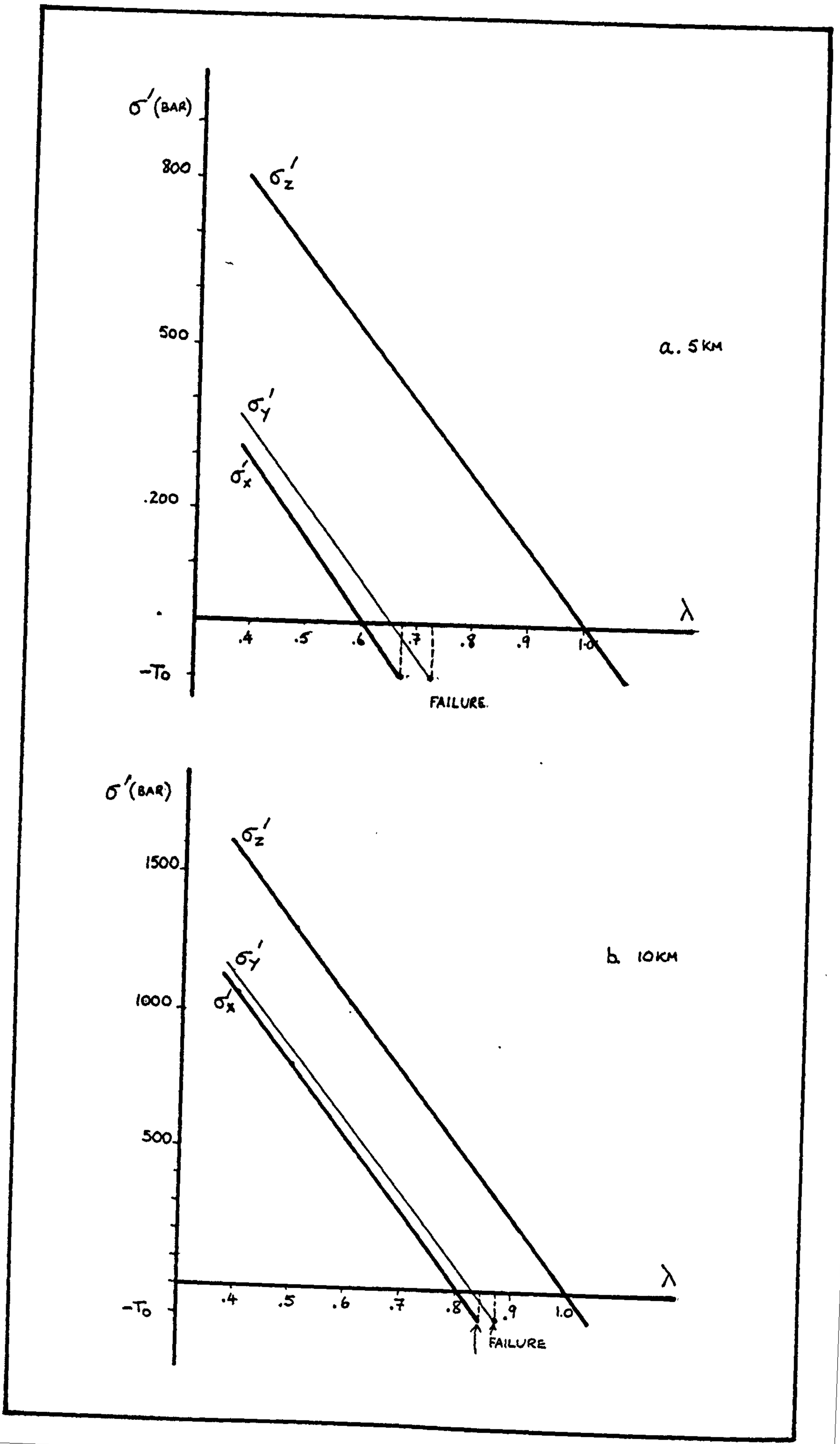
σ'(BAR)
800
500
.200
-To
σz'
σy'
σx'
λ
.4
.5
.6
.7
.8
.9
1.0
FAILURE
a. 5KM
σ'(BAR)
1500
1000
500
-To
σz'
σy'
σx'
λ
.4
.5
.6
.7
.8
.9
1.0
FAILURE
b. 10KM

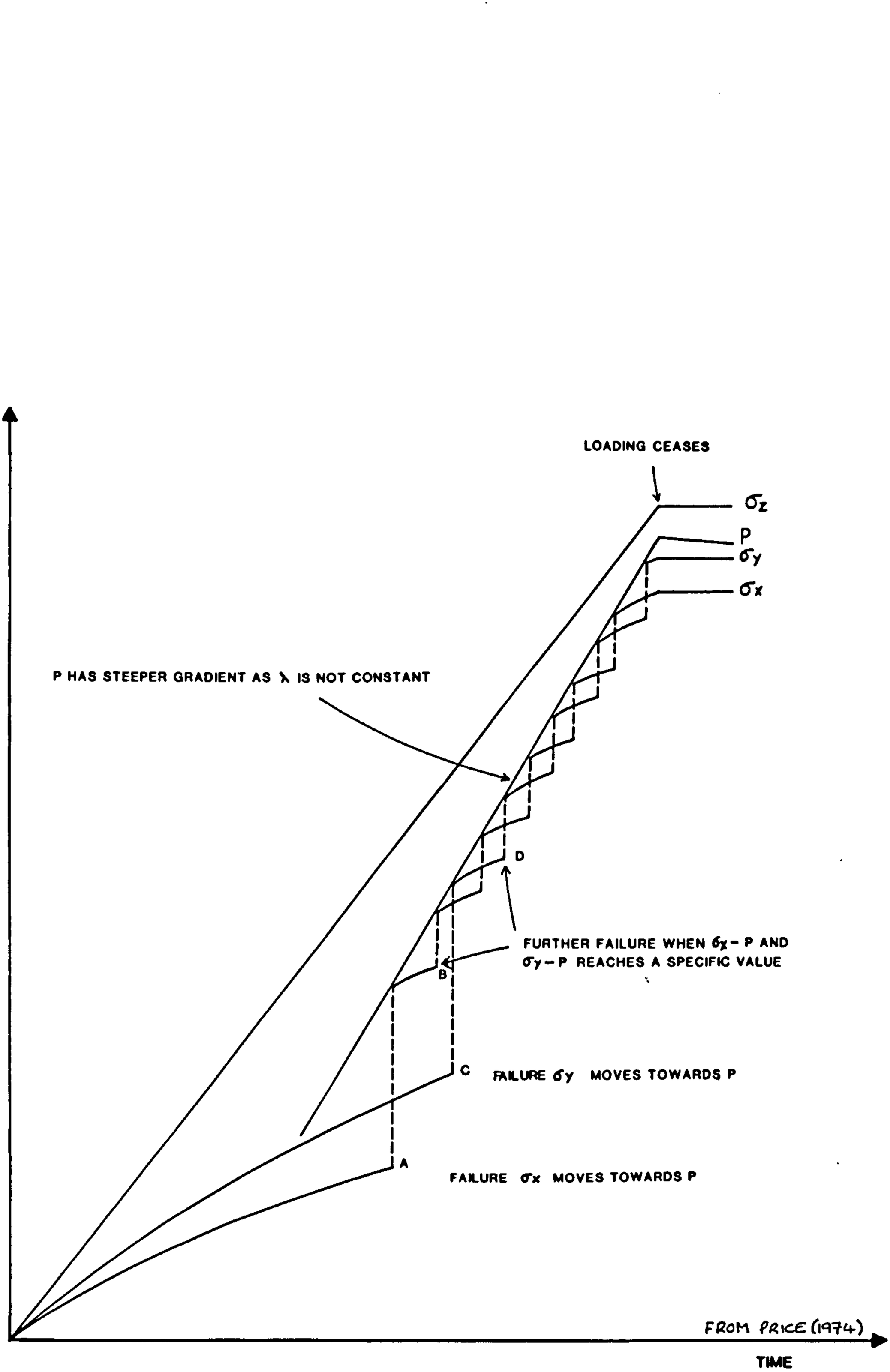

Fig.4.9.

Schematic graph to illustrate the stress history in Sheet IV during tectonic loading against time. With failure when $\sigma_x = \sigma_3$ and $\lambda =$ 0.65, σ_x will approach the value of p and σ_y will then become σ_3, if λ = 0.7-0.8 failure can occur and σ_y will also approach the value of p. After failure and with continued loading σ_x and σ_y will again start to increase. Further failure will occur when σ_x- p reaches a critical value, likewise for σ_y. The two lateral stresses will increase step wise until loading ceases.

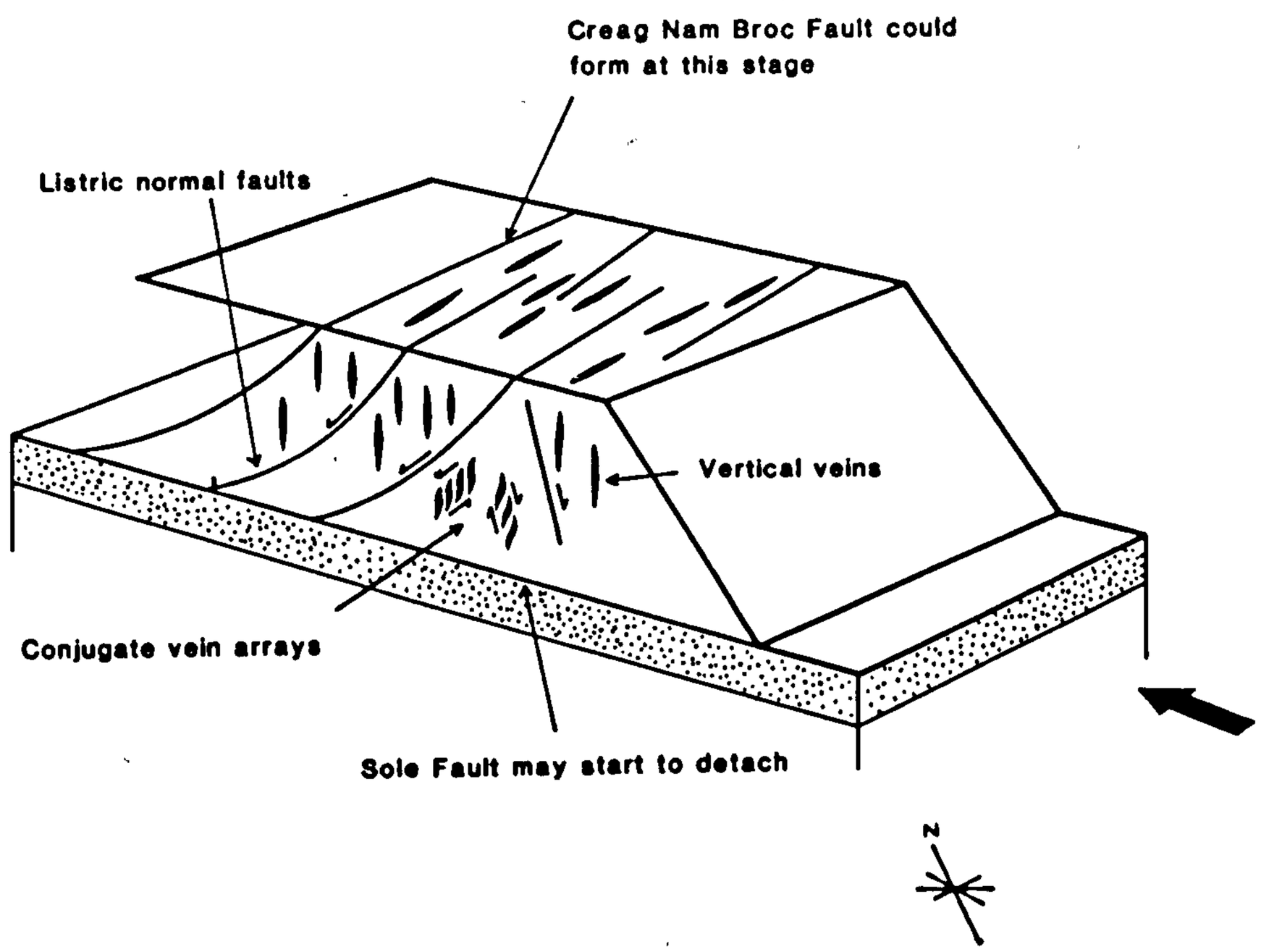

Fig.4.10.

Block diagram (not to scale) to illustrate the structures which form with failure when λ =0.65 and $\sigma_x = \sigma_3$. The faults are the N.E.-S.W set in Sheet IV.

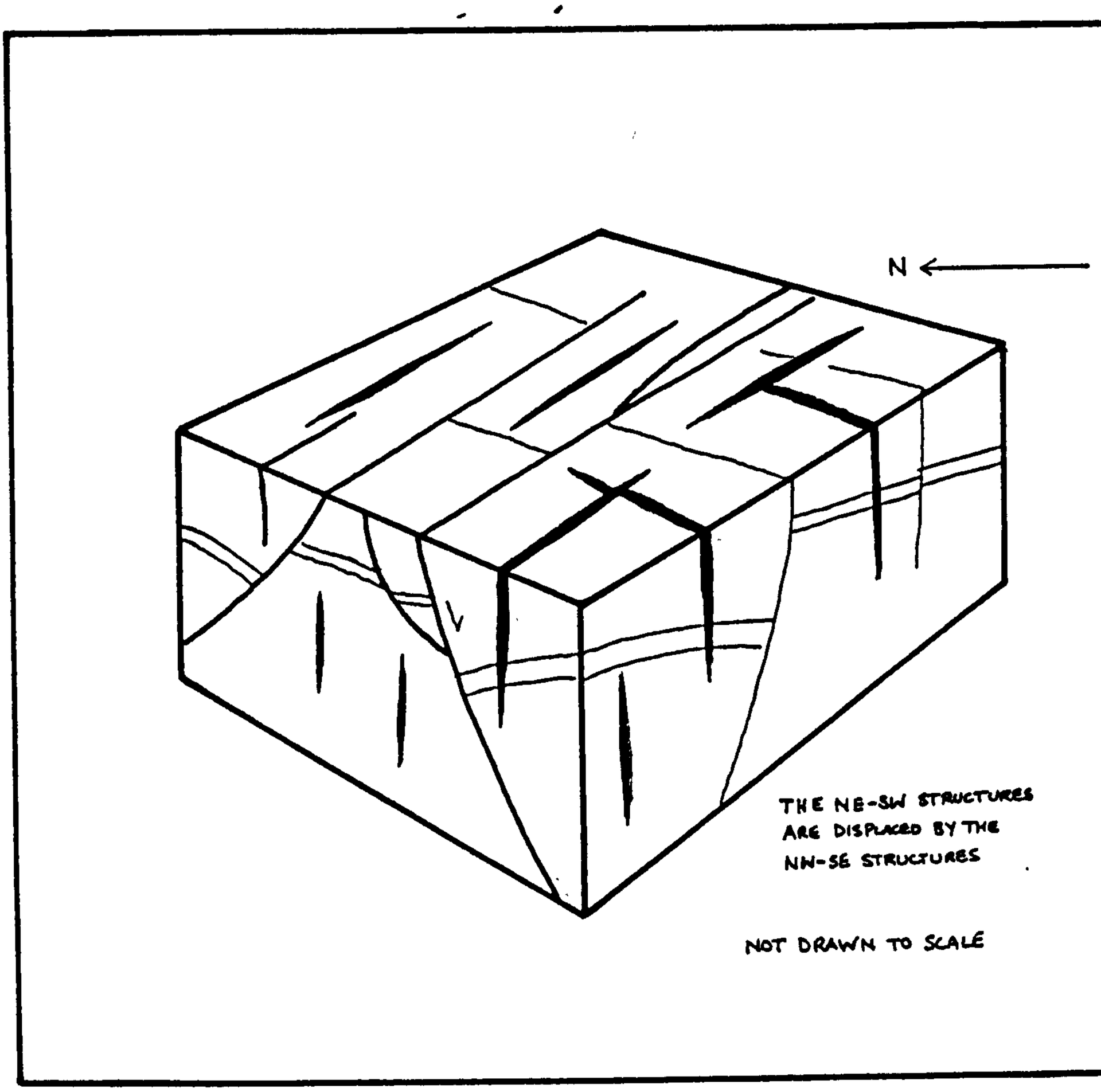

Fig.4.11.

Block diagram (not to scale) to show the style of structures which form with failure when $\sigma_y = \sigma_3$. The resulting N.W-S.E faults and concomittant veins crosscut the N.E.-S.W set of structures.

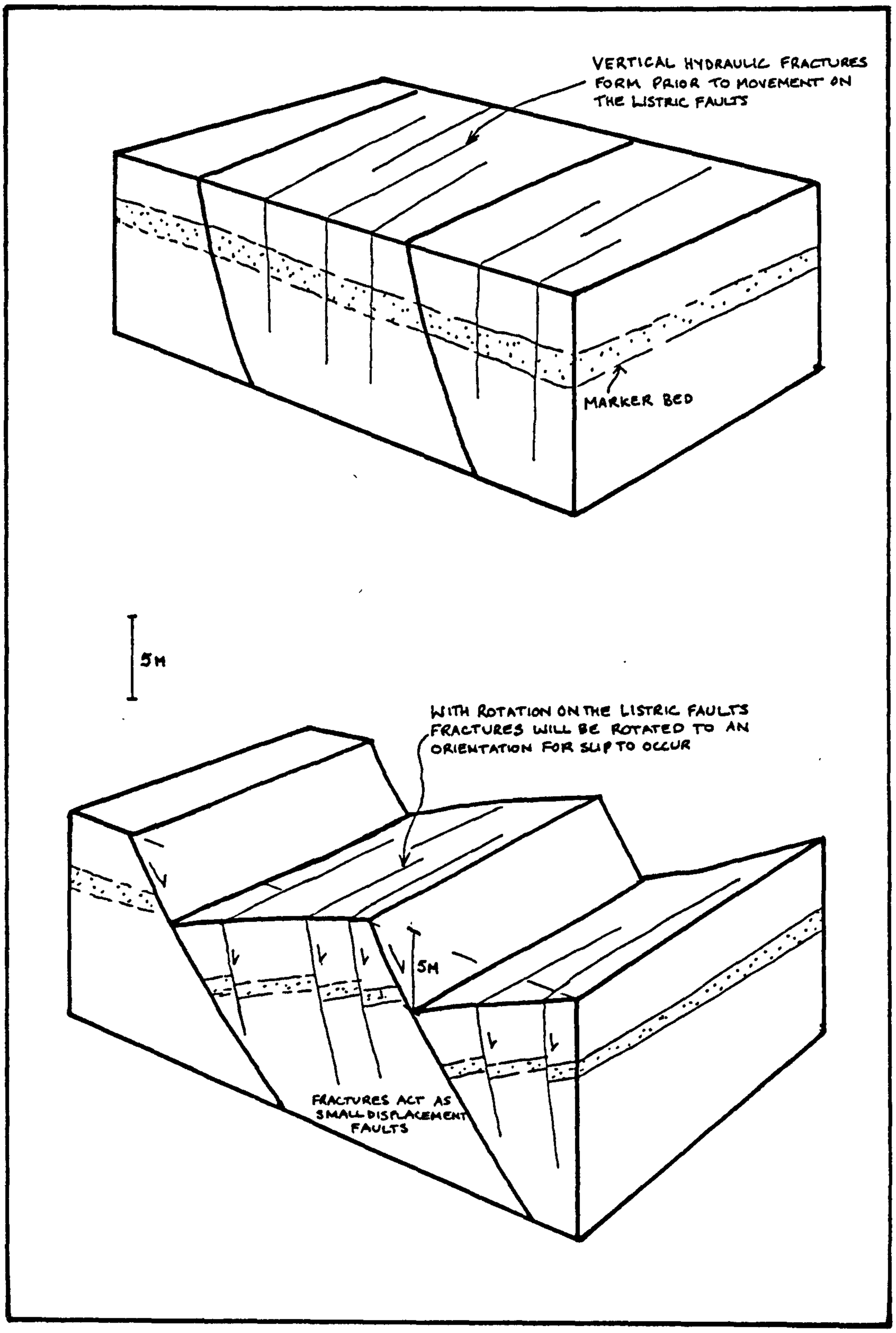

Fig.4.12.

Schematic block diagrams to show rotation of originally upright hydraulic fractures so that slip can occur along them.

Fig.4.13.

Diagrammatic graph to show the changes in the principal stresses with time during erosion. Note that at first the lateral stresses decrease more rapidly than p, and so when $\sigma_x - p$ further slip is possible. The lateral stress will decrease more slowly than the overburden stress and hence a situation may arise when $\sigma_y > \sigma_z$. If $\sigma_y = 3.\sigma_x$ then failure can occur producing strike slip faults. This has happened in SheetIV ,see section 2.5.1.3c, and the strike slip faults cut both sets of extension faults.

Fig.4.14.

Block diagram to show the geometry of the strike slip faults in Sheet IV in the Achall quarry.

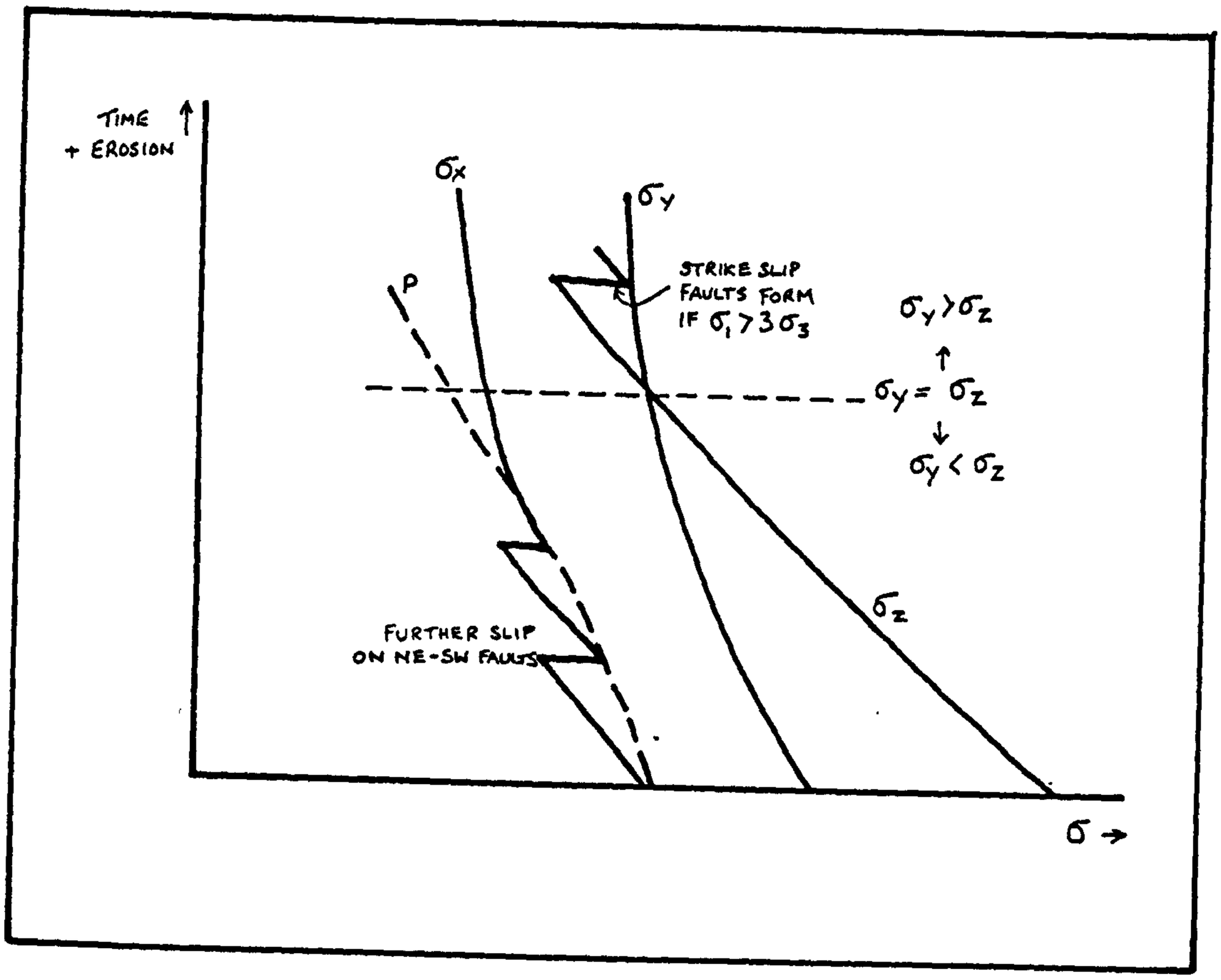
TIME ↑
+ EROSION
σ_x
σ_y
P
STRIKE SLIP FAULTS FORM IF $\sigma_1 > 3\sigma_3$
$\sigma_y > \sigma_z$
$\sigma_y = \sigma_z$
$\sigma_y < \sigma_z$
σ_z
FURTHER SLIP ON NE-SW FAULTS
σ →

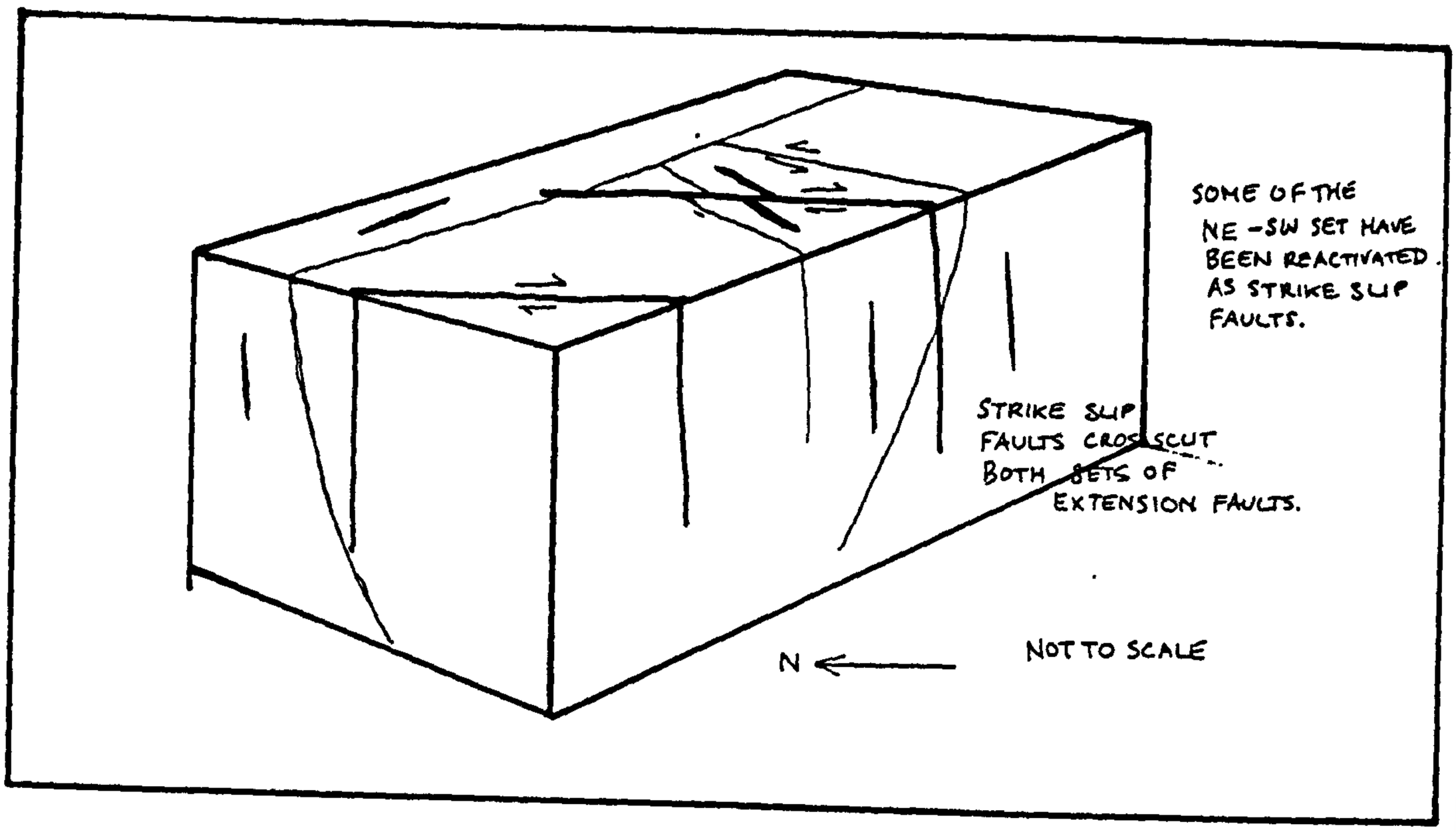
SOME OF THE NE-SW SET HAVE BEEN REACTIVATED AS STRIKE SLIP FAULTS.
STRIKE SLIP FAULTS CROSSCUT BOTH SETS OF EXTENSION FAULTS.
N ←
NOT TO SCALE

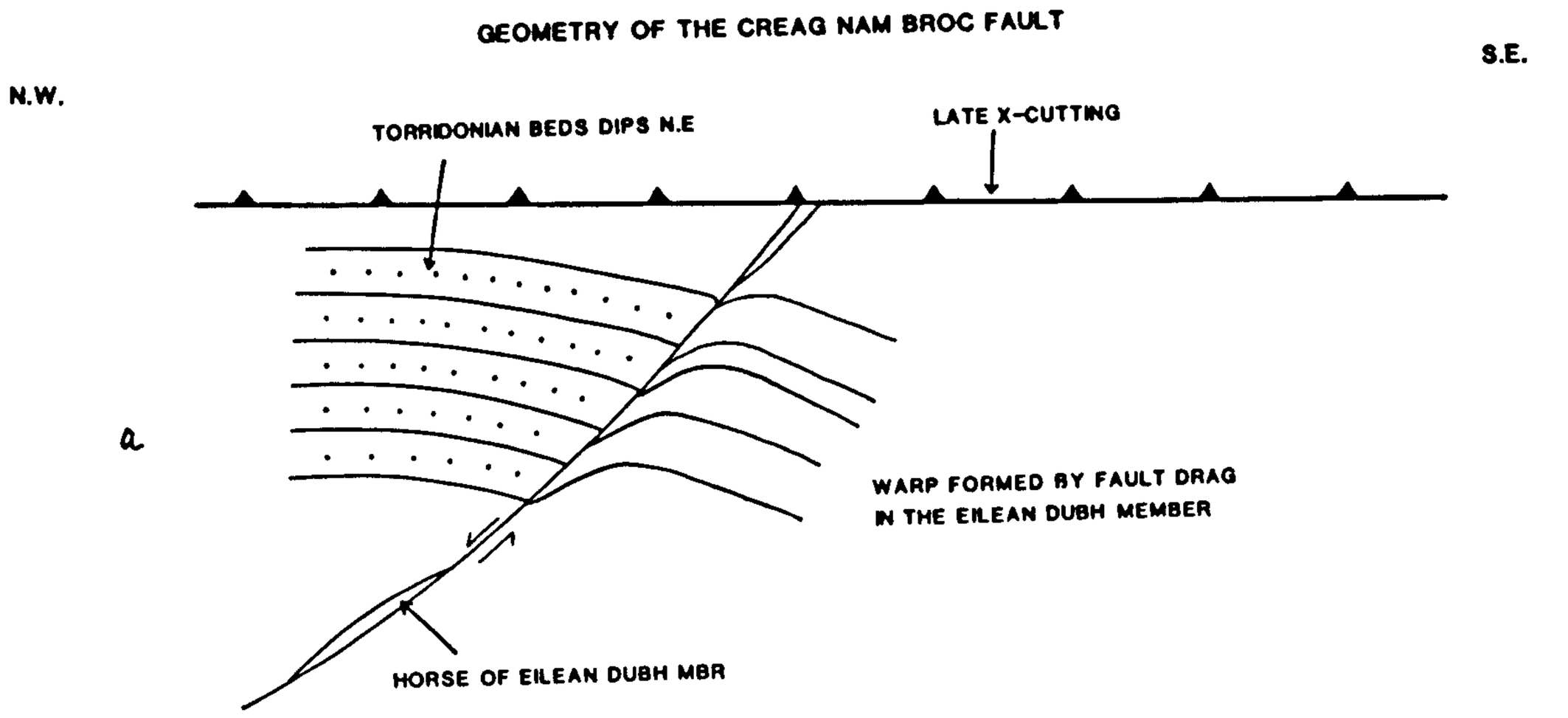

Fig.4.15.

Diagram to show the geometry of the Creag nam Broc fault.

(a) cross section illustrating the extensional geometry of the Creag nam Broc fault, see plate.4.1.

(b&c) these diagrams show the expected geometry if the Creag nam Broc fault was a folded thrust as interpreted by Peach et al. (1907) and Elliott & Johnson (1980).

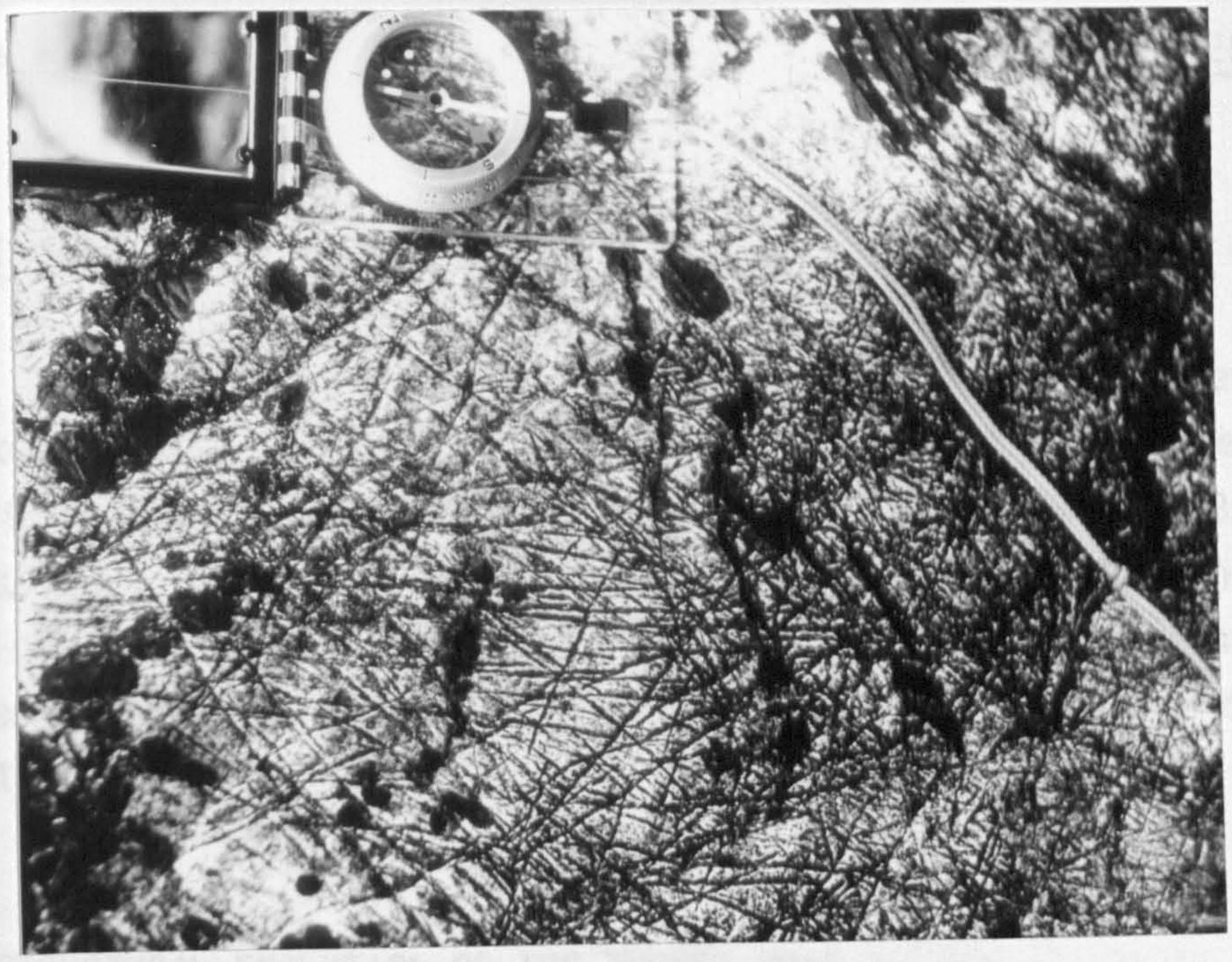

Plate .4.1 Intense veining in the Durness Formation below the Glencoul thrust at Loch Glencoul.

Chapter 5. STRUCTURAL EVOLUTION OF THE MOINE THRUST ZONE BETWEEN LOCH BROOM AND THE ASSYNT CULMINATION: A SUMMARY

5.1. INTRODUCTION.

The aim of this chapter is to bring together and synthesise the previous three chapters and to present a coherent picture of the structural evolution in the Moine thrust zone between Loch Broom and the Assynt culmination. The most effective method of doing this is to use hangingwall sequence diagrams for along strike sections. These diagrams are not drawn to scale and are diagrammatic in order that detail is presented more clearly.

5.2. STRUCTURAL EVOLUTION OF THE THRUST ZONE.

Because of the later extensional movement on the Moine thrust, little can be said of its original geometry. However, its original glide plane prior to the initiation and detachment of the Loch Broom thrust must have been in or above the Eilean Dubh Member, as two horses of the member occur beneath the present day Moine thrust near Loch na Maoile. Figure 5.1 is a diagrammatic hangingwall sequence diagram which represents the thrust geometry prior to the initiation of the Loch Broom thrust. Before much movement the geometry of the Loch Broom thrust was dominated by two large lateral ramps where the thrust climbed from the Lewisian gneiss (now seen at Langwell) up into the Eriboll Formation and then down the other lateral ramp back into the Lewisian gneiss at Loch Broom.

With movement the Loch Broom thrust climbed to the glide plane at the top of the An-t-Sron Formation, fig. 5.2, in so doing produced two antiforms above Glen Achall and Langwell and a wide synform, the Loch na Maoile synform. In its progress over 25 km of displacement, the Loch Broom thrust accreted a number of footwall horses of Eriboll Formation, the geometry of which show that they were derived from a ramp which cut through a fold. At Loch Broom, the Loch Broom thrust

was marked by a large lateral ramp where the glide planes at the top of the An-t-Sron Formation and in the Eriboll Formation are linked, fig. 5.2. At Knockan there are two large horses of Eriboll Formation which have been cut through by the late extensional movement on the Moine thrust. These horses were previously interpreted as klippen of the Ben More thrust sheet which is part of the Assynt culmination. Their geometry indicates that they were derived from a large asperity rather than a ramp.

Figure 5.2 shows the thrust zone just after the initiation of the Ullapool thrust which originated at the lateral ramp in the Loch Broom thrust as a means of smoothing off the ramp. After a displacement of about 3 km on the Ullapool thrust, Elliott & Johnson (1980), the portion of the Loch Broom thrust above the Ullapool thrust sheet ceased to move, fig. 5.3. At approximately the same time several large asperities of the Durness Formation caused ramping in the Loch Broom thrust at Langwell and Achall and on a smaller scale in the Ullapool thrust at Corry Bridge.

At Knockan, although the late movement on the Moine thrust makes any interpretation open to conjecture, the Moine thrust must have ramped laterally up into the Eilean Dubh Member because the thrust beneath the horses of Eriboll Formation has a glide plane in the Eilean Dubh Member.

Large asperities of the Durness Formation make up 'Sheet' IV, and these are internally deformed by complex extension faults caused by gravitational loading as the Loch Broom and Moine thrust sheets were emplaced over them. These extension faults flattened out onto the Sole fault which eventually detached, and when this occurred the roof thrusts over Sheet IV ceased to be active and the extension faults cut up into the overlying thrust sheets. The extension faults in Sheet IV were accompanied by tectonic veining, hydraulic fracture and the development of stylolites indicative of high pore fluid pressures. The high pore fluid pressure was built up by the rapid tectonic loading and by the restriction to fluid flow out of Sheet IV units by the surrounding impermeable fault rocks. The Moine thrust was then reactivated as a low angle extension fault which cut through earlier structures which had previously deformed it, fig. 5.4.

The deformation mechanisms of thrusting are entirely 'brittle' with the production of cataclasites. The cataclastic textures show that deformation occurred in cycles of cataclasis followed by induration and compaction when a crude pressure solution cleavage developed in areas of high strain. These cycles dictated periods of fluid flow as during cataclasis the cataclasite was permeable, whilst during the induration the cataclasite acted as a fluid flow restrictor.

This short chapter is a summary of the geological evolution of the Moine thrust zone between Ullapool and Knockan covered in the previous chapters, and shows that although the structure may look simple on the map, detailed study reveals complex geometries and structures. The deformation in this part of the thrust zone is characterised by elastic-brittle mechanisms, with no ductile deformation.

Fig.5.1.-5.4.

Hangingwall sequence diagrams to ilustrate the structural evolution of the Moine thrust zone between Knockan an Loch Broom. see text for details

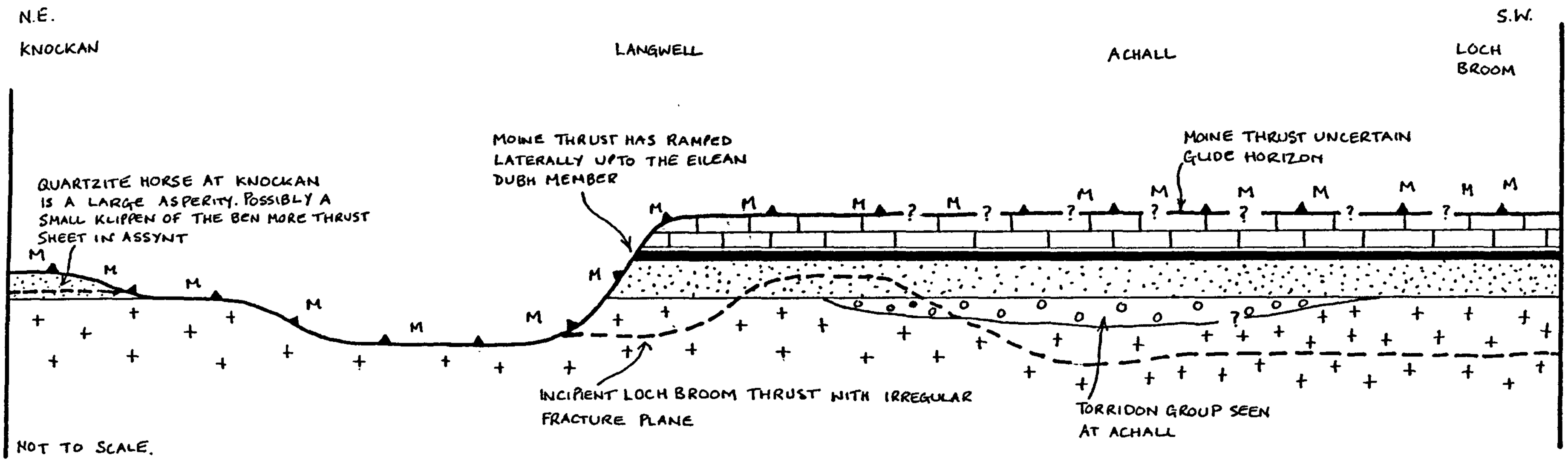
N.E.
KNOCKAN
LANGWELL
ACHALL
S.W.
LOCH BROOM
MOINE THRUST HAS RAMPED LATERALLY UPTO THE EILEAN DUBH MEMBER
MOINE THRUST UNCERTAIN GLIDE HORIZON
QUARTZITE HORSE AT KNOCKAN IS A LARGE ASPERITY. POSSIBLY A SMALL KLIPPEN OF THE BEN MORE THRUST SHEET IN ASSYNT
INCIPIENT LOCH BROOM THRUST WITH IRREGULAR FRACTURE PLANE
TORRIDON GROUP SEEN AT ACHALL
NOT TO SCALE.

FIG. 5.1.

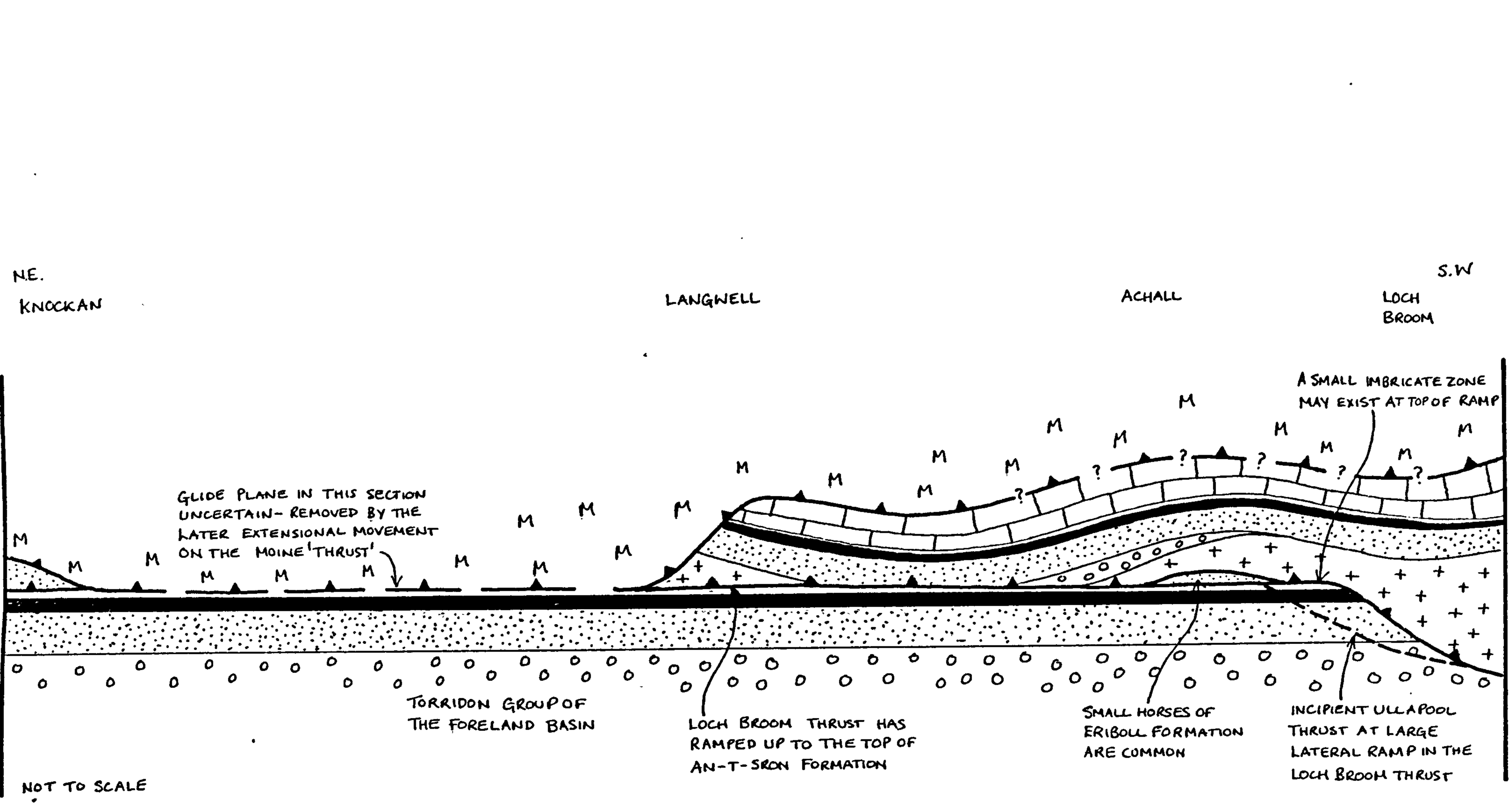
N.E.
KNOCKAN
LANGWELL
ACHALL
S.W
LOCH BROOM
A SMALL IMBRICATE ZONE MAY EXIST AT TOP OF RAMP
GLIDE PLANE IN THIS SECTION UNCERTAIN- REMOVED BY THE LATER EXTENSIONAL MOVEMENT ON THE MOINE 'THRUST'
TORRIDON GROUP OF THE FORELAND BASIN
LOCH BROOM THRUST HAS RAMPED UP TO THE TOP OF AN-T-SRON FORMATION
SMALL HORSES OF ERIBOLL FORMATION ARE COMMON
INCIPIENT ULLAPOOL THRUST AT LARGE LATERAL RAMP IN THE LOCH BROOM THRUST
NOT TO SCALE

FIG. 5.2.

N.E.
KNOCKAN

LANGWELL

ACHALL

LOCH BROOM

S.W.

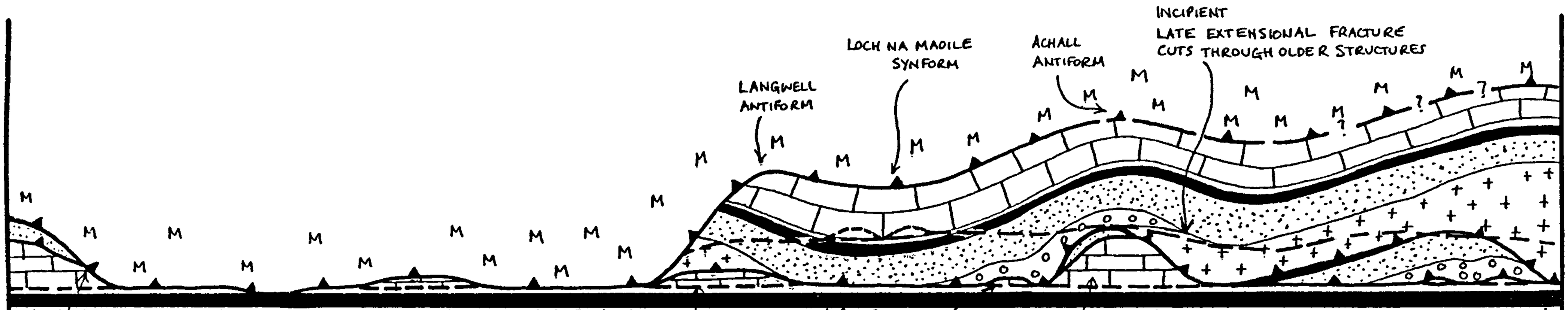

MOINE THRUST CLIMBS LARGE LATERAL RAMP INTO THE EILEAN DUBH MEMBER SOLE FAULT TO FORM AT BASE OF THE SHEET IV.

NOT TO SCALE

SHEET IV HORSES OF DURNESS FORMATION HAVE THE SOLE FAULT AS A FLOOR

THE LOCH BROOM THRUST HAS CLIMBED UP TO THE EILEAN DUBH MEMBER AT ACHALL TO FORM SHEET IV. RAPID RISES IN FLUID PRESSURE DUE TO FLUID FLOW RESTRICTION FROM THE SHEET. EXTENSION STRUCTURES AS A RESULT OF TECTONIC LOADING

EMPLACEMENT OF ULLAPOOL THRUST SHEET FOLDS OVERLYING THRUSTS.

FIG. 5.3.

N.E.

KNOCKAN

LANGWELL

ACHALL

S.W.

LOCH BROOM

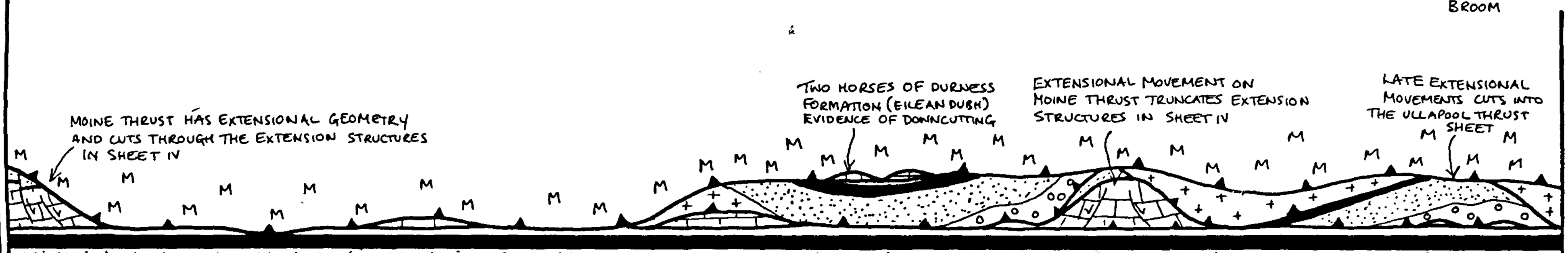

SOLE FAULT ACTIVE PRIOR TO EXTENSIONAL MOVEMENT ON THE MOINE THRUST

NOT TO SCALE

FIG. 5.4.

CHAPTER 6 THE THERMAL EFFECTS OF THRUSTING IN THE MOINE THRUST ZONE: THEIR TECTONIC AND REGIONAL IMPLICATIONS

6.1. INTRODUCTION.

The emplacement of thick thrust sheets causes a major upset in regional geothermal gradients which results in metamorphism of the footwall. If the displacement rates are sufficiently high, the distances moved are large and the thrust sheets sufficiently thick, then thrusting can cause inverted metamorphic zones and heat flow anomalies which are observable in the field.

Evidence of the former presence of
Inverted metamorphic gradients beneath large thrust sheets are now well established. Examples have been described from California, Graham & England (1976), Greece, Barton & England (1979), Newfoundland, Williams & Smythe (1975), the Himalaya, Le Fort (1975) and the Savoie Pre-Alps, Aprahamian & Pairis (1981). Thrusting causes disequilibrium of geothermal gradients, and re-equilibrium by the conductive heat transport from the thrust sheet has been described by Oxburgh & Turcotte (1974). In order to establish an inverted gradient, shear heating due to the frictional effects of movement on thrusts, Graham & England (1976), Barton & England (1979) or a combination of conductive heat transport and shear heating is necessary, Bickle et al. (1975), Brewer (1981). Numerical models of the effects of shear heating along thrust faults have been considered by Reitan (1968a, b, 1969) and Brewer (1981) has considered the combined effects of shear heating and thermal conduction. Both the theoretical models of Reitan (op cit), and Brewer (op cit), and the quantitative field studies of Graham & England (op cit) and Barton & England (op cit) show that in order to establish an inverted gradient by shear heating, displacements along the thrust need to be large, i.e. >50 km, in addition to high strain rates, shear stresses and differential stresses. Moderate strain rates and stresses are only feasible if the duration of thrusting is of the order of tens of my and the coefficients of friction of the rocks involved in the thrusting are high, Brewer (1981). Overthrust sheets for which shear heating has been

postulated usually consist of crystalline metamorphic or igneous rocks. However, the inverted gradient described in the Savoie Alps is confined entirely to sediments and the metamorphism is of a low grade, Aprahamian & Pairis (1981).

The aim of this chapter is to assess the thermal effects of thrusting in the Moine thrust zone. The lithologies involved in the thrusting do present a problem in that they are all thermally insensitive, i.e. quartzites, dolomites in the Cambro-Ordovician sequence and gneisses and arkoses in the Precambrian, and so are unhelpful in providing useful minerals in equilibration studies.

The method chosen for the thermal studies involved illite crystallinity and use of the b_o spacing indexes of white micas. The specimens were collected from the Fucoid Beds, shale partings and shale horizons within the quartzites of the Eriboll Formation, and the clay-sized matrix of the Torridon Group arkoses.

Downie (1981) estimated temperatures by using the colouration index of Acritarchs from the Fucoid Beds. With increase in temperature the Acritarchs change colour, and this colour change has been calibrated to give a colouration index. From this Downie (1981) showed that temperatures in the Cambro-Ordovician sequence ranged between 250-300°C, which agrees closely with the work on illite crystallinity presented here. Higgins (pers. comm. with Dr G.Oliver) reports that conodonts collected from the Durness Formation around Durness village have a colouration index (CAI) of 5 corresponding to temperatures of 300-400°C, Epstein et al. (1977). Oliver et al. (in press) have discussed the temperature calibration of the conodont colouration and note that in the Southern Uplands of Scotland, conodonts with CAI.=5 are found in association with spilites at Prehnite-Pumpellyite grade. Schiffman & Liou (1980) regard the maximum temperature at which prehnite and pumpellyite can co-exist to be 350°C at reasonable pressures.

6.2. THE METHODS USED: ILLITE CRYSTALLINITY AND b_0 SPACING.

Initially carbonates from the Durness Formation were collected from localities at Knockan and Glencoul, to test their suitability for calcite/dolomite thermometry. However, those samples tested by staining proved unsuitable, often being completely dolomitised

Illite crystallinity in shales and slates has been used to define the relative degree of diagenesis and metamorphism, Weber (1972), Kisch (1980a, b), and in relation to inverted gradients of low metamorphic grade by Aprahamian & Pairis (1981). These authors have shown that the width at half height of the 10Å illite peak on X-ray diffraction patterns decreases with an increase in metamorphic grade.

Recent work has shown that the b_0- spacing of potassic white micas depends on changes in the geobaric gradient with constant temperature, Sassi (1972), Sassi & Scolari (1974), Fettes et al. (1976), Padan et al. (1982). It was also shown by Sassi & Scolari (1974) that the b_0- spacing decreases with an increase in temperature depending upon the geothermal gradient, and hence can be used as a relative thermometer.

With the lack of any other 'thermal indicators', it was decided to use the above techniques on samples of Fucoid Beds from the An-t-Sron Formation, shale partings, thin shale beds from the quartzites of the Eriboll Formation, and the shale matrix of the 'Torridonian' arkoses.

6.2.1. Illite crystallinity - methodology.

6.2.1.1. Sample collection.

Because of the limited thickness of the Fucoid Beds, along with their somewhat sporadic outcrop, sampling from this horizon is not as systematic as originally hoped. Illite determinations from near to the Moine thrust are not as common as desired, and this reflects the rarity of outcrops of Fucoid Beds near to the Moine thrust. Also near to the Moine thrust the Fucoid Beds are unsuitable for analysis because they are often deeply weathered and in addition show chlorite growth which affects the illite peak, Sassi & Scolari (1974). Samples from immediately beneath the Sole fault were collected at equal intervals along strike from Glencoul to Loch Broom, and a number of samples were collected from the duplex zone at Loch Glencoul to see if there were any thermal effects beneath the Glencoul thrust, fig. 6.1.

Samples from the foreland were taken from two long traverses, and one short traverse. These traverses, see fig.6.1, were:-

(i) Skiag Bridge to Stoer Point.

(ii) Drumrunie to Reiff.

(iii) Loch Achall to Ullapool.

These were undertaken to ascertain if any large scale thermal effects had reached the foreland. The most complete sections are those at Ullapool, and from Drumrunie to Reiff.

On traverses (i) and (ii) samples were collected every 1 km, except where interrupted by exposures of Lewisian basement. On traverse (iii) samples were collected at closer intervals and collection was dictated by the occurrence of suitable lithologies (see fig. 6.2).

Because of the problems of varying provenance of illite and the effects of weathering, a number of samples were taken from each locality, and each sample population consisted of a number of specimens from different beds.

6.2.1.2. Sample preparaion.

The samples were crushed for ten seconds in a tema mill, and the resulting coarse grained powder disaggregated in an ultrasonic bath for fifteen minutes. Using a centrifuge the 2-6 u size fraction was separated and sedimented onto a glass side to dry.

6.2.1.3. Analytical method.

The first basal reflection of illite (001) is recorded five times and the mean of the peak widths at half height (hereafter called Hb, from the German word Halbwertsoreite, Weber (1972)) determined. Because of variation in machines from different laboratories, and possible instrument drift, quartz is used as an external standard with each sample analysis. These peaks of crushed quartz are measured for Hb both before and after each illite sample, and the mean determined. For each illite measurement the relative Hb is calculated.

$$Hb_{rel} = \frac{Hb\ (001)illite\ (mm)}{Hb\ (100)\ Quartz} \times 100$$

The figure is multiplied by 100 to avoid use of decimal points.

Instrument conditions are, Cukα, 36KV, 18MA. Monochrometer, goniometer scan speed 0.5 °/min. 'Chart speed 600 mm/hr, 1° divergence and 0.2° receiving slit, attenuation 2×10^2 to 4×10^2, detector voltage 412 volts.

6.2.1.4. Limitations of Illite crystallinity.

Three major factors will affect the Hbrel values from each locality:-

i) the varying provenance of illite.

ii) weathering, and

iii) rock composition.

These will produce a spread of Hbrel values and should be taken into account before interpretation.

6.2.1.4a. Provenance of Illite.

Illite occurs in sediments and low grade metamorphic rocks in two forms:-

i) as the product of degradation of clastic white micas, in the main muscovite from igneous and metamorphic source rocks. During sedimentary processes diagenesis and low grade metamorphism, the clastic mica reacts with circulating fluids to transform to illite by releasing K^+, and gaining Fe^{2+}, Mg^{2+}, H_2O and OH. Therefore, an inherited Hbrel from the least altered clastic micas may be present, the effect of inherited Hbrel is minimised by only analysing the 2-6 u fraction.

ii) Authigenic illite also grows during diagenesis from the breakdown of feldspars and montmorillonite clay, but there should be no inherited effect from this illite, as it is a direct result of heating.

6.2.1.4b. Effect of weathering.

Weathering of samples causes mixed layer clays to form. These clays e.g. ontmorillonite, have wide peaks which overlap the relatively narrow illite peaks, giving a larger value than unweathered specimens. The degree of weathering in samples is hard to estimate, but this effect is kept to the minimum by collecting only the freshest material available. Any obviously weathered material was discarded.

6.2.1.4c. Rock composition.

Sassi & Scolari (1974) maintain that rock composition can affect illite crystallinity, and therefore rocks of the same composition should be compared. However, the variation due to composition has not been quantified. Unfortunately there is a wide range of rock composition in the samples analysed from the Moine thrust area which may affect the data.

Because of the provenance and weathering effects, the mean value of a number of samples should be used rather than the value from an individual sample.

6.2.2. The b_0 spacing of white micas.

6.2.2.1. Sample collection.

The same samples were used for b_0 spacing analysis as for illite crystallinity.

6.2.2.2. The technique for measuring b_o spacing of Illite.

The sample used for measurement of b_o spacing in illites from the Moine thrust zone were the same as those for the illite crystallinity. A split was taken from the 2-6 μm size fraction used for Hbrel measurements and placed as a powder on a glass slide. The range from 59°2θ to 63°2θ was scanned in order that the quartz (211) peak could be used for internal standardisation of 2θ. The (060) illite peak was used for b_o spacing determination.

6.2.2.3. Limitations of b_o spacing.

There are several factors which should be considered during interpretation of the results.

i) Samples containing (a) high quartz content (b) K-feldspar as an essential component and (c) high chlorite content, should be treated with utmost caution as in all these cases the b_o spacings are abnormally high, Sassi & Scolari (1974).

ii) Carbonate-rich rocks will give a consistently low b_o spacing value, Sassi & Scolari (1974).

The Fucoid Beds contain appreciable amounts of both quartz and carbonate, and sandstone and limestone lenses are common sedimentary features. However, the effects on b_o- spacing due to both quartz and carbonates are minimised as the most shaly fraction of the formation was collected. The Fucoid Beds are also rich in potassium in K-feldspar which would tend to give high b_o spacings.

6.3. ANALYTICAL RESULTS

6.3.1. Illite crystallinity.

A histogram of all the Hbrel values is shown in fig. 6.2a. There is an obvious peak between 140-180 Hbrel, which represents the mean Hbrel. Although the results are spread over a wide range, the majority of results fall between 120-200 Hbrel. The range is likely to be due to compositional factors, i.e. widening of illite peaks by other clay minerals or weathering, and the varying provenance of illite. Therefore, the illite crystallinity is equivalent to temperatures of ~250°- ~300°C at 10 km and represents metamorphism to the transition zone between the Prehnite/Pumpellyite facies and the Upper Zeolite facies, or the middle to higher grade anchizone, Kisch (1980b), Padan et al. (1982).

Figure 6.2b shows the range of Hbrel for each of the localities. Sample populations 1-7 were collected from the foreland and no great change in Hbrel occurs along the strike of the thrust zone when compared with the map, fig. 6.1. The large traverses, Rieff-Drumrunie, Stoer-Inchnadamph, population 7, show a greater range of Hbrel, the significance of which is uncertain, as when the results are plotted on a map, fig. 6.1, and graph of Hbrel value versus depth below the thrust, fig. 6.3, there is no definite trend. This would seem to indicate that the range is either affected by variations due to compositional factors, or a time decrease, or increase in thermal gradient may occur but does not show as a trend because the temperature difference lies in the ±50°C confidence limits that are inherent in the illite crystallinity method. This may be resolved with the collection of more data. But on the data acquired the mean value does not differ significantly from the other foreland populations.

The Hbrel results from beneath the Glencoul thrust sheet show a range which indicates slightly higher temperatures than the foreland populations, but again the results lie within the error limits of the foreland temperatures, hence the rise may be insignificant and only further sampling may be able to pick out any real increase in temperature.

The sample populations from the Stack of Glencoul and within the Ben More thrust sheet were based on few samples and hence should be treated with caution, as their Hbrel may not be significant. However, it should be pointed out that the higher grade indicated by the Stack of Glencoul samples agrees with the lowest Greenschist facies/-Prehnite- Pumpellyite suggested by the metamorphic assemblages in the deformed sills and quartzites. These sills show chlorite-k-feldspar-quartz-muscovite assemblages, with the quartzites having a locally developed cleavage defined by new muscovite.

6.3.1.1. Summary of Illite crystallinity results.

i) All foreland, i.e. sub thrust zone, samples populations cover a similar range of Hbrel values, 123-225, with a mean of 174. This suggests relatively homogenous temperatures of around 250°-275°C, which corresponds to Upper Zeolite facies transition to Prehnite/Pumpellyite facies.

ii) The results show no inverted gradient beneath individual thrusts, or beneath the thrust zone into the foreland.

6.3.2. Analytical results of b_o spacing measurements.

The results are plotted in a histogram, fig. 6.4. The variability of the results is probably a result of the compositional effects discussed above, however, there are major peaks, and a mean value of 9.020 with a sample standard deviation ($\sigma_n - 1$) of 0.02, suggests a relatively low pressure metamorphism.

6.4. DISCUSSION.

6.4.1. Timespan of thrusting.

It is now considered that the Moine thrust has a displacement of at least 80 km, with displacements on the lower thrust sheets such as the Glencoul and Loch Broom thrust sheets variously estimated as 25-30 km, Elliott and Johnson (1980), Coward et al. (1980).

Gravity studies have shown that the Ross of Mull granite rests on an easterly dipping plane, possibly the Moine thrust plane since the granite separates highly deformed Moine metasediments from undeformed Torridon Group, Beckinsale & Obradovitch (1973). This granite has caused contact metamorphism both in the Torridon Group on Iona, and the Moine metasediments on Mull. Beckinsale & Obradovitch (op cit) obtained K-Ar dates of 423^{+4} Ma for biotite and 416 ± 4 Ma for hornblende, but more recently the intrusion has been dated as 414 ± 4 Ma using an Rb-Sr mineral isochron, Pankhurst (1982). The slightly older K-Ar dates may be due to excess argon. Therefore movement on the Moine thrust on Mull must have ceased prior to 414 ± 4 Ma.

Any diachroneity in the cessation of movement on the Moine thrust (i.e if the northern Moine thrust moved later than the southern Moine thrust) can be discounted, as any such movement would cause large strike slip shear zones and faults to develop in the Moine metasediments. These are not seen, Kelley (pers comm 1983).

Recent work by Kelley (in prep. 1983) along a traverse from the Fannich mountains in the inner part of the orogen to the Moine thrust at Ullapool, has shown that the whole of the Moine rocks along the traverse were uplifted virtually at the same time. Muscovites gave a mean K-Ar age of 425 ± 7 Ma, and co-existing biotites gave a mean age of 423 ± 5 Ma. Furthermore, there was no difference in ages in muscovites and biotites between those rocks which were strongly mylonitised and those which were unaffected by the mylonitisation, and this is taken to indicate that argon retention in the micas started during or immediately after the mylonitisation. Recent research has shown that the transition from ductile to brittle deformation in fault zones is a

continuous process, Stel (1981), White et al. (1982), and the amount of time involved in the process of transition is probably less than the error margins of the dating. The conclusion that these dates lead to is that cooling through the blocking temperatures of both micas was consequent on movement along the Moine and sub-Moine thrusts causing the Moines to cool simultaneously, Kelley (in prep). This conclusion is contrary to Dewey & Pankhurst (1970) who suggested that the Moine metasediments close to the Moine thrust cooled earlier than the central zone.

Parsons & McKirdy (1983) have shown that the Loch Borrolan intrusion post dates the Ben More thrust which, therefore, had ceased to be active prior to 430±4 Ma, the age of the intrusion obtained by van Breemen et al. (1979). If the concept of piggy-back thrusting is rigidly applied, then the Moine thrust must also have ceased to be active at 430 Ma. However, Parsons (1979), has shown that the Moine thrust has deformed the intrusions and thus disobeys the 'piggy-back' rules of thrusting and moved later than the Ben More thrust. Evidence of late movement by the Moine thrust is seen at Knockan, Coward 1983, Winter (in prep) and Ullapool, Winter (in prep), see 2.2.1. where the late movement on the Moine thrust truncates structures which had originally deformed it. This does not rule out any movement on the Moine thrust prior to 430 Ma, indeed, the Moine thrust has been folded by the emplacement of the lower thrust sheets and hence obeys the piggy-back rule. This means that there was movement on the Moine thrust prior to 430 Ma. Only the later movement post-dates the lower thrust structures. This concept of the largest thrust moving for the longest time has been applied to the Canadian Rockies, Jones (1972).

The late extensional movement on the Moine thrust truncates extension structures which are associated with movement on the Sole fault. The main movement and uplift on the Glencoul, Loch Broom and Moine thrusts occurred at around 425 Ma. Evidence at Ullapool shows that the extension faults displace the Loch Broom thrust, and therefore the extensional movement on the Moine thrust is post 425 Ma, but pre-414 Ma, the age of the Ross of Mull granite.

It is proposed the there were three stages of movement in the Moine thrust zone;

i). Pre-430 Ma but post the peak Caledonian metamorphism only occurs on the Moine thrust. This stage of movement was followed by the intrusion of the Assynt Alkaline intrusions.

ii) At 425 Ma, with movement on the Glencoul, Loch Broom and Moine thrusts.

iii) Post 425 but pre-414 Ma movement on the late extensional Moine thrust.

6.4.2. Temperatures of the base of the Moine thrust sheet during thrusting.

A knowledge of the temperature at the base of the Moine thrust sheet is necessary in order to interpret the metamorphism in the underlying thrust sheets and foreland. Blocking temperatures of micas are the best evidence available, although it must be kept in mind that there is some controversy as to whether the blocking temperature concept is valid, as recent work has shown that isotopic systems can be opened chemically, Chopin & Maluski (1981). However, there are some good estimates of blocking temperatures for simple cooling situations, Harrison & McDougall(1980) give an estimate for biotite of $280\pm40^{\circ}C_{\lambda}^{(K-Ar)}$, whilst Purdy & Jäger (1976) give the best estimate for muscovite at $350\pm50^{\circ}C_{\lambda}^{(K-Ar)}$. Therefore the temperature at the base of the Moine thrust sheet at 425±7 Ma was around 350°C. This is substantiated by the fact that mylonitisation commenced at biotite grade and retrogressed to chlorite grade during thrusting, Kelley & Powell (in press).

6.4.3. The age of the Illite event.

If the foreland metamorphism is a product of tectonic loading then both a Grampian age of Ca 500 Ma, Lambert & McKerrow (1976) and peak Caledonian age of ca 450-460 Ma for the metamorphism can be ruled out. There are no Caledonian structures seen in the foreland nor in the sub-Moine thrust sheets apart from thrusting and thrust related folding; as the mylonitisation and thrusting post-date the peak Caledonian metamorphism and deformation, Kelley & Powell (in press) the illite event must also post date the peak Caledonian metamorphism.

6.4.4. Interpretation of the results and the tectonic implications

Shear heating as a cause for the metamorphism can be ruled out. Using the charts of Brewer (1981) fig. 6.5, it is clear that for a thrust sheet 10 km thick displacement would have to be large, with a fast displacement rate, a high coefficient of friction for the rocks involved and a high shear stress. The Moine thrust, although it has a large displacement, had a foreland thrust type displacement rate of <1 cm/yr, Elliott(1976a), and with sliding on a cataclasite fault rock the coefficient of friction would be low. Hence any frictional heat which did build up would be small leaving little or no thermal effect such as an inverted metamorphic gradient.

The best way to interpret the illite event takes into account the effect of thrusting on an existing geothermal gradient, and follows the model of Oxburgh & Turcotte (1974). The model assumes that prior to the emplacement of the thrust sheet the temperature at the top of the overidden sequence was 0°C, see fig. 6.6a. With emplacement of the 10 km thrust sheet, the thermal gradient develops a sawtooth gradient, fig. 6.6b. The moment the thrust sheet is emplaced, the temperature at the interface between the thrust sheet and the footwall is 0.5T, where T is the temperature at the base of the thrust sheet prior to emplacement. For the movement on the Moine thrust at about 425 Ma T = 350°C, this results in a massive heat flux downwards into the footwall with consequent rapid heating of the footwall, and a simultaneous decrease in the temperature within the thrust sheet, fig. 6.7a, b, so that for the 10 km thick thrust sheet with a geothermal gradient of

35°C/km, the temperature at the interface was 175°C, fig. 6.6a, b. Figure 6.8 taken from Oxburgh & Turcotte (1974) shows the change in temperature at the interface through time. It is clear that the thinner the thrust sheet, the faster the thermal gradient equilibrates. For a 10 km sheet, from fig. 6.8 the footwall temperature would have increased to 0.7T after about 10 Ma, and 0.8T after approximately 24 Ma, hence it would have taken the footwall approximately 24 Ma to heat up to the 275° indicated by the illite crystallinity. At 275° the heating of the footwall ceased, indicating that cooling had begun; this presumably being caused by erosion of the overlying thrust sheet. Keeping the same geothermal gradient of 35°C/km, then the erosion needed amounts to approximately 2 km. From the mica dates and the date of the Loch Borrolan intrusion, discussed earlier, the emplacement of the thrust sheets on the Moine, Glencoul, and Loch Broom thrusts occurred at ca 425 Ma, hence the temperature of 275° in the footwall would have been reached at ca 401 Ma. This indicates that the metamorphism post dates the Loch Borrolan intrusion.

It is now known that the Borrolan intrusion post dates movement on the Ben More thrust, Parsons & McKirdy (1983), but the relationship between the intrusion and the Glencoul thrust is unclear. Displacement between the Glencoul thrust sheet and the Ben More thrust sheet is small, suggesting that there was little temporal gap between their movements. Elliott & Johnson (1980), however, noticed that the Breabag dome, which folds the Ben More thrust and which they considered to be part of the Glencoul thrust sheet plunges beneath the Borrolan intrusion and appears to fold it, hence the intrusion would pre-date movement on the Glencoul thrust. Assuming that the illite event in foreland is the same age beneath the Assynt culmination and at Ullapool, then the Glencoul thrust must have been active at ca 425 Ma, the same time as movement on the Moine thrust at Knockan and the Loch Broom thrust at Ullapool.

The Oxburgh & Turcotte (1974) model can be loosely applied to the Moine thrust at the top of the Glencoul and Ben More thrust sheets, this part of the thrust was active during stage 1. The quartzites of the Eriboll Formation which comprise the footwall are deformed by crystal plastic processes, hence temperatures must have been at least between 300-350°C, Weathers et al. (1979). The Moine mylonites of the hangingwall post date the peak Caledonian metamorphism at 450-460 Ma, Kelley & Powell (in press), but the mylonitisation initiated at biotite grade and retrogressed to chlorite grade during the thrusting, Kelley (pers. comm. 1982). Weathers et al. (1979) assume a 500°C temperature during the formation of the Moine mylonites, although this has not been confirmed by metamorphic studies. Using this temperature and a geothermal gradient of 35°C/km which gives the Moine thrust sheet a thickness of 15km, figure 6.9 shows that it would take the footwall 20Ma to heat up to 350°C or 0.7T. This would mean that the first stage of thrusting is rather close to the 450 Ma metamorphism. Given the vagueness of the thermal data from the Moine mylonites it is best to suggest that movement had started on the Moine thrust between 440-430 Ma, as time must be allowed for the Glencoul thrust sheet to heat up to at least 300°C.

Table 6.1 tabulates the thrusting chronology as implied by the cooling histories, and this chronology is diagrammatically illustrated in fig. 6.10.

The constraints placed on the dating of thrust movements by the cooling histories emphasises a pattern of short periods of thrust activity separated by longer periods of thrust inactivity. When the footwall was heating up movement may have recommenced due to the rise of fluid pressures in the sediments by aquathermal pressuring, Barker (1972) and which facilitated further movement. In the basement gneisses of the Glencoul sheet initial failure may have been represented by microcracking caused by heating and loading, allowing water to infiltrate. With failure and strain softening a ductile shear zone may have developed which with continued deformation narrowed to a single thrust plane, Armstrong & Dick (1974), Bartley (1982). During the longer periods of thrust inactivity deformation would have been by tectonic loading, see 4.2.1. A similar pattern of thrust activity and inactivity was suggested by Gretener (1981) in a theoretical study.

DATE	ASSYNT	ULLAPOOL
Pre 430 but post 450	Emplacement of 15 km thick Moine thrust sheet 500°C at base. Weathers et al (1979)	Moine thrust sheet emplaced, but evidence removed by late movements on the Moine Thrust
Ca 430 ma	Movement on Ben More thrust, and then intrusion of Loch Borrolan Syenite, 430±4 ma. Parsons & McKirdy (1983, van Breeman et al (1979).	
Ca 425 ma	Temperature reaches 350°C in Glencoul sheet, due to temperature equilibration after emplacement of Moine Sheet. Glencoul thrust moves Influx of heat down into foreland. Sole fault initiates and moves	Uplift of Moines on Moine thrust/Loch Broom thrust combination, 425±7 ma date in Muscovites corresponds to T of 350°C at base of Moine thrust sheet Kelley (in prep). Influx of heat down into foreland. Sole fault initiates and moves.
Post 425 but pre 414	Late movement on the Moine Thrust and surge zones of Coward (1982).	Late extensional movement on the Moine thrust
Ca 400 ma	Illite metamorphism temperatures reach 275°. Erosion reaches critical depth to start cooling of foreland 2 km removed.	Illite metamorphism temperatures reach 275. 2 km of erosion reaches critical depth to induce cooling.

Table 6.1 Table of relationship between age, structural history and thermal events.

Given that the periods of thrusting are temporally separated by 10-20 Ma, then the late extensional movement of the Moine thrust may follow this pattern and hence have been active ca 415Ma. Coward (1983) advocated that late movements on the Moine thrust were a result of gravity spreading caused by the major granitoid intrusions in the central Caledonides. These intrusions are dated 430-410, Brown (1979), Halliday et al. (1979) and are considered to be crustal additions, Brown (1979), and hence may have 'displaced' the crust laterally causing gravity spreading and thinning of the Moine thrust sheet, Smith (1981).

6.5. CONCLUSIONS

A widespread heating event has been recognized in the foreland of the Moine thrust zone. This has been interpreted as a partial re-equilibration of a thermal gradient perturbed by the emplacement of the thrust sheets. Temperatures in the foreland reached 275°C approximately 24 Ma after thrust sheet emplacement. Study of the cooling histories of the Glencoul thrust sheet and foreland, in relation to dating of igneous intrusions and the uplift of the Moine metasediments has established a chronology of thrusting. It can be inferred that movement on the Moine thrust occurred in relatively short periods separated by periods of 10-20 Ma, when movement was little or the thrusts were inactive. These periods of movement occurred at the estimated dates of ca 440 Ma, 425 Ma and 415 Ma. During the long periods of inactivity heating of the footwall by thermal conduction caused pore fluid pressures to rise by aquathermal pressuring hence facilitating further movement on the thrusts.

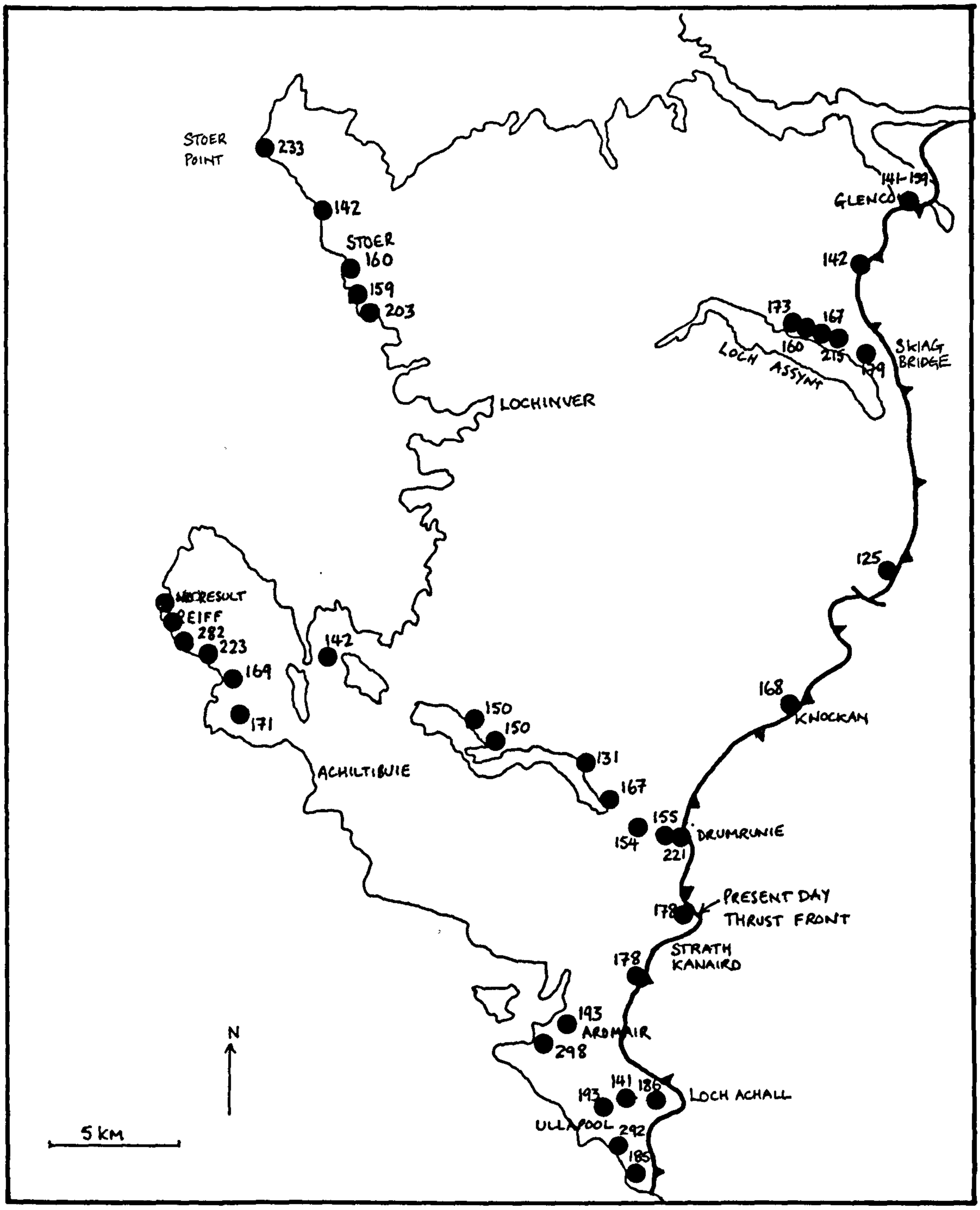

Fig. 6.1 Map to show sample localities with corresponding Hbrel values. Note that there is no real trend of values, and that low values of Hbrel occur at Stoer as well as near to the thrust.

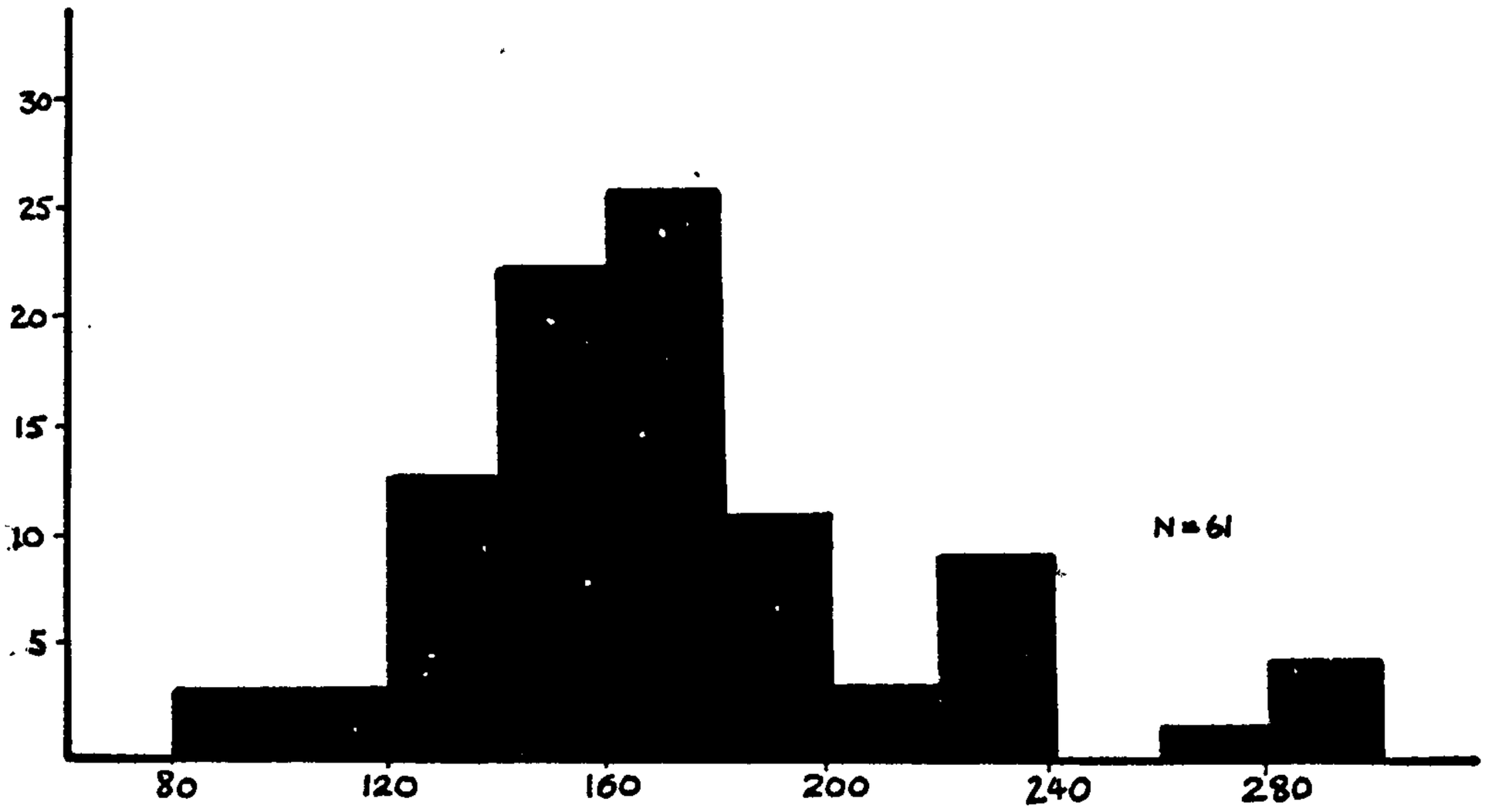

Fig. 6.2a A histogram of all Hbrel values, showing an obvious peak in the Hbrel range 140-180.

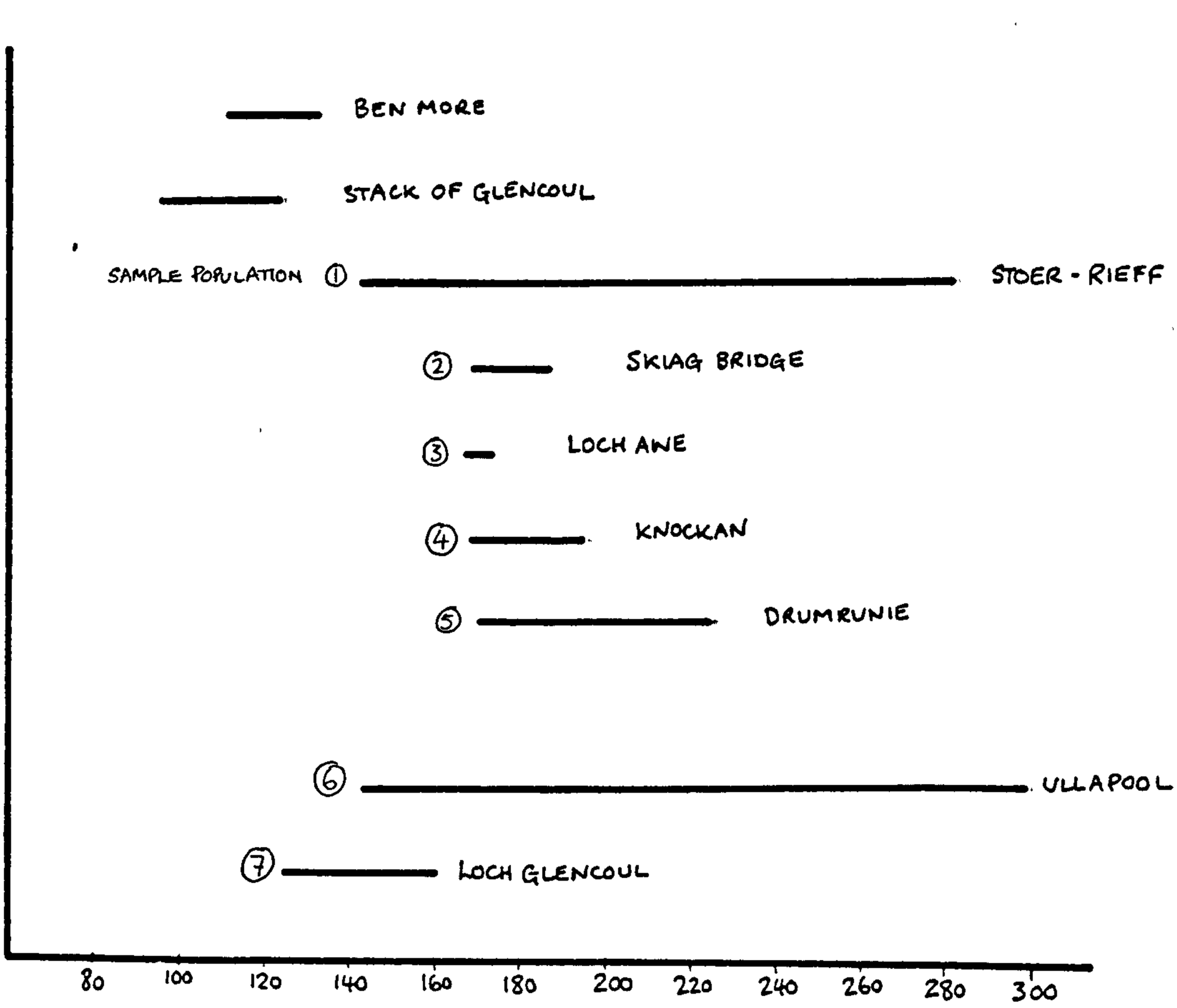

Fig. 6.2b Graph diagram to show range of Hbrel values for each sample population.

Fig. 6.3 Graph of Hbrel value against vertical distance below the thrust zone. Note the spread of values especially of the Stoer population. No marked thermal gradient is seen, however the wide spread may hide any gradient.

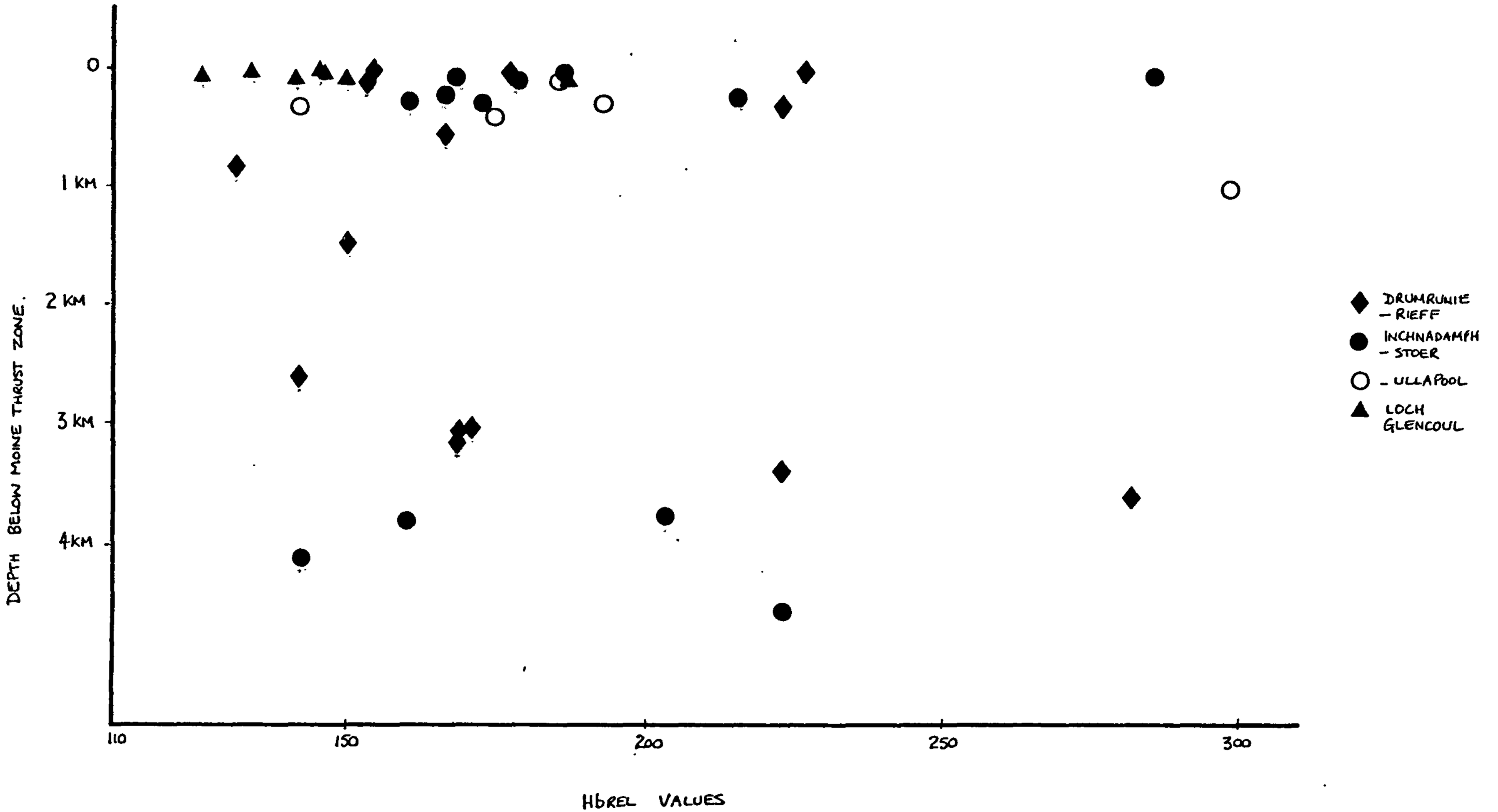
0
1 KM
2 KM
3 KM
4KM
DEPTH BELOW MOINE THRUST ZONE.
110
150
200
250
300
HbREL VALUES
DRUMRUNIE – RIEFF
INCHNADAMPH – STOER
– ULLAPOOL
LOCH GLENCOUL

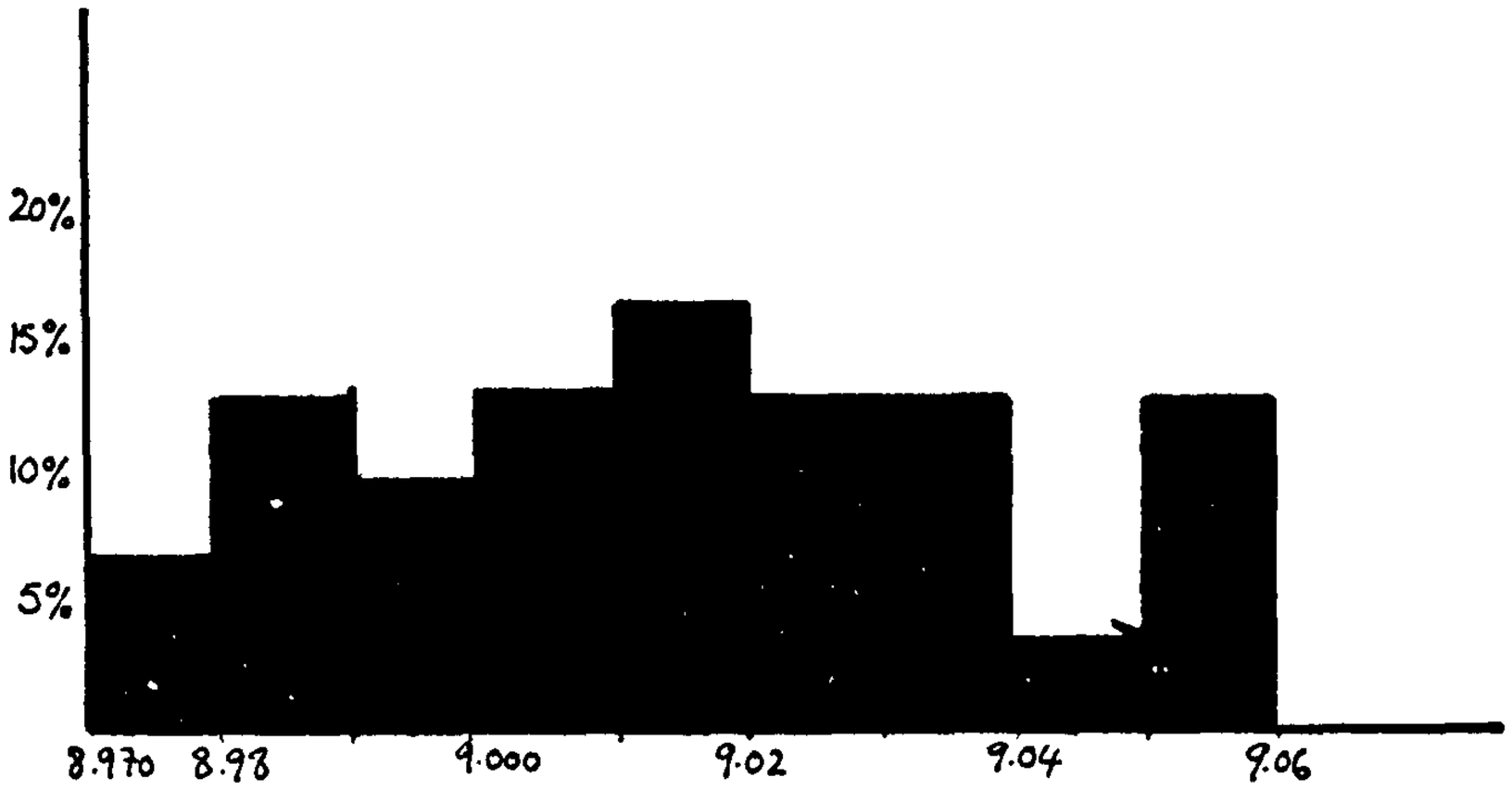

Fig. 6.4 A histogram of all b_o- spacing indexes. Note the widespread of values which is probably due to compositional effects, see text.

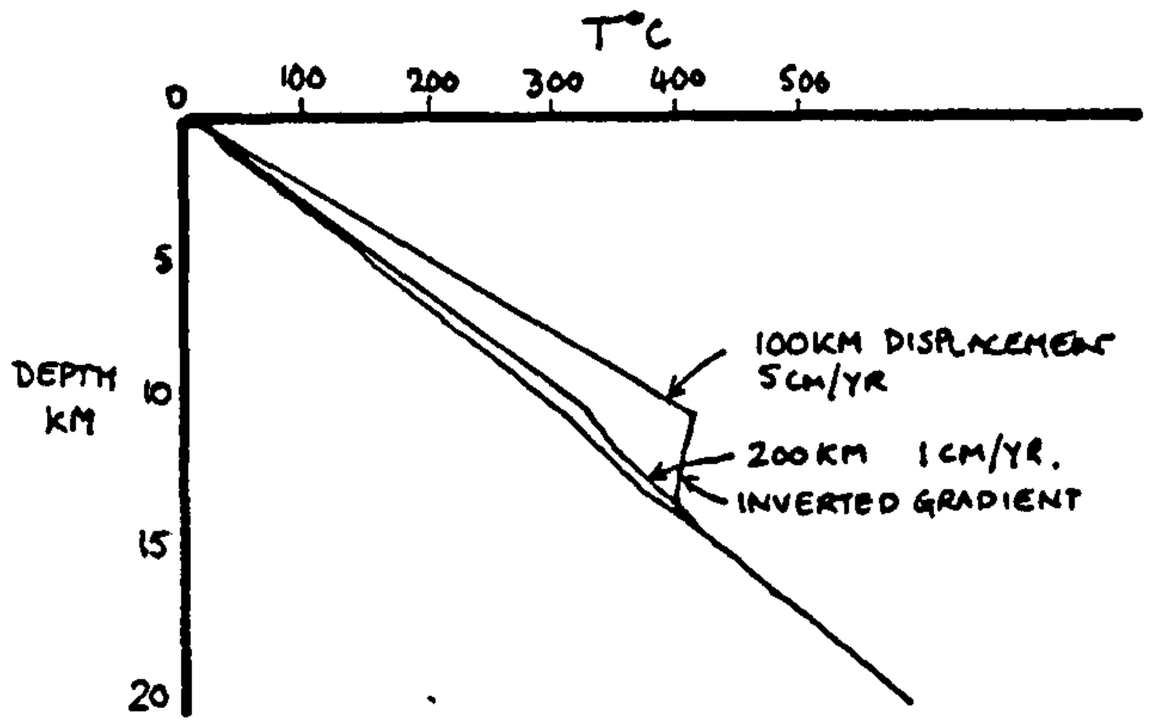

Fig. 6.5 Profiles of maximum temperatures developed by overthrusting 10 km thick thrust sheet for various parameter values. From Brewer (1981).

Fig. 6.6a Diagram to show simple thrust sheet emplacement model and configuration of thermal gradients before and immediately after thrusting.

Figure 6.6b. Sawtooth thermal gradient and relaxation thermal gradients produced after thrusting for a 10km thick thrust sheet. The relaxation profiles are obtained by referring to the thrust sheet/footwall interface temperatures in fig.6.8.

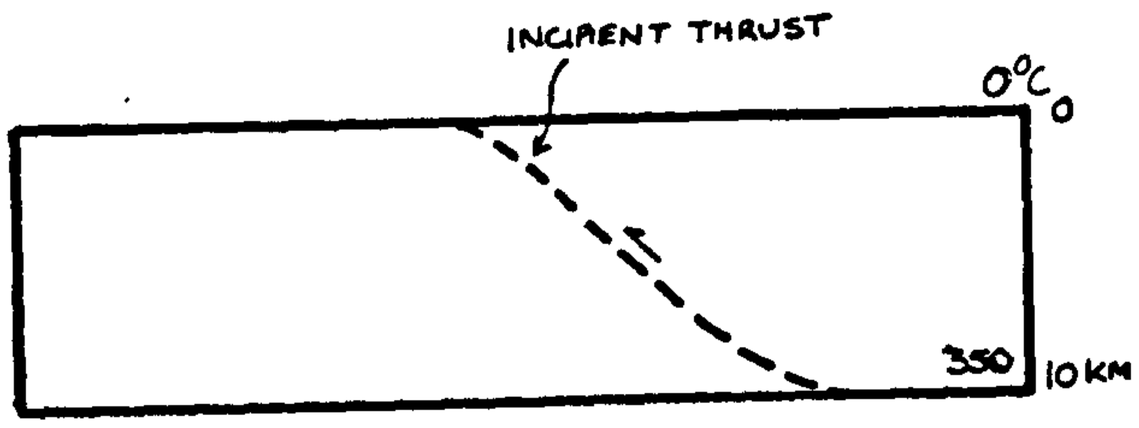

PRE - THRUSTING

FIG. 6. 6a.

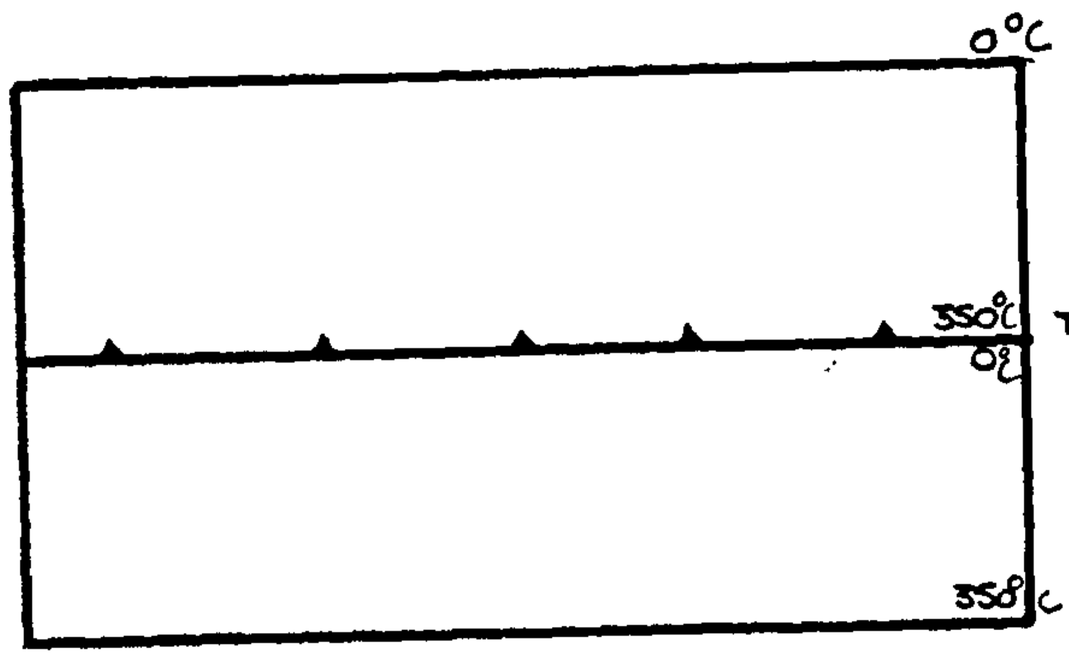

POST - THRUSTING.

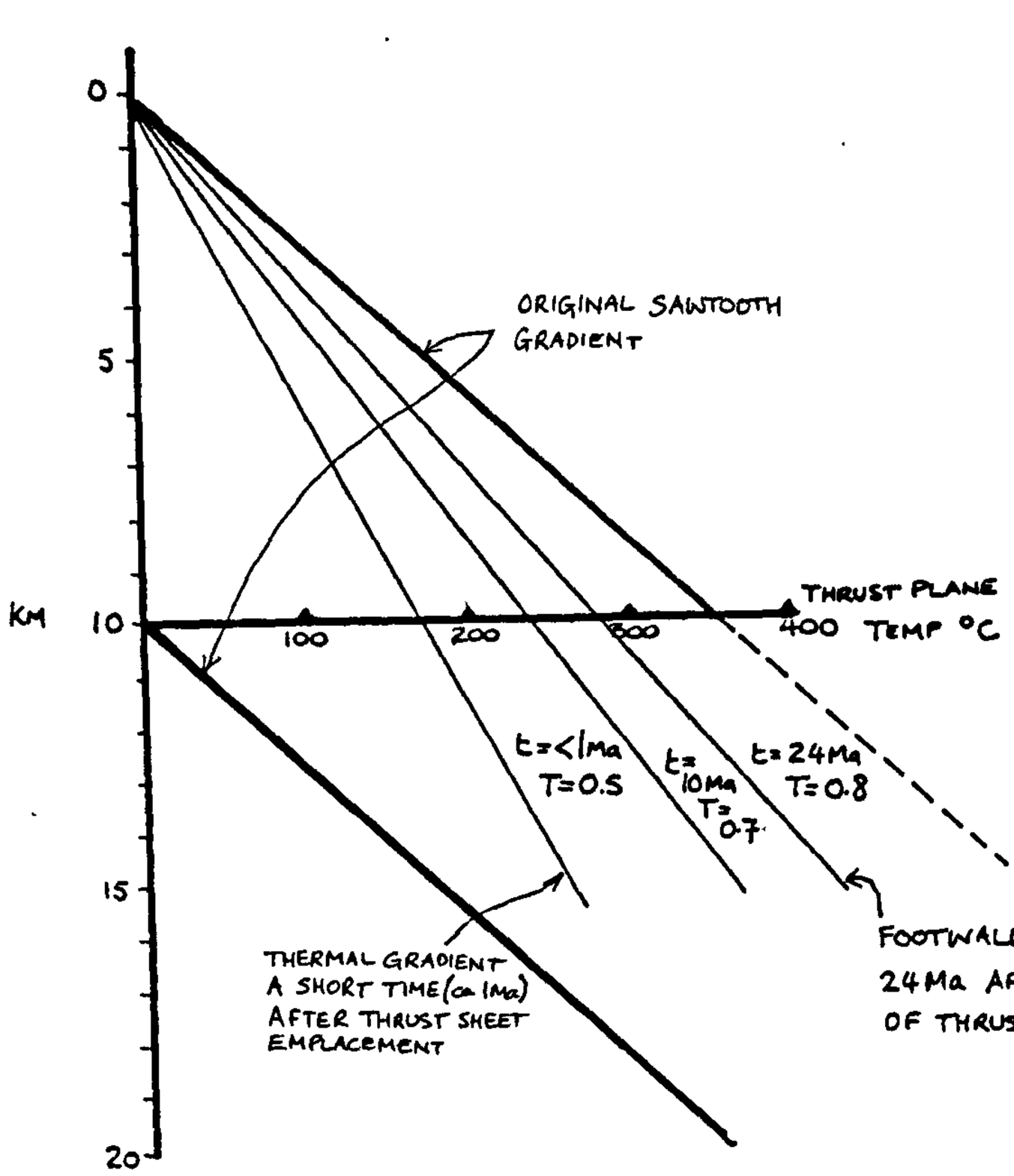

FIG. 6. 6b

Fig. 6.7a Graph to show change in temperature with time and depth with a thick thrust sheet. The initial rapid heat loss is clearly shown. Although illustrated for a 15 km thrust sheet, a 10 km thrust sheet will have similar profiles, from Oxburgh & Turcotte (1974).

Fig. 6.7b Graph to show temperature as a function of depth and time in the footwall of a thrust sheet 15 km thick. The initial heat flux into the footwall is obvious, from Oxburgh & Turcotte.(1974)

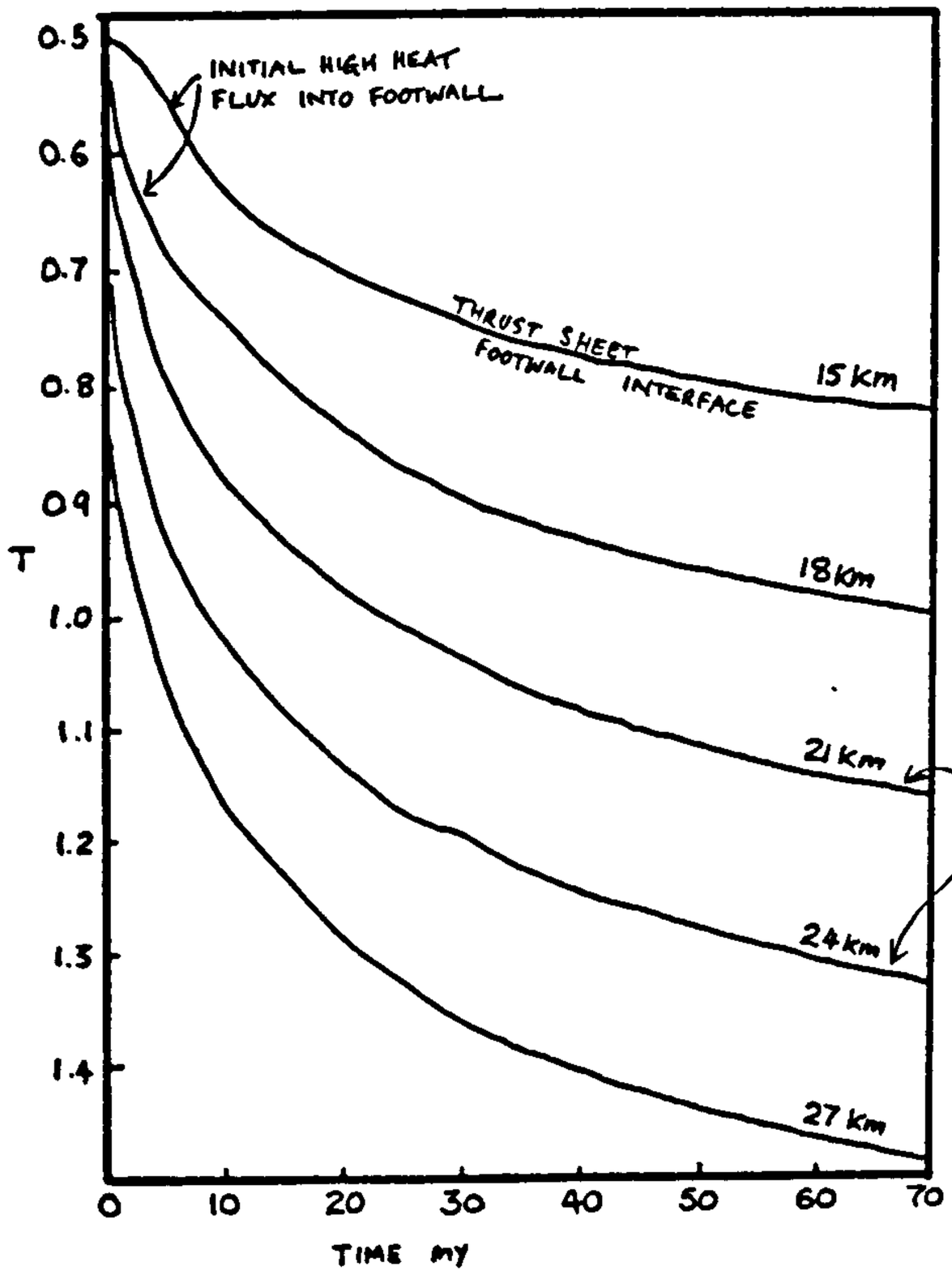

FIG. 6.7 b.

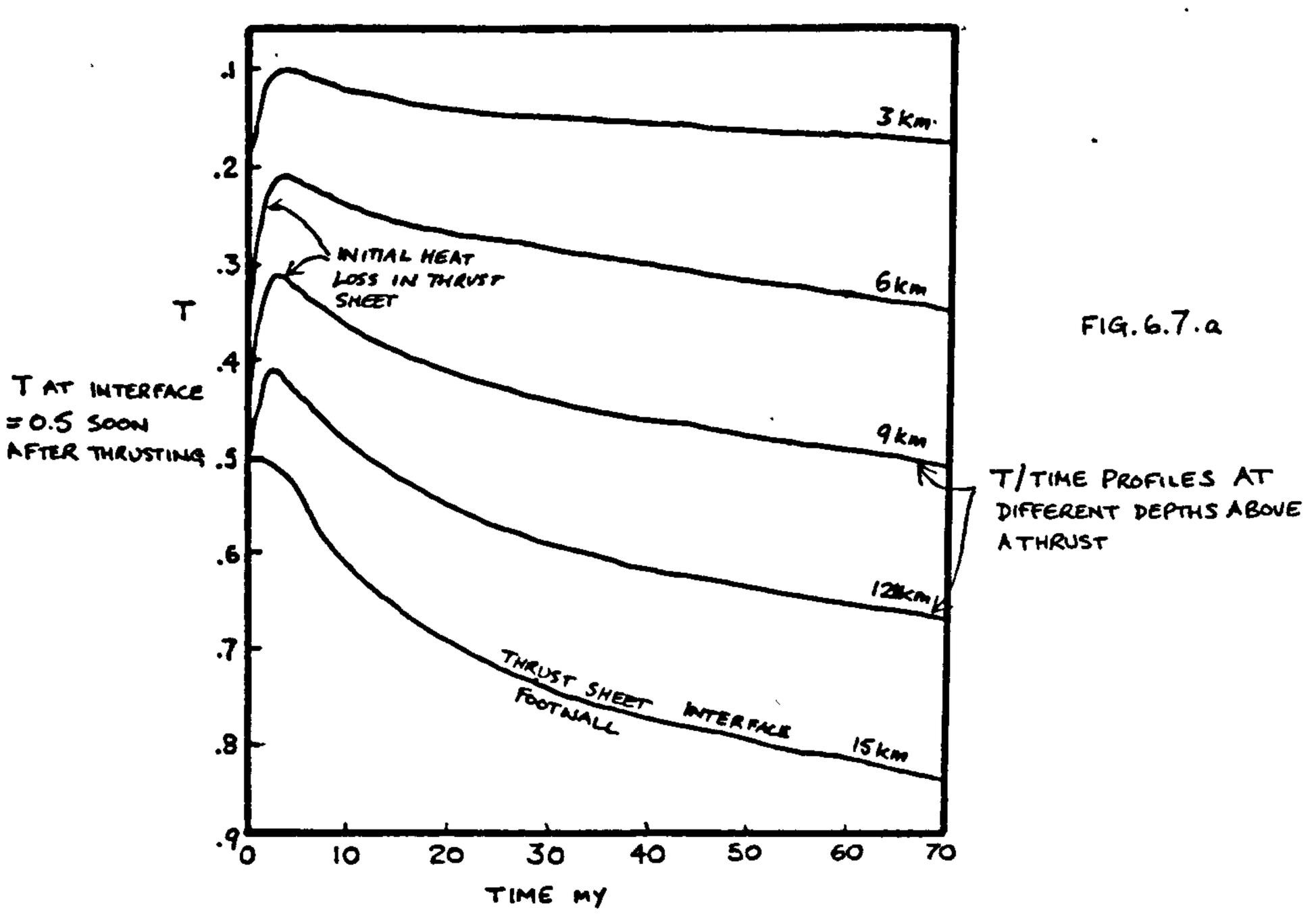

FIG. 6.7.a

T = 1.0 TOTAL TEMPERATURE AT BASE OF THRUST SHEET PRIOR TO THRUSTING.

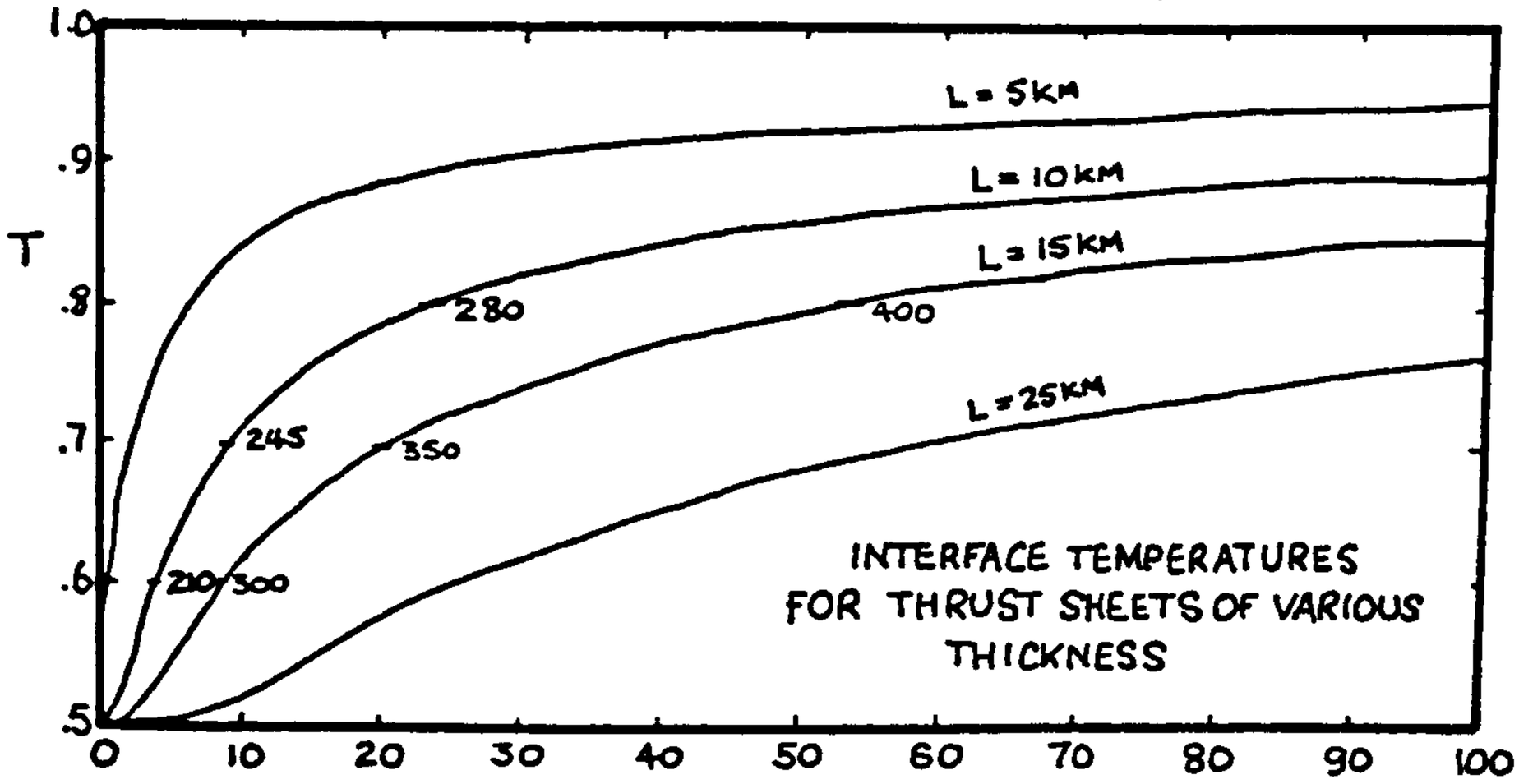

Fig. 6.8 Temperature as a function of time on the interface between the thrust sheet and the footwall. The temperatures on the 10 km thick thrust sheet profile are for the foreland metamorphism at the thrust, and the temperatures, for a 15 km thick thrust sheet, in the rocks beneath the Moine thrust at the Stack of Glencoul. See text for discussion.

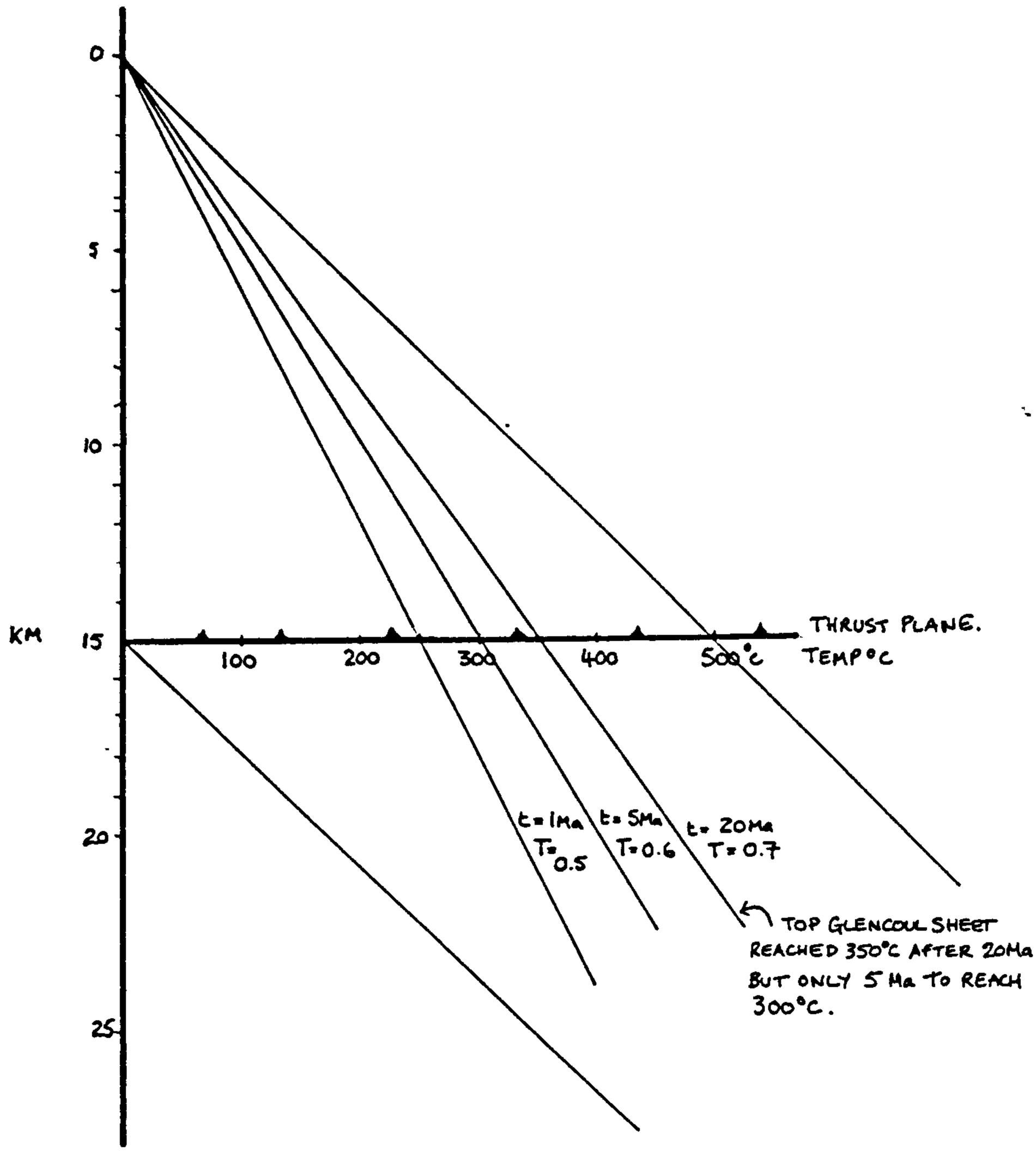

Fig. 6.9 Sawtooth thermal profile for the 15 km thick Moine thrust sheet on top of the incipient Glencoul thrust sheet. Relaxation profiles are added with time taken for that set of re-equilibration taken from Fig. 6.10.

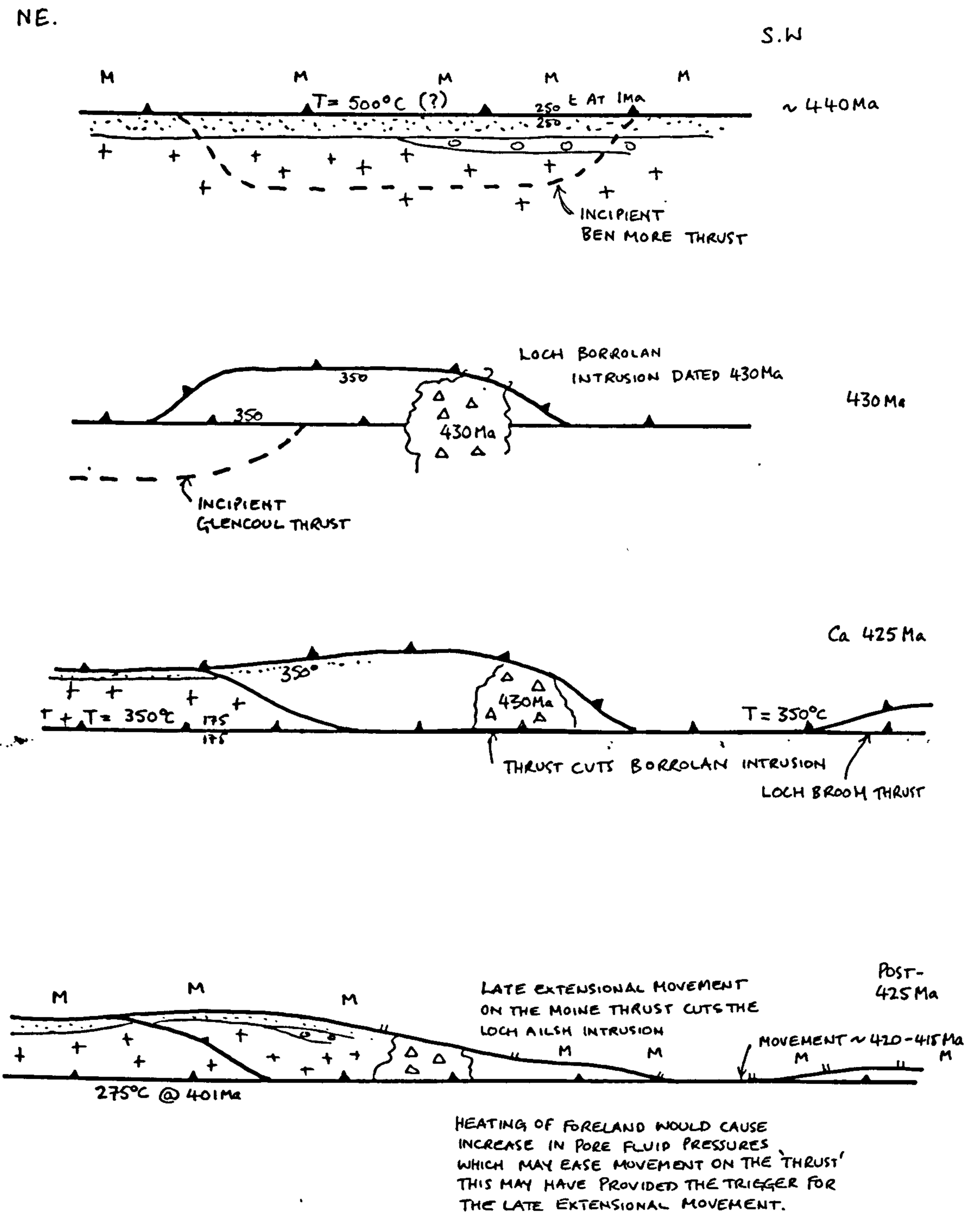

Fig. 6.10 Schematic diagram to show the relationship between the structural evolution of the thrust belt with the thermal events and their possible age relationships.

CHAPTER 7. CONCLUSIONS

1) Following recent studies in the Moine thrust zone, Elliott & Johnson (1980), Coward (1980, 1983), the geometry of the thrust sheets show that the thrusts propagated from E-W, i.e. from the hinterland towards the foreland with the older and higher thrusts deformed by structures formed by movement on the lower thrusts. Thus the Moine thrust was emplaced first, and subsequent movement on the Loch Broom thrust folded the Moine thrust into a broad culmination between Langwell and Loch Broom. Development of the Ullapool thrust sheet folded both the Loch Broom and Moine thrust sheets. However, new evidence from the geometrical relationships of the Moine thrust with the Loch Broom thrust sheet and with Sheet IV indicate that the Moine thrust was re-activated and cut through the structures which originally deformed it. This new evidence shows that the reactivation of the Moine thrust is more extensive than the localised occurrences described by Coward (1982, 1983) at Knockan and the Stack of Glencoul. The reactivation movement on the Moine thrust has an extensional geometry and 'disobeys' thrust rules by cutting down section in the direction of transport. This indicates that the driving mechanism behind these later extensional movements is gravitational, most likely gravity spreading, rather than a compressional push; thus supporting the thin skinned interpretation of the Moine thrust zone, Elliott & Johnson (1980), Coward (1980, 1983).

2) The fault rock products of the thrust planes are predominantly cataclasites with occasional ultracataclasites and microbreccias. These indicate deformation in the elastico-frictional regime of Sibson (1977) as all the fault rocks show brittle deformation. The cataclasites show a cyclicity of formation similar to that advocated by Sibson et al. (1975). Firstly as shear stress rises pre-failure dilatancy occurs causing a drop in the ambient fluid pressure as fluid flows into the fractures. With continuing stress rise the pore fluid pressure rises reducing the strength of the fault zone such that at a critical stress level, failure occurs. This causes a collapse of the dilatant zone. Post-failure deformation in the fault rock is compaction due to loading by the overlying thrust sheet, causing a rise in fluid pressures, hydraulic failure and the formation of tectonic veins. These veins then become incorporated into the cataclasite as

clasts during the next cataclasis cycle. The fault rock fabrics indicate that the thrusts moved in an episodic manner with short periods of movement followed by longer periods of inactivity when the deformation occurred by loading. Analogies with present day fault zones suggest that the pre-failure dilatancy followed by cataclasis may indicate an earthquake event, Sibson et al. (1975), Sibson (1977). The periods of dilatancy are shorter than the periods of post failure loading, Sibson et al. (1975). Further, during the loading deformation the fault zone would be relatively impermeable and during the pre-failure dilatancy porous and permeable. This could explain why fault zones can act as restrictions to fluid flow whilst they can also appear to have acted as fluid conduits.

3) Footwall horses are an important structural component of the studied portion of the Moine thrust zone and are formed at ramps and asperities in order to reduce friction. From observations of their geometry they can be classified as;

i) ramp related horses; these are foreland dipping and right way up if the ramp cut unfolded rocks, or hindward dipping and inverted if the horse originated from a ramp which cut through the steep limb of a fold. The horses produced from ramps will always be stratigraphically older or the same age as the footwall.

ii) asperity derived horses; these horses are hindward-dipping and right way up and may incorporate rocks which are stratigraphically younger than the footwall.

iii) horses from anastomosing thrust zones; these horses exhibit strong internal deformation which may destroy the original bedding. The age of the horses in anastomosing thrusts youngs towards the thrust.

4) In several localities along the thrust zone, Sheet IV occurs as ramp bounded horses of the Durness Formation floored by the Sole fault. These horses cause small culminations to develop where the thrusts ramp over them. Sheet IV exhibits remarkable normal faulting, hydraulic fracturing, tectonic veining and intense stylolite development. These structures are considered to have formed as a result of tectonic loading by the overlying thrust sheets. A semi-quantitative model shows how high pore fluid pressures are necessary to produce extension in a NE-SW direction. An important development of this model shows that differential stress can be estimated from natural structures given a knowledge of tensile strength of common rocks. When applied to Sheet IV the estimates agree closely with estimates from established methods. The estimated differential stress during the extension faulting was approximately 500 bar. However, estimates of differential stress from dolomite twins in the groundmass of the dolomites were approximately 1300 bar. This figure is interpreted as being a result of an early compression event during thrust initiation and propagation; thus the thrusting process can be divided into two stages. These are;

i) thrust initiation and propagation during which differential stresses were high, reflecting perhaps the amount of energy required to 'get things moving'.

ii) a translation stage where the predominant deformation in the footwall is tectonic loading under a low differential stress regime.

5) By using the illite crystallinity index measured from shales in the Fucoid Beds, Eriboll Formation and the 'Torridonian' rocks, it is shown that the foreland has suffered metamorphism with temperatures reaching around 275°C. This metamorphism is considered to be a result of the thermal effects produced by thrust sheet emplacement. Kelley and Powell (in press) show that the main uplift on the Moine thrust occurred at approximately 425 Ma, and the temperature at the base of the Moine thrust sheet was around 350°C. Using the simple cooling model of Oxburgh & Turcotte (1974) it can be shown that the temp-

erature reached 275°C at ca 400 Ma and that erosion had reached the critical depth to start cooling. These data show that some movement on the Moine thrust post dates the Assynt Alkaline intrusions dated at ca 430 Ma, van Breemen et al. (1979). However, the intrusions cut across the Ben More thrust, Parsons & McKirdy (1983), which indicates that there is also a pre 430 Ma component on movement on the Moine thrust, as the emplacement of the Ben More thrust has deformed it, i.e. piggy back thrusting. The later extensional movement on the Moine thrust post dates movement on the Sole fault, as the later Moine 'thrust' cross cuts the structures associated with the Sole fault. Therefore the later extensional movement on the Moine thrust must post date 425 Ma as the Sole fault-related structures deform the thrusts which carried the movement at 425 Ma. However, the extensional movement must be pre 414 Ma which is the age of the Ross of Mull granite. In conclusion there were three stages of movement on the Moine thrust-

i) Pre-430 but post-450 Ma; the Moine thrust first emplaced, the remnants of this movement only seen now along the Moine thrust proper above the Assynt culmination.

ii) ca 425; movement on the Glencoul thrust, the Moine thrust and the Loch Broom thrust. This represents the main uplift phase according to cooling history in the Moines, Kelly & Powell (in press).

iii) post-425 but-pre 414; late extensional movement on the Moine thrust cuts through structures which deform both the Loch Broom thrust and the original Moine thrust.

REFERENCES

ALVAREZ, W., ENGELDER, T. & LOWRIE, W. 1976. Formation of spaced cleavage and folds in brittle limestone by dissolution. Geology, 4, 698.-701

ANGELIER, J. & COLLETTA, B. 1983. Tension fractures and extensional tectonics. Nature, 301, 49-51.

ANDERSON, E.M. 1951. The Dynamics of Faulting. Oliver & Boyd, Edinburgh 2nd ed.

APRAHAMIAN, J. & PAIRIS, J-L. 1981. Very low grade metamorphism with a reverse gradient induced by an overthrust in Haute-Savoie (France: In McCLAY, K.P. & PRICE, N.J. Thrust and Nappe tectonics. Spec. Publ. Geol. Soc. Lond. 9, 159-166.

ARMSTRONG, R.L. & DICK, H.J.B. 1974. A model for the development of thin overthrust sheets of crystalline rock. Geology. 2 25-40.

ATKINSON, B.I. 1982. Subcritical crack propagation in rocks: Theory, experimental results and applications. J. Struct. Geol. 4, 41-56.

AYDIN, A. & JOHNSON, A.M. 1978. Development of faults as zones of deformation bands and as slip surface in sandstone. Pure. Appl. Geophys. 116, 931-942.

BAILEY, E.B. 1935. The Glencoul Nappe and the Assynt Culmination. Geol. Mag. 72, 151.-165

BAIRD, A.W. 1982. The Sgurr Beag Slide within Moine rocks at Loch Eilt, Inverness-shire. Jl. Geol. Soc. Lond. 139, 647-653.

BALLY, A.W., GORDY, P.L. & STEWART, G.A. 1966. Structure, seismic data and orogenic evolution of the southern Canadian Rocky Mountains. Bull. Can. Pet. Geol. 14, 337.-391

BALLY, A.W., BERNOULLI, D., DAVIS, G.A.,& MONTADERT, L. 1981. Listric normal faults. Oceanol. Acta. Proc. 26th Int. Geol. Cong. Geology of Continental Margins Symposium, Paris, 87-101.

BARBER, A.J. & MAY, F. 1976. The history of the western Lewisian in the Glenelg inlier, Lochalsh, northern Highlands. Scott. J. Geol. 12 35-50.

BARKER, C. 1972. Aquathermal pressuring - Role of temperature in the development of abnormal pressure zones. Bull. Am. Assoc. Pet. Geol. 56, 2068.-2071

BARTLEY, J.M. 1982. Limited basement involvement in Caledonian deformation, Hinnoy, North Norway and its tectonic implications. Tectonophysics, 83, 185-203.

BARTON, C.M. 1978. An Appalachian view of the Moine thrust. Scott. J. Geol. 14, 247.-257

BARTON, C.M. & ENGLAND, P.C. 1979. Shear heating at the Olympos (Greece) thrust and the deformation properties of carbonates at geological strain rates. Geol. Soc. Am. Bull. 90 483-492.

BEACH, A. 1975. The geometry of en-echelon vein arrays. Tectonophysics 28, 245-263

BEACH, A. 1977. Vein arrays, hydraulic fractures and pressure solution structures in a deformed flysch sequence. South West England. Tectonophysics 40, 201-225

BEACH, A. 1980. Numerical models of hydraulic fracturing and the interpretation of syntectonic veins. Struct. Geol. 2, 425-438.

BEACH, A. & FYFE, W.S. 1972. Fluid transport and shear zones at Scourie, Sutherland: Evidence of overthrusting? Contrib. Min. & Pet. 36, 175-185

BECKINSALE, R.D. & OBRADOVITCH, J.D. 1973. Potassium-argon ages for minerals from the jRoss of Mull, Scotland. Scott. J. Geol. 9, 147-156.

BERGER, P. & JOHNSON, A.M. 1980. First order analysis of deformation of a thrust sheet at a ramp. Tectonophysics 70, T9-T24.

BERTHE, D. & BRUN, J.P. 1980. Evolution of folds during progressive shear in the South Armorican Shear Zone, France. J. Struct. Geol. 2 127-133.

BICKLE, M.J., HAWKESWORTH, C.J., ENGLAND, P.C. & ATHEY, D.R. 1975. A preliminary thermal model for regional metamorphism in the jEastern Alps. Earth & Planet. Sci. Letts, 26, 13-28.

BIOT, M.A. 1965. Mechanics of incremental deformations. Wiley.

BOYER, S.E. & ELLIOTT, D. 1982. Thrust Systems. Bull. Am. Assoc. Pet. Geol. 66, 1196-1230.

BRACE, W.F. 1968. The mechanical effects of pore water pressure on the fracturing of rocks. Geol. Surv. Can. Pap. 68-52, 113-124.

BRACE, W.F. & MARTIN, R.J. 1968. A test of the law of effective stress for crystalline rocks of low porosity. Inst. J. Rock. Mech. Min. Sci. 5 412-426.

BRADLEY, J.S. 1975. Abnormal formation pressure. Bull. Am. Assoc. Pet. Geol. 59, 957-973.

BREWER, J.A. 1981. Thermal effects of thrust faulting. Earth. Planet. Sci. Lett. 56, 233-244

BREWER, J.A., COOK, F.A., BROWN, L.D., OLIVER, J.E., KAUFMAN, S. & ALBAUGH, D.S. 1981. COCORP seismic profiling across thrust faults. In McClay, K.R. & Price, N.J. Thrust and Nappe Tectonics Spec. Publ. Geol. Soc. Lond. 9, 501-512.

BROOK, M., BREWER, M.S. & POWELL, D. 1976. Grenville ages for rocks in the Moine of northwest Scotland. Nature Lond. 260, 515-517.

BROOK, M., POWELL, D. & BREWER, M.S. 1977. Grenville events in the Moine rocks of the Northern Highlands, Scotland. J. geol. Soc. Lond. 133, 489-496.

BROWN, G.C. 1979. Geochemical and geophysical constraints on the origin and evolution of Caledonian granites. in Harris, A.L., Holland, C.H. and Leake, B.E. (Eds). The Caledonides of the British Isles - reviewed. Spec. Publ. geol. Soc. Lond. No. 8, 645-651.

BRUCE, C.H. 1973. Pressured shale and related sediment deformation: Mechanisms for the development of regional contemporaneous faults. Bull. Am. Assoc. Pet. Geol. 57, 878-886.

BURCHFIEL, B.C., WERNICKE, B., WILLEMIN, J.H., AXEN, G.J. & CAMERON, C.S. 1982 A new type of decollement thrusting. Nature 300, 513-515.

BUTLER, R.W.H. 1982a. The terminology of structures in thrust belts. J. Struct. Geol. 4, 239.-245

BUTLER, R.W.H. 1982b. A Structural Analysis of the Moine Thrust zone between Loch Eriboll and Foinaven, N.W. Scotland. J. Struct. Geol. 4. 19-29

CHAPPLE, W.M. 1978. Mechanics of thin-skinned fold and thrust belts. Bull. Geol. Soc. Am. 89, 1189-1198.

CHOPIN, C. & MALUSKI, H. 1980. ^{40}Ar - ^{39}Ar Dating of high pressure micas from the Gran Paradiso area (Western Alps): Evidence against the blocking temperature concept. Contrib. Mineral. Petrol. 74, 109-122.

CHRISTIE, J.M. 1960. Mylonitic rocks of the Moine Thrust Zone in the Assynt region, North-west Scotland. Trans. Edinb. Geol. Soc. 18, 79-93.

CHRISTIE, J.M. 1963. The Moine thrust zone in the Assynt region, N.W. Scotland. Univ. California Pulb. Geol. Sci, 40.

CHRISTIE, J.M. & ORD, A. 1980. Flow stress from microstructures of mylonites: Example and current assessment. Journ. Geophys. Res, 85 B11. 6253.-6262

CHU, C.L., WANG, C.Y. & LIN, W. 1981. Permeability and frictional properties of San Andreas gouges. Geophys. Res. Lett. 8, 565.-570

COWARD, M.P. 1980. The Caledonian thrust and shear zones of N.W. Scotland. J. Struct. Geol. 2 11-19.

COWARD, M.P. 1982. Surge zones in the Moine thrust zone of North West Scotland. J. Struct. Geol. 4, 247.

COWARD, M.P. 1983. The thrust and shear zones of the Moine thrust zone and the NW Scottish Caledonides. J. Geol. Soc. Lond. 140, 795-811.

COWARD, M.P. & KIM. J.H. 1981. Strain within thrust sheets. in Thrust and Nappe Tectonics, eds McClay and Price. Spec. Publ. Geol. Soc. Lond. 9, 275.-292

COWARD, M.P., KIM, J.H. & PARKE, J. 1980. A correlation of Lewisian structures across the lower thrusts of the Moine thrust zone, N.W. Scotland. Proc. geol. Assoc. London. 91, 327-37.

COWIE, J.W. 1974. The Cambrian of Spitsbergen and Scotland. In Holland, C.H. (Ed) Cambrian of the British Isles, Norden and Spitsbergen. Wiley, London 123-155.

DAHLSTROM, C.D.A. 1969. Balanced cross sections. Can. J. Earth. Sci,6, 743-757.

DAHLSTROM, C.D.A. 1970. Structural geology in the eastern margin of the Canaadian Rocky Mountains. Bull. Can. Pet. Geol. 18, 332-456

DEWEY, J.F. & PANKHURST, R.J. 1970. The evolution of the Scottish Caledonides in relation to their isotopic age pattern. Trans. R. Soc. Edin. 68,361-389

DICKEY, P.A. 1976. Abnormal Formation Pressure: Discussion. Bull. Am. Assoc. Pet. Geol. 60, 1124.-1127

DICKINSON, G. 1953. Geological aspects of abnormal resevoir pressures in the Gulf Coast, Louisiana, U.S.A. Bull. Am. Assoc. Pet. Geol. 37, 410-432

DOUGLAS, R.J.W. 1950. Callum Creek, Langford Creek and Gap areas, Alberta. Geol. Surv. Mem. Can. 255.

DOWNIE, C. 1962. So-called spores from the Torridonian. Proc. geol. Soc. Lond. 1600, 127-128

DOWNIE, C. 1981. Lower Cambrian acriarchs from Scotland, Norway, Greenland and Canada. Trans. R. Soc. Edin. 72, 257.-285

DURNEY, D.W. & RAMSAY, J.G. 1973. Incremental stains measured by syntectonic crystal growths. In: DE JONG, K. & SCHOLTEN, R. (eds), Gravity and Tectonics. Wiley 67-96.

ELLIOTT, D. 1976a. The motion of thrust sheets. J. Geophys. Res. 81, 949-963.

ELLIOTT, D. 1976b. The energy balance and deformation mechanisms of thrust sheets. Phil. Trans. R. Soc. Lond. A283, 289-312

ELLIOTT, D. & JOHNSON, M.R.W. 1980. Structural evolution in the northern part of the Moine Thrust Belt, N.W. Scotland. Trans. R. Soc. Edin. 71, 69-96.

ENGELDER, J.T. 1974. Cataclasis and the generation of fault gouge. Bull. Geol. Soc. Am. 85, 1515-1522.

ENGELDER, J.T. 1979. Evidence for a variation of friction along natural fault zones. in Proc. Conf. VIII. Analysis of Actual Fault Zones in Bedrock. U.S.G.S. Open File Rep. 79-1239, 377-393.

EPSTEIN, A.G., EPSTEIN, J.B. & HARRIS, L.D. 1977. Conodont colour alteration; an index to Organic metamorphism. Geol. Surv. Am. Prof. Paper 995, 1-27.

ETHERIDGE, M.A. 1983. Differential stress magnitudes during regional deformation and metamorphism: Upper bound imposed by tensile fraturing. Geology. 11, 231-234.

ETHERIDGE, M.A. & WILKIE, J.C. 1981. An assessment of dynamically recrystallised grainsize as a paleopiezometer in quartz-bearing mylonites zones. Tectonophysics. 78, 475-508.

EVANS, C.R. & TARNEY, J. 1964. Isotopic ages of Assynt dykes. Nature Lond. 204, 638-641.

FETTES, D.J., GRAHAM, C.M., SASSI, F.P. & SCOLARI, A. 1976. The basal spacing of potassic white micas and facies series variation across the Caledonides. Scott. J. Geol. 12, 227-236.

FISCHER, M.W. & COWARD, M.P. 1982. Strain within thrust sheets: the Heilam sheet of N.W. Scotland. Tectonophysics. 88, 291-312.

FYFE, W.S., PRICE, N.J. & THOMPSON, A.B. 1978. Fluids in the Earths Crust. Elsevier.

GEISER, P.A. & SANSOME, S. 1981. Joints, microfractures and the formation of solution cleavage in Limestone. Geology, 9, 280-285.

GILETTI, B.J., MOORBATH, S. & LAMBERT, R. ST. J. 1961. A geochronological study of the metamorphic complexes of the Scottish Highlands. Q. Jl. geol. Soc. Lond. 117, 233-272.

GRAHAM, C.M. & ENGLAND, P.C. 1976. Thermal regimes and regional metamorphism in the vicinity of overthrust faults: an example of shear heating and inverted metamorphic zonation from Southern California. Earth & Planet. Sci. Letts, 312, 142-152.

GRETENER, P.E. 1972. Thoughts on overthrust faulting in a layered sequence. Bull. Can. Pet. Geol. 20, 583-607.

GRETENER, P.E. 1977a. Pore Pressure: Fundamentals, General Ramifications and Implications for Structural Geolgoy. Am. Assoc. Pet. Geol. Course notes 4, 131.

GRETENER, P.E. 1977b. On the character of thrust faults with particular reference to basal tongues. Bull. Can. Petrol. Geol. 25, 110-122.

GRETENER, P.E. 1981. Pore pressure, discontinuities, isostasy and overthrusts. in Thrust and Nappe Tectonics. eds McClay, K. and Price, N.J. Spec. Publ. Geol. Soc. Lond. 9. 33-39

HAIMSON, B.C. & FAIRHURST, C. 1967. Initiation and extension of hydraulic fractures in rocks. Petrol. Trans. A.I.M.E. 240, 310-318

HALLAM, A. & SWETT, K. 1966. Trace fossils from the Lower Cambrian Pipe Rock of the northwest Highlands. Scott. J. Geol. 2, 101-105.

HALLIDAY, A.N., STEVENS, W.E. & HARMON, R.S. 1979. Petrogenetic significance of Rb-Sr and U-Pb isotopic systems in the c.400 My old British Isles granitoids and their hosts. in Harris, A.L., Holland, C.H. & Leake, B.E. (Eds). The Caledonides of the British Isles - reviewed. Spec. Publ. geol. Soc. Lond. No 8, 653-661.

HANDIN, J., HAGER, R.V., FRIEDMAN, M. & FEATHER, . 1963. Experimental deformation of sedimentary rocks under confining pressure: pore pressure tests. Bull. Am. Assoc. Pet. Geol. 47, 717-755.

HANKS, T.C. 1977. Earthquake stress drops, ambient tectonic stresses, and stresses that drive plate motions. Pure & Appl. Geophys. 115, 441-458.

HARRIS, L.D. & MILICI, R.C. 1977. Characteristics of thin-skinned style of deformation in the southern Appalachians and potential hydrocarbon traps. U.S. Geol. Surv. Prof. Pap. 1018.

HARRISON, M.T., & McDOUGALL, I. 1980. Investigations of an intrusive contact, northwest Nelson, New Zealand. I- Thermal, chronological and isotopic constraints. Geochim. Cosmochim. Acta. 44, 1985-2003.

HATCHER, Jr, R.D. 1981. Thrusts and nappes in the North American Appalachian Orogen. In McClay, D.R. & Price, N.J. Thrust and Nappe Tectonics Spec. Publ. Geol. Soc. Lond. 9, 491-500

HOUSE, W.M. & GRAY, D.R. 1982. ; Cataclasites along the Saltvile Thrust, U.S.A. and their implications for thrust sheet emplacement. J. Struct. Geol. 4, 257-269

HUBBERT, M.K. & RUBEY, . 1959. Role of fluid pressure in the mechanics of overthrust faulting. Bull. Geol. Soc. Am. 70, 115-205.

JACKSON, J. & McKENZIE, D. 1983. The geometrical evolution of normal fault systems. J. Struct. Geol. 5, 471-482.

JACOBEEN, R. & KANES, W.H. 1974. Structure of Broadtop synclinorium and its implications for Appalachian structural style. Bull. Am. Assoc. Pet. Geol. 58, 362-375

JACOBEEN, R. & KANES, W.H. 1975. Structure of Broadtop synclinorium, Wills mountain anticlinorium and the Allegheny frontal zone. Bull. Am. Assoc. Pet. Geol. 59, 1136-1150

JAEGER, J.C. & COOK, N.G.W. 1976. Fundamentals of Rock mechanics. 2nd Edition. Methuen.

JAMISON, W. & SPANG, J. 1976. Use of calcite twin lamellae to infer differential stress. Bull. Am. Geol. Soc. 87, 868-872.

JOHNSON, M.R.W. 1960. The structural history of the Moine thrust zone at Lochcarron Wester Ross. Trans. R. Soc. Edin. 64, 139-168.

JOHNSON, M.R.W. 1961. Polymetamorphism in movement zones in the Caledonian thrust belt of northwest Scotland. J. Geol. 69, 417-432.

JOHNSTONE, G.S. 1975. The Moine Succession. In Precambrian, Harris, A.L., Shackleton, R.M., Watson, J.V., Downie, C., Harland, W.B. and Moorbath, S. (eds) Special Report 6 Geol. Soc. Lond. 30-43

JOHNSTONE, G.S., SMITH, D.I. & HARRIS, A.L. 1969. The Moinian assemblage of Scotland. In Kay, M. (ed) Noreth Atlantic geology and continental drift: a symposium. Mem. Am. Assoc. Petrol. Geol. 12, 159-180.

JONES, P.B. 1971. Folded faults and sequence of thrusting in Alberta foothills. Am. Assoc. Petrol. geol. Bull. 55, 292-306.

KEHLE, R.O. 1970. Analysis of gravity sliding and orogenic translation. Bull. Geol. Soc. Am. 81, 1641-64.

KELLY, S.P. & POWELL. D. 1984 in press. Relationships between marginal thrusting and internal, major, ductile shear displacements in the N. Highland Caledonides, Scotland. J. Struct. Geol
.

KENT, P.E. 1975. The tectonic development of Great Britain and the surrounding seas. In: WOODLAND, A.W. (ed) Petroleum geology of the continental shelf of N.W. Europe vol I. Geology. 3-28

KISCH, H.J. 1980a. Incipient metamorphism of Cambro-Silurian clastic rocks from the Jamtland Supergroup, central Scandinavian Caledonides: illite crystallinity and 'vitrinite' reflectance. J. Geol. Soc. Lond,137. 271-288.

KISCH, H.J. 1980b. Illite crystallinity and coal rank associated with lower grade metamorphism of the Taveyanne greywacke in the Helvetic zone of the Swiss Alps. Ecologae. Geol. Helv.,73, 753-777.

LACHENBRUCH, A.H. & SASS, J.H. 1980. Heat flow and energetics of the San Andreas fault zone: Journ. Geophys. Res. 85, 6185-6222.

LAMA, R.D. & VUTUKURI, V.S. 1978. Handbook on mechanical properties of rocks. Volume II. Clausthal, Trans. tech. Publ. 481p.

LAMBERT, R.St.J. & McKERROW, W.S. 1976. The Grampian Orogeny. Scot. J. Geol. 12, 271-293.

LATJAI, E.Z. 1977. A mechanistic view of some aspects of jointing in rocks. Tectonophysics 38, 327-338.

LAUBSCHEER, 1973. Jura Mountains in De Jong, K.A. and Scholten, R. (eds) Gravity and Tectonics. Wiley, New York 217-227.

LeFORT, P. 1975. Himalayas, the collided range. Present knowledge of the continental arc. Am. J. Sci, 275-A, 1-44.

LYON, T.D.B., PIDGEON, R.T., BOWES, D.R. & HOPGOOD, A.M. 1973. Geochronological investigation of the quartzofeldspathic rocks of the Lewisian of Rona. Inner Hebrides. Jl. Geol. Soc. Lond. 129, 389-404.

MAGARA, K. 1975a. Re-evaluation of montmorrillonite dehydration as the cause of abnormal pressure and hydrocarbon migration. Bull. Am. Assoc. Pet. Geol. 59, 292.-302

MAGARA, K. 1975b. Importance of aquathermal pressuring effect in the Gulf coast. Bull. Am. Assoc. Pet. Geol. 59, 2037.-2045

McGARR, A. & GAY, N.C. 1978. State of stress in Earth's crust. Ann. Rev. Earth Planet. Sci. 6, 405-436.

MOORBATH, S. 1969. Evidence for the age of deposition of the Torridonian sediments of Northwest Scotland. Scott. J. Geol. 5, 154-170.

MOORBATH, S., WELKE, H.J. & GALE, N.H. 1969. The significance of lead isotope studies in ancient high grade metamorphic complexes, as exemplified by the Lewisian rocks of Northwest Scotland. Earth. Planet. Sci. Lett. 6, 245-256.

MORROW, C.A., SHI, L.Q. & BYERLEE, J.D. 1981. Permeability and strength of San Andreas fault gouge under high pressure. Geophys. Res. Lett. 8 325.-328

MORROW, C.A., SHI, L.Q. & BYERLEE, J.D. 1982. Strain hardening and strength of clay rich fault gouges. Journ. Geophys. Res. 87, 6771-6780.

NARASIMHAN, T.N., HOUSTON, W.N. & NUR, A.M. 1980. The role of pore pressure in deformation in geologic processes. Geology 8, 349.-351

NORRIS, R.J. & HENLEY, R.W. 1976. Dewatering of a metamorphic pile. Geology 4, 333.-336.

OXBURGH, E.R. :& TURCOTTE, D.L. 1974. Thermal gradients and regional metamorphism in overthrust terrains with special reference to the eastern Alps. Schweiz. Mineral. Petrogr. Mitt. 54, 641.

PADAN, A., KISCH, H.J. & SHAGAM, R. 1982. Use of lattice parameter, b_o of dioctahedral Illite/Muscovite for the characterisation of P/T gradients of incipient metamorphism. Contrib. Mineral. Petrol, 79, 85-95.

PANKHURST, R.J. 1982. Geochronological tables for British igneous rocks. in 'Igneous Rocks of the British Isles' Sutherland, D.S. (Ed). John Wiley & Sons, 575-581.

PARSONS, I. 1979. The Assynt Alkaline Suite. In HARRIS, A.L., HOLLAND, C.H. & LEAKE, B.E. (eds). The Caledonides of the British Isles - Reviewed. Spec. Publ. geol. soc. Lond. 8, 677-81.

PARSONS, I. & McKIRDY, A.P. 1983. Inter-relationships of igneous activity and thrusting in Assynt: excavations at Loch Borralan. Scot. J. Geol. 19, 59-66.

PEACH, B.N., HORNE, J., GUNN, W., CLOUGH, C.T., HINXMAN, L.W. & CADELL, H.M. 1907. The geological structure of the North West Highlands of Scotland. Mem. Geol. Surv. U.K., 668p.

PHILLIPS,W.J. 1972. Hydraulic fracturing and mineralization. J. Geol. Soc. Lond. 128, 337-359

PIERCE, W.G. 1973. Principal features of the Heart Mountain fault and the mechanism problem. in De Jong, K.A. and Scholten, R. (eds) Gravity and Tectonics, Wiley, New York 457-7.

POWELL, D. 1974. Stratigraphy and structure of the western Moine and the problem of Moine orogenesis. Jl. Geol. Soc. Lond. 130, 575-593.

POWELL, D., BROOK. M., & BAIRD. A.W. 1982. Structural dating of a Precambrian pegmatite in Moine rocks of northern Scotland and its bearing on the status of the 'Morarian Orogeny'. J. Geol. Soc. Lond.140,813-824.

PRICE, N.J. 1966. Fault and joint development in brittle and semi-brittle rock. Pergamon, Oxford.

PRICE, N.J. 1974. The development of stress systems and fracture patterns in undeformed sediments. Proc. Third. Congr. Int. Soc. Rock. Mech. in Advances in rock Mechanics, I, Part A. 487-96. National Academy of Sciences, Washington, D.C.

PRICE, N.J. 1975. Fluids in the crust of the earth. Sci. Prog. Lond. 62, 59-87.

PRICE, N.J. 1977. Aspects of gravity tectonics and the development of listric faults. J. Geol. Soc. Lond. 133, 311-327.

PRICE, N.J. & HANCOCK, P. 1972. Development of fracture cleavage and kindred structures. Proc. 24th Int. Geol. Congr. Sect 3, 584.

PRICE, R.A. 1973. Large scale gravitational flow of supracrustal rocks, south Canadian Rockies. In De Jong, K. & Scholten, R. (eds). Gravity and tectonics, Wiley, 491-501.

PURDY. J.W. & JAGER. E. 1976. K-Ar ages of rock forming minerals from the Central Alps. Mem. Inst. Geol. Mineral. Univ. Padova. 30. 1-32.

QUINQUIS, H., AUDREN, CL. BRUN, J.P. & COBBOLD, P.R. 1978. Intense progressive shear in the Ile de Groix blueschists and compatibility with subduction or obduction. Nature, Lond. 273, 43-45.

RAMSAY, J.G. 1963. Structure and metamorphism of the Moine and Lewisian of the Northwest Caledonides. In Johnson, M.R.W. & Stewart, F.H. (eds). The British Caledonides, 143-175.

RAMSAY, J.G. 1980a. The crack seal mechanism of rock deformation. Nature, 284, 135.

RATHBONE, P.A. & HARRIS, A.L. 1979. Basement cover relationships at Lewisian inliers in the Moine rocks. In Harris, A.L., Holland, C.H. & Leake, B.E. (eds). The Caledonides of the British Isles - reviewed. Spec. Pub. Geol. Soc. Lond. 8, 101-107.

REITAN, P.H. 1968. Frictional heat during metamorphism, 1. Quantitative evaluation of concentration of heat in time. Lithos, 1, 151-163.

REITAN, P.H. 1968. Frictional heat during metamorphism, 1. Quantitative evaluation of concentration of heat in time. Lithos, 1, 151-163.

REITAN, P.H. 1969. Temperatures with depth resulting from frictionally generated heat during metamorphism. Geol. Soc. Am. Mem. 115, 495-512.

RICH, J.L. 1934. Mechanics of Low-Angle overthrust faulting as illustrated by the Cumbeerland thrust block, Virginia, Kentucky, Tenessee. Am. Assoc. Petrol. Geol. 18, 1584-96.

ROBERTS, D.G. 1974. Structural development of the British Isles, the continental margin and the Rockall Plateau. In: BURKE & DRAKE (eds) The geology of continental margins, New York. 343.–359

RODGERS, D.A. & RIZER, W.D. 1981. ; Deformation and secondary faulting near the leading edge of a thrust fault. in Thrust and Nappe Tectonics. eds McClay, K. and Price, N.J. Spec. Publ. Geol. Soc. Lond. 9, 65-77.

ROYSE, R. Jr, WARNER, M.A. & REESE, D.L. 1975. Thrust belt structural geometry and related stratigraphic problems, Wyoming-Idaho-northern Utah. Symp. Rocky. Mt. Ass. Geol. 41–54.

SASSI, F.P. 1972. The petrologic and geologic significance of b_o value of potassium white micas in low grade metamorphic rocks. An application to the Eastern Alps. Tschermaks. Mineral. Petrogr. Mitt.,18, 105-113.

SASSI, F.P. & SCOLARI, A. 1974. The b_o value of the potassium white micas as a barometric indicator in low grade metamorphism of pelitic schists. Contrib. Mineral Petrol. 45, 143-152.

SCHIFFMAN, P. & LIOU, J.G. 1980. Synthesis and stability relations of Mg-Al Pumpellyite $Ca_4Al_5MgSi_6O_{21}(OH)_7$. J. Petrol.21, 441-474.

SECOR, D.T. 1975. Role of fluid pressure in jointing. Am. J. Sci. 263 633-46.

SECOR, D.T. 1968. Mechanics of natural extension fracturing at depth in the earth's crust. Geol. Surv. Can. Pap. 68, 52. 3-48.

SERRA, S. 1977. Syles of deformation in ramp regions of overthrust faults. Trans. Am. Geophys. Union 58, 507 (abstr.).

SHEARMAN, D.J., MOSSOP, G., DUNSMORE, H. & MARTIN, M. 1972. Origin of gypsum veins by hydraulic fracture. Trans. Inst. Min. Metall. 81, B149-B155.

SIBSON, R.H. 1974. Frictional constraints on thrust, wrench and normal faults. Nature Lond. 249, 542-4.

SIBSON, R.H. 1975. Generation of pseudotachylyte by ancient seismic faulting. Geophys. J. R. Astr. Soc.43,775-794.

SIBSON, R.H. 1977. Fault rocks and fault mechanisms. J. Geol. Soc. Lond. 133, 191-213.

SIBSON, R.H. 1980. Power dissipation and stress levels on faults in the upper crust. J. Geophys. Res. 85 B11, 6239-6247.

SIBSON, R.H. 1981. Controls on low stress, hydro-fracture dilatancy in thrust, wrench and normal fault terrains. Nature 289, 665-667.

SIBSON, R.H., MOORE, & RANKIN, 1975. Seismic pumping, a hydro-thermal fluid transport mechanism. J. Geol. Soc. Lond. 131, 653-659.

SMITH, A.G. 1981. Subduction and coeval thrust belts with particular reference to North America. in Price N.J. and McClay, K.R. (Eds). 'Thrust and Nappe Tectonics', Spec. Publ. Geol. Soc. Lond. 9, 111-124.

* SOPER, N.J. & BARBER, A.J. 1979. Proterozoic folds on the north-western Caledonian foreland. Scott. J. Geol. 15, 1-11.

SOPER, N.J. & BARBER, A.J. 1982. A model for the deep structure of the Moine thrust zone. J. Geol. Soc. Lond. 39, 127-138.

SOPER, N.J. & WILKINSON, P. 1975. The Moine thrust and Moine nappe at Loch Eriboll, Sutherland. Scott. J. Geol. 11, 339-359.

SPRY, A. 1969. Metamorphic textures. Pergamon Press, Oxford, 350 pp.

STEL, H. 1981. Crystal growth in cataclasites: diagnostic micro-structures and implications. Tectonophysics, 78, 585-600.

STEWART, A.D. 1969. Torridonian rocks of Scotland reviewed. In Kay, M. (ed) North Atlantic-geology and continental drift in a symposium. Mem. Am. Assoc. Petrol. Geol. 12, 595-608.

SUTTON, J. & WATSON, J. 1951. The pre-Torridonian metamorphic history of the Loch Torridon and Scourie areas in the Northwest Highlands and its bearing on the chronological classification of the Lewisian. Quart. Jl. Geol. Soc. Lond. 106, 241-307.

* SMITH. R.L., STEARN. J.E.F. & PIPER. J.D.A. 1983. Palaeomagnetic studies of Torridonian sediments, N.W. Scotland. Scott. J. Geol, 19, 29-46

SWETT, K. 1969. Interpretation of depositional and diagenetic history of the Cambrian-Ordovician succession of northwest Scotland. In Kay, M (ed). North Atlantic geology and continental drift. Mem. Am. Assoc. Petrol. Geol. 12, 630-646.

SWETT, K., KLEIN, G de V. & SMITH, D.E. 1971. A Cambrian tidal sand body - the Eriboll sandstone of northwest Scotland; An ancient-recent analog. J. Geol. 79, 400-415.

TANNER, P.W.G. 1971. The Sgurr Beag Slide - a major-tectonic break within the Moinian of the western Highlands of Scotland. Q. J. Geol. Soc. Lond. 126, 425-63.

TANNER, P.W.G., JOHNSTONE, G.S., SMITH, D.I. & HARRIS, A.L. 1970. Moinian Stratigraphy and the problem of the Central Ross-shire inliers. Bull. Geol. Soc. Am. 81, 299-306.

TERZAGHI, K. 1950. Mechanics of landslides. Bull. Geol. Soc. Am., Berkeley Vol., 83-123.

TWISS, R.J. 1977. Theory and applicability of a recrystallised grainsize palaeopiezometer. Pure & Appl. Geophys. 115, 227-244.

VAN BREEMAN, O., PIDGEON, R.T. & JOHNSON, M.R.W. 1974. Precambrian and Palaeozoic pegmatites in the Moines of northern Scotland. J. geol. Soc. Lond. 130, 493-507.

VAN BREEMAN, O., AFTALION, M. & JOHNSON, M.R.W. 1979. Age of the Loch Borrolan complex, Assynt and late movements on the Moine thrust. J. gol. Soc. Lond. 136, 489-96.

WALLACE, R.E. & MORRIS, H.T. 1979. Characteristics of faults and shear zones as seen in mines at depths as much as 2.5km below the surface. in Proc. Conf.VIII. Analysis of actual Fault Zones in Bedrock. U.S.G.S. Open File Rep.79-1239, 276.

WALTON, E.K. 1983. Lower Palaeozoic-structure and palaeogeography. In Craig, G.Y. (ed) The Geology of Scotland. Scottish Academic Press, 105-166.

WATSON, J.V., 1983. Lewisian. In Craig, G.Y. (ed). The Geology of Scotland, Scottish Academic Press, 23-47.

WATTS, N.L. 1983. Microfractures in chalks of Albuskjell Field, Norwegian Sector, North Sea: Possible origin and distribution. Am. Assoc. Petrol. Geol. Bull. 67, 201-234.

WEATHERS, M.S., BIRD, J.M., COOPER, R.E. & KOHLSTEDT, D.L. 1979. Differential stress determined from deformation induced microstructures of the Moine Thrust Zone. Journ. Geophy. Res. 84, B13, 7495.-7509

WEBER, K. 1972. Notes on the determination of Illite crystallinity. Neues Jarb. Mineral. Monatsh. 6, 267-276.

* SUTTON. J. & WATSON. J. V. 1962. An interpretation of Moine-Lewisian relations in Central Ross-shire. Geol. Mag, 99, 527-541

WERNICKE, B. & BURCHFIEL, B.C. 1982. Modes of extensional tectonics. J. Struct. Geol. 4, 105-115.

WHITE, S.H. 1979a. Difficulties associated with palaeo-stress estimates. Bull. Mineral, 102, 210-215.

WHITE, S.H. 1979b. Palaeo-stress estimates in the Moine thrust zone. Eriboll. Scotland. Nature, 280, 222-224

WHITE, S.H., EVANS, D.J. & ZHONG, D.L. 1982. Fault rocks of the Moine thrust zone. Textures and Microstructures, 5, 33-61.

WHITTEN, E.H.T. 1966. Structural geology of folded rocks. Rand. McNally, Chicago. 663 p.

WILLIAM, H. & SMYTHE, W.R. 1973. Metamorphic aureoles beneath ophiolite suites and Alpine peridotites; tectonic implications with West Newfoundland examples. Am. J. Sci, 273, 594-621

WILTSCHKO, D.V. 1979a. A mechanical model for thrust sheet deformation at a ramp. J. Geophys. Res. 84 B3, 1091-1104

WILTSCHKO, D.V. 1979b. Partitioning of energy in a thrust sheet and implications concerning driving forces. J. Geophys. Res. 84 B11, 6050-6058

WILTSCHKO, D.V. 1981. Thrust sheet deformation at a ramp: summary and extension of an earlier model. in thrust and Nappe Tectonics eds McClay, K. and Price, N.J. Spec Publ. Geol. Soc. Lond. 9, 55-59